Norwegian University of Life Sciences
Faculty of Environmental Sciences
and Natural Resource Management

Philosophiae Doctor (PhD)
Thesis 2022:34

Microplastic particles from roads and traffic – occurrence and concentrations in the environment

Mikroplastpartikler fra veg og trafikk – forekomst og konsentrasjoner i miljøet

Elisabeth Støhle Rødland

Microplastic particles from roads and traffic – occurrence and concentrations in the environment

Mikroplastpartikler fra veg og trafikk – forekomst og konsentrasjoner i miljøet

Philosophiae Doctor (PhD) Thesis

Elisabeth Støhle Rødland

Norwegian University of Life Sciences
Faculty of Environmental Sciences and Natural Resource Management

Ås (2022)

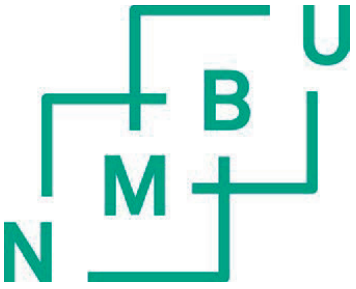

Thesis number 2022:34
ISSN 1894-6402
ISBN 978-82-575-1906-3

Burn some dust. Eat my rubber.

- Clark Griswold

Supervisors and Evaluation Committee

Supervisors

Doctor Sondre Meland

Norwegian Institute for water Research (NIVA)

Section for Catchment Biogeochemistry

Centre for Environmental Radioactivity (CERAD) CoE

Faculty of Environmental Sciences and Natural Resource Management (MINA)

Norwegian University of Life Sciences (NMBU)

E-mail: sondre.meland@niva.no

Professor Ole Christian Lind, PhD

Centre for Environmental Radioactivity (CERAD) CoE

Faculty of Environmental Sciences and Natural Resource Management (MINA)

Norwegian University of Life Sciences (NMBU)

E-mail: ole-christian.lind@nmbu.no

Doctor Lene Sørlie Heier

Norwegian Public Roads Administration (NPRA)

Division for Construction

E-mail: lene.sorlie.heier@vegvesen.no

Doctor Malcolm Reid

Norwegian Institute for water Research (NIVA)

Section for Environmental Chemistry and Technology

E-mail: malcolm.reid@niva.no

Evaluation Committee

Doctor Stephan Wagner

Hof University of Applied Science

Research group of Anthropogenic Water Cycles

Email: stephan.wagner@hof-university.de

Professor Yvonne Andersson-Sköld

The Swedish National Road and Transport Research Institute (VTI)

Environment and Transport

Email: yvonne.andersson-skold@vti.se

Professor Dag Anders Brede

Centre for Environmental Radioactivity (CERAD) CoE

Faculty of Environmental Sciences and Natural Resource Management (MINA)

Norwegian University of Life Sciences (NMBU)

Email: dag.anders.brede@nmbu.no

Acknowledgements

This PhD-project is a collaboration between the Norwegian Institute for Water Research (NIVA), the Norwegian University of Life Sciences (NMBU) and the NordFoU-project REHIRUP, consisting of the Norwegian Public Roads Administration (NPRA), the Swedish Transport Administration and the Danish Road Directorate (http://www.nordfou.org).

To my main supervisor Dr. Sondre Meland (NIVA/NMBU); without your efforts I would never have had the chance to come to NIVA and NMBU, and I am forever grateful for everything you have taught me about road pollution, statistics, patience during tunnel wash sampling and for safe use of life vests.

To the rest of my supervisor-team: thank you all for your expertise, hard questions and dedication. I would like to thank Professor Ole Christian Lind (NMBU) for insightful discussion on particle pollution and for sharing your knowledge on μXRF-techniques, Dr. Malcolm Reid (NIVA) for your help with analytical chemistry and method developments, as well as great advices for looking at "the bigger picture" and last but not least, I would like to thank Dr. Lene Sørlie Heier (NPRA) for your expertise on road pollution and for always asking great questions to steer me in the right direction.

To all my co-authors; thank you all for your knowledge, hard work and important contribution to this thesis. To my fellow pyrolysis enthusiast Dr. Elvis Okoffo (QAEHS); thank you for sharing your knowledge and being a great support in Brisbane and over Zoom. To Dr. Cassie Rauert (QAEHS); thank you for contributing your insights on tire particles and for helping me get my samples free from quarantine at QAEHS! To Professor Kevin Thomas (QAEHS); thank you for your contribution, your expert knowledge on microplastics have been a great asset to our work. To Dr. Saer Samanipour (UVA/NIVA); your positive attitude towards any challenge was truly helpful and I appreciate immensely your contribution to this thesis. To Dr. Brynhild Snilsberg (NPRA) and siv.ing Dagfin Gryteselv (NPRA); thank you both for your invaluable expertise on road particles and road surfaces, and for contributing with field sampling with the WDS. To my very best office neighbor, lab partner and Swede Emelie Skogsberg (NIVA/NMBU);

thank you for your filtration and sieving stamina, for all your help in R and most of all, thank you for bringing joy to my office days.

I would also like to thank Alfhild Kringstad (NIVA), Kine Bæk (NIVA) and Bert van Bavel (NIVA) for sharing your expertise in GC/MS and organic analyses with me. And I want to thank the great microplastic team at NIVA that I have had the pleasure to work with the last four years; Dr. Rachel Hurley, Nina Buenaventura, Dr. Amy Lusher, Dr. Inger Lise Nerland Bråte, Cecilie Singdahl-Larsen, Elena Martinez-Frances and Emilie Kallenbach. To Jacqueline Knutson (NIVA), thank you for helping me avoid complicated sentences and always mixing up my was/were's! Rachel and Nina, you have made these years fantastic.

I also want to thank my parents, my family and my friends for all your support and cheers during this work, and to my daughter Sophia for filling my days with both laughter, tears and a lot of creativity. And to Therese, thank you for always listening, for making me take breaks and focus on the things that matter.

Elisabeth,
Oslo, April 2022

Table of Contents

Abbreviations and definitions

µg/kg	Micrograms of microplastic particles per kilo
µm	Micrometer
µx	Mean number of particles (used for LOD and LOQ)
σx	Standard deviation (used for used for LOD and LOQ)
g/km	Grams per kilometre
Km	Kilometre
s.d.	Standard deviation
ATR-FT-IR	Attenuated Total Reflectance - Fourier Transformed Infra-Red Spectrometry
A	Acrylic
BR	Butadiene Rubber
BRP	Black rubber-like particles
CA	Concrete asphalt
CaCl2	Calcium chloride
d5-Pb	Deuterated polybutadiene
d6-PS	Deuterated polystyrene
DCM	Dichloromethane
EP	Ethylene propylene
ER	Epoxy resin
EVA	Ethylene vinyl acetate
FT-IR	Fourier-Transform Infrared spectroscopy
GC-MS	Gas chromatography mass spectrometry
HPDE	High Density Polyethylene
LOD	Limit of Detection
LOQ	Limit of Quantification
MgCl2	Magnesium chloride
MP	Microplastic

MP/kg	Number of microplastic particles per kilo
NaCl	Sodium chloride
NR	Nitrile rubber
PC	Polycarbonate
PE	Polyethylene
PEE	Polyester epoxide
PET	Polyethylene terephthalate
PLE	Pressurized liquid extraction
PMMA	Poly-(methyl methacrylate)
PP	Polypropylene
PS	Polystyrene
PUR	Polyeruthane acrylic resin
PVC	Polyvinyl chloride
PYR-GC/MS	Pyrolysis gas chromatography mass spectrometry
QAQC	Quality control and quality assurance
RAMP	Road-associated microplastic particles
RDA	Redundancy analysis
RO	Reverse osmosis
RS	Rock salt
RWPPMB	Road wear particles polymer-modified bitumen
RMP	Road marking particles
SBR	Styrene butadiene rubber
SBS	Styrene butadiene styrene
SEBS	Styrene ethylene butadiene styrene
SIS	Styrene isoprene styrene
SMA	Stone mastic asphalt
TED-GC/MS	Thermal desorption gas chromatography mass spectrometry
TSS	Total suspended solids
TRWP	Tire and road wear agglomerate particles
TWP	Tire wear particles

List of papers

Paper I: Elisabeth S. Rødland, Elvis D. Okoffo, Cassandra Rauert, Lene S. Heier, Ole Christian Lind, Malcolm J. Reid, Kevin V. Thomas, Sondre Meland. 2020. Road de-icing salt: assessment of a potential new source and pathway of microplastic particles from roads. Science of the Total Environment. Volume 738, 10. October 2020, Article no.139352. DOI: https://doi.org/10.1016/j.scitotenv.2020.139352

Paper II: Elisabeth S. Rødland, Saer Samanipour, Cassandra Rauert, Elvis D. Okoffo, Malcolm J. Reid, Lene S. Heier, Ole Christian Lind, Kevin V. Thomas, Sondre Meland. 2021. A novel method for the quantification of tire and polymer-modified bitumen particles in environmental samples by pyrolysis gas chromatography mass spectroscopy. Journal of Hazardous Materials. Volume 423, Part A, 5. February 2022, Article no. 127092. DOI: https://doi.org/10.1016/j.jhazmat.2021.127092

Paper III: Elisabeth S. Rødland, Ole Christian Lind, Malcolm J. Reid, Lene S. Heier, Elvis D. Okoffo, Cassandra Rauert, Kevin V. Thomas, Sondre Meland. 2022. Occurrence of tire and road wear particles in urban and peri-urban snowbanks, and their potential environmental implications. Science of the Total Environment. Volume 824, 10. June 2022, Article no. 153785. DOI: https://doi.org/10.1016/j.scitotenv.2022.153785

Paper IV: Elisabeth S. Rødland, Ole Christian Lind, Malcolm J. Reid, Lene S. Heier, Emelie Skogsberg, Brynhild Snilsberg, Dagfin Gryteselv, Sondre Meland. Characterization of Tire and Road Wear Microplastic Particle contamination in a Road Tunnel: from surface to release. Accepted for publication in Journal of Hazardous Materials (April 26th, 2022)

Abstract

The impact of roads and traffic on the environment have been studied for several decades, and negative impact on both the terrestrial and aquatic environment from pollutants have been demonstrated. Road pollution is typically related to high concentrations of particles, such as mineral particles (quartz, feldspar) and micro- and nanoparticles from the abrasion of tires and road surfaces. In recent years, the research interest for tire and road wear particles have increased substantially due to the increased research interest in micro- and nanoparticle pollution. As tires and some types of road surfaces contain synthetic rubbers, these particles are also included in the plastic pollution terminology as tire wear particles (TWP), tire wear particles combined with mineral particles (TRWP) and road wear particles with polymer-modified bitumen (RWP_{PMB}). Road pollution is also typically high in particle-associated pollutants, such as metals (zinc (Zn), copper (Cu), cadmium (Cd), nickel (Ni), lead (Pb)) and organic micropollutants such as polycyclic aromatic hydrocarbons compounds (PAC), organophosphates compounds (OPC), benzothiazoles, hexa(methoxymethyl)melamine (HMMM) and N-1,3-dimethylbutyl-N 0-phenyl-p-phenylenediamine-quinone (6-PPD-quinone). Especially the acute toxic effect of 6-PPD-quinone and benzothiazoles in the environment have been linked to the release of tire wear particles. Roads and traffic are estimated as the largest source of microplastic particles (MP) from land to the marine environment, and TWP are estimated to be the main microplastic source, with abrasion particles from road markings (RMP) and RWP_{PMB} as the second and third source.

Road transport is an essential part of modern society and predictions estimate that the number of vehicles will almost double over the next 30 years. It is therefore crucial for the environment on the planet that road-associated microplastic particles (RAMP) are assessed and mitigated. To reliably assess the levels of RAMP and ensure correct and efficient mitigation measures, there is an urgent need for more environmental data. However, comparisons between current available data on RAMP are hampered by the lack of standardized methods for both sampling and analysis. There are currently several initiatives in the research community and on

governmental level to harmonize the assessments of MP, such as Horizon2020-project EUROqCHARM (https://www.euroqcharm.eu/en). There are also efforts made to unify the analytical methods for TWP/TRWP specifically, such as the European TRWP Platform (https://www.csreurope.org/trwp). At the national level, several countries have implemented action plans against plastic pollution. In the National Transport Plan (NTP, 2022-2033), the Norwegian government have incorporated the need to improve the knowledge of microplastic release from roads and traffic and how to reduce the negative impact on the environment. The presented thesis aimed to contribute knowledge on the sources of MPs from roads and traffic, on the occurrence and concentrations of microplastic in different environmental compartments and to assess possible remedial actions for road-associated microplastic particles.

To investigate potential new sources of RAMP, the microplastic concentrations in road de-icing salt from both sea salt and rock salt sources were assessed, and the annual release of microplastic particles from road de-icing salt in Scandinavia was estimated (Paper I). The results demonstrated that MPs are present in road de-icing salt in Scandinavia, however the contribution was negligible compared to the other three sources of RAMP previously identified. The annual release of MPs from road de-icing salt was estimated to contribute to less than 0.003% of the total estimated microplastic release, compared to TWP (90%), RM (9%) and RWP_{PMB} (0.5%). However, the results support the need to identify and assess all sources of RAMP in order to evaluate the realistic levels of microplastic pollution and to reduce the negative impact on the environment. Although the work of this thesis focused on the high road salt consumption in Scandinavia, high salt consumption is also observed in several other countries, such as Germany, the United Kingdom, Ireland, the US, Canada and China. As different road de-icing salts are used in different countries, future research should assess the microplastic levels in the salts used locally to realistically address the annual release of microplastic particles from this source.

One of the challenges with describing the environmental impact of MPs, including TWP and RWP_{PMB}, is knowing what the relevant environmental concentrations are. Thus, reliable and comparable quantification methods must be developed so that these levels can be assessed across different studies in time and

space, and between different environmental compartments. Current available literature presents several different analytical methods for analysing RAMP, mostly focused on TWP. For single-particle analysis, methods such as Fourier Transform Infrared Spectroscopy (FTIR) and Raman Spectroscopy, Scanning Electron Microscopy with Energy Dispersive X-Ray Analysis (SEM-EDX) and Micro-X-ray Fluorescence (μXRF) have been utilized. For mass concentration analysis, Inductively Coupled Plasma Mass Spectrometry (ICP-MS), Liquid-Chromatography Mass Spectrometry (LC-MS/MS), Thermal Desorption Gas Chromatography Mass Spectroscopy (TED-GC/MS) and Pyrolysis Gas Chromatography Mass Spectroscopy (PYR-GC/MS) are the most used methods in current literature. For mass-based analysis, the challenge is finding suitable marker compounds that are reliable for both reference material and environmental samples, stable in different types of matrices and accessible for a high throughput of samples in order to establish environmental concentration levels across different types of samples. For PYR-GC/MS, the International Organization for Standardization (ISO) has published two technical specifications for quantifying TWP/TRWP in soil/sediment and air samples. However, these methods are currently not adjusted for the presence of synthetic rubbers in the road surface wear layer (RWP_{PMB}), such as styrene butadiene styrene rubbers (SBS) or scrap tires, which as applied in many countries for roads with high traffic volume. As SBS is currently the only rubber added to RWP_{PMB} on state and county roads as well as some municipality roads of Norway, the current thesis aimed to improved quantification methods for TWP/TRWP and RWP_{PMB}.

The improved method (Paper II) proposed in this thesis utilizes multiple pyrolysis markers for the quantification of styrene butadiene rubber (SBR) and butadiene rubber (BR) from tires and SBS from the road surface in environmental samples. The suggested markers were *benzene* (mz 78), *α-methylstyrene* (mz 117), *ethylstyrene* (mz 118) and *butadiene trimer* (mz 91). The proposed markers substantially lowered the standard deviation of the results to 40% s.d. compared to 62% (4-VCH), 77% (SB dimer) and 85% (SBB trimer) for the single marker compounds proposed in previous studies. The multiple pyrolysis markers also demonstrated good recoveries in complex road matrices (88–104%), which further validated the strength of the method. The proposed method also included an improved calculation step from the

measured rubber concentration to the mass of TWP and RWP_{PMB}. This step included the use of local emission factors, traffic data and locally relevant reference tires. The calculations were performed with Monte Carlo simulation. The use of Monte Carlo simulation also enabled the uncertainties related to these calculations to be reported. Incorporating assessments of the uncertainty is important, as the rubber concentration in commercial tires are highly variable. The average percentage of SBR+BR rubbers in personal and heavy vehicles tires reported in the current thesis were 31% (of total tire tread) and 33%, respectively. However, for personal vehicles and heavy vehicles, the variation between different tire types and brands were large. These results differ substantially from previous studies were 40-50% SBR+BR have been assumed for all personal vehicle tires and 50% natural rubber (NR) have been proposed for truck tires. Thus, the use of locally relevant reference tires will improve the quantification of TWP in environmental samples. As TWP in the environment are exposed to other road particles on the road surface, tire wear particles are often reported as agglomerate particles mixed with mineral particles from the road, defined as tire and road wear particles (TRWP). Based on a limited number of studies, previous quantification methods assume that all TRWP particles contain TWP and minerals in a 1:1 ratio. In the present thesis, we propose an improved method for calculating TRWP based on the concentration of TWP and the current data available on mineral content for TRWP. The calculations for TRWP are also performed with Monte Carlo simulation. Even though the proposed method is hampered by the limited knowledge on mineral content of TRWP, it demonstrates the possibility to optimize quantification methods for locally relevant data, such as different road surfaces, different driving patterns or other variables, as future publications contribute with improved data.

The improved quantification methods for TWP, RW_{PMB} and TRWP were further used to analyse the concentration levels in roadside snow (Paper III) and in different compartments of a road tunnel (Paper IV). The TWP concentrations in roadside snow (76.0–14 500 mg/L meltwater; 222–109 000 mg/m^2 mass loads) far exceeded concentration levels reported for snow and road runoff in previous studies, as well as the concentrations reported for tunnel wash water (TWW) in the present thesis (untreated: 14.5-47.8 mg/L; treated: 6.78-29.4 mg/L). As concentrations of RW_{PMB}

had not been assessed in previous studies, only comparison between the roadside snow (14.8–9550 mg/L; 50.0–28 800 mg/m^2), the tunnel road surface (0.578-258 mg/m^2) and the TWW (untreated: 11.5-38.1 mg/L; treated: 5.40-23.4 mg/L), in which the roadside snow has substantially higher concentrations compared to the tunnel samples. This demonstrates the potential for snow piles to accumulate RAMP and potentially pose a higher acute release risk to the environment compared to road runoff and tunnel wash water. Compared to the mass of total particles in the snow (TSS), the percentage of TWP and RW_{PMB} combined were 5.7% (meltwater) and 5.2% (mass load).

For the road tunnel, the concentrations of TWP, RWP_{PMB} and TRWP were assessed for the road surface, the gully-pots and the TWW, including TWW after sedimentation treatment. The concentration on the road surface were significantly higher in the side bank area (TWP: 2650 ± 1120, RWP_{PMB} : 2110 ± 892; TRWP: 3840 ± 1620 mg/m^2) and the outlet area (TWP: 1520 ± 2210, RWP_{PMB} : 1210 ± 1760; TRWP: 2200 ± 3200 mg/m^2) compared to the other surface areas, suggesting that these are important areas for accumulation. The mass percentage of TWP, RWP_{PMB} and TRWP were higher in the bank area (3.8%, 3.0% and 5.5%) and the outlet (6.4%, 5.1% and 9.2%) compared to the average mass percentage. For gully pots (GP), the highest concentration of TWP, RWP_{PMB} and TRWP were reported from the inlet GP (TWP: 24.7 ± 26.9 mg/g, RWP_{PMB}: 17.3 ± 48.8 mg/g, TRWP: 35.8 ± 38.9 mg/g). The mass percentage of TWP (5.4%), RWP_{PMB} (4.3%) and TRWP (7.8%) were also higher at the inlet GP compared to the other gully pots. For the tunnel wash water, the mass percentage of TWP, RWP_{PMB} and TRWP did not change substantially from the untreated TWW (TWP 2.1%, RWP_{PMB} 1.7% and TRWP 3.0%) to the treated TWW (TWP 2.5%, RWP_{PMB} 2.0% and TRWP 3.6%), although there was a small increase in the percentage for the treated water. The concentrations of TWP, RWP_{PMB} and TRWP were 38.3 ± 10.5, 26.8 ±7.33 and 55.3 ±15.2 mg/L in the untreated TWW and 14.3 ± 6.84, 9.99 ±4.78 mg/L and 20.7 ±9.88 mg/L in the treated TWW, respectively. The current treatment of TWW for this tunnel (sedimentation) retained 63% of the RAMP and 69% of the TSS, indicating a lower retention efficiency for microplastic particles compared to the total particle load.

The study on roadside snow also explored the different variables potentially explaining the variation of RAMP concentrations along roads. The road types (peri-urban highway, urban highway and urban city roads) were the most important variable explaining the variation, however, the main traffic variable was speed limit. This is contradictory to previous road studies, were Annual Average Daily Traffic (AADT) has been reported as the main explanatory variable. Other statistically significant explanatory variables were distance from the road and the combination of speed and AADT.

The reported concentrations of TWP, RWP_{PMB} and TRWP in roadside snow and the road tunnel both validates the improved analytical method proposed in this thesis and contributes new data on the environmental concentrations of RAMP. More data on environmental concentrations are needed in order to assess and evaluate the levels of microplastics from roads and traffic, from different types of roads, such as highways, urban roads and country-side areas, and for different traffic variables such as speed, AADT, inclination and road maintenance. It is also necessary to evaluate the efficiency of different types of measures taken to mitigate negative environmental impacts from road pollution, including MP. To be able to evaluate and assess the efficiency of different types of mitigation measures and types of water treatments used for road and tunnel runoff, it is important to increase the number of studies across different countries, climates, road types and driving patterns, as well as using comparable methods for sampling and analysis.

In short, the presented thesis provides a validated analytical method for mass quantification of microplastic particles from tire and road wear in different environmental matrices, new knowledge on the concentration levels of RAMP in different environmental compartments including the retention efficiency of TWW treatment and new knowledge on potential new sources of MPs from roads and traffic. This thesis answers to the needs defined by Norwegian government (NTP, 2022-2033), as well as providing new and improved knowledge for the research community.

Sammendrag

Miljøpåvirkningen av vei og trafikk har blitt studert i flere tiår, og det er påvist at veiforurensing kan ha negativ påvirkning på både det terrestriske og akvatiske miljøet. Veiforurensning er typisk relatert til høye konsentrasjoner av partikler, som mineralpartikler (kvarts, feltspat) og mikro- og nanopartikler fra slitasje av bildekk og veidekker. De siste årene har forskningsinteressen for dekk- og veislitasjepartikler økt betydelig på grunn av den økte interessen for mikro- og nanoplast. Siden bildekk og enkelte typer veidekker inneholder syntetisk gummi, er disse slitepartiklene også inkludert i plastforurensningsterminologien som dekkslitasjepartikler (TWP), dekk og veislitasjepartikler (TRWP) og veislitasjepartikler med polymermodifisert bitumen (RWP_{PMB}). Veiforurensning inneholder også typisk høye konsentrasjoner av partikkelbundet forurensning, som for eksempel metaller (sink (Zn), kobber (Cu), kadmium (Cd), nikkel (Ni), bly (Pb)) og organiske miljøgifter, som polysykliske aromatiske hydrokarbon-forbindelser (PAC), organofosfat-forbindelser (OPC), benzotiazoler, heksa(metoksymetyl)melamin (HMMM) og N-1,3-dimetylbutyl-N 0-fenyl-p-fenylendiamin-kinon (6-PPD-kinon). Særlig de akutte toksiske effektene av 6-PPD-kinon og benzotiazoler i miljøet har vært knyttet til utslipp av dekkslitasjepartikler. Vei og trafikk er estimert som den største kilden til mikroplastpartikler (MP) fra land til havmiljø, og TWP/TRWP er estimert til å være den viktigste mikroplastkilden, med slitasjepartikler fra veimerking (RM) og veislitasjepartikler med polymermodifisert bitumen (RWP_{PMB}) som de nest største og tredje største kildene.

Siden veitransport er en vesentlig del av det moderne samfunnet og estimater anslår at antall kjøretøy vil nesten dobles i løpet av de neste 30 årene, er det avgjørende for miljøet på planeten at veiassosiert mikroplastforurensning (RAMP) evalueres og reduseres. For å pålitelig vurdere nivåene av RAMP og sikre korrekte og effektive avbøtende tiltak, er det behov for mer miljødata. Mangel på standardiserte metoder for både prøvetaking og analyse påvirker mulighetene til å sammenligne mellom nåværende kunnskap om RAMP. Det er for tiden flere initiativer i forskningsmiljøet og på myndighetsnivå for å harmonisere metoder for å

evaluere mikroplast (MP) i miljøet, for eksempel Horizon2020-prosjektet *EUROqCHARM* (https://www.euroqcharm.eu/en). Det finnes også initiativer for å forene kunnskapen om TWP spesifikt, slik som den europeiske TRWP-plattformen (https://www.csreurope.org/trwp). På nasjonalt nivå har flere land iverksatt handlingsplaner mot plastforurensning. I Nasjonal Transportplan (NTP, 2022-2033) har den norske regjeringen beskrevet behovet for å bedre kunnskapen om utslipp av mikroplast fra veg og trafikk, samt kunnskap om hvordan man kan redusere den negative påvirkningen på miljøet. Denne PhD-avhandlingen hadde som mål å bidra med kunnskap om kilder til MP fra vei og trafikk, om forekomst og konsentrasjoner av mikroplast i ulike typer miljøprøver og å vurdere mulige tiltak for å hindre spredning av RAMP.

For å undersøke potensielle nye kilder til RAMP, ble MP i veisalt fra både havsalt- og steinsaltkilder analysert, og det årlige utslippet av MP fra veisalt i Skandinavia ble estimert (Artikkel I). Resultatene viste at MP er tilstede i veisalt i Skandinavia, men bidraget var ubetydelig sammenlignet med de tre tidligere identifiserte kildene til RAMP. Det årlige utslippet av MP fra veisalt ble estimert å bidra med mindre enn 0,003 % av det totale estimerte mikroplastutslippet, sammenlignet med TWP (90 %), RM (9 %) og RWP_{PMB} (0,5 %). Resultatene støtter imidlertid behovet for å identifisere og vurdere alle kilder til RAMP, slik at vurderingen av mikroplastforurensing til miljøet kan baseres på målte konsentrasjonsnivåer. Selv om deler av arbeidet med denne avhandlingen har fokusert på det høye veisaltforbruket i Skandinavia så er veisaltforbruket også høyt i andre land, som Tyskland, Storbritannia, Irland, USA, Canada og Kina. Forskjellige typer veisalt med ulikt produksjonsopphav, brukes i forskjellige land. Derfor bør fremtidige studier vurdere mikroplastnivåer i salt som brukes lokalt og vurdere de årlige utslippene fra veisalt som en kilde til mikroplast fra vei.

En av utfordringene med å karakterisere miljøpåvirkningen fra mikroplast, deriblant TWP og RWP_{PMB}, er å definere hva som er relevante konsentrasjoner i miljøet. For å kunne vurdere det så er det behov for å utvikle pålitelige og sammenlignbare kvantifiseringsmetoder, slik at disse nivåene kan vurderes på tvers av ulike studier i tid og rom, og mellom ulike matrikser. Nåværende publiserte studier presenterer flere forskjellige analytiske metoder for å analysere RAMP,

hovedsakelig fokusert på TWP. For å analysere enkeltpartikler så er det blant annet benyttet metoder som Fourier Transform Infrared Spectroscopy (FTIR) og Raman Spectroscopy, Scanning Electron Microscopy with Energy Dispersive X-Ray Analysis (SEM-EDX) og Micro-X-ray Fluorescence (μXRF). For kvantifisering av massekonsentrasjon er Induktivt koblet plasma massespektrometri (ICP-MS), Væskekromatografi massespektrometri (LC-MS/MS), Termisk Desorpsjons-Gasskromatografi Massespektroskopi (TED-GC/MS) og Pyrolyse Gasskromatografi Massespektroskopi (PYR-GC/MS) blant de mest brukte metodene i nåværende litteratur. For analyse av massekonsentrasjon er det å finne egnede markører for RAMP den største utfordringen, hvorav disse markørene må være pålitelige og stabile for kvantifisering i både referansemateriale og ulike typer miljøprøver, samt kunne benyttes til å analysere et stort antall prøver. Den internasjonale standardiseringsorganisasjonen ISO (International Organization for Standardization) har publisert to tekniske spesifikasjoner for kvantifisering av TWP/TRWP i jord/sediment og luftprøver. Disse metodene er imidlertid ikke tilpasset miljøprøver hvor det også finnes syntetisk gummi fra slitasje av veidekket (RWP_{PMB}). I mange land benyttes styren-butadien-styrengummi (SBS) eller kasserte bildekk i bitumenblandingen på veier med høyt trafikkvolum (årsdøgntrafikk, ÅDT). For alle riks- og fylkesveier i Norge, samt enkelte kommunale veier, benyttes det kun SBS i RWP_{PMB}. Et av delmålene for denne avhandlingen var derfor å inkludere SBS-gummi i metoder for massekvantifisering av TWP/TRWP og RWP_{PMB}.

Den nye analysemetoden som presenteres i denne avhandlingen benytter flere pyrolysemarkører for kvantifisering av styren-butadiengummi (SBR) og butadiengummi (BR) fra dekk og SBS fra veibanen i miljøprøver (Artikkel II). De foreslåtte markørene var *benzen* (mz 78), ***α**-metylstyren* (mz 117), *etylstyren* (mz 118) og *butadien-trimer* (mz 91), hvorav summen av signalene fra alle fire markører benyttes til kvantifiseringen. De foreslåtte markørene reduserte standardavviket for resultatene betydelig (40 % s.d.) sammenlignet med enkeltmarkørene som er foreslått av tidligere studier (4-VCH: 62 %); SB-dimer: 77%; SBB-trimer: 85 %. De foreslåtte markørene viste også gode resultater i komplekse prøvematriser, hvor 88–104% av tilsatt testmateriale ble korrekt kvantifisert, noe som ytterligere validerte metoden. Den foreslåtte metoden inkluderte også en forbedret beregningsmetode

for TWP basert på den målte gummikonsentrasjonen, samt inkluderte beregning av mengden RWP_{PMB}. Denne beregningen inkluderte bruk av lokale utslippsfaktorer, trafikkdata og lokale referansedekk. Beregningene ble utført med Monte Carlo-simulering. Bruken av Monte Carlo-simulering gjorde det også mulig å rapportere usikkerheten knyttet til disse beregningene. Det er viktig å inkludere vurderinger av usikkerheten, da gummikonsentrasjonen i kommersielle dekk er svært varierende. Den gjennomsnittlige prosentandelen av SBR+BR-gummi i bildekk for personbiler og tunge kjøretøy rapportert i denne avhandlingen var henholdsvis 31 % (av total dekkmengde) og 33 %, men med store forskjeller mellom dekktypene. Disse resultatene skiller seg vesentlig fra tidligere studier hvor det er antatt at alle personbildekk inneholder 40-50 % SBR+BR og alle bildekk for tunge kjøretøy inneholder 50 % naturgummi (NR). Ved å benytte gumminivåene i lokale referansedekk, kan analysemetodene tilpasses de faktiske lokale forhold og dermed forbedre kvantifiseringen av TWP i miljøprøver. Ettersom TWP i miljøet er eksponert for andre veipartikler på veibanen, rapporteres dekkslitasjepartikler ofte som agglomerater, hvor bildekkpartikler er blandet med mineralpartikler fra veien. Disse er definert som dekk- og veislitasjepartikler (TRWP). Basert på et begrenset antall studier er det antatt i tidligere kvantifiseringsmetoder at alle TRWP-partikler inneholder TWP og mineraler i et 1:1 forhold. I denne oppgaven foreslår vi en forbedret metode for å beregne TRWP basert på konsentrasjonen av TWP og gjeldende data som er tilgjengelige for mineralinnhold i TRWP. I likhet med metodene for TWP og RWP_{PMB} er beregningene for TRWP er også utført med Monte Carlo-simulering. Selv om den foreslåtte metoden påvirkes av det nåværende datagrunnlaget for mineralinnhold i TRWP, demonstrerer den muligheten for å optimalisere kvantifiseringsmetoder for lokalt relevante data når disse blir tilgjengelig, som for eksempel data om ulike veidekker, ulike kjøremønstre eller andre variabler.

De forbedrede kvantifiseringsmetodene for TWP, RWP_{PMB} og TRWP ble videre benyttet til å analysere konsentrasjonsnivåene i veinær snø (Artikkel III) og i ulike deler av en vegtunnel (Artikkel IV). TWP-konsentrasjonene i snø (76,0–14 500 mg/L smeltevann; 222–109 000 mg/m^2 snømasse) rapportert i denne avhandlingen var langt høyere enn det som tidligere er rapportert for veinær snø og veiavrenning,

samt høyere enn konsentrasjonene som ble rapportert for tunnelvaskevann (TWW) i denne avhandlingen (ubehandlet TWW: 14,5-47,8 mg/L; behandlet TWW: 6,78-29,4 mg/L). Ettersom konsentrasjoner av RWP_{PMB} ikke er vurdert i tidligere studier så sammenlignes disse konsentrasjonene kun mellom studier gjennomført i denne avhandlingen. Konsentrasjonene for RWP_{PMB} var høyest i snø (14,8–9550 mg/L; 50,0–28 800 mg/m^2) sammenlignet med veioverflaten i tunnel (0,578-258 mg/m^2) og sammenlignet med TWW (ubehandlet: 11,5-38,1 mg/L; behandlet: 5,40-23,4 mg/L). Prosentandelen av TWP og RWP_{PMB} i snø sammenlignet med den totale mengden partikler (TSS) var 5,7 % (smeltevann) og 5,2 % (snømasse). Disse funnene demonstrerer at RAMP kan akkumulere i veinær snø i store konsentrasjoner, og potensielt utgjøre en høyere akutt risiko for negativ påvirkning på miljøet sammenlignet med veiavrenning og tunnelvaskevann.

Konsentrasjonene av TWP, RWP_{PMB} og TRWP i tunnel ble kvantifisert i veistøv fra vegdekket, i sandfang og i vaskevann (TWW) før og etter rensing (sedimentasjon). Konsentrasjonen på veibanen var betydelig høyere i sidearealet (bankett) (TWP: 2650 ± 1120, RWP_{PMB}: 2110 ± 892; TRWP: 3840 ± 1620 mg/m^2) og utløpet av tunnelen (TWP: 1520 ± 2110, RWP_{PMB}: 1210 ± 1760; TRWP: 2200 ± 3200 mg/m^2) sammenlignet med andre områder av vegbanen, noe som tyder på at dette er viktige områder for akkumulering. Masseprosenten av TWP, RWP_{PMB} og TRWP var høyere i sidearealet (3,8 %, 3.0 % og 5,5 %) og ved utløpet (6,4 %, 5,1 % og 9,2 %) sammenlignet med gjennomsnittlig masseprosent. De høyeste konsentrasjonene i sandfang (GP) ble målt ved innløpet (TWP: 24,7 ± 26,9 mg/g, RWP_{PMB}: 17,3 ± 48,8 mg/g, TRWP: 35,8 ± 38,9 mg/g). Masseprosenten av TWP (5,4 %), RWP_{PMB} (4,3 %) og TRWP (7,8 %) var også høyere i sandfang ved innløpet sammenlignet med de andre sandfangene i tunnelen. For tunnelvaskevannet endret ikke masseprosenten av TWP, PMB og TRWP seg vesentlig fra urenset TWW (TWP 2.1%, RWP_{PMB} 1.7% and TRWP 3.0%) til renset (TWP 2.5%, RWP_{PMB} 2.0% and TRWP 3.6%). Konsentrasjonene av TWP, RWP_{PMB} and TRWP var henholdsvis 38.3 ± 10.5, 26.8 ±7.33 og 55.3 ±15.2 mg/L i urenset TWW, og 14.3 ± 6.84, 9.99 ±4.78 mg/L and 20.7 ±9.88 mg/L i renset TWW. Den nåværende rensemetoden for tunnelvaskevann (sedimentasjonsbasseng) holdt tilbake 63% RAMP og 69% av TSS i

tunnelvaskevannet, noe som indikerer at tilbakeholdelsen av totalpartikler fra vei er noe høyere enn tilbakeholdelsen av mikroplastpartikler fra vei.

Sammenhengen mellom konsentrasjonene av RAMP i snø og ulike forklaringsvariabler ble også undersøkt (Artikkel III), og veitypene (motorveier, urbane motorveier og urbane byveier) var den viktigste variabelen som forklarer variasjonen. For trafikk-relaterte variabler ble fartsgrense funnet til å være den viktigste variabelen, noe som strider mot tidligere studier hvor ÅDT er rapportert som hovedforklaringsvariabel. Andre statistisk signifikante forklaringsvariabler var avstand fra vei og kombinasjonen av hastighet*ÅDT.

De rapporterte konsentrasjonene av TWP og, RWP_{PMB} og TRWP i snø og tunnel validerer den forbedrede analysemetoden foreslått i denne avhandlingen og bidrar med ny kunnskap om konsentrasjonene av RAMP i miljøet. Flere konsentrasjonsdata er nødvendig for å vurdere og evaluere nivåene av veirelatert mikroplast fra ulike typer veier, som motorveier, urbane veier og landområder, samt sammenhengen med ulike trafikkvariabler som hastighet, ÅDT, helning på veien og vedlikehold. For å redusere de negative påvirkningene på miljøet er det også nødvendig å vurdere hvilken effekt ulike typer tiltak implementert mot veiforurensning generelt har for RAMP. For å kunne evaluereeffektiviteten av ulike typer avbøtende tiltak og ulike rensetiltak som brukes for vei- og tunnelavrenning, er det viktig å øke antallet studier på tvers av ulike land, klima, veityper og kjøremønstre, samt benytte sammenlignbare metoder for prøvetaking og analyse.

Oppsummert så er det i denne avhandlingen presentert en ny validert analytisk metode for massekvantifisering av mikroplastpartikler fra dekk- og veislitasje i ulike miljømatriser, ny kunnskap om konsentrasjonsnivåene av RAMP i ulike miljøprøver, inkludert rensegrad av tunnelvaskevann og ny kunnskap om potensielle nye kilder til MP fra vei og trafikk. Denne oppgaven svarer ut behovene beskrevet av norske myndigheter i NTP (2022-2033), samt bidrar med ny og forbedret kunnskap om mikroplast fra vei og trafikk til forskningsmiljøet.

1 Introduction

1.1 Road transport – an integral part of modern society

Road networks are essential to societies, connecting both people and commodities across the world. In 2020 it was reported that there were 1.3 billion vehicles on the planet, and it is predicted that this number will rise to 2 billion by 2035 and possibly 2.5 billion by 2050 (Ceder, 2021). In order to make sure that future cities are sustainable, the transportation sector also needs to consider sustainable transportation methods and innovative solutions for densely populated cities. Sustainable transport is one of the goals (no. 11) in the United Nations Sustainable Development Goals (UN, 2015), where the overall goal is to make sure the global community can achieve a more sustainable future. Several countries have their own national plan for future transportation, where areas in need of development and plans for reducing negative impact are described. In the Norwegian National Transport Plan (NTP, 2022-2033), shifts towards more green mobility, with electrified vehicles and zero emission policies for both transport and construction are described (MT, 2021). One goal put forward in the NTP is to contribute to reducing the emissions from the transport sector 50% by 2030, following the Norwegian Climate Plan (2021-2030) (MCE, 2021). It is also described in the NTP that pollution to air, soil, water and general negative impact on ecosystems due to transportation should be reduced. One of the topics that was especially mentioned was the release of plastic pollution from roads, which has gained a lot of attention in recent years, as roads and traffic has been named one of the main sources of microplastic pollution on land (Boucher et al., 2020; Sundt et al., 2021). The National Transport Plan states that the transport sector should improve knowledge of microplastic sources and how to reduce the release from roads and traffic (MT, 2021).

1.2 Road-related pollution

Roads and traffic are also closely associated with a large range of pollutants, coming from both the road surface itself and from the vehicles driving on the roads. Pollution from road traffic has been a topic of interest for both researchers and environmental authorities for several decades, as both exhaust and non-exhaust sources contribute to pollution of air, soil, water and biota (Cadle and Williams, 1979; Rogge et al., 1993; Thorpe and Harrison, 2008). In recent years, microplastic contamination has gained a global interest as an immediate threat to the environment, with recent discoveries of plastic contamination on every continent, from the deep oceans (Bergmann et al., 2017; Kanhai et al., 2019) to remote mountain areas (Allen et al., 2019; Napper et al., 2020). Road traffic is estimated to be one of the major sources of microplastic particles to the environment (Boucher et al., 2020; Knight et al., 2020), and the release of synthetic rubbers from tire wear particles (TWP) is the main contribution from roads. However, these estimates are associated with large uncertainties as environmental data on road-related microplastic particles (RAMP) are limited. Accurate and reliable environmental data is needed to evaluate how traffic and road-related variables are contributing to the mass balance of RAMP, and to understand the process of transport from the road surface into the environment. Reliable data is also important for evaluating mitigation efforts, such as retention treatment of road runoff. The current limitation in environmental data is mainly due to challenging analytical methods (Baensch-Baltruschat et al., 2020; Wagner et al., 2018), as well as large uncertainties stemming from the variability of chemical composition in tires (Rauert et al., 2021) and in road surface types from different commercial suppliers (EAPA, 2018).

1.3 Research hypotheses

The overarching aim of the present thesis is to contribute knowledge of the sources of microplastic particles from roads and traffic, of the occurrence and concentrations of microplastics in different environmental compartments and to assess possible remedial actions for road-associated microplastic particles. Thus, the

present thesis aims to provide new knowledge that could contribute to the development of more sustainable transport systems, which is in line with the United Nations Sustainable Development Goals. This work also aims to provide new knowledge about road-related microplastic particles that could contribute to reduce emission from the transport sector according to the Norwegian National Transport Plan (2022-2033).

Hypothesis 1

Non-negligible amounts of microplastic particles from road de-icing salt is left unaccounted for as model estimates mainly focus on tire wear, road wear and road marking.

Identification and characterization of potential additional sources of microplastic particles related to road activity and traffic will contribute to the overall assessment of impacts on the environment from microplastic particles. Previous studies have demonstrated the presence of microplastic particles in both sea salt and rock salt used for food consumption. Increased knowledge on the potential levels of microplastic particles from new sources such as road de-icing salts will improve the model estimates of road-associated microplastic particles in the environment.

Hypothesis 2

Methods for mass quantification of tire and road wear particles can be improved by utilizing multiple pyrolysis markers for styrene butadiene rubbers, incorporate relevant reference tires for calculation of tire wear and relevant levels of mineral content in tire and road wear-agglomerate particles.

Current mass quantification methods have focused on determination of TWP in different environmental samples. These methods have not adjusted for the presence of synthetic rubbers in the road surface wear layer (RWP_{PMB}), such as styrene butadiene styrene rubbers or scrap tires, which is applied in many countries

for roads with high traffic volume. To be able to incorporate these rubbers in the mass quantifications, new and adjusted quantification methods are needed. Current quantification methods for tire wear particles assume that all tires have a fixed percentage of synthetic rubbers, although research show a large variation in different commercial tires. This variation needs to be addressed and incorporated in improved methods. The current literature also assumes that all tire and road wear agglomerate particles (TRWP) have a tire tread to mineral content ratio of 1:1, although the present environmental data suggests a large variation in mineral encrustment of TRWP.

Hypothesis 3

Tire and road wear particles are deposited close to roads and the main variable contributing to the particle emissions is the Annual Average Daily Traffic.

According to the current literature on road-associated particle pollution, such as metals and polycyclic aromatic compounds, the highest concentrations of pollutants are found close to the roadsides as the particles are retained in the road structures such as grass-filled swales or gully-pots. It is reasonable to assume that microplastic particles follow a similar transport route from roads and do not differ significantly from other road particles. Current road pollution studies also show that the main traffic variable impacting the concentrations of road pollutants is the traffic volume, measured as the Annual Average Daily Traffic (AADT), and it is assumed that this is also true for road-associated microplastic particles.

Hypothesis 4

Road tunnels represent local "hot-spots" sources for the release of tire and road wear particles to the environment.

Previous research on pollution levels in road tunnels have demonstrated that road tunnels are pollution "hot spots", with high concentrations of both particle-related pollutants and dissolved pollutants accumulating inside the tunnels over time. These pollutants are released to the environment through wind and air

deposits at the tunnel inlet and outlet, and to the aquatic environment through the washing of tunnels and release of tunnel wash water to water recipients. Improved knowledge on the distribution of TWP/TRWP and RWP_{PMB} in different tunnel compartments will contribute to better treatment methods for road-associated microplastic particles in tunnels.

1.4 Research objectives

To test the research hypotheses, three objectives (Figure 1) have been defined;

1) Investigate road de-icing salt as a potential new source to RAMP (Paper I)

The goal of this objective is to identify, estimate and characterize microplastic particles potentially present in road de-salt originating from evaporated marine waters (sea salt). Sea salt may be a possible fourth source of microplastic particles from roads, alongside tyres, road paint and polymer modified bitumen in asphalt. Road salt originating from microplastic polluted marine sources will be compared with road salt originating from rock salt.

2) Develop a validated, mass-based quantification method for tire and road wear particles in environmental samples (Paper II)

The goal of this objective is to develop a new analytical method that quantifies both TWP and RWP_{PMB} in environmental samples, incorporate relevant reference tires for calculation of tire wear in the samples and assess the levels of uncertainties with the method.

3) Assess the concentration level of tire and road wear particles in different road and tunnel compartments (Papers III and IV).

The goal of this objective is to utilize the established mass quantification method to assess the level of TWP/TRWP and RWP_{PMB} in different environmental samples, from both roads and tunnels.

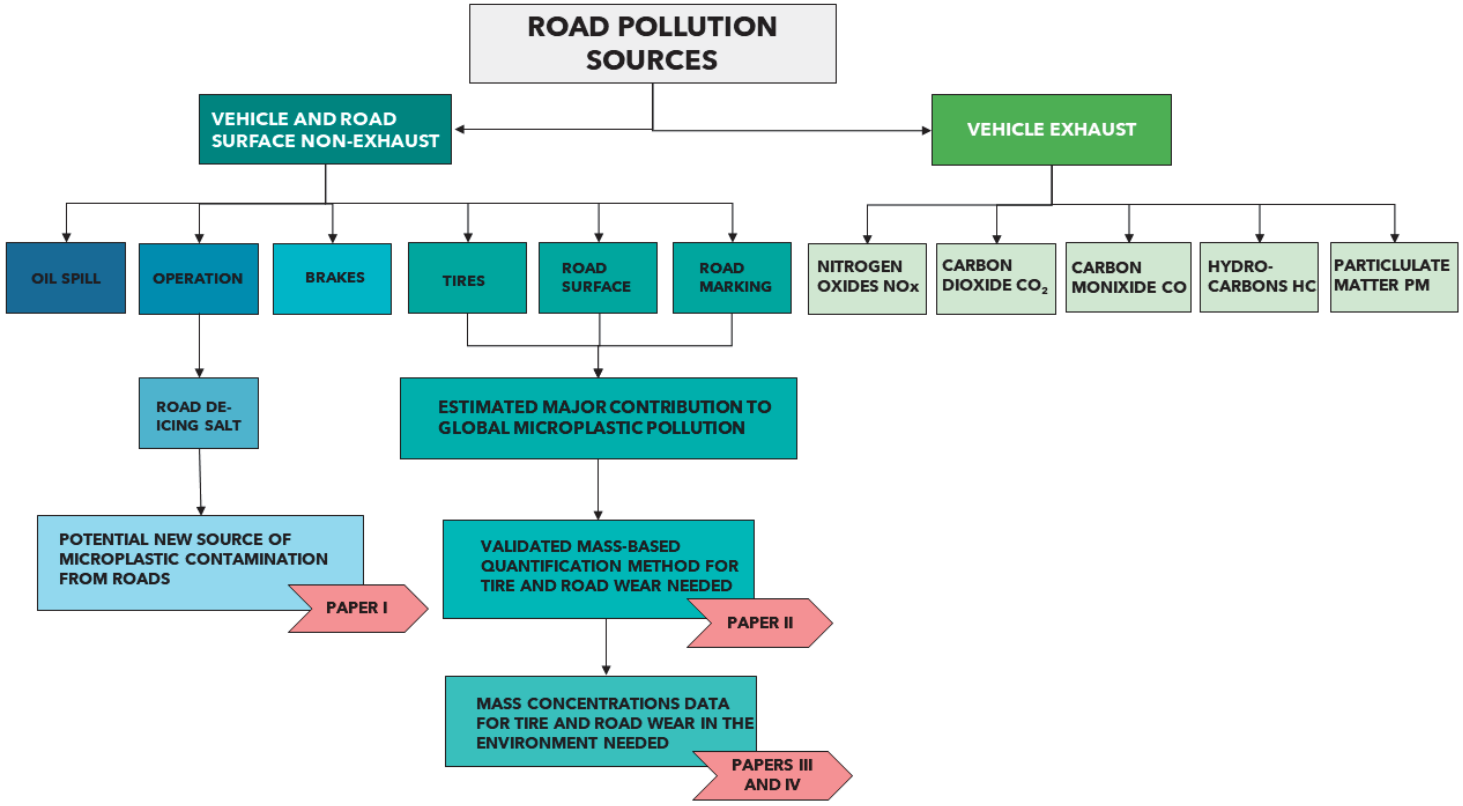

Figure 1. An overview of the main sources of pollution related to roads, separated by the two categories vehicle exhaust and vehicle and road surface non-exhaust. The illustration shows which areas of road pollution the present thesis has focused on. (Illustration: E. Rødland)

2 Background

2.1 Global pollution

The term "pollution" includes a large range of negative impacts on the environment caused by anthropogenic activities. Any substance that is introduced to the environment by human activities in levels that can cause harm to organisms are considered "pollutants". This includes, but are not restricted to, the release of chemicals such as metals, organic compounds and radioactive substances, the release of greenhouse gases (carbon dioxide (CO_2), nitrogen oxides (NOx)), excess nutrients (nitrogen N and phosphorus P) and aerosol particles ($PM_{2.5}$, PM_{10}). The impacts on the environment and the planet are so extensive that researchers have introduced a new geological age, the Anthropocene, arguing that the rapid changes by mankind have thrown us into a new geological period different to the Holocene period that has lasted for over 11 700 years (Crutzen, 2016).

The potential global impact of the rising levels of pollution were described with the term "planetary boundaries" by Rockström et al. (2009) in which thresholds of no return are described. Exceeding these thresholds means that irreversible effects that threaten life on whole continents or the whole planet are inevitable. In this work, nine planetary boundaries were suggested; climate change (CO_2), ocean acidification, ozone depletion, change in the N and P cycles, global freshwater use, land system change, biodiversity loss, chemical pollution and atmospheric aerosol loading. These planetary boundaries assess what the limits for the Earths functioning systems are and how close our activities currently are for damaging these vital systems. The planetary boundary for chemical pollution was renamed "novel entities" by Steffen et al. (2015) to also include all new types of human made materials or organisms alongside substances previously defined as anthropogenic pollutants. According to Steffen et al. (2015) these novel entities reach a level of threat to the planet when they are characterized as persistent and mobile in the environment, as well as causing negative effects on the Earths systems. Several studies have argued that plastic pollution is an important part of the novel entities planetary boundary, and

that the impact of plastic contamination is close to the planetary boundary (Arp et al., 2021; Villarrubia-Gómez et al., 2018). According to a recent publication (Persson et al., 2022), the rate at which chemical pollution and plastic pollution is released exceeds the planet's ability to both assess and reverse the effects, and they argue that the planetary boundary of novel entities is currently being exceeded. Thus, irreversible effects caused by chemical and plastic pollution will be a significant part of the future of the planet.

2.2 Road pollution

Road pollution is typically linked to high levels of particles, such as mineral particles (quartz, feldspar), road asphalt abrasion particles and micro- and nanoparticles from the abrasion of tires and road surfaces with synthetic rubbers present. Road pollution is also typically high in particle-associated pollutants, such as metals (zinc (Zn), copper (Cu), cadmium (Cd), nickel (Ni)) (Hallberg et al., 2014; Meland et al., 2010a), road salt (sodium chloride (NaCl), magnesium chloride ($MgCl_2$)) (Bäckström et al., 2004; Mahrosh et al., 2014; Meland et al., 2010a), nutrients (nitrogen (N), phosphorous (P)) (Reddy et al., 2013; Winston and Hunt, 2017) and organic micropollutants such as polycyclic aromatic compounds (PAC), organophosphate compounds (OPC), benzothiazoles, hexa(methoxymethyl)melamine (HMMM) and N-1,3-dimethylbutyl-N 0-phenyl-p-phenylenediamine-quinone (6-PPD-quinone), (Allan et al., 2016; Grung et al., 2017; Grung et al., 2021; Meland et al., 2010a; Peter et al., 2018; Tian et al., 2021). High levels of pollutants have been reported in different environmental compartments, such as road dust accumulating on the road surface (Asheim et al., 2019; Gustafsson et al., 2019; NPRA, 2017; NPRA, 2021b; Rogge et al., 1993), in the roadside soil (Cao et al., 2022; Werkenthin et al., 2014; Zhang et al., 2018), in road and tunnel runoff (Grung et al., 2021; Gunawardena et al., 2015; Hallberg et al., 2014; Kumata et al., 2002; Meland et al., 2010b; Meland and Rødland, 2018; Wik et al., 2008), in roadside snow (Baumann and Ismeier, 1998; Bäckström, 2003; Seiwert et al., 2022; Vijayan et al., 2021; Viklander, 1996; Viklander, 1998; Viklander, 1999) and in freshwater recipients (Johannessen et al., 2022; Meland et al., 2010a; Ni et al., 2008; Zakaria et

al., 2002). Release of tunnel wash water have been found to be both acute and chronically toxic to aquatic organisms (Meland et al., 2010b; Petersen et al., 2016). Studies have also demonstrated that solids and associated road pollutants may be retained in treatment measures such as grass-filled swales or bioretention filters (Blecken, 2016; Bäckström et al., 2004; Flanagan et al., 2018; Hatt et al., 2009), gully-pots (Deletic et al., 2000; Huber et al., 2016; Pitt and Field, 2004; Rietveld et al., 2021), sedimentation basin (Andersson et al., 2018; Barbosa and Hvitved-Jacobsen, 2001), raingardens (Robinson et al., 2019) and treatment facilities combining sedimentation and filtration (Huber et al., 2016; Marsalek et al., 2006). Heavy metals and PAHs are especially correlated to the concentration of particles in the runoff, and measures such as sedimentation ponds and filter treatment has been proven to be highly effective (Flanagan et al., 2018; Huber et al., 2016; Paruch and Roseth, 2008).

Studies have also demonstrated that stormwater and road runoff are dominated by particles <20µm (Cristina and Sansalone, 2003; Kayhanian et al., 2012; Li et al., 2005), which have been difficult to retain in grass-filled swales (Bäckström, 2002) or sedimentation ponds (Pettersson, 1998). Recently, new attention has been given to road pollution, as the focus on microplastic particles has increased. Synthetic rubbers from TWP have been estimated to be one of the largest sources of microplastic particles released into the environment (Boucher et al., 2020; Knight et al., 2020; Sundt et al., 2021).

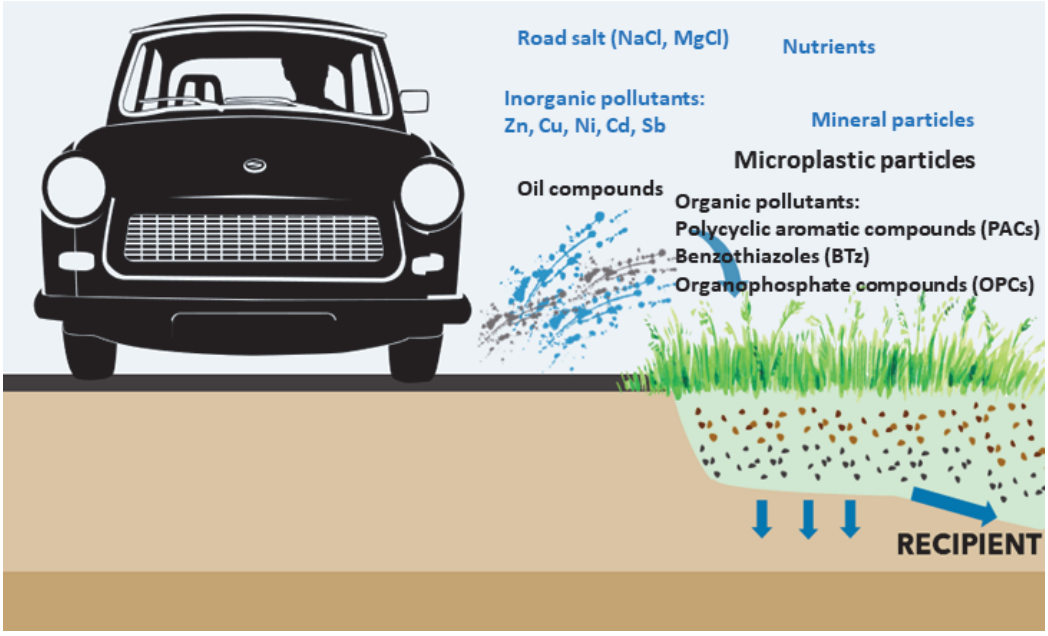

Figure 2. Illustration of road runoff pollution entering the environment. Examples of inorganic pollutants in runoff (blue text) are road salt (NaCl, $MgCl_2$), sinc (Zn), copper (Cu), nickel (Ni), cadmium (Cd), antimon (Sb), minerals (quartz, feldspar) and nutrients (N, P). Examples of organic pollutants in road runoff (in black) are oil compounds, polycyclic aromatic compounds (PACs), benzothiazoles (BTz), organophosphate compounds (OPCs), hexa(methoxymethyl)melamine (HMMM) and N-1,3-dimethylbutyl-N 0-phenyl-p-phenylenediamine-quinone (6-PPD-quinone) and microplastic particles. (Illustration: Modified from Furuseth and Rødland (2021))

2.3 Microplastic particles

Plastic pollution has gained a global interest in the last few decades, with ongoing research continuously describing new environmental compartments polluted by plastics and new species affected (SAPEA, 2019). Over 400 million tonnes of plastic is produced every year on a global scale (UNEP, 2021), where more than 80% of the plastic is unaccounted for and assumed to be in landfills or released to the environment (UNEP, 2021). The impact of plastic pollution on a global scale and how to handle it, has been a topic of debate in the research community, environmental organizations and among the countries of the world. In March 2022 at the United Nations Environment Assembly (UNEA-5-2), 175 countries agreed to a plastic resolution on ending plastic pollution and making a legally binding agreement on this by 2024 (UNEP, 2022).

Plastic and rubber are made from synthetic or semisynthetic organic material, either as mixtures of different polymer components or one single polymer. The most common plastic types produced are polyethylene (PE 32%), polypropylene (PP 15%), polyethylene terephthalate (PET 10%), polystyrene (PS 6%), polyurethane (PUR 5%) and polyvinyl chloride (PVC 5%) (UNEP, 2021), where the main sources of these plastics are packaging (46%), textiles (15%) and consumer products (12%). The most common synthetic rubber types are styrene butadiene rubber (SBR), butadiene rubber (BR), styrene butadiene styrene (SBS), and acrylonitrile butadiene styrene (ABS). The SBR and BR are mainly used in vehicle tires (Wagner et al., 2018) and the SBS is mainly applied in road surfaces, pavements and roofs (Polymerdatabase, 2022). The ABS rubber is more commonly used in the building and construction industry (Omnexus, 2022).

Plastics can be divided into different size ranges and several published studies have argued for different size definitions, as summarized by Hartmann et al. (2019). However, agreeing on the size definitions is crucial for comparison between studies, and the following definition have been proposed (Hartmann et al., 2019) as a compromise between previous studies: macroplastic >1000 mm, mesoplastic 1-<10 mm, microplastic 1 - <1000µm and nanoplastic 1 - >1000nm. Microplastic particles

have gained the most attention by research, as the size of the particles and density of the different polymer materials enables the microplastic particles to be transported by both atmospheric deposition and water, as well as potentially being ingested by various organisms of different trophic levels (Bråte et al., 2017; Lusher et al., 2017; Su et al., 2018; Wright et al., 2013), including the marine environment (Lundebye et al., 2022), the freshwater environment and the terrestrial environment (Bråte et al., 2017; Kallenbach et al., 2022; Lundebye et al., 2022; Lusher et al., 2017; Su et al., 2018; Wright et al., 2013). However, the current knowledge on ecotoxicity of microplastic particles is limited, and future studies need to incorporate both the physical impact of the particles themselves as well as the related chemicals to fully understand the impact of microplastic particles on organisms (Gomes et al., 2022).

Microplastic particles are also in a size range that has been manageable for different analytical approaches, assessing both single particles using techniques such a Fourier-Transform Infrared Spectroscopy (FTIR) and Raman Spectroscopy, and mass of microplastic particles using techniques such as Thermal Desorption Gas Chromatography Mass Spectrometry (TED-GC/MS) and Pyrolysis Gas Chromatography Mass Spectrometry (PYR-GC/MS).

Due to the vast interest, microplastic particles have been reported from all environmental matrices (air, water, soil, plants, organisms) and from urban to remote areas, including remote tropical islands, the Arctic, the Antarctic, mountains and deep-sea sediments (GESAMP, 2016; SAPEA, 2019). Plastic nanoparticles, with sizes smaller than microplastic particles, are possibly an even bigger challenge for the environment. Experimental studies have shown that plastic nanoparticles can be taken up by plant roots from the water and transported to the shoots (del Real et al., 2022), as well as across the blood-brain barrier in mice and eventually accumulate in the brain (Shan et al., 2022). Although the first reports of plastic particles in the nanosize range was in 2015 (Gigault et al., 2016; Lambert and Wagner, 2016) and uptake in organisms in experimental studies have been demonstrated, the environmental data on plastic nanoparticles are still limited, mainly due to analytical challenges (Kumar et al., 2021). Although several analytical techniques, such as laser diffraction and electrophoretic light scattering, have been efficient tools for nanoparticle assessments, these are less suited to separate plastic nanoparticles

from other nanoparticles, and less suitable for mass quantification (Kumar et al., 2021). Some analytical techniques currently used for microplastic studies show more promise for plastic nanoparticles, such as FTIR and PYR-GC/MS (Kumar et al., 2021; Wagner and Reemtsma, 2019)

2.4 Road-associated microplastic particles

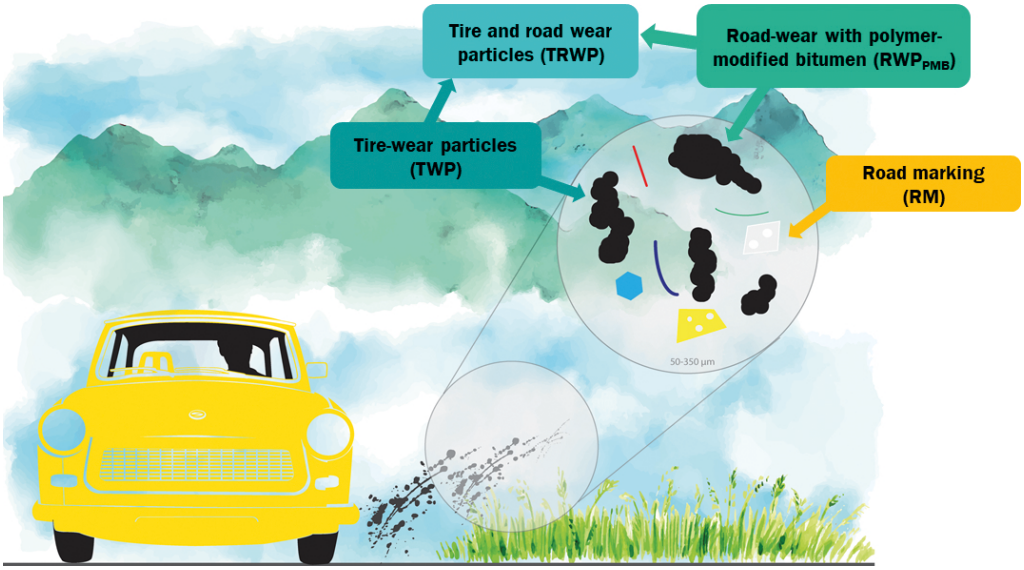

Figure 3. Schematic illustration of the known sources of road-associated microplastic particles (RAMP). Microplastic particles from litter and degradation of macroplastic is not covered by the RAMP definition and therefore not included. (Illustration: E. Rødland)

Overall, roads are estimated as the largest single source of microplastic particles from land to the marine environment (Boucher et al., 2020; Sundt et al., 2021), where tire wear particles are estimated to be the main microplastic source. The annual release of TWP is estimated at 0.6 – 5.5 kg/capita estimated for different countries

across the globe (reported by Baensch-Baltruschat et al. (2020) based on previously published data (Kole et al., 2017; Magnusson et al., 2017; Sundt et al., 2014; Unice et al., 2013; Wagner et al., 2018)

Synthetic rubbers are used in vehicle tires and in the road surface of many types of roads (polymer-modified bitumen (PMB) in road asphalt or asphalt concrete), and these rubbers are released through the friction between tires and the road surface, causing the release of tire wear particles (TWP) and road wear particles with PMB (RWP_{PMB}) (Figure 3). Road markings (RM) used on the road surface also contain different synthetic polymers, which are released during weathering and traffic. Collectively, TWP, RWP_{PMB} and RM are defined as road-associated microplastic particles (RAMP), and they all have in common that their source is intentionally applied to vehicles or on the road surface (Vogelsang et al., 2018). An overview of the characteristics of RAMP is given in Table 1.

2.4.1 Characteristics of Road-associated Microplastic Particles

Tire wear particles

Tire producers have their own recipes for different types of tires, and the exact formulations are proprietary information. According to current literature, tires contain 40-50% rubber (SBR, BR, NR), 30-35% filler (carbon black, silica, others), 15% softener (oils, resin), 2-5% vulcanization agents (ZnO, S) and 5-10% additives (preservatives, anti-oxidants, desiccants, plasticizers, processing aids) (Baensch-Baltruschat et al., 2020; Sommer et al., 2018; Wagner et al., 2018; Wagner et al., 2022). The shape of tire particles can vary, but most studies have reported them as elongated hetero-aggregates of TWP mixed together with mineral components from the road surface and environment, which are then reported as tire and road wear particles (TRWP). The percentage of minerals in the TRWP is variable according to current literature, with estimates of 6-53% (Klöckner et al., 2021b; Kreider et al., 2010; Sommer et al., 2018). The size of TRWP is expected to be in the range 50-350 µm (85% of particles) and <50 µm (15% of particles) (Kreider et al. 2010; Broeke et al. 2008), however it is suggested that most of TWP has sizes <50µm, which dominate in road tunnels (Klöckner et al., 2021b). Asphalt and minerals such as

quartz, have high densities (2.4 g/cm^3, 2.7 g/cm^3, respectively), whereas the density of pure TWP is 1.2 g/cm^3 (Degaffe and Turner, 2011). The density of TRWP depends on the percentage of mineral content and has been reported in the range 1.2 - 2.1 g/m^3 ((Jung and Choi, 2022; Kayhanian et al., 2012; Klöckner et al., 2021b)).

Road wear particles

Road wear particles (RWP) in general are reported to include particles with similar size range and shape as TWP/TRWP, although a variation in different shapes were reported (Kreider et al., 2010; Sommer et al., 2018). Studies also report a variation in composition for RWP, including 94-95% minerals (quartz, feldspar, pyroxene, amphibole, mica) and different elements (Si, Al, Ca, Na, K, Mg; Fe, S), held together as aggregated particles by the bitumen (5-6%) from the road asphalt (Sommer et al., 2018). There is currently no morphology study available for RWP_{PMB}, so it is assumed that RWP and RWP_{PMB} share similar characteristics (Vogelsang et al., 2018), although the rubber content of RWP_{PMB} may contribute to differences and should be investigated in future research. For RWP_{PMB} between 3-10% (d.w.) synthetic polymers or rubbers are added to the bitumen to increase resistance to cracking and deformation (rutting) of the road surface (Saba et al., 2012)

PMB can be used with different types of road surfaces, such as stone mastic asphalt (SMA) and concrete asphalt (CA), and are applied in several countries such as Norway, Australia, China, Denmark, Russia, Sweden and the United Kingdom (EAPA, 2018). Different polymers or rubbers can be applied, such as styrene butadiene styrene (SBS), styrene ethylene butadiene styrene (SEBS), low-density polyethylene (LDPE), ethylene vinyl acetate (EVA), polypropylene (PP) and styrene isoprene styrene (SIS) (Chen et al., 2002; Giavarini et al., 1996; Becker et al., 2003; Panda and Mazumdar, 1999; Polacco et al., 2005; Polacco et al., 2006; Sengoz et al., 2009). Some countries also utilize scrap tires as the rubber component of PMB (Bouman et al., 2020). Approximately 6% (3282 km) of the state and county road network in Norway has PMB in the road surface (SSB, 2019; Vegvesen, 2020). Only SBS is used for road surfaces in Norway (NVF, 2013).

Road marking particles

Particles from road marking (RM) are expected to be in the size ranges 50-4000 µm (Vogelsang et al., 2018). RM differs from the other two RAMP particles by being more square-like fragments formed by the breaking of road marking layers and are found both with and without glass beads present. RM is expected to have lower densities (>1.2 g/m^3) than both TWP/TRWP and PMB, depending on the amount of glass beads in each particle.

Two types of road marking are used in Norway, thermoplastic markings and water-based polymer paint (Sundt et al., 2021; Sundt et al., 2014; Sundt et al., 2016). In the thermoplastic type, the polymer content is 1-5% (Sundt et al., 2014). According to the producers of road markings in Norway, the binding agent constitutes 20% of the total road marking mass. However, the polymer mass in the binding agent is only 2% and the rest is made of natural or synthetic resins and oils (Geveko, 2018). The polymers used are either Styrene Isoprene Styrene (SIS) or ethylene-vinyl acetate copolymer resin (EVA) in the white markings, and SIS or polyamid in the yellow markings (Geveko, 2018). Further the markings have 5-7% pigments (Ti, organic pigment), 30-35% fillers (dolomites, quartz), and 40% glass beads made from recycled glass (old glass windows).

Table 1: Summary of the known size, shape, density and chemical composition of RAMP.

	Tire wear particles (TWP/TRWP)	*Road wear particles (RW_{PMB})*	*Road marking (RM)*	*ILLUSTRATION*
Size	85% 50-350 µm	Assumed similar to TWP, however more research is needed.	50-4000 µm	TWP/TRWP and RW_{PMB} 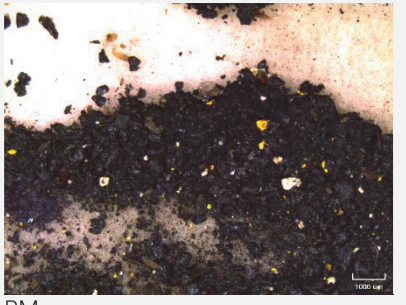 RM 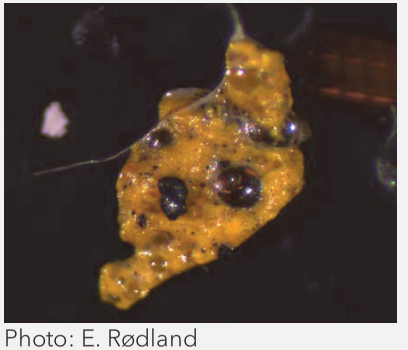 Photo: E. Rødland
Shape	15% <50 µm Elongated, sausage-like particles	Assumed similar to TWP, however more research is needed.	Squared-like flakes	
Density	1.2-2.1 g/m3	Assumed similar to TWP, however more research is needed.	>1.2 g/cm3	
Chemical composition	40-50% of polymers (SBR, BR, NR) 30-35% filler (carbon black, silica, others) 15% softener (mineral oils, resin) 2-5% vulcanization agents (ZnO, S) 5-10% additives (preservatives, antioxidants, desiccants, plasticizers, processing aids) TRWP: 50% TWP and 50% mineral (quartz, feldspar, ferromagnesian silicates)	94-95% minerals (quartz, feldspar, pyroxene, amphibole, mica) 5-6% bitumen (3-10% polymer/rubber) Different elements (Si, Al, Ca, Na, K, Mg; Fe, S)	20% binding agent (2% polymer: SIS, EVA, 18% natural or synthetic resins), 5-7% pigments (Ti, organic pigment), 30-35% fillers (dolomites, quartz), 40% glass beads	
References	Kreider et al., (2010); Broeke et al., (2008); Wang et al., (2017); Kayhanian et al., (2012); Baench-Baltruschat et al., 2020), Jung and Choi, (2022)	Statens vegvesen, (2014); Vogelsang et al., (2018), Kreider et al., (2010); Sommer et al., (2018)	Vogelsang et al., (2018); Geveko, (2018).	

2.5 Road-associated microplastic particles in the environment

2.5.1 Pathways

Tire and road wear particles

The current literature on road-related microplastic particles is focused mainly on tire wear particles, as these are estimated to be the main source of microplastic into the environment (Boucher et al., 2020; Knight et al., 2020). Tire and road wear particles are initially deposited on the road surface. However, from the road surface, the particles may take different pathways into the environment or they might be retained and removed by different treatment systems (Furuseth and Rødland, 2021; Kole et al., 2017) (Figure 4). Based on probabilistic models, Sieber et al. (2020) reported that 74% of the TRWP were deposited on the roadsides, whereas 22% were transported to surface water and 4% to soils. Figure 5 summarizes the reported mass concentration levels for TRWP for different environmental compartments. It should also be emphasized that the current knowledge on TWP/TRWP mass concentrations in the environment are based on several different analytical techniques, and these should be compared with caution. The analytical challenges related to analysis of RAMP are further described in chapter 2.6.

Road surface deposition

Particles larger than 10µm are potentially deposited on the road surface, and from there the pathways are dependent on local conditions. Particles may be transported short distances (0-30 m) into the terrestrial environment (Cadle and Williams, 1979; Vogelsang et al., 2018), by turbulence generated by traffic and the splash and spray effect caused by traffic during precipitation (Denby et al., 2013). During heavy precipitation, the runoff water from the surface is usually quickly removed due to road inclination (Brodie, 2007), and flows into the nearby roadsides, into the nearest recipient or into the road drainage system. The tire and road wear particles in road dust have been assessed by several studies, with concentrations between 0.7-124 mg/g (Eisentraut et al., 2018; Hopke et al., 1980; Klöckner et al.,

2020; Kumata et al., 2000; Kumata et al., 2002; Rogge et al., 1993; Zakaria et al., 2002) (Figure 5). The surface tunnel dust has also been assessed, where values so far are significantly higher than the reported values for road dust (2.7-210 mg/g) (Klöckner et al., 2021b; Kumata et al., 2000; Wik and Dave, 2009) (Figure 5).

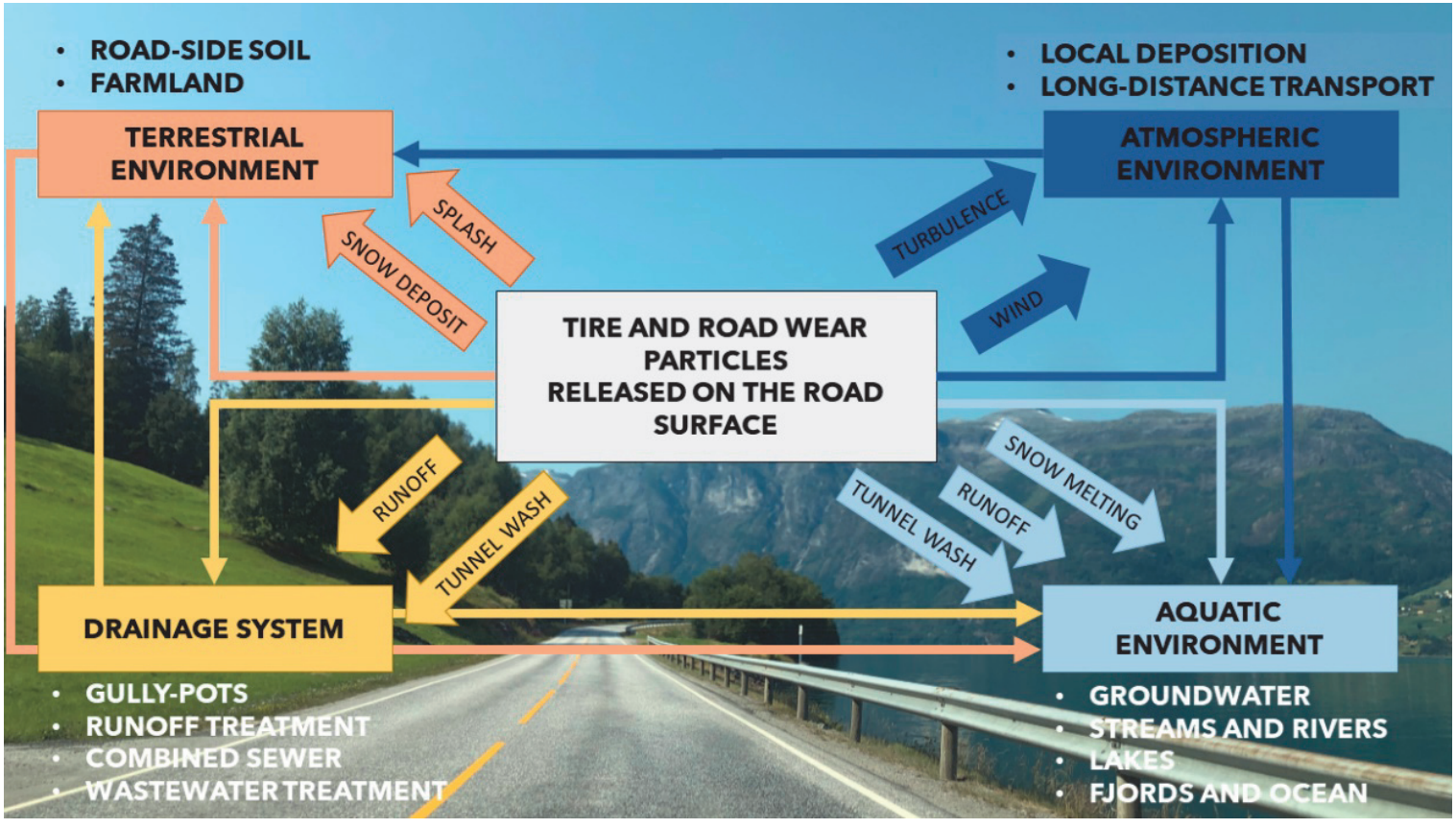

Figure 4. Potential pathways of tire and road wear particles from the road surface and into the atmospheric environment (dark blue), aquatic environment (light blue), terrestrial environment (orange) and the drainage system (yellow) (Illustration: E. Rødland)

Atmospheric environment

Small particles, typically in the size range of <10µm (PM_{10} and $PM_{2.5}$), are potentially transported by wind and turbulence to the atmosphere and deposited into the terrestrial or aquatic environment. Previous studies have estimated that only between 0.1 and 10% of the tire and road wear are transported by air, although some studies reported up to 30% (Grigoratos and Martini, 2014). The contribution from non-exhaust sources to PM_{10} is estimated between 50 and 85%, where road wear is considered the main source and tire wear is estimated to contribute <10% (Grigoratos and Martini, 2014). One study (Panko et al., 2019) has reported the tire concentration in $PM_{2.5}$ (0.012-0.042 µg/m_3) and PM_{10} (0.095-1.91 µg/m_3) from London, LA and Tokyo (Figure 5). Due to limited data available there are currently no data on the distribution of airborne tire and road wear particles between the terrestrial and aquatic environment (Kole et al., 2017).

Aquatic environment

The concentration of TWP in road runoff have so far been reported by several studies in the range of 3-180 mg/L (Baumann and Ismeier, 1998; Kumata et al., 2000; Kumata et al., 1997; Kumata et al., 2002; Parker-Jurd et al., 2021; Reddy and Quinn, 1997; Wik and Dave, 2009) (Figure 5). In the Nordic countries, the most common pathway of road runoff is infiltration into the grass-filled swales in the roadsides or in open trenches that transport the runoff to the nearest recipient (Andersson et al., 2018; Meland, 2016; Vogelsang et al., 2018).

Studies have modelled the transport of TWP/TRWP into the aquatic environment and reported that between 6 and 23% potentially end up in marine recipients (Wagner et al., 2018), whereas 18-22% of TWP/TRWP end up in freshwater recipients (Sieber et al., 2020; Unice et al., 2019). The transport of tire wear particles from Sweden's largest river Göta into the marine recipient Kattegat was modelled in the study of Bondelind et al. (2020), where only one third of the TWPs (average size 20µm, density 1.7g/cm^3) were reported to settle in the river. However, size and density were reported to have a large impact, and larger (75µm) and heavier (1.9g/cm^3) particles mainly settled in the river (Bondelind et al., 2020). Although the number of studies assessing TWP and TRWP in the aquatic environment is limited,

the current studies show large variations of mass concentrations for both freshwater sediment (0.036-155 mg/g) (Reddy and Quinn, 1997; Spies et al., 1987; Unice et al., 2013; Wik et al., 2008) and river water (0.8-18.5 mg/L) (Kumata et al., 2000; Ni et al., 2008; Rauert et al., 2022; Reddy and Quinn, 1997).

During winter, especially in the northern hemisphere, roadside snow is also an important matrix for tire and road wear deposition. Although several studies have shown high concentrations of pollutants in snow (Moghadas et al., 2015; Vijayan et al., 2021; Viklander, 1999), the number of studies reporting tire and road wear concentrations are limited. Only one study has so far reported mass concentrations of TWP in snow (563 mg/L; Baumann and Ismeier (1998)) (Figure 5). However, a few studies have reported the presence of tire wear particles based on visual analysis (Bergmann et al., 2019; Vijayan et al., 2019). One recent study also reported concentrations of 6-PPD-quinone (tire anti-ozonant) in roadside snow from Germany, confirming the presence of TWP in these samples (Seiwert et al., 2022). Due to limited data, there are currently no estimates on the retention of tire and road wear particles from snowmelt. For road pollution in general, larger particles are expected to be retained where the snow deposit is situated and only the smaller particles and dissolved pollutants will follow the drainage system or natural flow into recipients nearby (Borris et al., 2021).

Drainage system

For runoff entering the road drainage system, different roads may have different solutions. Most highways have gully-pots, or sedimentation traps, which are designed to retain large debris, gravel/sand litter as well as large particles in order to keep the drainage system from clogging. Studies have reported high retention efficiency (>75%) for large particles (400µm) (Rietveld et al., 2021). However, the retention decreases with the size of the particles, and for particles <180µm, less than 50% is expected to be retained in the gully-pots (Deletic et al., 2000; Pitt and Field, 2004; Rietveld et al., 2020; Rietveld et al., 2021)). Only one study has so far reported mass concentrations of TRWP in gully-pots (0.8-150 mg/g; Mengistu et al. (2021b)) (Figure 5), thus demonstrating the need for more data to assess the retention potential for gully-pots

Some highways, especially those with high traffic volumes, close to vulnerable recipients or in urban areas, may have different treatment systems for the retention of road runoff (Andersson et al., 2018; Vogelsang et al., 2018). These treatment systems are typically referred to as sustainable urban drainage systems (SUDS), best management practices (BMP) or nature-based solutions (NBS). NBS are currently implemented in several countries, where urban runoff can be treated and utilized as a part of the blue-green infrastructure of the city (Oral et al., 2020). Examples of these are retention basins (constructed wet basins with a permanent water level), detention basins (temporary detention/delay of the release during stormwater events), and different types of ponds (non-constructed) designed to either retain or detain runoff from roads (Meland, 2016; Vollertsen et al., 2019). Previous studies have reported concentrations of 0.0023-130 mg/g of TRWP in the sediment of retention basins (Klöckner et al., 2019; Wik and Dave, 2009) and 0.38-2.0 mg/g TRWP (mean concentrations) in settling ponds (Klöckner et al., 2019). Urban roads may also have drainage systems connected with waste-water treatment plants (WWTP) (Kole et al., 2017). Several studies have investigated the retention of microplastic particles in WWTP and reports suggest that 93-99.9% is retained (Carr et al., 2016; Horton et al., 2017; Mintenig et al., 2014). Only two studies have so far reported mass concentrations of TWP from WWTP, although both of these also demonstrate a potentially high retention. One study reported the mass concentration levels of TWP from the inlet of one WWTP through a whole year, with 45 ± 78 µg/L during normal weather and 300 ± 240 µg/L during heavy rainfall (Vogelsang et al., 2020). However, in the same study, no TWP were detected in the effluent, thus, the retention of tire wear particles was potentially 100% in this WWTP. Another study analysed effluent water from four different WWTPs during both dry and wet weather conditions and reported TWP concentrations of 20 ± 10 µg/L (Parker-Jurd et al., 2021) (Figure 5). Although the inlet concentrations were not assessed in this study, the concentrations of the effluent were lower compared to the reported inlet concentrations in Vogelsang et al. (2020), which indicates that WWTP are capable of retaining TWP. In the case of road runoff entering the WWTP, there is also a potential for tire and road wear particles to re-enter the environment due to the application of biosolids from WWTP to agricultural soil as fertilizers (Hurley and Nizzetto, 2018). In many cases, the

road drainage systems directly lead the road runoff into the nearest recipient, either freshwater lakes, streams, rivers or a marine recipient (Meland et al., 2010a; Rauert et al., 2022). This is also the case for many road tunnels, where only a smaller percentage of these may have treatment systems (Meland et al., 2010a; Meland and Rødland, 2018).

Terrestrial environment

Tire and road wear particles may be retained in the soil, demonstrated by the high concentrations of TWP reported for roadside soils along a highway in Germany (Müller et al., 2022a). Concentrations of TWP were highest 0.2m from the road (18 700 mg/kg, topsoil 0-2cm) (Figure 5) with decreasing concentrations towards 5m distance (1060 mg/kg). The study also reported a decreasing trend for the deeper soil layers (2-10cm depth) compared to the topsoil. Several other studies have also reported TWP concentrations from roadside soils; 0-1m (0.6-158 mg/g), >1m (n.d.-3 mg/g) to <20m (n.d.-0.9 mg/g) (Figure 5), demonstrating that most tire particles are deposited within a few meters from the road (Kumata et al., 2011; Unice et al., 2013). Although no studies have so far reported retention efficiencies for tire and road wear particles in swales, studies have demonstrated high retention capabilities (>70%) for total suspended solids from road runoff (Bäckström, 2002; Bäckström, 2003).

Uptake or retention in organisms

For assessment of environmental impact, it is also necessary to demonstrate the effect that TWP/TRWP has on organisms. Currently there are only a few studies where uptake or retention in the environment has been confirmed with chemical characterisation methods, such as FTIR or PYR-GC/MS (Bråte et al., 2018; Bråte et al., 2020). Several other studies have demonstrated uptake of TWP in experimental lab exposure for both aquatic species (Cunningham et al., 2022; Khan et al., 2019; LaPlaca and van den Hurk, 2020; Redondo-Hasselerharm et al., 2018; Sheng et al., 2021) and terrestrial species (Sheng et al., 2021).

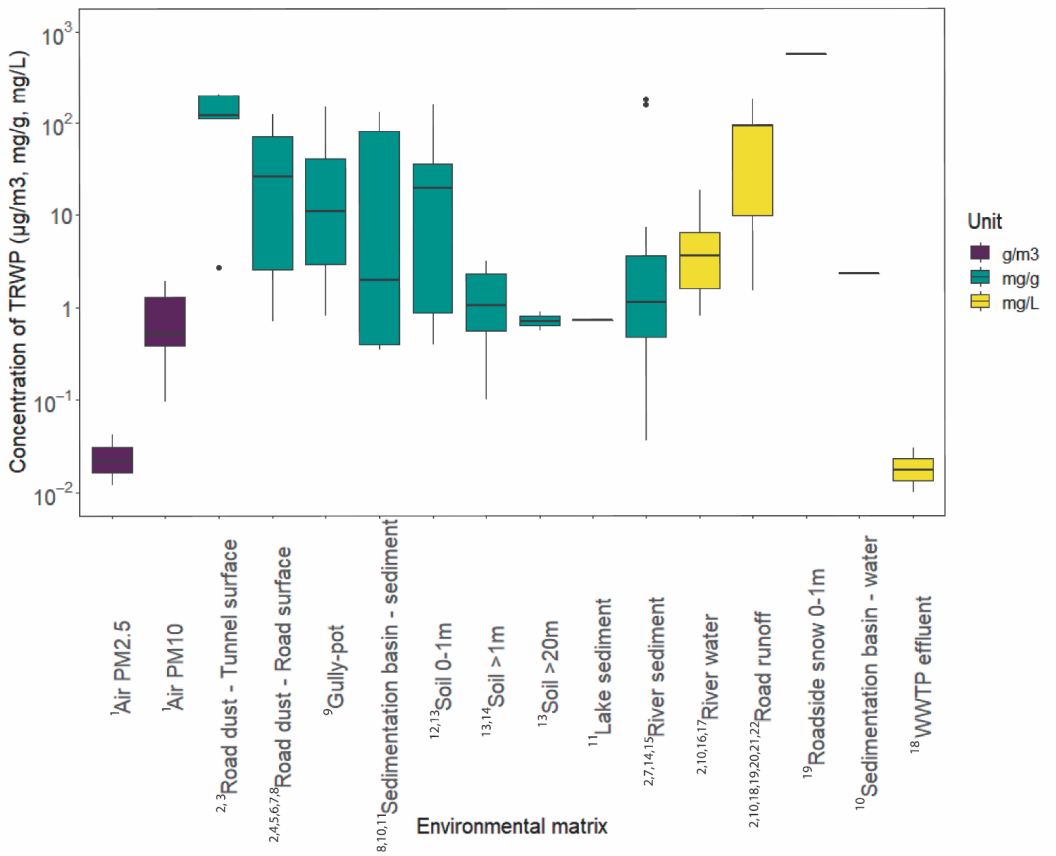

Figure 5: The figure shows a boxplot of TRWP concentrations in the environment, in g/m^3 for air samples, mg/g for solid samples and mg/L for water samples. Each data entry is a mean value, and the figure summarizes several different studies from 1974 – 2022. The figure is based on previously published data 1) Panko et al. (2019), 2) Kumata et al. (2000), 3) Klöckner et al. (2021b), 4) Hopke et al. (1980), 5) Rogge et al. (1993), 6) Kumata et al. (2002), 7) Zakaria et al. (2002), 8) Eisentraut et al. (2018), 9) Mengistu et al. (2021b), 10) Reddy and Quinn (1997), 11) Klöckner et al. (2019), 12) Kocher et al. (2008), 13) Müller et al. (2022a), 14) Unice et al. (2013), 15) Spies et al. (1987), 16) Ni et al. (2008), 17) Rauert et al. (2022), 18) Parker-Jurd et al. (2021), 19) Baumann and Ismeier (1998), 20) Kumata et al. (1997), 21) Kumata et al. (2002), 22) Zeng et al. (2004).

Road wear particles with polymer-modified bitumen

For tire and road wear particles, there are currently no studies reporting the concentrations of road wear particles with polymer-modified bitumen (RWP_{PMB}). However, it is assumed based on particle characterization, that TWP and RWP_{PMB} will have similar pathways from the road surface into the environment due to the similarities in characteristics, such as size and density (Table 1). Therefore, the pathways of tire and road wear particles are described together (Figure 3).

Road markings

The current knowledge on how particles from road markings are transported from the road surface into the environment, and the level of contamination in different matrices, is limited. The first study to report the presence of particles from road marking in the environment was Horton et al. (2017a), however the number of particles in the river sediment was not reported. Another study has reported the number of particles in road sweep sand (up to 10 000 particles/kg), in tunnel wash water (44 particles/L) and in stormwater (38 particles/L) (Järlskog et al., 2020). So far, no studies have reported the mass concentration of road marking particles.

2.5.2 Environmental impact of road-associated microplastic particles

Tire wear particles

For TWP/TRWP, especially zinc (Zn) has been pointed out as one of the toxic compounds to aquatic organisms. Zn has been found to accumulate in high concentrations in fish gills and liver, directly related to acute toxicity, as well as lead to sublethal effects such as reducing the motility of fish sperm (Giardina et al., 2009; Nelson et al., 1994).

In addition to various rubber content in different types and brands of tires, they potentially also contain different additives to accommodate seasonality or regional differences such as UV-exposure or temperature. In fact, more than 214 different organic chemicals have been identified in tires (Müller et al., 2022b), in which 145 compounds were found to be leachable from the tire particles into the environment. Some of these compounds have been found to be harmful to organisms, such as hexa(methoxymethyl)melamine (HMMM), N-1,3-dimethylbutyl-N 0-phenyl-p-phenylenediamine-quinone (6-PPD-quinone), benzothiazoles, aniline, 1,3-diphenylguanidine (DPG) and different polycyclic aromatic hydrocarbons (PAHs) (Brinkmann et al., 2022; Halsband et al., 2020; Marwood et al., 2011; Peter et al., 2018; Seiwert et al., 2020; Tian et al., 2022; Tian et al., 2021; Unice et al., 2015). Both HMMM and 6-PPD-quinone have been related to acute toxicity and mass-deaths of salmon species (coho salmon *Oncorhyncus kisutch*, rainbow trout *Oncorhynchus mykiss*, brook trout *Salvelinus fontinalis*) in North America (Brinkmann et al., 2022; Peter et al., 2018; Tian et al., 2021), and following these initial studies, both compounds and their transformation products have been detected in various environmental compartments across different continents (Cao et al., 2022; Challis et al., 2021; Johannessen et al., 2022; Johannessen et al., 2021; Klöckner et al., 2021b; Rauert et al., 2022; Rauert et al., 2020; Seiwert et al., 2022). Although several studies have replicated the toxicity tests with 6-PPD and 6-PPD-quinone with other species such as Arctic char (*Salvelinus alpinus*), white sturgeon (*Acipenser transmontanus*), zebrafish (*Danio rerio*), water flea (*Daphnia magna*), Japanese medaka (Oryzias latipes), amphipod (*Hyalella azteca*), no acute toxicity was observed with these

species at relevant environmental concentrations (Brinkmann et al., 2022; Hiki et al., 2021; Varshney et al., 2022).

As the data describing toxicity effects for different organisms and the behaviour of these compounds in the environment are still limited, more research is needed to evaluate the true effect of TWP/TRWP on organisms in the terrestrial and aquatic environment. Another aspect which is currently hampered by limited data is the retention of TWP/TRWP particles in organisms. If TWP/TRWP are retained in an organism, for example in the gills, compounds such as HMMM and 6-PPD-quinine could potentially continue to leach from the particles over time until depletion of the particles.

Road wear and road markings

Compared to TWP/TRWP, the current knowledge of environmental conditions and toxicity of RM and RWP_{PMB} is limited. According to estimates, the concentrations of both are expected to be far lower than for TWP. For RWP_{PMB}, the main component is minerals (quartz, feldspar, pyroxene, amphibole, mica), in which current literature does not indicate any toxicity effect related to these. However, the bitumen component contains naphthene acids, which has been found to be both cytotoxic and cause endocrine disruption and has been found to cause adverse effects in both fish and mammals (Headley and McMartin, 2004).

For RM, the density is expected to be lower than for TWP, which might cause it to float more easily and thus be more bioavailable to aquatic organisms than TWP. When it comes to the toxicity, most of the road paint is made of quartz, dolomites and glass beads (70-75%), but it also includes TiO_2, which has been found to cause different adverse effects, such as cell damage, genotoxicity and inflammation (Skocaj et al., 2011). Also, the glass beads that makes up about 40% of the road marking, are mainly made from recycled glass, usually old windows. Many old windows contain lead (Pb), arsenic (As) and antimony (Sb), which can be toxic to organisms (dos Santos et al., 2013).

Mixture toxicity

RAMP are a complex rubber and polymer matrix mixed with minerals, metals and a range of different chemicals. Several of the chemical compounds found in RAMP particles can be acute or chronically toxic to different organisms at different concentrations by themselves. In the environment, RAMP will always be present together with other road-related substances, which also have possible toxic effects, such as Zn (non-tyre related), Cd, Ni, Cu and organic pollutants such as PAH. Recent studies have also shown that alkylated PAHs dominate in sedimentation ponds and are related to DNA damage in dragonfly nymphs (Meland et al., 2019). Previous toxicity studies with road runoff have confirmed that the presence of road salt (NaCl), which is commonly used for de-icing purposes in many countries, increases the toxicity observed in aquatic organisms (Mahrosh et al., 2014; Meland et al., 2010b). This has also been demonstrated for the 6-PPD compound (Klauschies and Isanta-Navarro, 2022), where the toxicity effects caused by 6-PPD in the freshwater rotifer (*Brachionus calyciflorus*) were enhanced by the presence of NaCl. Although the concentrations tested in this study were above the environmentally relevant concentrations, the combination effect of multiple stressors is important to consider, as organisms are not exposed to these organic pollutants as single compounds, but rather in complex mixtures together with high amount of suspended solids, metals, salts and other road-related compounds (Meland et al., 2010b; Meland et al., 2010c; Salbu et al., 2005; Salbu et al., 2019).

It may be difficult to distinguish between the effects of TWP/TRWP, RM, RWP_{PMB} and road runoff in general when assessing environmental toxicity. Also, distinguishing between road-associated microplastic particles, meaning the particles with polymers in them, and other road-associated particles, might well be an artificial and less optimal way of studying road runoff. As seen by the available toxicity studies on TWP/TRWP, the toxicity observed is related to the chemicals and additives associated with the tire particles, and not the rubber content itself.

2.6 Analytical Challenges of Road-associated microplastic particles

2.6.1 Current Analytical Methods of Road-associated microplastic particles

Microplastic particles have typically been analysed as single particles by visual analysis coupled with chemical identification methods such as Fourier-Transform Infrared Spectroscopy (FTIR) or Raman Spectroscopy (Hale et al., 2022). These techniques have proven to be useful for particles down to 10-20 µm in size (Vinay Kumar et al., 2021; Xu et al., 2019). Visual analysis are possible efficient techniques for road marking particles, as these are expected to be >50µm in size, with bright colors and typically also contain glass beads used for reflection (Horton et al., 2017a). However, using infrared spectroscopy to identify the polymer content in black particles, such as potential tire and road wear particles, has been challenging due to absorption of the IR in the black material. Variations in carbon black filler in tires have demonstrated that it is possible to identify some tire particles using FTIR. However, in most cases these potential tire particles cannot be confirmed which results in uncertainty of their true rubber content (Wagner et al., 2018). Thus, other analytical techniques have been explored for tire particles, such as the elemental composition using Scanning Electron Microscopy with Energy Dispersive X-Ray Analysis (SEM-EDX) and laser induced breakdown spectroscopy (LIBS). Additionally, micro-X-ray fluorescence (µXRF) is proposed as a possible analytical approach for tire particles, however, current published literature has so far focused on other microplastic particles, especially paint particles (Table 2).

Another challenge when it comes to analyzing TRWP is the potential large number of particles present in a sample, as well as the mixture of TRWP and pure asphalt or road wear particles making it difficult to choose individual particles to analyze. Due to these challenges, several approaches have been made to analyze the mass of TRWP in samples instead of single particles. The techniques that have been tested by various studies utilize different marker compounds to calculate the mass of TRWP and/or road markings, including techniques such as Inductively Coupled Plasma Mass Spectrometry (ICP-MS), Liquid-chromatography mass spectrometry (LC-MS/MS), TED-GC/MS and PYR-GC/MS (Table 2).

Table 2. Overview of different analytical techniques used to identify and quantify road-related microplastic particles (tire and road wear particles and road marking particles).

Analytical technique	Type of analysis	Marker compound	Reference
Fourier-Transform Infrared Spectroscopy (FTIR)	Specific wavenumbers fingerprints for SBR and BR rubber	SBR+BR	Fernández-Berridi et al. (2006)
Simultaneous Thermal Analysis (STA), Fourier Transform Infra-Red (FTIR), and Parallel Factor Analysis (PARAFAC)	Specific wavenumbers fingerprints for SBR and BR rubber	SBR+BR	Mengistu et al. (2021b); Mengistu et al. (2019)
Raman Spectroscopy	Specific wavenumbers fingerprints for road marking polymers	SBR+BR	Horton et al. (2017b)
Scanning Electron Microscopy with Energy Dispersive X-Ray Analysis (SEM-EDX)	Elemental composition	Zn:S	Kovochich et al. (2021a); Kovochich et al. (2021b); Sommer et al. (2018)
Laser induced breakdown spectroscopy (LIBS)			Lucchi et al. (2021); Prochazka et al. (2015)
Micro-X-ray fluorescence (μXRF)		Zn:S	Leistenschneider et al. (2021)
Inductively Coupled Plasma Mass Spectrometry (ICP-MS)		Zn	Klöckner et al. (2019), Klöckner et al. (2020)
Liquid-chromatography mass spectrometry (LC-MS/MS)	Organic compounds/tire additives	N-formyl-6-PPD, QDI-OH, and 6-PPDQ	Klöckner et al. (2021a)

	Organic compounds/tire additives	Benzothiazoles (benzothiazole, 2-methylthiobenzothiazole, thianaphthene, triphenylene, 2-morpholin-4-yl-benzothiazole, 2-hydroxy-benzothiazole, 2-thio-benzothiazole, 2-methylthio-benzothiazole, and 2-amino-benzothiazole)	Asheim (2018); Asheim et al. (2019); Baumann and Ismeier (1998); Bye and Johnson (2019); Kumata et al. (2000); Kumata et al. (2002); Ni et al. (2008); Spies et al. (1987); Kumata et al. (1997); Parker-Jurd et al. (2021)
Thermal Desorption Gas Chromatography Mass Spectroscopy (TED-GC/MS)	SBR+BR and NR decomposition products	4-Vinylcyclohexene (SBR+BR), Cyclo-hexenyl benzene (SBR) Isoprene (NR),	Eisentraut et al. (2018; Klöckner et al. (2019; Klöckner et al. (2020; Müller et al. (2022a)
Pyrolysis Gas Chromatography Mass Spectroscopy (PYR-GC/MS)	SBR+BR and NR decomposition products	4-Vinylcyclohexene (SBR+BR), Isoprene (NR)	ISO (2017a); ISO (2017b); Panko et al. (2013); Panko et al. (2019); Rauert et al. (2022); (Rauert et al., 2021); Sun et al. (2022); Unice et al. (2012a); Unice et al. (2013); Youn et al. (2021)
	SBR+BR decomposition products	4-Vinylcyclohexene SBB, SB (SBR+BR),	Goßmann et al. (2021); Rauert et al. (202)1
	SBR+BR and SBS decomposition products	Benzene, α-methylstyrene, ethylstyrene and butadiene trimer (SBR+BR+SBS)	Rødland et al. (2022a); Rødland et al. (2022b); Rødland et al., (2022c, accepted April 26th)
Pyroprobe Pyrolysis Gas Chromatography Mass Spectroscopy (PYR-GC/MS)	SBR+BR decomposition products	Benzothiazole	Parker-Jurd et al., 2021)
Gas Chromatography Mass Spectroscopy	Organic compounds/tire additives	Oleamide	Chae et al. (2021

For mass-based analysis, the challenge is finding suitable marker compounds that are reliable for both reference material and environmental samples, stable in different types of matrices and accessible for a high analysis throughput in order to establish environmental concentration levels across different types of matrices. These challenges are currently the main bottle neck for analysis of road-associated microplastic particles. The focus in the research community has been in quantifying tire particles, as they are estimated to be the largest source of microplastics in most part for the world so far (Boucher et al., 2020; Knight et al., 2020). This has resulted in different analytical approaches being tested and reported, where the results are not necessarily comparable between studies. Even within the same analytical technique, different studies are applying different markers and calculations when reporting concentration levels, which makes comparison difficult. The thermal decomposition techniques TED-GC/MS and PYR-GC/MS are similar techniques where the decomposition products from SBR and BR rubber can be used to calculate the amount of rubber present in the sample, which in turn can be used to calculate the amount of tire present. However, current studies are not unified in which of these decomposition products should be used and how calculations from rubber to tire particles should be performed (Goßmann et al., 2021; Miller et al., 2022; Miller et al., 2021; Rauert et al., 2021; Rødland et al., 2022b). Thus, several different methods using TED-GC/MS and PYR-GC/MS are proposed.

For PYR-GC/MS there is also the possibility of applying different types of pyrolyzers, such as the resistive PYR-GC/MS (Miller et al., 2022), Curie point PYR-GC/MS (Miller et al., 2022; Panko et al., 2013; Panko et al., 2019; Unice et al., 2012a; Unice et al., 2013) and the microfurnace PYR-GC/MS (Goßmann et al., 2021; Rauert et al., 2021; Rødland et al., 2022a; Rødland et al., 2022b; Youn et al., 2021). These have different characteristics in terms of how samples are thermally decomposed and how much material can be analyzed for each sample. The differences between them and their accuracy for tire wear particles in environmental samples were assessed by Miller et al. (2022), where the microfurnace type displayed the highest accuracy, followed by the curie point type, whereas the resistive pyrolyzer was reported to be less useful for quantitative analysis.

Another important aspect of mass-based techniques is the limit of detection. For PYR-GC/MS, there is a limit to the mass of rubber (SBR+BR) that can be analyzed in a sample, whereas the lower limit is set as the lowest mass reliably detectable above the signal to noise ratio (S/N). The lower limit reported in previous PYR-GC/MS studies are

between 0.1 and 28 µg SBR (Goßmann et al., 2021; Rauert et al., 2021; Unice et al., 2012b; Unice et al., 2013), however this depends on the background noise present in the sample from the environmental matrix, as well as the sensitivity of the instruments used. These lower limits may therefore vary and should be reported in all studies. For the upper limit of detection, the detector can be saturated to a point where the signal increase is no longer following the calibration curve and the quantification will be affected. For SBR+BR, this level is typically found around 150 µg of rubber in the sample, however, this is also subject to variations caused by the environmental matrix and the instrumental set-up.

3 Experimental details

3.1 Sample collection

3.1.1 Reference material

Tire material for method testing consisted of new, unused tires (n=31) donated by different tire companies through the Norwegian tire recycling organization *Norsk Dekkretur*, which is owned by the tire import companies of Norway. The tires were selected to represent the most used tires in Norway. For personal vehicles a total of 18 tires were analyzed (eight summer tires, five winter tires with studs and five winter tires without studs) and 13 tires for heavy vehicles (one all year tire and 12 summer tires). Samples were collected using ceramic knives with disposable blades (Slice TM), or with taping knives (Ironside TM), using separate blades for each tire to avoid cross-contamination.

For PYR-GC/MS analysis of microplastic particles in road salt (Paper I), 7 reference polymers and 1 rubber were analyzed for quantification: PE (Sigma-Aldrich, St. Louis, MO, USA), Poly (methyl-methacrylate) (PMMA: Sigma-Aldrich, St. Louis, MO, USA), Polystyrene (PS: Sigma-Aldrich, St. Louis, MO, USA), Polyvinylchloride (PVC: Sigma-Aldrich, St. Louis, MO, USA), Polypropylene (PP: NIVA, Oslo, Norway), Polyethylene terephthalate (PET: Goodfellow, Cambridge, UK) and Polycarbonate (PC: NIVA, Oslo, Norway), Styrene butadiene rubber (SBR) (SBR1500: Polymer Source, Quebec, Canada). The internal standards used were deuterated Polystyrene (d5-PS, Polymer Source, Quebec, Canada) and deuterated Polybutadiene (d6-Pb, Polymer Source, Quebec, Canada). For PYR-GC/MS of tire and road-wear particles, the two reference rubbers analyzed for quantification were Styrene butadiene rubber (SBR) (SBR1500: Polymer Source, Quebec, Canada) and Styrene butadiene styrene (SBS) (Kraton D: Nynäs AB, Norway).

3.1.2 Environmental samples

Snow samples were collected as snow cores (Figure 6) using a metal snow corer (inner diameter 4.2cm, NIVA, 2019) in snowbanks at approximately 0m (0-1m), 1m (1-2m) and 3m (3-4m) m from the road. From each snowbank, 5-10 cores were collected, depending on the height of the snow. Samples were collected in zip-lock bags (Polythylene (PE)) and kept frozen until analysis.

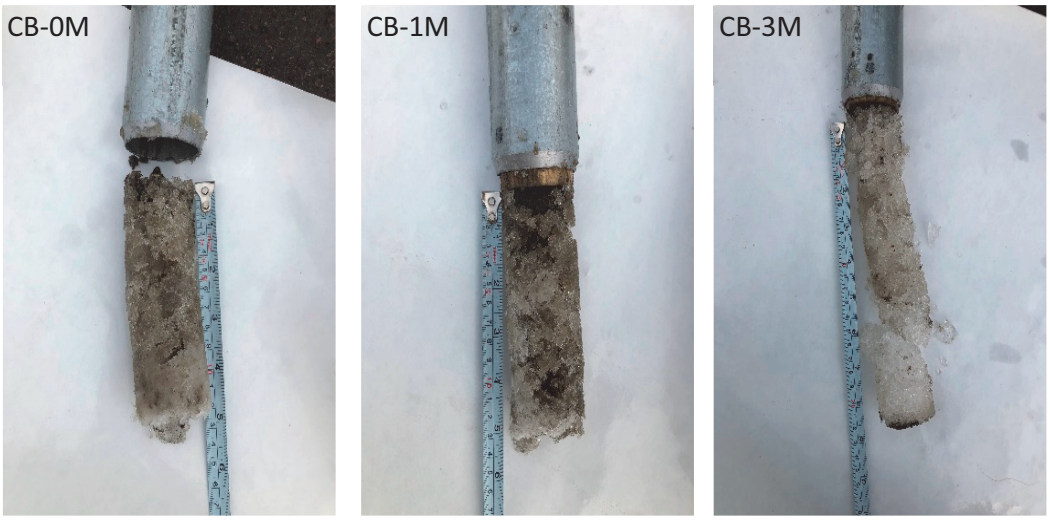

Figure 6. Snow cores collected at Carl Berner (Oslo, Norway) at 0m, 1m and 3m distance from the road. Photos: E. Rødland)

Tunnel samples were divided into four categories: 1) road surface samples collected with a Wet Dust Sampler (WDS; Lundberg et al. (2019), Figure 7), 2) gully-pot sediment collected with a small van Veen grab and 3) untreated tunnel wash water (TWW) collected in the pump house with a small drain pump submerged in the water column and 4) treated TWW collected directly from the outlet to the raingarden.

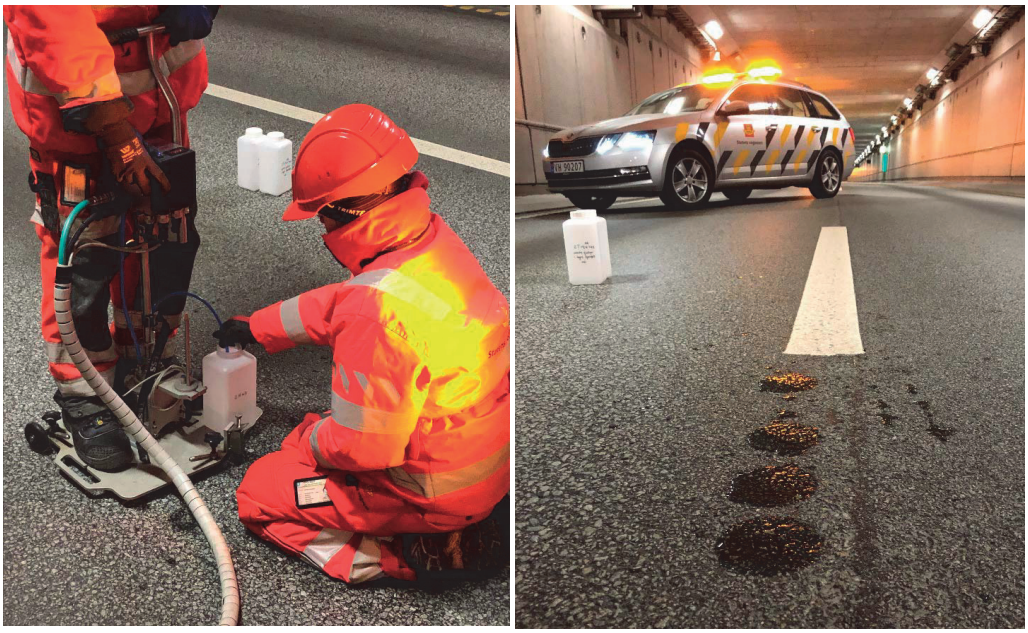

Figure 7. Sampling of tunnel road dust in the Smestad tunnel (Oslo, Norway) using the Wet Dust Sampler (left image: WDS; Lundberg et al. (2019)). Four consecutive areas were sampled for each location, leaving a wet stain on the road surface (right image). Sampling method is described in detail in Paper IV (Photos: E. Rødland)

3.2 Treatment of samples

All samples were either treated as a solid sample (snow, gully-pot sediment, soil and tire material) or as a water sample (road surface wet dust sample, tunnel wash water (Figure 8).

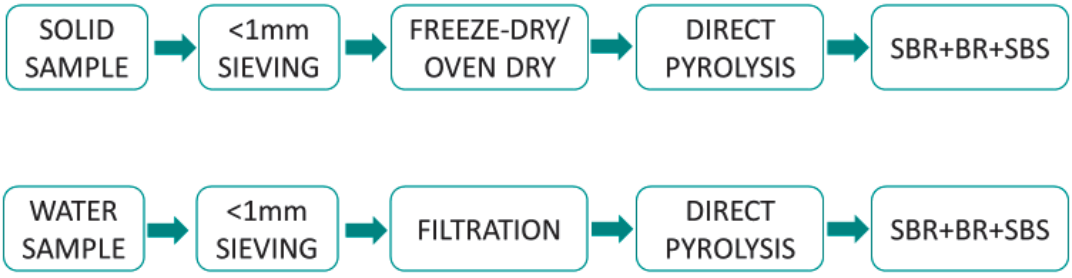

Figure 8. Schematic illustration for the pretreatment process of samples before analysis. (Illustration: E. Rødland)

Snow samples were thawed, sieved (<1mm pore size) and subsampled (16mL). The subsamples were re-frozen and freeze-dried (Figure 9A). Gully-pot sediments were freeze-dried and dry-sieved (<1mm). Roadside soil was oven dried and dry-sieved (<1mm). Dry samples were weighed directly into pyrolysis cups on a microbalance. Water samples (WDS, tunnel wash water) were filtered through a 1mm sieve onto glass fiber filters (GF-F, 1.6 µm pore size, 13mm diameter, Whatman) (Figure 9B). Glass fiber filters were dried in a muffle furnace and weighed before filtration. After filtration, the filters were dried in room temperature for 24 hours and weighed. The volume filtered and total mass of particles retained on the filter was registered. The filter was then rolled and inserted into the pyrolysis cup (Figure 9C).

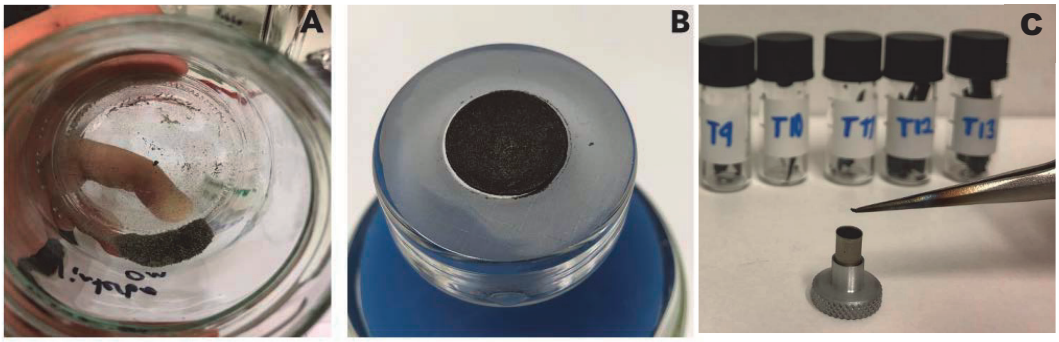

Figure 9. Free-dried snow sample (A), filtered tunnel wash water (B) and reference tire tread (C). (Illustration: E. Rødland)

3.3 Analytical approach

3.3.1 Microplastic analysis – Fourier Transform Infrared Spectroscopy

Road de-icing salt samples were analyzed using FTIR. The largest fragments (>200µm, longest axis) were analyzed with single point measurement Attenuated Total Reflectance - Fourier Transformed Infra-Red Spectrometry (ATR-FT-IR) using a Cary 630 FT-IR Spectrometer (Agilent). The particles <200µm (longest axis) and all fibers were analysed with a FT-IR diamond compression cell in µ-transmission using a Spotlight 400 FT-IR Imaging system (Perkin Elmer) (Figure 10). The particles were analysed with the full wavelength of the FT-IR (4000–600 cm^{-1}) and resolution of 4 cm^{-1}. The libraries used to identify the polymers were the Agilent Polymer Handheld ATR Library and the Elastomer O-ring and Seal Handheld ATR Library for the analysis done on the ATR. For the µFT-IR the reference database from Primpke et al. (2018), the Perkin Elmer ATR Polymer Library and three inhouse reference libraries for rubbers, reference polymers and non-plastic particles were used for identification. For all analyses, the spectra were manually inspected and only the matches of 0.6 and above were accepted.

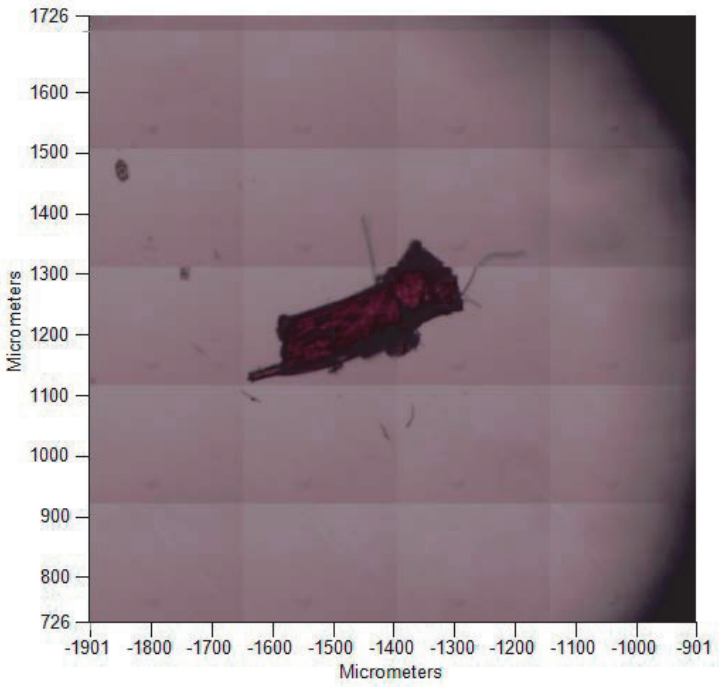

Figure 10. Polypropylene fragment (0.915 match score) from rock salt, analyzed with µFTIR. (Photo: E. Rødland)

3.3.2 Microplastic analysis – Pyrolysis GC/MS

All samples were analysed with a Multi-Shot Pyrolyzer (EGA/PY-3030D) equipped with an Auto-Shot Sampler (AS-1020E) (Frontier lab Ltd., Fukushima, Japan) coupled to gas chromatography mass spectrometer (GC/MS) (5977B MSD with 8860 GC, Agilent Technologies Inc., CA, USA) (Figure 11). The pyrolysis markers used for quantification of SBR+BR+SBS rubber from TWP and RWP_{PMB} were *benzene* (mz 78), ***α**-methylstyrene* (mz 117), *ethylstyrene* (mz 118) and *butadiene trimer* (mz 91). The method and instrument settings are described in detail in Paper II.

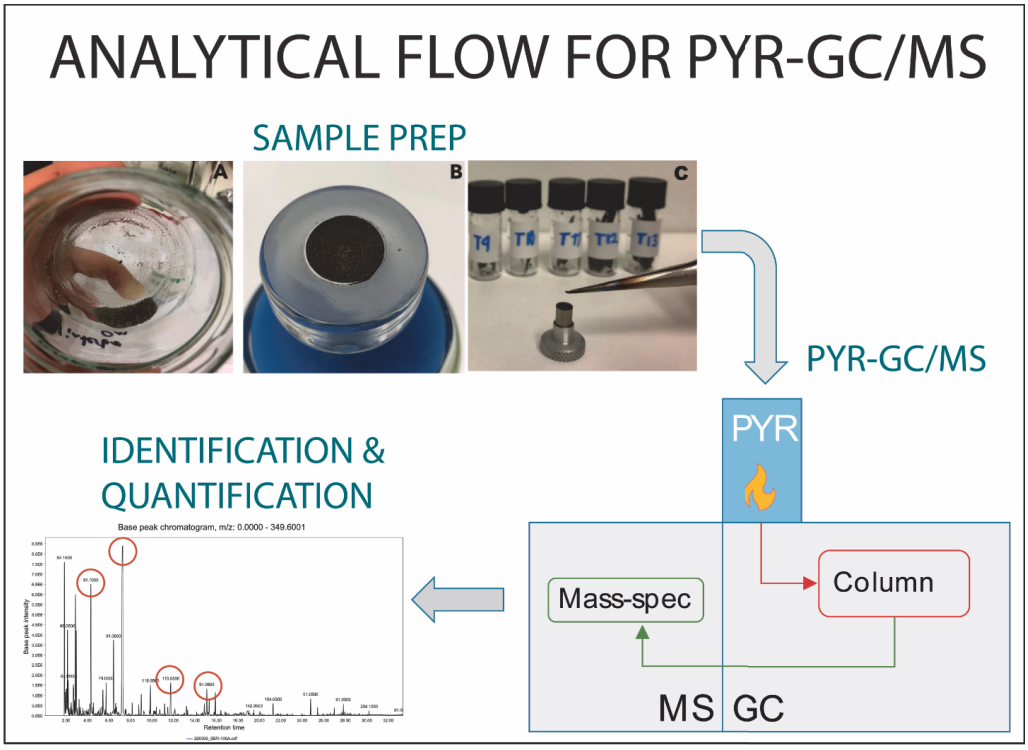

Figure 11. Schematic illustration of the analytical method flow for PYR-GC/MS used for papers I, II, III & IV (Illustration: E.Rødland)

3.4 Statistical methods

3.4.1 Univariate statistics

The statistical analysis of the data was conducted in RStudio 1.3.109 (Team, 2020), R version 4.0.4 (2021-02-15), specifically using the ggplot2-package (Lai et al., 2016) (gplot2_3.3.3), the car-package (Fox J and Weisberg S . A, 2019) and the dplyr-package (Wickham et al., 2018) for creating boxplot graphs (Papers I, II, II, IV), linear regression (paper III and IV) and for performing Analysis of Variance (ANOVA) (paper III and IV).

All ANOVAs were performed on log-transformed data. The assumption of normal distribution of residuals was tested using Andersen-Darling normality test. If the assumption of normality was not met, ANOVA was still applied when number of samples (n) in each group were >15. The assumption of equal variance was tested using Levene's Test of Homogeneity of Variance. Whenever this assumption was not met, Welch's one-way ANOVA was used. The statistically significant level was set to p=0.05.

Linear regression was used to assess the relationship between total suspended solids (TSS) and total concentration of rubbers (Papers III and IV). The residuals of the regression model were checked for normality using Andersen Darling Normality test. If assumption of normality was not met, the linearity was tested using assumption free Redundancy analysis (RDA) combined with Monte Carlo permutation tests, with rubber concentration as response variable and TSS concentration as the explanatory variable (see more details about RDA in Ch.3.4.2).

3.4.2 Multivariate statistics

Redundancy analysis (RDA) was used to explore the observed variation in response variables using explanatory variables (Papers I, III, IV), which are then tested with Monte Carlo permutations for significance. All multivariate statistical analyses were conducted in Canoco 5.12 (Braak and S̃milauer, 2018). In Paper III, the dataset was log-transformed by the default transformation setting in Canoco. Two variants of RDA were tested in Paper III. First, a constrained RDA with all variables were performed to explore the total variation

explained by all identified variables. Second, RDA with forward selection was tested, where the explanatory variables contributing the most to the variation can be selected until there is no more variation to explain. In the forward selection mode, both the simple effects (the effect of each independent variable) and the constrained effects (the effect of the variable considering the other variables) were tested. In Paper IV, Aitchison-weighted-log-ratio-RDA (Aitchison, 1983; Greenacre and Lewi, 2009) was performed on the particle size distribution in tunnel wash water. This variant of RDA is useful when analysing weighted data, for example compositional data such as percentage, where the sum of the multiple response variables adds up to 1. The use of log-ratios, the logarithm of pairwise ratios of the components, ensures that the data is "sub-compositional coherent", meaning that the removal or addition of any of the components does not change the result of the others. The use of weighted data ensures that log-ratio RDA is also "distributionally equivalent", meaning that any of the components could be merged or separated without this affecting the distance between samples in the RDA (Greenacre and Lewi, 2009). The significance level in the RDA is derived by Monte Carlo permutation tests (4999 permutations performed). For all tests, $p<0.05$ is set as the level of significance.

3.4.3 Monte Carlo-based prediction modelling

The TWP and RWP_{PMB} concentrations reported in Papers II, III and IV were calculated and predicted by Monte Carlo Simulation (Crystal Ball Add-In, Microsoft Excel), according to the method described in Paper II. The TRWP concentrations were calculated and predicted according to the method described in Paper IV. Monte Carlo simulations are a series of probability simulations that can be used to estimate the likely outcomes from an uncertain event based on a range of input data. In Monte Carlo simulations, a model is built based on the dependent variables that will be predicted and the input variables that will drive the prediction. The input variables are assigned a probability distribution (such as normal distribution, uniform distribution or other) and the outcome of the model is recalculated multiple times using random values within the minimum and maximum range of the model. This results in a predicted outcome of the model, generate the statistical outputs such as mean, standard deviation, median, minimum, maximum, confidence interval and more. The model is typically run for

thousands or more times to increase the statistical power of the model. The application of Monte Carlo predictions allows for; 1) reduction of uncertainties related to variable input data, such as the large variation in rubber content of commercial tires, by predicting the likely outcome and the range of possible outcome values, and 2) assessment of the remaining uncertainty, such as the predicted standard deviation, and which input data drives the uncertainty of the model (sensitivity analysis).

For the prediction of TWP (the dependant variable) in Papers II, III, IV, the input variables were the concentration of SBR+BR+SBS rubbers that was measured in a sample and the specific percentage of personal vehicles (PV) and heavy vehicles (HV) for the sample location. The ratio of SBS calculated for the specific sample was applied with a probability distribution (triangle distribution). In Papers II and III, a logistic probability distribution of the SBR+BR concentration in personal vehicles and heavy vehicles from the reference tire dataset was assigned by the Crystal Ball application as the best fit and used for the model predictions. However, the distribution generated a large range of predicted values within the minimum and maximum values, which were unrealistic (negative minimum values) and large standard deviations (100-200%) from the predicted mean. For Paper IV, normal distribution was chosen for both the PV and the HV dataset, which resulted in more realistic minimum and maximum TWP values, and a predicted standard deviation of 9.4% for all samples.

For the RWP_{PMB} prediction (Papers II, III and IV), the dependant variable PMB was calculated by the input variable SBR+BR+SBS and with the SBS ratio (triangle distribution). The model was run 100 000 time. For the calculation of TRWP (Paper IV), the input variables were the predicted concentrations of TWP and the probability distribution of mineral encrustment (triangle distribution). All simulations were run 100 000 times.

4 Results

4.1 Investigating potential new sources to Road-associated Microplastic Particles

Paper I: Road de-icing salt: Assessment of a potential new source and pathway of microplastic particles from roads

According to the estimates, the main sources of microplastic contamination from roads and traffic are TWP/TRWP, RW_{PMB} and RM. However, in the Scandinavian countries, as well as in the US and Canada, large quantities of road salt are applied to roads during winter for de-icing purposes. Previous studies have demonstrated that both sea salts and rock salts used for food applications may contain high concentrations of microplastic particles. In Paper I, microplastic contamination in road-deicing salt was quantified and the possibility of road de-icing salt as an additional source of road-related microplastic contamination was assessed.

The road salts tested were sea salts from two sites in Tunisia and one site in Spain as well as one rock salt from Germany. ATR-FT-IR, μFT-IR and PYR-GC-MS were employed to identify and quantify the polymer content in these four types of road salts. The particle number of MP in sea salts (range 4-240 MP/kg, mean ± s.d. = 35 ± 60 MP/kg and rock salt (range 4-192 MP/kg, 424 ± 61 MP/kg) were similar, whereas MP mass concentrations were higher in sea salts (range 0.1-7650 μg/kg, 442 ± 1466 μg/kg) than in rock salts (1-1100 μg/kg, 322 ± 481 μg/kg). The results from FTIR demonstrated the impact of carbon black on the analysis. Black rubber-like particles (BRP) constituted 96% of the total concentration of microplastics (Figure 12) and 86% of all particles in terms of number of particles/kg. A subset of the BRP was analysed with both ATR-FT-IR and μFT-IR, however, no chemical identification was possible due to absorption of the infrared light caused by carbon black. The FTIR libraries included particles with carbon black and all of the BRPs tested had a match (>0.7) with these. Although vehicles are used at all the production sites, the shape and morphology of most of the BRPs did not match that of tire wear particles from previous studies. Another possibility would be that these are wear particles

from conveyer belts. All the production sites use conveyer belts for the transport of salt, and many of these are made of carbon black-reinforced PVC. This was further supported by the results from the PYR-GC/MS, where 77% of the total microplastic particle mass quantified were PVC. In this 77% we also would find other possible PVC particles that are not part of the BRPs. However, the results from the FTIR showed that the presence of other microplastic particles in the sample only contributed 4% of the mass, and included polyethylene terephthalate (PET), polyvinylchloride (PVC), nitrile butadiene rubber (NBR), polyethylene (PE), polypropylene (PP), polyurethane (PUR), acrylic (A), epoxy resin (ER), ethylene propylene (EP) and polyester epoxide (PEE). Thus, the contribution from non-black PVC in the salt samples should be very low compared to the PVC particles attributed to BRP. In addition to the suggestion that black PVC particles originate from conveyer belts, some of the BRPs are also likely tire wear particles, as 4% of the mass volume reported with PYR-GC/MS were styrene butadiene rubber (SBR) which mainly originate from vehicle tires. The results from PYR-GC/MS also reported the mass concentrations of PE (13% of the total mass of polymers), PET (5%), PP (0.6%) and polystyrene (PS) (0.3%) in the samples. Road salt contribution to MP on state and county roads in Norway was estimated at 0.15 tonnes/year (0.003% of total road MP release), 0.07 tonnes/year in Sweden 0.008%) and 0.03 tonnes/year in Denmark (0.0004-0.0008%) Thus, microplastics in road salt is a negligible source of microplastics from roads compared to other sources.

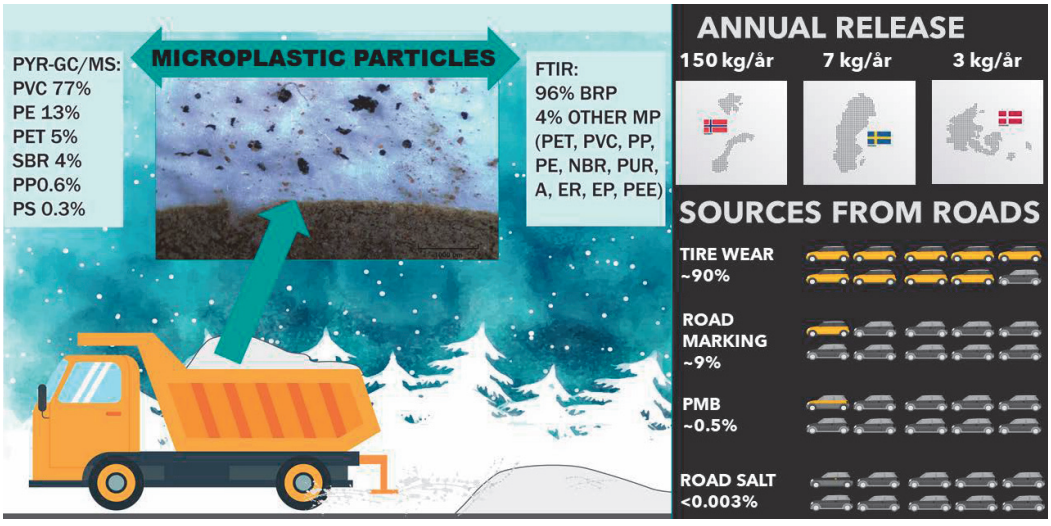

Figure 12. Graphical summary of the main findings of Paper I.

4.2 Development of a validated, mass-based quantification method for tire and road wear particles in environmental samples

Paper II A Novel Method for the Quantification of Tire and Polymer-modified Bitumen Particles in Environmental Samples by Pyrolysis Gas Chromatography Mass Spectroscopy

Tire and road wear particles may constitute the largest source of microplastic particles in the environment. However, the quantification of these particles are associated with large uncertainties due to inadequate analytical methods. In this study we presented a new method for quantifying tire and road wear particles in environmental samples based on synthetic rubbers and applying PYR-GC/MS. The study confirmed that SBR rubber from TWP and SBS rubber from RWP_{PMB} in road asphalt were indistinguishable by PYR-GC/MS. The proposed method therefore applies multiple pyrolysis marker compounds to measure the combined mass of these rubbers in samples.

The presented method also includes an improved step of calculating the amount of tire and road wear particles based on the measured rubber content from PYR-GC/MS, by applying site-specific traffic data and Monte Carlo simulation (Figure 13). First, the predicted tire and road wear concentrations are calculated with emission factors for each location. The emission factors for tire wear related to the driving pattern (highway driving, urban driving) and the percentage of personal and heavy vehicles is used for the calculations, where a concentration of tire wear particles is estimated. From this, the expected concentration of SBR+BR at the site is reported. The emission factors for road abrasion are related to the different road surface types (stone mastic asphalt, asphalt concrete), the percentage of personal and heavy vehicles, and the use of studded and non-studded tires. From the mass of road wear particles, the mass of RWP_{PMB} and subsequently SBS can be estimated. By comparing the concentrations of SBR+BR and SBS from the location, the expected ratio between them is calculated. This ratio is applied to the concentration of SBR+BR+SBS in order to separate SBR+BR from SBS. For the Monte Carlo simulations, the rubber content of relevant reference tires is applied together with the expected ratio of rubber from RWP_{PMB} in order to predict the likely concentration of TWP and RWP_{PMB} in a sample. This approach makes it possible to

quantify the uncertainty related to variable rubber content in tires. The method provided good recoveries of 83-92% for a simple matrix (tire tread) and 88-104% for a complex matrix (road sediment). The validated method was applied to urban snow, roadside soil and gully-pot sediment samples. Large variations in the concentrations of TWP were reported, from 0.1-17.7 mg/mL (snow) to 0.6 – 68.3 mg/g (soil/sediment). Large variations were also reported for the concentration of RWP_{PMB}, from 0.03-0.42 mg/mL (snow) to 1.3-18.1 mg/g (soil/sediment).

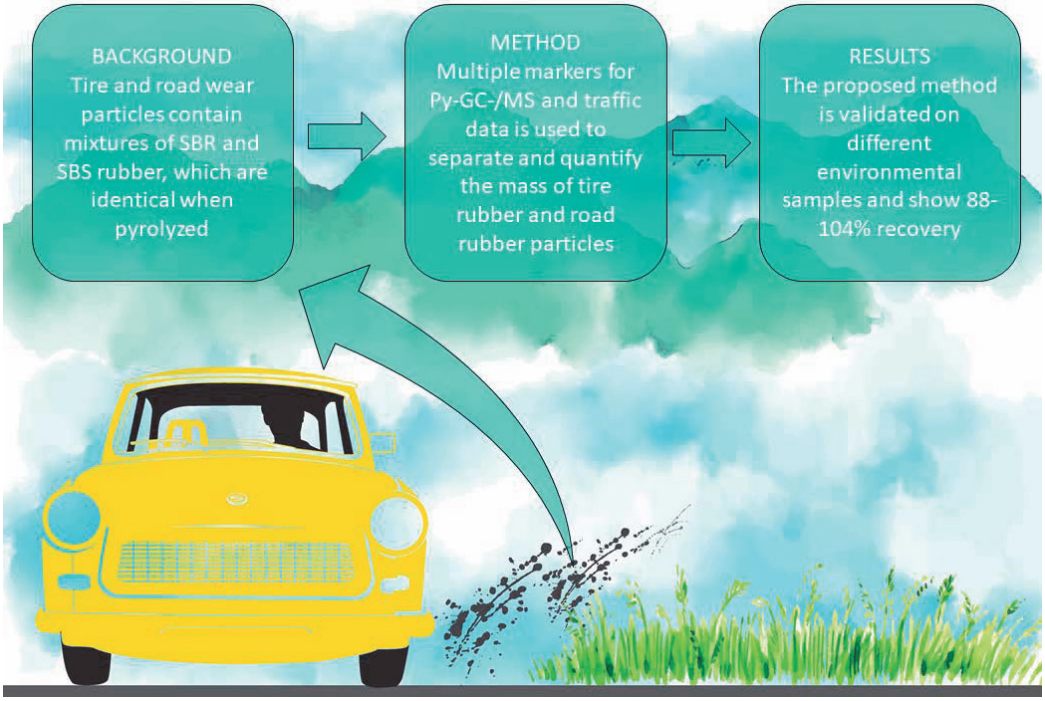

Figure 13. Graphical summary of the main findings of Paper II.

4.3 Assessment of the concentration level of tire and road wear particles in different road compartments

Paper III: Occurrence of tire and road wear particles in urban and peri-urban snowbanks, and their potential environmental implications

Available data on local emissions and transport of tire and road wear particles into environmental compartments are associated with large uncertainties, which highlights the need to provide more and reliable data on inventories and fluxes of these particles. This paper focused on providing mass concentrations and snow mass load of TWP and RWP_{PMB}, which to our knowledge is the first study to do so. Roadside snow and meltwater from three different road types (peri-urban, urban highway and urban) were collected using a snow corer and a multiple sample approach, and then analysed by PYR-GC/MS. The analytical method and calculation method used are described in Paper II.

The concentration of TWP and RWP_{PMB} in the roadside snow were reported as meltwater concentrations in mg/L and as mass load concentrations in mg/m^2. The mass load concentration is calculated from the snow depth and snow density, and is useful when comparing levels between different sites, such as snow that has frozen and thawed at different rates. Across all sites, the TWP concentration varied greatly, from 76 mg/L to 14 500 mg/L for meltwater (Figure 14), and from 222 mg/m^2 to 109 000 mg/m^2 for mass load. The reported mass concentrations far exceeded the levels previously reported for roadside snow and road runoff (3-563 mg/L). Large variations were also observed for the RWP_{PMB} concentrations, from14.8 mg/L to 9550 mg/L in meltwater and 50.0 mg/m^2 to 28 800 mg/m^2 in meltwater, as the results from the present paper provides the first mass concentrations of RWP_{PMB} in environmental samples. The combined mass percentage of TWP and RWP_{PMB} compared to the total mass of particles (TSS) were 5.7% (meltwater) and 5.2% (mass load). This demonstrates that although the concentration of TWP and RWP_{PMB} were high compared to previous studies, roadside snow contains a high concentration of particles, in which most of these particles are not attributed to RAMP. The large variation between sites in the study was investigated using redundancy analysis (RDA) of the possible explanatory variables. Contradictory to previous road studies, speed limit was found to be one of the most important variables explaining the variation in mass concentrations, whereas Annual Average Daily Traffic (AADT) was found to be

less important compared to traffic speed. Other statistically significant explanatory variables in addition to speed and AADT were road types, distance from the road and the combination of speed*AADT. All identified variables explained 69% and 66%, for meltwater and mass load concentrations, respectively. The results show that roadside snow contain total suspended solids in concentrations far exceeding release limits of tunnel and road runoff, as well as tire particles in concentrations comparable to levels previously reported to cause toxicity effects in organisms. These findings strongly indicate that roadside snow should be treated before release into the environment, especially in urban areas and areas with higher speed limits.

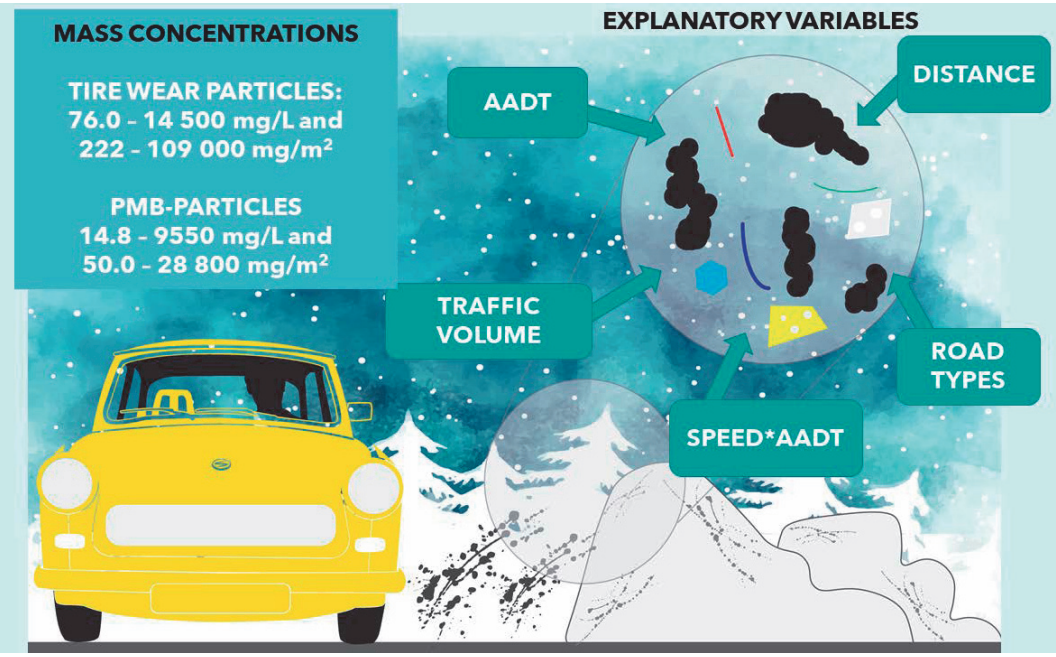

Figure 14. Graphical summary of the main findings of Paper III.

Paper IV: Tire and Road Wear Microplastic Particles in a Road Tunnel System: from surface to release

Road tunnels are known as pollution hotspots and the environmental impacts of pollutants in discharge of tunnel wash water to nearby water recipients have been studied for decades. The use of road tunnels for pollution studies are ideal, because they are semi-closed systems, and the accumulation of pollutants makes it possible to study these over a time-period. In this study we aimed to explore the distribution of TWP, RWP_{PMB} and TRWP in different tunnel compartments such as road surface, gully-pots and tunnel wash water, as well as the treatment efficiency of tunnel wash water before release to the environment.

The analytical method and calculation method used were described in Paper II. The present study also aimed to contribute an improved method for calculating the mass of tire and road wear particle agglomerates (TRWP) using previously published data on TRWP mineral content and Monte Carlo simulation.

The average mass percentage of TWP, RWP_{PMB} and TRWP compared to the total particle mass did not differ substantially between the tunnel compartments (Figure 15). The average percentage of TWP, RWP_{PMB} and TRWP compared to the total mass of particles were 1.8%, 1.5% and 2.7% at the road surface, 2.2%, 1.7% and 3.1% in the gully pots, 2.1%, 1.7% and 3.0% in the untreated TWW and 2.5%, 2.0% and 3.6% in the treated TWW, respectively. However, the concentration of TWP, RWP_{PMB} and TRWP at the road surface was significantly higher in the side bank area (TWP: 13.4 ± 5.67, RWP_{PMB}: 9.39 ± 3.96; TRWP: 22.9 ± 8.19 mg/m^2) and the outlet area (TWP: 7.72 ± 11.2, RWP_{PMB}: 5.40 ± 7.84; TRWP: 11.2 ± 16.2 mg/m^2) compared to the other surface areas, suggesting that these are important areas for accumulation. The mass percentage of TWP, RWP_{PMB} and TRWP were higher in the bank area (3.8%, 3.0% and 5.5%) and the outlet (6.4%, 5.1% and 9.2%) compared to the average level. The highest percentage contribution from TWP, RWP_{PMB} and TRWP of all the tunnel compartments were also reported from the tunnel outlet. This confirms that these areas have a higher affination towards TWP, RWP_{PMB} and TRWP particles compared to other road surface areas of the tunnel. A similar pattern was found in the gully pots. The gully pot closest to the tunnel inlet (GP-1) had the highest concentration of TWP, RWP_{PMB} and TRWP compared to the other gully pots, with concentrations of 24.7 ± 26.9 mg/g, 17.3 ± 48.8 mg/g and 35.8 ± 38.9 mg/g,

respectively. The mass percentage of TWP (5.4%), RWP_{PMB} (4.3%) and TRWP (7.8%) were also higher in GP1 compared to the other gully pots. For the tunnel wash water, the mass percentage of TWP, RWP_{PMB} and TRWP did not change substantially from the untreated (TWP 2.1%, RWP_{PMB} 1.7% and TRWP 3.0%) to the treated TWW (TWP 2.5%, RWP_{PMB} 2.0% and TRWP 3.6%), although there was a small increase in the percentage for the treated water. As the sedimentation treatment only retained 63% of the TWP, RWP_{PMB} and TRWP particles and as much as 69% of the total particles in the tunnel wash water, the small change observed for the mass percentage might indicate that the sedimentation treatment is better suited for other road particles than the microplastic-related particles, removing more of these at the same time as close to half of the TWP, RWP_{PMB} and TRWP particles were not retained. The concentrations of TWP, RWP_{PMB} and TRWP were 38.3 ± 10.5, 26.8 ±7.33 and 55.3 ±15.2 mg/L in the untreated TWW and 14.3 ± 6.84, 9.99 ±4.78 mg/L and 20.7 ±9.88 mg/L in the treated TWW, respectively. The relationship between the total particles (TSS) and the rubbers from TWP and RWP_{PMB} (SBR+BR+SBS) were also explored, and a strong linear relationship (R^2-adj=0.88, $p<0.0001$) was established. This strong relationship indicates the possibility of using TSS for monitoring the road-associated microplastic particles in future studies.

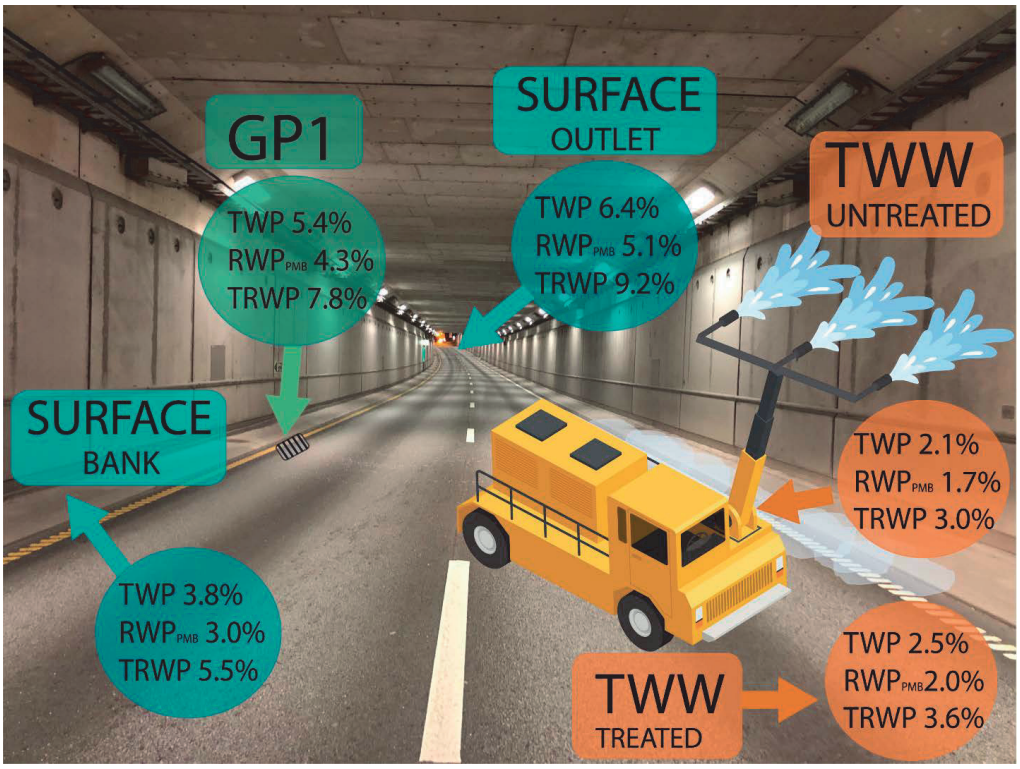

Figure 15. Graphical summary of the main findings of Paper IV. The figure shows the mass percentages of tire wear particles (TWP), road wear particles with polymer-modified bitumen (RWP_{PMB}) and tire and road wear particles (TRWP) compare to total mass of particles for the road surface side bank area (BANK), the road surface outlet area (OUTLET), the inlet gully pot (GP1), the tunnel wash water before treatment (TWW UNTREATED) and the tunnel wash water after treatment (TWW TREATED).

5 Discussion

5.1 Sources of road-associated microplastic particles

The current available literature suggests that the three main sources of microplastic particles (MP) to the environment from roads and traffic are derived from wear of tires, road surface and road marking (Sundt et al., 2021; Sundt et al., 2014; Sundt et al., 2016; Vogelsang et al., 2018) , and these are defined as road-associated microplastic particles (RAMP) as they originate from sources purposely used on roads, such as vehicle tires (Vogelsang et al., 2018). The results from Paper I demonstrate that road de-icing salt is also a source of MP. Although the contribution of MPs from road salt was insignificant compared to the other three sources of RAMP in Norway, it is still a source of contamination that needs to be addressed. Paper I focused on the high road salt consumption in Scandinavia, however, high salt consumption is also observed in several other countries in Europe, such as Germany (700 000 tonnes/year, 2018/2019), Austria (400 000 tonnes/year, 2018/2019) and Ireland (200 000 tonnes /year, 2018/2019) (CEDR, 2019) (Figure 16). For comparison, the consumption in Norway in the same season (2018/2019) was 320 000 tonnes/year (CEDR, 2019). Other parts of the world also report high road salt consumptions, such as in the US (22 million tonnes/year, (Kelly et al., 2019; Schuler and Relyea, 2018)), Canada (7 million tonnes/year, (CE, 2012))) and China (600 000 tonnes/year, (Ke et al., 2013; Li et al., 2014b)). The salt consumption in the US and Canada are comparable to Norway when adjusting for total road length, with approximately 5 tonnes of salt per kilometer road. Due to increasing temperatures during winter (de Coninck et al., 2018), there will be more days with freezing and thawing, which increases the need for road de-icing salts to prevent ice-formation on the road surface. Thus, the release of MPs due to road salt should also be addressed in other countries where the use of road salt is an important part of the winter road maintenance. The reported MP concentrations and MP types did not differ significantly between sea salts produced from marine water and rock salt produced in salt mines. The results in Paper I indicate that the main contamination of these salts is contributed by the production, packaging and transportation, which should be addressed by the salt industry in order to reduce the MP contamination in salts.

Recent studies have also identified and quantified other MP in various samples related to road pollution, such as urban runoff and stormwater (Monira et al., 2022; O'Brien et al., 2021). One study has compared the mass concentrations of TWP/TRWP to other MP in road and environmental matrices, where the mass of TWP far exceeded the mass of other MPs present in road samples (Goßmann et al., 2021). The results from these previous studies demonstrate that TWP/TRWP are the dominating source of microplastic particles in road dust, and that TWP/TRWP are also present in different environmental matrices. They also demonstrate that road compartments are contaminated with MPs from different sources, not just the road-related sources.

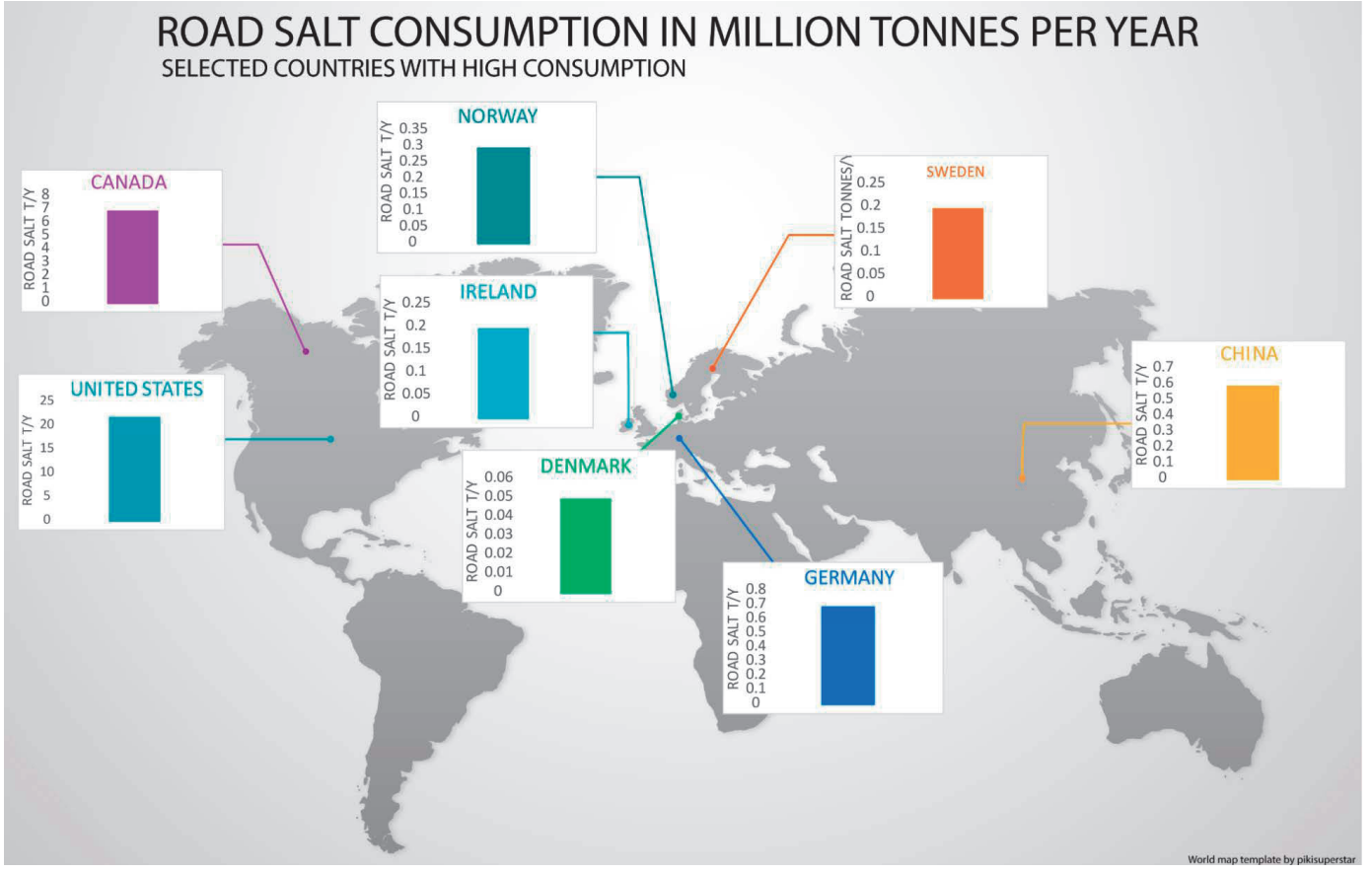

Figure 16. Map showing the yearly road salt consumption (million tonnes per year (t/y)) for selected countries with high consumption (CE, 2012; CEDR, 2019; Ke et al., 2013; Kelly et al., 2019; Li et al., 2014b; Schuler and Relyea, 2018). (Illustration: E. Rødland, map template by freepik/pikisuperstar)

5.2 Method Harmonization and Uncertainties

5.2.1 Sampling of road-associated microplastic particles

After defining the specific research questions in a project, ensuring representative sampling is the next, and perhaps most important step. Without relevant and representative sampling, our data and results will not be useful even with the most accurate methods available. Hence, sampling should be specific for the research questions, the matrices investigated and the sample locations of interest. Previous studies of road pollution have described different sampling strategies, such as multiple increment sampling for soil samples (Hadley and Petrisor, 2013; Aaneby and Johnsen, 2019) and for snow piles (Vijayan et al., 2021), where multiple samples are collected from a defined area and then mixed as composite samples before subsampling for analysis. As demonstrated by the snow samples, the increased number of samples resulted in decreased variance, and the use of composite samples yielded lower variation compared to discrete samples (Vijayan et al., 2021).

The sampling strategy of composite samples was applied in Papers I-IV. For the road salt samples (Paper I), multiple samples were collected from the piles of salt at the distribution site (sea salt from Zarziz and Ben Gardene, Tunisia) and collected as a composite sample. The soil samples tested in Paper II were initially collected for analysis of general road pollution with the multiple increment strategy (Aaneby and Johnsen, 2019). For snow samples (Paper III), the snow piles were collected with a snow corer from top to bottom, and 5-10 snow cores from each snow pile were collected as composite samples. This strategy is in line with the proposed snow pile sampling by Vijayan et al. (2021). For the road surface samples (Paper IV), samples were collected with the Wet Dust Sampler (WDS II), by flushing high pressurized water onto the road surface and collecting the water with the road particles in a sample bottle. This method has been validated for sampling road dust from the road surface in several studies (Asheim, 2018; Asheim et al., 2019; Gustafsson et al., 2019; Järlskog et al., 2020; Lundberg et al., 2019; NPRA, 2017). A recent publication (NPRA, 2021b) also demonstrated that to be able to collect 90% of particles <180µm and 60% of particles 180-5000 µm, a minimum of three samples (sample shots) from the same surface area is needed. Thus, both the sampling equipment and the sampling strategy are important for sampling the road surface, and

without harmonization between studies it will be difficult to compare results. For the gully-pot samples (Paper IV), the samples were collected with a small van Veen grab, and multiple grab samples from the same gully pot were mixed before subsamples were collected. For studies of tunnel wash water, previous studies have typically been sampled by manually collecting multiple subsamples for each time period and pooling these together. In Paper IV, the tunnel wash samples before treatment were collected with a drain pump suspended in the water column and the samples after treatment were collected directly from the outlet pipe. Both sample types were collected in time intervals. Compared to previous studies where samples have been collected at the beginning, middle and end of a wash event (Meland and Rødland, 2018), the approach used in Paper IV with continuous samples over a time scale could provide more information on the change of concentrations of pollutants through the tunnel wash and through the release of treated water. Another aspect which would increase the sample strength is sampling multiple occasions, which was demonstrated in recent studies of road runoff (Parker-Jurd et al., 2021). In many cases there is a need to adjust the number of samples analyzed for cost reasons. According to the research questions in each project, it is therefore necessary to assess if the questions are best answered by high resolution (multiple samples) for a limited number of sample events or low resolution (limited samples) for multiple sampling events. The use of multiple increment samples is useful in reducing the number of samples per sampling event. As demonstrated by the various sampling procedures chosen by different studies, there is an urgent need for standardization of sampling procedures for different road matrices, with evaluation of sampling equipment and number of samples needed.

5.2.2 Analytical methods of road-associated microplastic particles

One of the challenges of describing the environmental impact of MPs, including tire wear particles, is knowing what the relevant environmental concentrations are. Thus, reliable and comparable quantification methods must be developed so that these levels can be assessed across different studies in time and space, and between different environmental compartments. The need for harmonized methods for MP has been argued by several researchers (Provencher et al., 2020; Rochman et al., 2017), stating that both harmonization and validation of methods are essential for the scientific progress of microplastic research (Lusher et al., 2021). Harmonization is not only needed

for the analytical part, it also needs to be included in the experimental set up, the sampling and sample treatment procedures, as well as data reporting and criteria for publishing (Cowger et al., 2020; Hale et al., 2022; Provencher et al., 2022). Some efforts have been launched to unify the research community and agree on analytical methods for microplastics in general, such as the ongoing Horizon2020 project EUROqCHARM (https://www.euroqcharm.eu/en). There are also efforts made to unify the analytical methods for tire wear with the European TRWP Platform (https://www.csreurope.org/trwp), where both governments and the research community meet and discuss challenges and future perspectives. The International Organization for Standardization (ISO) has also published two technical specifications for quantifying TWP/TRWP in soil/sediment and air samples with PYR-GC/MS (ISO, 2017a; ISO, 2017b) based on the methods described in Unice et al. (2012b). However, the number of studies on TWP/TRWP has increased exponentially over the last decade and several different analytical methods for TWP/TRWP have been published, as described in detail in chapter 2.6.2. Comparison between different studies and methods is necessary to assess the environmental impact, however, comparisons between studies using different analytical methods should be done with careful consideration. The current literature on both snow and road runoff have quantified TWP using different benzothiazoles (BTs) as marker compounds (Baumann and Ismeier, 1998; Kumata et al., 2000; Kumata et al., 1997; Kumata et al., 2002; Parker-Jurd et al., 2021; Reddy and Quinn, 1997). However, it has been demonstrated that BTs ability to transform during different environmental conditions impacts their reliability as marker compounds (Asheim, 2018; Bye and Johnson, 2019; Zhang et al., 2018), thus the reliability of the mass concentrations put forward by these studies needs to be addressed. In the study of Wik and Dave (2009), total zinc (tot-Zn) was used as the marker in surface runoff water. The use of tot-Zn as a marker for tire wear has been debated due to the presence of other Zn sources (galvanized steel construction, road surface) in the road environment (Blok, 2005; Councell et al., 2004; Unice et al., 2013; Wagner et al., 2018)). Other studies have proposed organic Zn (org-Zn) as potential markers for tire wear (Fauser et al., 1999; Klöckner et al., 2019), although the reliability of org-Zn as a marker for TWP has also been questioned due to difficulty in extracting the org-Zn from TWP in samples (Unice et al., 2012a; Unice et al., 2013). Recent studies demonstrated that tot-Zn can be a reliable maker when used in combination with density separation to target the TWP/TRWP

fraction in the sample (Klöckner et al., 2019; Klöckner et al., 2020). Density separation is, however, difficult due to the wide range in density (1.2-2.1 g/m^3) reported for TWP/TRWP (Jung and Choi, 2022; Kayhanian et al., 2012; Klöckner et al., 2021b). (Jung and Choi, 2022; Kayhanian et al., 2012; Klöckner et al., 2021b) Density separation is further complicated when there is RWP_{PMB} present in the sample, as these might increase the density in the higher end of the density scale due to the high content of road asphalt (2.4 g/cm^3) and mineral particles (2.7 g/cm^3). A recent study also suggests improvements to density separation by removing asphalt particles from the mixture of road dust samples by dissolving the bitumen with chloroform (Jung and Choi, 2022).

Although PYR-GC/MS has been validated as a sensitive and reliable analytical approach for tire wear (Miller et al., 2022), there is uncertainty between the different markers proposed for PYR-GC/MS, including the markers proposed by Paper II and markers proposed by other studies (Goßmann et al., 2021; Unice et al., 2012a). Thus, current methods recommended by the ISO and by the research community should be discussed in an open, international forum and recommendations for "best practice" methods should be made. Different methods may be considered "best practice", depending on the sample matrix and the research questions at hand.

The method presented in Paper II, builds on the previous methods put forward by ISO, however, there are considerable differences that contribute new perspectives to the analysis of tire and road wear in environmental samples. The method in Paper II applies four different pyrolysis products in combination *(benzene + **α**-methylstyrene+ ethylstyrene + butadiene trimer*) as the marker for SBR+BR rubber, whereas previous methods in general apply only one marker to quantify SBR+BR, as well as including marker for NR (Unice et al., 2012a). Previous studies have reported that heavy vehicle tires contain mainly NR, which supported the inclusion of NR in the quantification methods. However, this has been disputed in recent studies (Rauert et al., 2021), where substantial concentrations of SBR+BR was also reported for heavy vehicle tires. Thus, both personal and heavy vehicle tires can be quantified based on the SBR+BR concentrations alone. Another reason for excluding NR from the quantification methods is the possible interference from plant material in environmental samples, as both NR and plant material produce dipentene (polyisoprene) when pyrolyzed (Eisentraut et al., 2018). The presented method in Paper II have therefore focused on markers for quantifying SBR+BR+SBS.

By applying multiple markers, the variation observed in commercial tires were reduced to <40% s.d. (115 - 682 µg/mg, n=31) compared to large variation (62-85% s.d.) observed for the single markers (4-VCH, SB dimer and SBB trimer) (Goßmann et al., 2021; Unice et al., 2012b). For studies applying mass-based methods such as PYR-GC/MS, the use of reliable pyrolysis markers with low variability is crucial. This has been discussed as a major issue when it comes to analysing tire particles, as different pyrolysis products have displayed large variations in different reference tires tested (Rauert et al., 2021; Rødland et al., 2022b). The major impacting factor causing variability is the different microstructures in the composition of SBR and BR rubber, which can cause variability in the pyrolysis products (Choi, 2001; Choi and Kwon, 2020; Miller et al., 2021). The use of different types of SBR in tires, such as emulsion-SBR and solution-SBR has a been brought to attention in Paper II, as well as previous literature (Miller et al., 2021). Another important aspect is the need to address how aging of tire particles in the environment impacts the SBR+BR content and the pyrolysis products used as marker compounds (Wagner et al., 2022). For TWP/TRWP, both abiotic (photooxidation, thermo-oxidation, leaching) and biotic factors (microbial degradation) could cause the particles to change their physico-chemical structure, such as leaching of chemical additives causing depletion of the particles over time, as well as breaking the particles into smaller sizes with time (Wagner et al., 2022). These changes might be the main drivers behind environmental harm, as potentially toxic chemicals such as HMMM and 6-PPD-quinone are leached out to the environment (Peter et al., 2018; Tian et al., 2021). It might further affect the identification and quantification of TWP/TRWP in environmental samples, if the environmentally impacted tire particles contain a different chemical profile compared to tire particles created in lab-conditions, such as road simulator particles or cryo-milled particles. Other aspects of importance are how the rubber materials potentially differ in aged tire particles compared to pure rubber or new tires, which could also impact how tire particles are quantified using thermal desorption methods such as PYR-GC/MS or TED-GC/MS. Fungi and bacteria present in the environment, especially in soils, have been found to degrade rubber material (Sarkar B. and S., 2020; Wagner et al., 2022), after antioxidants and other components added to protect tires from degradation have leached out (Marchut-Mikołajczyk et al., 2019). This might also impact the identification and quantification of TWP/TRWP in the terrestrial environment. For future studies, aging should also be considered for SBS rubber in RWP_{PMB}. The presence of SBS rubber in

environmental samples has so far only been addressed for Norwegian roads (Papers II, III and IV), however, several countries such as Australia, the United Kingdom, Russia, Denmark and Sweden apply PMB asphalt on roads with high traffic volume (EAPA, 2018). As various polymers and rubbers, not just SBS can be applied, it is important to investigate the presence of SBS in the road surface before analysing samples for SBR+BR. SBR and SBS have identical pyrolysis products, as well as BR sharing overlapping products with SBS, so without separation between SBR+BR and SBS, TWP/TRWP concentrations will be overestimated in a sample that contains both. The method presented in Paper II proposes a calculation method to separate between SBR+BR and SBS to avoid overestimation of TWP/TRWP as well as report the concentrations of RWP_{PMB} for roads were PMB is applied to the road surface.

5.2.3 Prediction modelling of tire and road wear particles

Previous studies have calculated the mass of TWP based on the assumption that all tires contain 50% SBR+BR (ISO, 2017a; ISO, 2017b; Unice et al., 2013) and the mass of TRWP based on the assumption that all tire and road wear particles contain 50% tire and 50% minerals (Kreider et al., 2010; Unice et al., 2013). This approach, however, does not take into account the large variability of SBR+BR content in different commercial tires (Goßmann et al., 2021; Rauert et al., 2021; Rødland et al., 2022b) nor the variability of mineral encrustment reported by literature (Klöckner et al., 2020; Klöckner et al., 2021b; Kreider et al., 2010; Sommer et al., 2018). The previous methods have not addressed the issue of SBS rubber present in samples from RWP_{PMB} either, which would impact the calculated concentration of both TWP and TRWP. The improved method proposed for prediction of TWP and RWP_{PMB} concentrations applying Monte Carlo simulation (Paper II) reduces the uncertainty related to assuming a fixed ratio of rubber present in all tires, as well as calculating the concentration of RWP_{PMB} also present in the sample by separating between SBR+BR and SBS. This allows the uncertainty related to reported mean values to be evaluated and communicated. The variation of the predicted TWP values is mainly influenced by the large variation of SBR+BR content in the PV tires (96.8%, Crystal ball sensitivity analysis), which underlines the need for relevant and reliable reference tires. The estimated SBS rate contributes 2.4% to the variation, whereas the SBR+BR variation in HV tires only contributes 0.8% of the variation. For the PMB

particles, the variation of SBS reported in PMB asphalt is low compared to the variation in tires because the input data has a lower variance and the model is only influenced by the SBS ratio for Smestad (100%, Crystal Ball sensitivity analysis), and therefore the % predicted standard deviation of RWP_{PMB} concentrations is lower (11%).

For the TRWP, current literature suggests that urban roads with lower speed limits and lower traffic density have a high percentage of encrusted particles (>73%, Klöckner et al. (2020)) compared to highways with higher speed limits and higher traffic density (<10%: Sommer et al. (2018); 25%: Klöckner et al. (2021b)). Increased speed limit and traffic density increases the distance a tire wear particle is transported from the point of release (Gustafsson et al., 2009; Rødland et al., 2022a), thus, decreasing the potential mixing with mineral particles from the road surface. Since the mineral encrustment of TRWP exists in a range and not a fixed ratio (Klöckner et al., 2021b; Kreider et al., 2010; Sommer et al., 2018), a new method for calculation of TRWP using the same Monte Carlo principles as for RWP_{PMB} were suggested (Paper IV). However, as the range of mineral encrustment is based on only three published studies, there is a substantial uncertainty related to the calculation of TRWP. Even so, the use of Monte Carlo prediction modelling based on published data gives the opportunity for presenting the TRWP values as predicted mean values with standard deviations and communicating the uncertainty related to these calculations at the same time. The variation of predicted TRWP concentrations were influenced by the variation in mineral encrustment (100%, Crystal Ball sensitivity analysis) and displayed an overall standard deviation of 14.2% for all samples.

The use of Monte Carlo simulations for predicting the expected TWP, RWP_{PMB} and TRWP concentrations in the sample is promising and the models can be improved by increasing the data available for relevant reference tires and the data for road abrasion for PMB-roads. For TRWP, there is a need to generate more data on mineral encrustment, including the impact on mineral content by different variables such as driving conditions (highway, urban, rural), traffic speed, the use of studded tires and different types of road surfaces. As the input variable in the TRWP model is the predicted TWP values, the TRWP model is also subject to the variations in tire reference data. Thus, improving both the data available for mineral encrustment and SBR+BR content in relevant reference tires will improve the prediction of TRWP.

Another aspect not mentioned in any previous literature is how road wear particles with polymer-modified bitumen interact with and impact the TRWP. In Papers II, III and IV, TWP and RWP_{PMB} particles are reported and discussed as separate particles. This is mainly because there is not enough research available on how these particles interact with each other in the environment. To fully understand the transport mechanisms and the possibilities with mass-based analysis, more research is needed on the impact of PMB particles on TRWP.

5.3 Environmental impact of road-associated microplastic particles

5.3.1 Environmental concentrations

The results presented in the work of Papers III and IV contributes data on the levels of tire and road wear particles in the environment. The TWP concentrations in roadside snow (Paper III) far exceeded previous studies of TWP (Figure 17) in both snow (Baumann and Ismeier, 1998) and runoff (Baumann and Ismeier, 1998; Kumata et al., 2000; Kumata et al., 1997; Kumata et al., 2002; Parker-Jurd et al., 2021; Reddy and Quinn, 1997; Wik and Dave, 2009). This demonstrates that snow piles left on the sides of the road can accumulate tire wear over time and potentially pose a higher acute release risk to the environment compared to road runoff. This is also in line with previous research on other road pollutants in snow, such as metals and PAH (Viklander, 1996).

The concentrations of TWP/TRWP in tunnel road dust (Paper IV) also exceeded previously reported concentrations for both tunnel dust collected by pressure washer and wet vacuum cleaner (Klöckner et al., 2021b) and road dust outside tunnels collected by road sweepers (Klöckner et al., 2020). Comparing the concentrations of rubbers (SBR+BR), the levels found for tunnel dust (Paper IV) were also 40 times higher compared to street dust collected as road runoff (Eisentraut et al., 2018). These results suggest that the accumulation of tire wear on the road surface is higher inside tunnels compared to outside of tunnels. One possible reason why higher concentration of tire and road wear are observed inside the tunnels is that the tunnels are semi-closed. This inhibits particles from entering the atmosphere by winds and turbulence from the traffic, and the side

areas of the road, as it would do outside of the tunnel. Close to the inlet and outlet of the tunnel there may be some particles that would end up on the outside due to the turbulent air created by traffic, however, it is more likely that particles kept in suspension will be transported with the direction of traffic through the tunnel due to air being forced through by the traffic ("piston effect", Moreno et al. (2014)). This is further supported in Paper IV, where the concentrations of tire and road wear particles were significantly higher on the road surface by the outlet compared to the inlet and middle areas of the tunnel. Another possible explanation for the observed differences is the sampling techniques. The WDS applied in Paper IV is a validated method for collecting particles accumulating on the road surface, and especially efficient for particles <180µm trapped in the road macrostructure (NPRA, 2021b). However, previous studies have demonstrated that even with the WDS, multiple samples from the same surface area are needed to collect all particles present on the surface. Other studies of road dust have applied different sampling equipment and sampling strategies. However, evaluation of which method is preferable is hampered by the fact that different methods have not been compared to each other on the same road surface.

For the gully-pots, the sediment had TWP/TRWP concentrations presented in Paper IV comparable to concentrations from gully-pots from municipality roads (Mengistu et al., 2021a) and comparable to levels reported in sediment from a road runoff treatment (Klöckner et al., 2019). These results show that gully-pots are capable of retaining tire and road wear particles, in contradiction to previous assumptions (Blecken, 2016; Vogelsang et al., 2018). However, it should be stressed that the retention efficiency of gully-pots was not assessed in Paper IV, and future research should include retention experiments for gully-pots to assess their efficiency as treatment options for RAMP.

The levels of TWP/TRWP in the untreated tunnel wash water were comparable to TWP/TRWP levels in road runoff (Baumann and Ismeier, 1998) and runoff (Baumann and Ismeier, 1998; Kumata et al., 2000; Kumata et al., 1997; Kumata et al., 2002; Parker-Jurd et al., 2021; Reddy and Quinn, 1997; Wik and Dave, 2009), although significantly lower compared to the roadside snow reported in Paper III. Paper III and IV are also currently the only publications reporting levels of RWP_{PMB}, and the highest levels found in the untreated tunnel wash were 4 times lower compared to the highest levels found for roadside snow. The average concentrations of total rubbers (SBR+BR+SBS) in the tunnel wash water after 21 days with sedimentation treatment was reduced by 63% (69% for

total suspended solids, TSS). This demonstrates that sedimentation treatment can retain tire and road wear particles. It should, however, be noted that the retention in this current treatment system was lower than what was expected for sedimentation basins from previous studies of TSS and road pollution (Garshol et al., 2015; NPRA, 2021a; Nyström et al., 2019)). The untreated and treated tunnel wash water was also analyzed for the presence of potential nanosized particles. As the initial samples for Paper IV were filtered onto 1.6µm GF-filters, the remaining water samples passing through were collected in bulk, subsampled and filtered again with 0.7µm GF filters (unpublished results from the work of Paper IV) and analyzed with PYR-GC/MS. For the untreated tunnel water, the concentrations of TWP and RWP_{PMB} particles <1.6µm were 0.18 mg/L and 0.14 mg/L, respectively. For the tunnel water that had been subject to treatment, the concentrations of TWP and RWP_{PMB} were reduced by 22% (14 mg/L) and 14% (0.12 mg/L), respectively. The results demonstrate that there are nanosized tire and road wear particles present in the tunnel wash, with substantially lower retention by sedimentation treatment compared to RAMP.

For both the tunnel wash water and the snow samples, the relationship between TSS and the SBR+BR+SBS rubber was explored. The linear relationship was strongest for the tunnel wash water (adjusted R^2= 0.88, p <0.0001) compared to the snow (R^2-adj =0.48, p<0.0001), although both datasets indicate possibilities for applying TSS as a proxy for monitoring SBR+BR+SBS, TWP/TRWP and RWP_{PMB} in future studies.

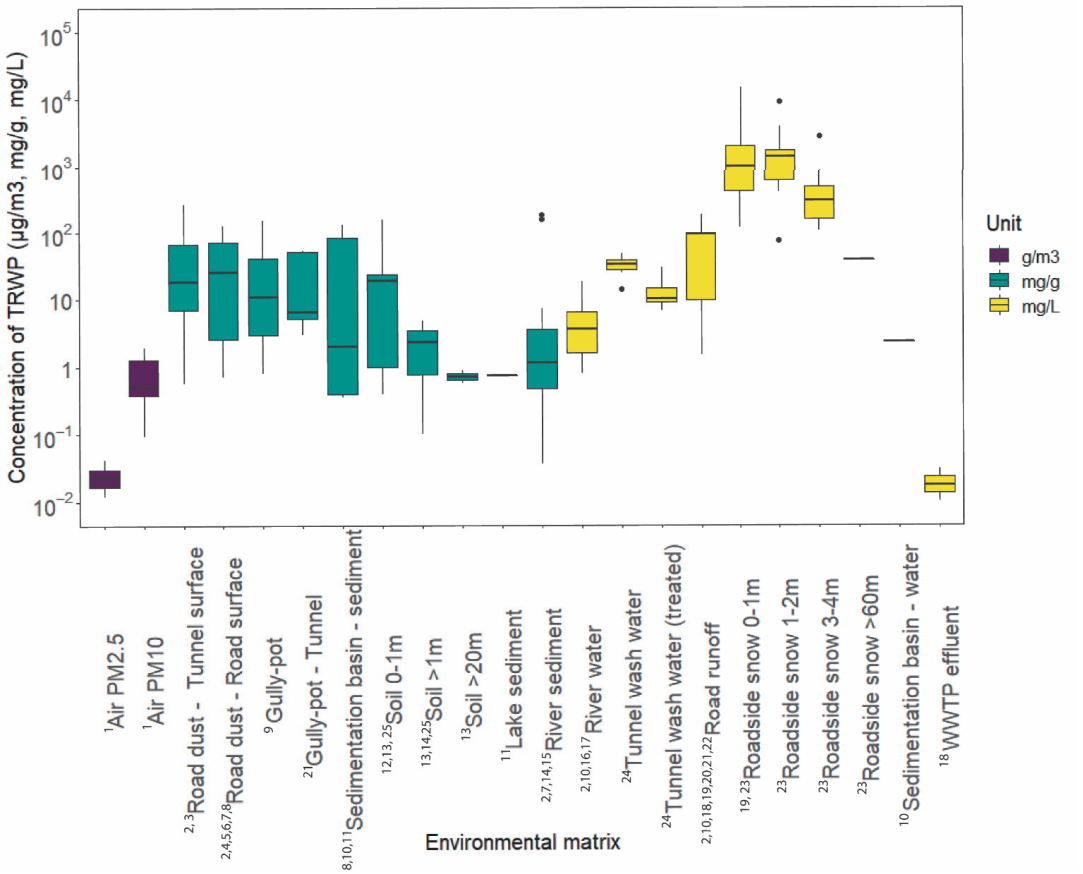

Figure 17: The figure shows a boxplot of TRWP concentrations in the environment, in g/m^3 for air samples, mg/g for solid samples and mg/L for water samples. The figure summarizes previously published data (Figure 5) and the data presented in this thesis (papers I, II, III and IV), from 1974-2022. Each data entry is a mean value. 1) Panko et al. (2019), 2) Kumata et al. (2000), 3) Klöckner et al. (2021b), 4) Hopke et al. (1980), 5) Rogge et al. (1993), 6) Kumata et al. (2002), 7) Zakaria et al. (2002), 8) Eisentraut et al. (2018), 9) Mengistu et al. (2021b), 10) Reddy and Quinn (1997), 11) Klöckner et al. (2019), 12) Kocher et al. (2008), 13) Müller et al. (2022a), 14) Unice et al. (2013), 15) Spies et al. (1987), 16) Ni et al. (2008), 17) Rauert et al. (2022), 18) Parker-Jurd et al. (2021), 19) Baumann and Ismeier (1998), 20) Kumata et al. (1997), 21) Kumata et al. (2002), 22) Zeng et al. (2004), 23) Rødland et al. (2022a), 24) Rødland et al. (2022b), 25) Rødland et al., (2022c, accepted April 26th)

5.3.2 Exploring the variation of road-associated microplastic particles

To assess the environmental fate of RAMP and possible mitigations, it is crucial to understand which variables are related to the production of RAMP. Previous studies have identified the Annual Average Daily Traffic (AADT, v/d) as one of the main drivers behind the variation of road-related pollutants in roadside soil (Werkenthin et al., 2014), road dust (Gunawardena et al., 2015), roadside snow (Li et al., 2014a; Moghadas et al., 2015; Viklander, 1999) and in tunnel wash water (Meland and Rødland, 2018). As the number of vehicles increases, the release of both exhaust and non-exhaust pollution, such as the abrasion of tires and the road surface, increases. For roadside snow (Paper III) AADT was found to be less important for explaining the large variation of SBR+BR+SBS concentrations. The main explanatory variable was the road type, where the urban highway road (13 600-58 500 v/d, speed limit 70 km/h) and the city urban road (6000-14 100 v/d, 40-50 km/h) explained more than half of the combined variation, followed by the speed limit, the distance from the road, the combination of AADT and speed limit, and then the AADT. The peri-urban road type, dominated by highway driving (12 200-71 300 v/d, 80 km/h) was not a significant variable. As the urban road types were the most dominant factors, this suggests that the characteristics of these roads are important, such as traffic lights, crossings, roundabouts and other obstacles. Although AADT as a factor by itself was found to be less important compared to road types, speed and distance, AADT is an important part of the characteristics of the different road types and should still be considered an important explanatory variable in combination with other variables. The different road types may also have different practices for road maintenance, such as different snow handling. Especially in the city, there is less available space for snow storage on the sides, so snow tends to be transported and stored at certain areas where there is available space. The importance of snow handling for pollution load has also been discussed in previous publications (Viklander, 1998).

For the road dust, gully-pots and tunnel wash water, only one tunnel was assessed (Paper IV), thus, exploration of traffic variables was not possible. However, the results for both the tunnel road surface and the gully pots demonstrated that tire and road wear particles accumulate in different parts of the tunnel. For the road surface, the highest concentrations were observed at the side bank area close to the tunnel walls. This is in line with previous studies of road pollution in tunnels (NPRA, 2017; NPRA, 2021b) and highlights the importance of removing the accumulated road dust in these areas before

washing the tunnel walls. For the road surface, the highest concentrations were observed in the outlet of the tunnel, which was in contradiction to previous studies of tunnel road dust (NPRA, 2017; NPRA, 2021b), and in contradiction to the results for gully-pots in the same tunnel, where the concentrations in the inlet were significantly higher compared to the outlet. One possible explanation for the observed pattern for both road surface and gully pots is the impact of runoff from the outside of the tunnel. The inlet of the tunnel is at the highest point of the tunnel, so the runoff from road surface outside the tunnel will likely flow into the gully-pots at the inlet area. The runoff entering the inlet area of the tunnel may also remove part of the tire and road wear particles from the road surface as it flows past and into the gully pots. This was also supported by observation, were the middle and outlet gully-pots had drier sediment.

5.4 Identified gaps for future research

Although there has been an increasing number of studies assessing the concentration levels and fate of RAMP in different compartments the last 5-10 years, there is still a need to improve the current knowledge. Published studies have mainly focused on assessing TWP/TRWP, as demonstrated by number of published environmental science papers with the words "tire wear", "tyre wear" or "TRWP" in the search fields (title, abstract, key words) increasing from the first published article in 1975 to 125 articles in 2021and 29 articles published so far in 2022 (April 12th, 2022) (Figure 18, Clarivate (2022).

Future research needs to include assessments RWP_{PMB} and RM in environmental samples as well. For yearly emission estimates it is also important to enhance the data available on abrasion of different types of road surfaces, especially with RWP_{PMB} present. There is currently also a general lack of knowledge on other microplastic particles (MP) present in road-associated environmental compartments, and to fully assess the levels of contamination and how the MPs impact the quantification of RAMP, these should also be assessed.

One of the key gaps that need to be filled in future studies is the harmonization of methods used for assessing RAMP. The current limitation of data is partly hindered by inadequate and/or non-harmonized data, which makes comparison between studies difficult. There is a need for the research community working with RAMP to agree on

standardized methods for sampling different road matrices, with evaluation of sampling equipment and sampling procedures. There is also an urgent need for standardization of analytical methods for different road matrices. The analytical methods for TWP/TRWP put forward by the International Organization for Standardization (ISO, 2017a; ISO, 2017b) as a technical specifications needs to be evaluated (Rauert et al., 2021) and currently available methods for identification and quantification (section 2.6.2) need to be assessed and evaluated for future standardized methods. Future research should also focus on improving the analytical methods for plastic nanoparticles, including nanoparticles from tire wear and road wear, to address the true impact on the environment from these particle types.

As a part of the future standardization of analytical methods, efforts should also be made to create a reference database for tires, where tires could be classified based on the countries/regions where they are used, if they are used for different seasons, personal vehicles, buses, trucks, motorcycles, electric vehicles or other classifications. The database should be openly available for all researchers and could potentially include a range of data for identification and quantification of rubber content and other relevant components, such as elemental composition and additives.

For tire-related additives and leachates, future research should continue the work on toxicity studies for different organisms, as well as assessing the levels of these in different environmental compartments. Uptake and retention of RAMP in organisms also need to be assessed by both laboratory studies and environmental conditions. Relevant environmental levels are needed to assess the level of impact on organisms, and to date most toxicity studies have predated the studies quantifying the level of TWP/TRWP and tire leachates in the environment.

For mitigation measures, there is a need to evaluate the retention efficiencies for particles and leachates in different types of treatments, such as different sedimentation treatments, filter treatment and gully-pots. For this to be possible, both sampling and analytical methods should be harmonized, so that comparisons can be made between different countries and continents.

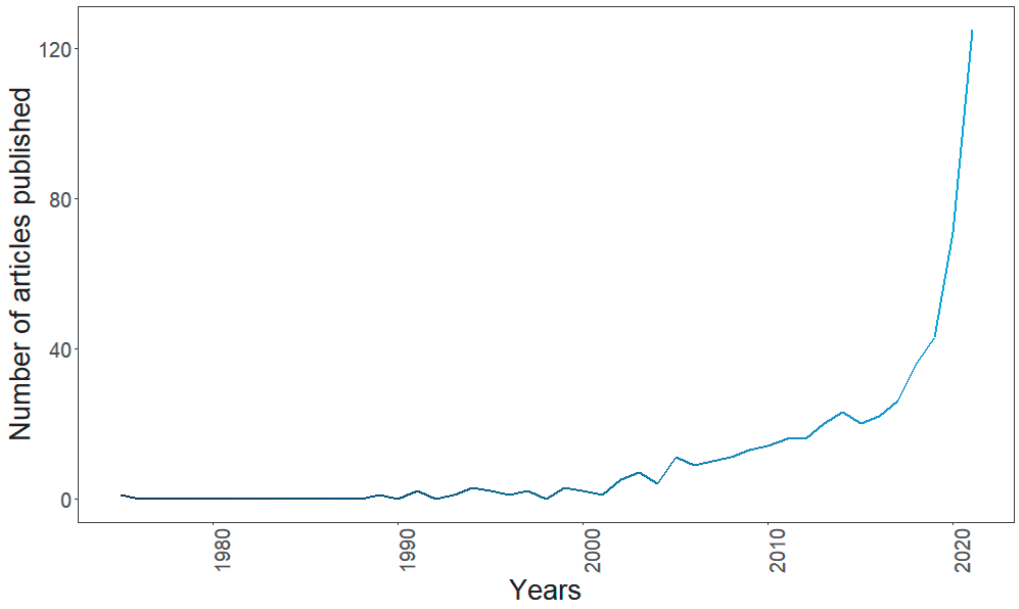

Figure 18. Graph showing the number of articles published in environmental science journals with the search words "tire wear", "tyre wear" and "TRWP" in any searchable field (title, abstract, keywords) from the first appearance in 1975 to the so far highest number of articles reported in 2021. Data are based on metrics from ISI Web of Knowledge.

6 Conclusions

As with all environmental assessments, it is important to put the pollutant of concern into a wider perspective. Although current models and estimates suggest that tire wear particles are one of the main sources of microplastic particles, it is important to highlight that these national or global estimation studies do not necessarily consider the processes on a local scale, such as in a freshwater lake or a river, nor do they consider sources of microplastic particles that could be of importance on a local scale. Hypotheses 1 of the present thesis suggested that the current model estimates of RAMP have left non-negligible sources of microplastic unaccounted for, which lead to the first objective of this thesis; to investigate if road de-icing salt could be a substantial source of microplastic particles from roads and traffic. As demonstrated in Paper I, there are other sources of microplastic particles from roads than tire wear, road wear and road markings. In Paper I, the concentration levels of microplastic particles from a new source, road de-icing salt, was assessed and the yearly release of microplastic particles from this source was estimated. The results from Paper I refuted Hypothesis 1; and the microplastic contribution from road de-icing salt was found to be negligible. However, together with recent publications on microplastic particles (non-road sources) in road samples, the results from Paper I highlight the need to investigate all possible sources of microplastic particles to road matrices, as well as evaluating the possible impact on the environment from the combined microplastic particle load and not just tire wear particles as the estimated main source.

As roads and traffic have been estimated to be one of the largest sources of microplastic particles to the environment, the need for validating these estimates with environmental data is imminent. However, the lack of standardized analytical methods and possibilities for local adaptations have hampered the development within this research area. Due to this, there are currently numerous different analytical methods for mass quantification of tire wear particles, as synthetic tire rubber (SBR, BR) has been estimated as the largest source of microplastics within the road and traffic area. The current methods used are based on different analytical techniques and instruments, different marker compounds for the tire rubber and different mass calculations of rubber present in tires. Another important issue with current methods is that they have not

considered the presence of synthetic rubbers (SBS, scrap tire, others) in the wear layer of road surface. Many countries use polymer-modified bitumen (PMB) as the binder in road asphalt or concrete asphalt, where SBS or scrap tires are often used as the polymer blend. The styrene and butadiene components of SBS rubber are derived from the same monomers as the styrene and butadiene in SBR rubber used in tires, and when these are thermally decomposed, for example using PYR-GC/MS, they will break down into identical pyrolysis products. As demonstrated in Paper II, it is not possible to separate between SBR and SBS when analysing an environmental sample with both present. Also, BR rubber used in tires is derived from the same butadiene monomers as the butadiene in SBR and SBS and will therefore also have overlapping pyrolysis products for butadiene. One of the main goals of this thesis has been to improve the mass quantification method for RAMP, and it was suggested in Hypothesis 2 that the use of multiple pyrolysis markers would improve the quantification method of both tire and road wear styrene butadiene rubbers. This hypothesis was supported by the results in Paper II. The set of multiple pyrolysis markers proposed in Paper II, substantially lowered the standard deviation of the results to 40% s.d. compared to 62% (4-VCH), 77% (SB dimer) and 85% (SBB trimer) for the single marker compounds proposed in previous studies. The multiple pyrolysis markers also demonstrated good recoveries in complex road matrices (88–104%), which further validate the strength of the method. For the second part of the method, expected local ratio between TWP and RWP_{PMB} is calculated based on emission factors and traffic data. Though this method relies on available traffic data, there is an increasing level of data being collected for roads and traffic, especially in European countries, which enables the possibilities for locally adapted methods. This makes the measurements and reported data more relevant compared to using global statistics and release estimates. A simpler version of the method could also be applied without traffic data (Paper II).

The second part of the mass quantification method presented in Paper II is to apply the concentrations of SBR+BR and SBS to Monte Carlo simulations, together with rubber data from locally relevant reference tires and predict the mass concentrations of both tire particles and RWP_{PMB} particles in a sample. The average percentage of SBR+BR rubbers in personal and heavy vehicles tires reported in Paper II were 31% (of total tire tread) and 33%, respectively. These results differ substantially from previous studies were 50% SBR+BR have been assumed for all personal vehicle tires and 50% NR have been

proposed for truck tires, and strongly support the second part of Hypothesis 2, that the incorporation of locally relevant reference tires would improve the quantification method for tire wear.

As tire wear particles in the environment are exposed to other road particles on the road surface, an increasing number of studies have reported tire wear particles as agglomerate particles mixed with minerals from the road, defined as tire and road wear particles (TRWP). However, the calculation from TWP to TRWP particles has been based on a limited number of studies and a broad assumption that all TRWP contain 50% tire tread and 50% minerals. In Paper IV, we propose an improved method for calculating TRWP based on the concentration of tire particles obtained by the methods in Paper II. This method is based on the same principles as the methods of Paper II, where Monte Carlo simulation is applied to a set of relevant data for the sample area. Even though the proposed method in Paper IV is hampered by the limited number of studies reporting mineral content of TRWP, it represents a more optimized method than using a global percentage and it demonstrates the possibilities for adapting the calculations to better report environmental data from roads with different pavements, different driving patterns or other variables, as more data on TRWP is available. These results further support Hypothesis 2, with improvements of the mass quantification methods for tire and road wear particles.

Road pollution is very much a local-scale issue, and previous studies of road pollution such as zinc, nickel, cadmium, PAHs, total particles and tire wear particles have been reported to accumulate in close vicinity of the road, in the roadsides or a nearby recipient (Figure 4). The results from Paper III support previous reports from road pollution studies and demonstrates that the concentrations of tire and road wear particles are higher close to the road (0-1m) compared to further away (3-4m, 60m). Thus, the first part of Hypothesis 3, that tire and road wear are deposited adjacent to roads, are supported. The results from Paper III did, however, show that there are several different variables that impact the concentration levels of tire and road wear particles along roads, and in contradiction to previous studies on road pollution, AADT was not found to be the main explanatory variable. Traffic speed and road types (highway road, urban road) were found to have the biggest impact on the concentration levels, although AADT, distance from the road and the combined variable AADT*traffic speed were also

statistically significant variables. Thus, the second part of Hypothesis 2 was refuted based on the results of Paper III.

The impact of local sources of tire and road wear is also important to consider for areas that have road tunnels. Currently, the public road network in Norway has over 1100 road tunnels, with various length and AADT. All road tunnels are semi-closed structures, where pollution accumulates over time and is mainly released to the environment through the release of tunnel wash water. According to Hypothesis 4, road tunnels are potentially important "hot-spots" for tire and road wear on a local scale. The concentration levels of tire and road wear particles reported for different compartments of the tunnel in Paper IV demonstrated that these particles do accumulate in different parts of the tunnel; the side bank areas of the road surface and close to the outlet of the tunnel, as well as in the inlet gully-pots. It also demonstrated that on the road surface, the concentrations of tire and road wear particles were substantially higher compared to previous studies of road dust from both roads and tunnels. For gully-pots, however, the concentration levels were comparable to previous studies of roadside gully-pots. For the tunnel wash water, the concentrations levels in the untreated water were comparable to levels reported in other studies, although lower compared to the concentration levels reported for roadside snow in Paper III. As the tire and road wear particles from the tunnel are mainly released into the environment through the untreated or treated tunnel wash water, these results support the rejection of Hypothesis 4.

The reported concentrations of tire and RWP_{PMB} and TRWP in roadside snow (Paper III) and different compartments of a road tunnel (Paper IV) both validate the analytical method in Paper II and contribute new data on the environmental concentrations of road-related microplastic particles. More data on environmental concentrations are needed to assess and evaluate the levels of microplastics from different types of roads, such as highways, urban roads and country-side areas, and for different traffic variables such as speed, AADT, inclination and road maintenance. It is also necessary to evaluate different types of measures against road pollution and their efficiency in reducing the negative impacts on the environment from microplastic pollution. Paper IV presents an efficiency assessment of sedimentation treatment based on retention of tire and road wear particles from tunnel wash water. To be able to evaluate and assess the efficiency of different types of mitigation measures and types of water treatments used for road and tunnel runoff, it is important to increase the number of studies across different

countries, climates, road types and driving patterns, as well as using comparable methods for sampling and analysis.

The work presented in this thesis provides new knowledge about road-associated microplastic particles that could contribute to developing more sustainable transportation systems and is in line with the United Nations Sustainable Development Goals. This work also answers the call from the Norwegian government put forward by the NPT 2022-2033 by 1) providing a validated analytical method for mass quantification of microplastic particles from tire and road wear in different environmental matrices (Paper II), 2) providing new knowledge on the concentration levels of microplastic particles from roads in different environmental compartments (Paper III & Paper IV), and 3) assessing potential new sources of microplastic particles from roads and traffic (Paper I).

7 References

Aitchison J. Principal Component Analysis of Compositional Data. Biometrika 1983; 70: 57-65.

Allan IJ, O'Connell SG, Meland S, Bæk K, Grung M, Anderson KA, et al. PAH Accessibility in Particulate Matter from Road-Impacted Environments. Environmental Science & Technology 2016; 50: 7964-7972.

Allen S, Allen D, Phoenix VR, Le Roux G, Jimenez PD, Simonneau A, et al. Atmospheric transport and deposition of microplastics in a remote mountain catchment. Nature Geoscience 2019; 12: 339-+.

Andersson J, Mácsik J, van der Nat D, Norström A, Albinsson M, Åkerman S, et al. Reducing Highway Runoff Pollution (REHIRUP). Sustainable design and maintenance of stormwater treatment facilities. 2018:155, 2018.

Arp HPH, Kühnel D, Rummel C, MacLeod M, Potthoff A, Reichelt S, et al. Weathering Plastics as a Planetary Boundary Threat: Exposure, Fate, and Hazards. Environmental Science & Technology 2021; 55: 7246-7255.

Asheim J. Benzotriazoles, Benzothiazoles and Inorganic Elements as Markers of Road Pollution Sources in a Sub-Arctic Urban Setting (Trondheim, Norway), 2018, pp. 125.

Asheim J, Vike-Jonas K, Gonzalez SV, Lierhagen S, Venkatraman V, Veivåg I-LS, et al. Benzotriazoles, benzothiazoles and trace elements in an urban road setting in Trondheim, Norway: Re-visiting the chemical markers of traffic pollution. Science of The Total Environment 2019; 649: 703-711.

Baensch-Baltruschat B, Kocher B, Stock F, Reifferscheid G. Tyre and road wear particles (TRWP) - A review of generation, properties, emissions, human health risk, ecotoxicity, and fate in the environment. Science of The Total Environment 2020; 733: 137823.

Barbosa AE, Hvitved-Jacobsen T. Infiltration Pond Design for Highway Runoff Treatment in Semiarid Climates. Journal of Environmental Engineering 2001; 127: 1014-1022.

Baumann W, Ismeier M. Emissionen beim bestimmungsgemässen Gebrauch von Reifen. Kautschuk und Gummi, Kunststoffe 1998; 51: 182-186.

Becker MY, Müller AJ, Rodriguez Y. Use of rheological compatibility criteria to study SBS modified asphalts. Journal of Applied Polymer Science 2003; 90: 1772-1782.

Bergmann M, Mützel S, Primpke S, Tekman MB, Trachsel J, Gerdts G. White and wonderful? Microplastics prevail in snow from the Alps to the Arctic. Science Advances 2019; 5: eaax1157.

Bergmann M, Wirzberger V, Krumpen T, Lorenz C, Primpke S, Tekman MB, et al. High Quantities of Microplastic in Arctic Deep-Sea Sediments from the HAUSGARTEN Observatory. Environmental Science & Technology 2017; 51: 11000-11010.

Blecken GW. Kunskapssammanställning – Dagvattenrening. In: Vatten S, Utveckling., editors, 2016.

Blok J. Environmental exposure of road borders to zinc. Science of the Total Environment 2005; 348: 173-190.

Bondelind M, Sokolova E, Nguyen A, Karlsson D, Karlsson A, Björklund K. Hydrodynamic modelling of traffic-related microplastics discharged with stormwater into the Göta River in Sweden. Environmental Science and Pollution Research 2020; 27: 24218-24230.

Borris M, Österlund H, Marsalek J, Viklander M. Snow pollution management in urban areas: an idea whose time has come? Urban Water Journal 2021; 18: 840-849.

Boucher J, Billard G, Simeone E, Sousa JT. The marine plastic footprint. 2831720281. IUCN, Gland, Switzerland, 2020.

Bouman E, Meland S, Furuseth IS, Tarrasón L. Feasibility study for asphalt rubber pavements in Norway. 'Rubber Road' feasibility study. NILU, 2020.

Brinkmann M, Montgomery D, Selinger S, Miller JGP, Stock E, Alcaraz AJ, et al. Acute Toxicity of the Tire Rubber-Derived Chemical 6PPD-quinone to Four Fishes of Commercial, Cultural, and Ecological Importance. Environmental Science & Technology Letters 2022.

Brodie IM. Prediction of stormwater particle loads from impervious urban surfaces based on a rainfall detachment index. Water Science and Technology 2007; 55: 49-56.

Bråte ILN, Hurley R, Iversen K, Beyer J, Thomas KV, Steindal CC, et al. Mytilus spp. as sentinels for monitoring microplastic pollution in Norwegian coastal waters: A qualitative and quantitative study. Environmental Pollution 2018; 243: 383-393.
Bråte ILN, Hurley R, Lusher A, Buenaventura N, Hultman M, Halsband C, et al. Microplastics in marine bivalves from the Nordic environment. In: report NCoM, editor, 2020, pp. 127.
Bråte ILN, Huwer B, Thomas KV, Eidsvoll DP, Halsband C, Almroth BC, et al. Micro-and macro-plastics in marine species from Nordic waters. Nordic council of Ministry Report 2017.
Bye N, Johnson JP. Assessment of tire wear emission in a road tunnel, using benzothiazoles as tracer in tunnel wash water Master of Science. Norwegian University of Life Sciences., 2019.
Bäckström M. Sediment transport in grassed swales during simulated runoff events. Water Science and Technology 2002; 45: 41-49.
Bäckström M. Grassed swales for stormwater pollution control during rain and snowmelt. Water Science and Technology 2003; 48: 123-132.
Bäckström M, Karlsson S, Bäckman L, Folkeson L, Lind B. Mobilisation of heavy metals by deicing salts in a roadside environment. Water Research 2004; 38: 720-732.
Cadle SH, Williams RL. Gas and Particle Emissions from Automobile Tires in Laboratory and Field Studies. Rubber Chemistry and Technology 1979; 52: 146-158.
Cao G, Wang W, Zhang J, Wu P, Zhao X, Yang Z, et al. New Evidence of Rubber-Derived Quinones in Water, Air, and Soil. Environmental Science & Technology 2022.
CE. Five-year Review of Progress: Code of Practice for the Environmental Management of Road Salts. In: Environment C, editor, 2012.
Ceder A. Urban mobility and public transport: future perspectives and review. International Journal of Urban Sciences 2021; 25: 455-479.
CEDR. A review of applications of de-icing chemicals, representative for European countries. In: Muthanna TM, Jan-Willem Knegt JW, Bink S, van der Veen I, van Tol J, editors. Conference of European Directors of Roads, 2019.
Chae E, Jung U, Choi S-S. Quantification of tire tread wear particles in microparticles produced on the road using oleamide as a novel marker. Environmental Pollution 2021; 288: 117811.
Challis JK, Popick H, Prajapati S, Harder P, Giesy JP, McPhedran K, et al. Occurrences of Tire Rubber-Derived Contaminants in Cold-Climate Urban Runoff. Environmental Science & Technology Letters 2021; 8: 961-967.
Chen JS, Liao MC, Tsai HH. Evaluation and optimization of the engineering properties of polymer-modified asphalt. Practical Failure Analysis 2002; 2: 75-83.
Choi S-S. Characteristics of pyrolysis patterns of polybutadienes with different microstructures. Journal of Analytical and Applied Pyrolysis 2001; 57: 249-259.
Choi S-S, Kwon H-M. Considering factors on determination of microstructures of SBR vulcanizates using pyrolytic analysis. Polymer Testing 2020; 89: 106572.
Clarivate. Web of Science Database, 2022.
Councell TB, Duckenfield KU, Landa ER, Callender E. Tire-wear particles as a source of zinc to the environment. Environmental science & technology 2004; 38: 4206-4214.
Cowger W, Booth AM, Hamilton BM, Thaysen C, Primpke S, Munno K, et al. Reporting Guidelines to Increase the Reproducibility and Comparability of Research on Microplastics. Applied Spectroscopy 2020; 74: 1066-1077.
Cristina CM, Sansalone JJ. “First Flush,” Power Law and Particle Separation Diagrams for Urban Storm-Water Suspended Particulates. Journal of Environmental Engineering 2003; 129: 298-307.
Crutzen PJ. Geology of Mankind. In: Crutzen PJ, Brauch HG, editors. Paul J. Crutzen: A Pioneer on Atmospheric Chemistry and Climate Change in the Anthropocene. Springer International Publishing, Cham, 2016, pp. 211-215.
Cunningham B, Harper B, Brander S, Harper S. Toxicity of micro and nano tire particles and leachate for model freshwater organisms. Journal of Hazardous Materials 2022; 429: 128319.
de Coninck H, Revi A, Babiker M, Bertoldi P, Buckeridge M, Cartwright A, et al. Strengthening and Implementing the Global Response. Global warming of 1.5°C: Summary for policy makers. IPCC - The Intergovernmental Panel on Climate Change, 2018, pp. 313-443.
Degaffe FS, Turner A. Leaching of zinc from tire wear particles under simulated estuarine conditions. Chemosphere 2011; 85: 738-743.

del Real AEP, Mitrano DM, Castillo-Michel H, Wazne M, Reyes-Herrera J, Bortel E, et al. Assessing implications of nanoplastics exposure to plants with advanced nanometrology techniques. Journal of Hazardous Materials 2022; 430: 128356.
Deletic A, Ashley R, Rest D. Modelling input of fine granular sediment into drainage systems via gully-pots. Water Research 2000; 34: 3836-3844.
Denby BR, Sundvor I, Johansson C, Pirjola L, Ketzel M, Norman M, et al. A coupled road dust and surface moisture model to predict non-exhaust road traffic induced particle emissions (NORTRIP). Part 1: Road dust loading and suspension modelling. Atmospheric Environment 2013; 77: 283-300.
dos Santos ÉJ, Herrmann AB, Prado SK, Fantin EB, dos Santos VW, de Oliveira AVM, et al. Determination of toxic elements in glass beads used for pavement marking by ICP OES. Microchemical Journal 2013; 108: 233-238.
EAPA. HEAVY DUTY SURFACES THE ARGUMENTS FOR SMA. Technical review. In: Association EAP, editor, Brussels, Belgium, 2018.
Eisentraut P, Dümichen E, Ruhl AS, Jekel M, Albrecht M, Gehde M, et al. Two Birds with One Stone—Fast and Simultaneous Analysis of Microplastics: Microparticles Derived from Thermoplastics and Tire Wear. Environmental Science & Technology Letters 2018; 5: 608-613.
Fauser P, Tjell JC, Mosbaek H, Pilegaard K. Quantification of tire-tread particles using extractable organic zinc as tracer. Rubber Chemistry and Technology 1999; 72: 969-977.
Fernández-Berridi MJ, González N, Mugica A, Bernicot C. Pyrolysis-FTIR and TGA techniques as tools in the characterization of blends of natural rubber and SBR. Thermochimica Acta 2006; 444: 65-70.
Flanagan K, Branchu P, Boudahmane L, Caupos E, Demare D, Deshayes S, et al. Field performance of two biofiltration systems treating micropollutants from road runoff. Water Research 2018; 145: 562-578.
Fox J, Weisberg S . A. n R Companion to Applied Regression. Thousand Oaks CA.: Sage, 2019.
Furuseth IS, Rødland ES. Reducing the Release of Microplastic from Tire Wear: Nordic Efforts. Nordiske Arbejdspapirer ; 2020:909, Copenhagen, 2021, pp. 41.
Garshol FK, Estevez MM, Eftekhar Dadkhah M, Stang P, Rathnaweera SS, Sahu A, et al. Laboratorietester – rensing av vaskevann fra Nordbytunnelen. Inklusive datarapport og resultater med vann hentet 31.08. 2014 og 18.03.2015. In: NORWAT, editor. Report No. 521, Norway, 2015, pp. 131.
GESAMP. Sources, fate and effects of microplastics in the marine environment: part two of a global assessment. Joint Group of Experts on the Scientific Aspects of Marine Environmental Protection, 2016, pp. 220.
Giardina A, Larson SF, Wisner B, Wheeler J, Chao M. Long-term and acute effects of zinc contamination of a stream on fish mortality and physiology. Environmental Toxicology and Chemistry 2009; 28: 287-295.
Giavarini C, De Filippis P, Santarelli ML, Scarsella M. Production of stable polypropylene-modified bitumens. Fuel 1996; 75: 681-686.
Gigault J, Pedrono B, Maxit B, Ter Halle A. Marine plastic litter: the unanalyzed nano-fraction. Environmental Science: Nano 2016; 3: 346-350.
Gomes T, Bour A, Coutris C, Almeida AC, Bråte IL, Wolf R, et al. Ecotoxicological Impacts of Micro- and Nanoplastics in Terrestrial and Aquatic Environments. In: Bank MS, editor. Microplastic in the Environment: Pattern and Process. Springer International Publishing, Cham, 2022, pp. 199-260.
Goßmann I, Halbach M, Scholz-Böttcher BM. Car and truck tire wear particles in complex environmental samples – A quantitative comparison with "traditional" microplastic polymer mass loads. Science of The Total Environment 2021; 773: 145667.
Greenacre M, Lewi P. Distributional Equivalence and Subcompositional Coherence in the Analysis of Compositional Data, Contingency Tables and Ratio-Scale Measurements. Journal of Classification 2009; 26: 29-54.
Grigoratos T, Martini G. Non-exhaust traffic related emissions. Brake and tyre wear PM. JRC Science and Policy Reports 2014: 53.

Grung M, Kringstad A, Bæk K, Allan IJ, Thomas KV, Meland S, et al. Identification of non-regulated polycyclic aromatic compounds and other markers of urban pollution in road tunnel particulate matter. Journal of Hazardous Materials 2017; 323: 36-44.
Grung M, Meland S, Ruus A, Ranneklev S, Fjeld E, Kringstad A, et al. Occurrence and trophic transport of organic compounds in sedimentation ponds for road runoff. Science of The Total Environment 2021; 751: 141808.
Gunawardena J, Ziyath AM, Egodawatta P, Ayoko GA, Goonetilleke A. Sources and transport pathways of common heavy metals to urban road surfaces. Ecological Engineering 2015; 77: 98-102.
Gustafsson M, Blomqvist G, Gudmundsson A, Dahl A, Jonsson P, Swietlicki E. Factors influencing PM10 emissions from road pavement wear. Atmospheric Environment 2009; 43: 4699-4702.
Gustafsson M, Blomqvist G, Järlskog I, Lundberg J, Janhäll S, Elmgren M, et al. Road dust load dynamics and influencing factors for six winter seasons in Stockholm, Sweden. Atmospheric Environment: X 2019; 2: 100014.
Hadley PW, Petrisor IG. Incremental Sampling: Challenges and Opportunities for Environmental Forensics. Environmental Forensics 2013; 14: 109-120.
Hale RC, Seeley ME, King AE, Yu LH. Analytical Chemistry of Plastic Debris: Sampling, Methods, and Instrumentation. In: Bank MS, editor. Microplastic in the Environment: Pattern and Process. Springer International Publishing, Cham, 2022, pp. 17-67.
Hallberg M, Renman G, Byman L, Svenstam G, Norling M. Treatment of tunnel wash water and implications for its disposal. Water Science and Technology 2014; 69: 2029-2035.
Halsband C, Sørensen L, Booth AM, Herzke D. Car Tire Crumb Rubber: Does Leaching Produce a Toxic Chemical Cocktail in Coastal Marine Systems? Frontiers in Environmental Science 2020; 8.
Hartmann NB, Hüffer T, Thompson RC, Hassellöv M, Verschoor A, Daugaard AE, et al. Are We Speaking the Same Language? Recommendations for a Definition and Categorization Framework for Plastic Debris. Environmental science & technology 2019; 53: 1039-1047.
Hatt BE, Fletcher TD, Deletic A. Hydrologic and pollutant removal performance of stormwater biofiltration systems at the field scale. Journal of Hydrology 2009; 365: 310-321.
Headley JV, McMartin DW. A review of the occurrence and fate of naphthenic acids in aquatic environments. Journal of Environmental Science and Health, Part A 2004; 39: 1989-2010.
Hiki K, Asahina K, Kato K, Yamagishi T, Omagari R, Iwasaki Y, et al. Acute Toxicity of a Tire Rubber-Derived Chemical, 6PPD Quinone, to Freshwater Fish and Crustacean Species. Environmental Science & Technology Letters 2021; 8: 779-784.
Hopke PK, Lamb RE, Natusch DF. Multielemental characterization of urban roadway dust. Environmental science & technology 1980; 14: 164-172.
Horton AA, Svendsen C, Williams RJ, Spurgeon DJ, Lahive E. Large microplastic particles in sediments of tributaries of the River Thames, UK - Abundance, sources and methods for effective quantification. Marine Pollution Bulletin 2017a; 114: 218-226.
Horton AA, Svendsen C, Williams RJ, Spurgeon DJ, Lahive E. Large microplastic particles in sediments of tributaries of the River Thames, UK – Abundance, sources and methods for effective quantification. Marine Pollution Bulletin 2017b; 114: 218-226.
Huber M, Hilbig H, Badenberg SC, Fassnacht J, Drewes JE, Helmreich B. Heavy metal removal mechanisms of sorptive filter materials for road runoff treatment and remobilization under de-icing salt applications. Water Research 2016; 102: 453-463.
Hurley RR, Nizzetto L. Fate and occurrence of micro(nano)plastics in soils: Knowledge gaps and possible risks. Current Opinion in Environmental Science & Health 2018; 1: 6-11.
ISO. ISO/TS 20593: Ambient air - Determination of the mass concentration of tire and road wear particles (TRWP) - Pyrolysis-GC-MS method. International Organization for Standardization, Geneve, Switzerland, 2017a.
ISO. ISO/TS 21396: Rubber — Determination of mass concentration of tire and road wear particles (TRWP) in soil and sediments — Pyrolysis-GC/MS method. International Organization for Standardization, Genève, Switzerland, 2017b.
Johannessen C, Helm P, Lashuk B, Yargeau V, Metcalfe CD. The Tire Wear Compounds 6PPD-Quinone and 1,3-Diphenylguanidine in an Urban Watershed. Archives of Environmental Contamination and Toxicology 2022; 82: 171-179.

Johannessen C, Helm P, Metcalfe CD. Detection of selected tire wear compounds in urban receiving waters. Environmental Pollution 2021; 287: 117659.
Jung U, Choi S-S. Classification and Characterization of Tire-Road Wear Particles in Road Dust by Density. Polymers 2022; 14: 1005.
Järlskog I, Strömvall A-M, Magnusson K, Gustafsson M, Polukarova M, Galfi H, et al. Occurrence of tire and bitumen wear microplastics on urban streets and in sweepsand and washwater. Science of The Total Environment 2020; 729: 138950.
Kallenbach EMF, Rødland ES, Buenaventura NT, Hurley R. Microplastics in Terrestrial and Freshwater Environments. In: Bank MS, editor. Microplastic in the Environment: Pattern and Process. Springer International Publishing, Cham, 2022, pp. 87-130.
Kanhai LK, Johansson C, Frias J, Gardfeldt K, Thompson RC, O'Connor I. Deep sea sediments of the Arctic Central Basin: A potential sink for microplastics. Deep-Sea Research Part I-Oceanographic Research Papers 2019; 145: 137-142.
Kayhanian M, McKenzie ER, Leatherbarrow JE, Young TM. Characteristics of road sediment fractionated particles captured from paved surfaces, surface run-off and detention basins. Science of The Total Environment 2012; 439: 172-186.
Ke C, Li Z, Liang Y, Tao W, Du M. Impacts of chloride de-icing salt on bulk soils, fungi, and bacterial populations surrounding the plant rhizosphere. Applied Soil Ecology 2013; 72: 69-78.
Kelly VR, Findlay SEG, Weathers KC. Road Salt: The Problem, The Solution, and How To Get There. Cary Institute of Ecosystem Studies, 2019, pp. 16.
Khan FR, Halle LL, Palmqvist A. Acute and long-term toxicity of micronized car tire wear particles to Hyalella azteca. Aquatic Toxicology 2019; 213: 105216.
Klauschies T, Isanta-Navarro J. The joint effects of salt and 6PPD contamination on a freshwater herbivore. Science of The Total Environment 2022; 829: 154675.
Klöckner P, Reemtsma T, Eisentraut P, Braun U, Ruhl AS, Wagner S. Tire and road wear particles in road environment – Quantification and assessment of particle dynamics by Zn determination after density separation. Chemosphere 2019; 222: 714-721.
Klöckner P, Seiwert B, Eisentraut P, Braun U, Reemtsma T, Wagner S. Characterization of tire and road wear particles from road runoff indicates highly dynamic particle properties. Water Research 2020; 185: 116262.
Klöckner P, Seiwert B, Wagner S, Reemtsma T. Organic Markers of Tire and Road Wear Particles in Sediments and Soils: Transformation Products of Major Antiozonants as Promising Candidates. Environmental Science & Technology 2021a; 55: 11723-11732.
Klöckner P, Seiwert B, Weyrauch S, Escher BI, Reemtsma T, Wagner S. Comprehensive characterization of tire and road wear particles in highway tunnel road dust by use of size and density fractionation. Chemosphere 2021b; 279: 130530.
Knight LJ, Parker-Jurd FNF, Al-Sid-Cheikh M, Thompson RC. Tyre wear particles: an abundant yet widely unreported microplastic? Environ Sci Pollut Res Int 2020; 27: 18345-18354.
Kocher B, Brose S, Siebertz S. Schadstoffgehalte von Bankett - Bundesweite Datenauswertung. Verkehrstechnik - Berichte der Bundesanstalt für Straßenwesen Heft. 167, 2008.
Kole PJ, Lohr AJ, Van Belleghem FGAJ, Ragas AMJ. Wear and Tear of Tyres: A Stealthy Source of Microplastics in the Environment. International Journal of Environmental Research and Public Health 2017; 14.
Kovochich M, Liong M, Parker JA, Oh SC, Lee JP, Xi L, et al. Chemical mapping of tire and road wear particles for single particle analysis. Science of The Total Environment 2021a; 757: 144085.
Kovochich M, Parker JA, Oh SC, Lee JP, Wagner S, Reemtsma T, et al. Characterization of Individual Tire and Road Wear Particles in Environmental Road Dust, Tunnel Dust, and Sediment. Environmental Science & Technology Letters 2021b.
Kreider ML, Panko JM, McAtee BL, Sweet LI, Finley BL. Physical and chemical characterization of tire-related particles: Comparison of particles generated using different methodologies. Science of the Total Environment 2010; 408: 652-659.
Kumar M, Chen H, Sarsaiya S, Qin S, Liu H, Awasthi MK, et al. Current research trends on micro- and nano-plastics as an emerging threat to global environment: A review. Journal of Hazardous Materials 2021; 409: 124967.

Kumata H, Mori M, Takahashi S, Takamiya S, Tsuzuki M, Uchida T, et al. Evaluation of Hydrogenated Resin Acids as Molecular Markers for Tire-wear Debris in Urban Environments. Environmental Science & Technology 2011; 45: 9990-9997.
Kumata H, Sanada Y, Takada H, Ueno T. Historical Trends of N-Cyclohexyl-2-benzothiazolamine, 2-(4-Morpholinyl)benzothiazole, and Other Anthropogenic Contaminants in the Urban Reservoir Sediment Core. Environmental Science & Technology 2000; 34: 246-253.
Kumata H, Takada H, Ogura N. 2-(4-Morpholinyl)benzothiazole as an Indicator of Tire-Wear Particles and Road Dust in the Urban Environment. Molecular Markers in Environmental Geochemistry. 671. American Chemical Society, 1997, pp. 291-305.
Kumata H, Yamada J, Masuda K, Takada H, Sato Y, Sakurai T, et al. Benzothiazolamines as Tire-Derived Molecular Markers: Sorptive Behavior in Street Runoff and Application to Source Apportioning. Environmental Science & Technology 2002; 36: 702-708.
Lai FY, O'Brien J, Bruno R, Hall W, Prichard J, Kirkbride P, et al. Spatial variations in the consumption of illicit stimulant drugs across Australia: A nationwide application of wastewater-based epidemiology. Science of The Total Environment 2016; 568: 810-818.
Lambert S, Wagner M. Characterisation of nanoplastics during the degradation of polystyrene. Chemosphere 2016; 145: 265-8.
LaPlaca SB, van den Hurk P. Toxicological effects of micronized tire crumb rubber on mummichog (Fundulus heteroclitus) and fathead minnow (Pimephales promelas). Ecotoxicology 2020; 29: 524-534.
Leistenschneider C, Burkhardt-Holm P, Mani T, Primpke S, Taubner H, Gerdts G. Microplastics in the Weddell Sea (Antarctica): A Forensic Approach for Discrimination between Environmental and Vessel-Induced Microplastics. Environmental Science & Technology 2021; 55: 15900-15911.
Li X, Jiang F, Wang S, Turdi M, Zhang Z. Spatial distribution and potential sources of trace metals in insoluble particles of snow from Urumqi, China. Environmental Monitoring and Assessment 2014a; 187: 4144.
Li Y, Lau S-L, Kayhanian M, Stenstrom MK. Particle Size Distribution in Highway Runoff. Journal of Environmental Engineering 2005; 131: 1267-1276.
Li Z, Liang Y, Zhou J, Sun X. Impacts of de-icing salt pollution on urban road greenspace: a case study of Beijing. Frontiers of Environmental Science & Engineering 2014b; 8: 747-756.
Lucchi J, Gluck D, Rials S, Tang L, Baudelet M. Tire Classification by Elemental Signatures Using Laser-Induced Breakdown Spectroscopy. Applied Spectroscopy 2021; 75: 747-752.
Lundberg J, Blomqvist G, Gustafsson M, Janhäll S, Järlskog I. Wet Dust Sampler—a Sampling Method for Road Dust Quantification and Analyses. Water, Air, & Soil Pollution 2019; 230: 180.
Lundebye A-K, Lusher AL, Bank MS. Marine Microplastics and Seafood: Implications for Food Security. In: Bank MS, editor. Microplastic in the Environment: Pattern and Process. Springer International Publishing, Cham, 2022, pp. 131-153.
Lusher AL, Hollman PC, Mendoza-Hill J. Microplastics in fisheries and aquaculture, 2017.
Lusher AL, Hurley R, Arp HPH, Booth AM, Bråte ILN, Gabrielsen GW, et al. Moving forward in microplastic research: A Norwegian perspective. Environment International 2021; 157: 106794.
Magnusson K, Eliasson K, Fråne A, Haikonen K, Hultén J, Olshammar M, et al. Swedish sources and pathways for microplastics to the marine environment: A review of existing data. IVL Swedish Environmental Research Institute, 2017.
Mahrosh U, Kleiven M, Meland S, Rosseland BO, Salbu B, Teien H-C. Toxicity of road deicing salt (NaCl) and copper (Cu) to fertilization and early developmental stages of Atlantic salmon (Salmo salar). Journal of Hazardous Materials 2014; 280: 331-339.
Marchut-Mikołajczyk O, Drożdżyński P, Januszewicz B, Domański J, Wrześniewska-Tosik K. Degradation of ozonized tire rubber by aniline – Degrading Candida methanosorbosa BP6 strain. Journal of Hazardous Materials 2019; 367: 8-14.
Marsalek J, Watt WE, Anderson BC. Trace metal levels in sediments deposited in urban stormwater management facilities. Water Science and Technology 2006; 53: 175-183.
Marwood C, McAtee B, Kreider M, Ogle RS, Finley B, Sweet L, et al. Acute aquatic toxicity of tire and road wear particles to alga, daphnid, and fish. Ecotoxicology 2011; 20: 2079.

MCE. Meld. St. 13 (2020–2021) Klimaplan for 2021–2030. In: Environment MoCa, editor. Norwegian Government, 2021.
Meland S. Management of contaminated runoff water. Current practice and Future Research Needs. Conference of European Directors of Roads (CEDR), Brussels, 2016.
Meland S, Borgstrøm R, Heier LS, Rosseland BO, Lindholm O, Salbu B. Chemical and ecological effects of contaminated tunnel wash water runoff to a small Norwegian stream. Science of The Total Environment 2010a; 408: 4107-4117.
Meland S, Gomes T, Petersen K, Håll J, Lund E, Kringstad A, et al. Road related pollutants induced DNA damage in dragonfly nymphs (Odonata, Anisoptera) living in highway sedimentation ponds. Scientific Reports 2019; 9: 16002.
Meland S, Heier LS, Salbu B, Tollefsen KE, Farmen E, Rosseland BO. Exposure of brown trout (Salmo trutta L.) to tunnel wash water runoff — Chemical characterisation and biological impact. Science of The Total Environment 2010b; 408: 2646-2656.
Meland S, Rødland E. Pollution in tunnel wash water – a study of 34 road tunnels in Norway. VANN 2018; 01.
Meland S, Salbu B, Rosseland BO. Ecotoxicological impact of highway runoff using brown trout (Salmo trutta L.) as an indicator model. Journal of Environmental Monitoring 2010c; 12: 654-664.
Mengistu D, Heistad A, Coutris C. Tire wear particles concentrations in gully pot sediments. Science of The Total Environment 2021a; 769: 144785.
Mengistu D, Heistad A, Coutris C. Tire wear particles concentrations in gully pot sediments. Sci Total Environ 2021b; 769: 144785.
Mengistu D, Nilsen V, Heistad A, Kvaal K. Detection and Quantification of Tire Particles in Sediments Using a Combination of Simultaneous Thermal Analysis, Fourier Transform Infra-Red, and Parallel Factor Analysis. International Journal of Environmental Research and Public Health 2019; 16: 3444.
Miller JV, Chan K, Unice KM. Evaluation of three pyrolyzer technologies for quantitative pyrolysis-gas chromatography-mass spectrometry (Py-GC-MS) of tire tread polymer in an artificial sediment matrix. Environmental Advances 2022: 100213.
Miller JV, Maskrey JR, Chan K, Unice KM. Pyrolysis-Gas Chromatography-Mass Spectrometry (Py-GC-MS) Quantification of Tire and Road Wear Particles (TRWP) in Environmental Matrices: Assessing the Importance of Microstructure in Instrument Calibration Protocols. Analytical Letters 2021: 1-13.
Moghadas S, Paus KH, Muthanna TM, Herrmann I, Marsalek J, Viklander M. Accumulation of Traffic-Related Trace Metals in Urban Winter-Long Roadside Snowbanks. . Water, Air & Soil Pollution 2015; 226: 404.
Monira S, Roychand R, Bhuiyan MA, Hai FI, Pramanik BK. Identification, classification and quantification of microplastics in road dust and stormwater. Chemosphere 2022; 299: 134389.
Moreno T, Pérez N, Reche C, Martins V, de Miguel E, Capdevila M, et al. Subway platform air quality: Assessing the influences of tunnel ventilation, train piston effect and station design. Atmospheric Environment 2014; 92: 461-468.
MT. Nasjonal transportplan 2022–2033. In: Transport Mo, editor. Norwegian Government, 2021.
Müller A, Kocher B, Altmann K, Braun U. Determination of tire wear markers in soil samples and their distribution in a roadside soil. Chemosphere 2022a; 294: 133653.
Müller K, Hübner D, Huppertsberg S, Knepper TP, Zahn D. Probing the chemical complexity of tires: Identification of potential tire-borne water contaminants with high-resolution mass spectrometry. Science of The Total Environment 2022b; 802: 149799.
Napper IE, Davies BFR, Clifford H, Elvin S, Koldewey HJ, Mayewski PA, et al. Reaching New Heights in Plastic Pollution-Preliminary Findings of Microplastics on Mount Everest. One Earth 2020; 3: 621-630.
Nelson S, Mueller G, Hemphill D. Identification of tire leachate toxicants and a risk assessment of water quality effects using tire reefs in canals. Bulletin of environmental contamination and toxicology 1994; 52: 574.

Ni H-G, Lu F-H, Luo X-L, Tian H-Y, Zeng EY. Occurrence, Phase Distribution, and Mass Loadings of Benzothiazoles in Riverine Runoff of the Pearl River Delta, China. Environmental Science & Technology 2008; 42: 1892-1897.
NPRA. Road cleaning in tunnel and street, 2016. Strindheim tunnel and Haakon VII street in Trondheim, Stordal tunnel in Møre and Romsdal. In: Snilsberg B, Gryteselv D, editors. Norwegian Public Roads Administration, Trondheim, 2017.
NPRA. Håndbok N200 Vegbygging Norwegian Public Roads Administration 2021a.
NPRA. Tunnel cleaning experiment 2019-2020. Reduced washing frequency in the Strindheim tunnel. In: Snilsberg B, Gryteselv D, Veivåg ILS, Peckolt Fordal K, Indo K, Monsen E, editors. Norwegian Public Roads Administration, Trondheim, 2021b.
NVF. Trender innen belegningsbransjen i Norden: Belegningstrender i Norge. Nordiskt Vägforum, Utvalg for Belegninger,, 2013, pp. 61.
Nyström F, Nordqvist K, Herrmann I, Hedström A, Viklander M. Treatment of road runoff by coagulation/flocculation and sedimentation. Water Science and Technology 2019; 79: 518-525.
O'Brien S, Okoffo ED, Rauert C, O'Brien JW, Ribeiro F, Burrows SD, et al. Quantification of selected microplastics in Australian urban road dust. Journal of Hazardous Materials 2021; 416: 125811.
Omnexus. A Detailed Guide on Acrylonitrile Bitadiene Styrene. SpecialChem, 2022.
Oral HV, Carvalho P, Gajewska M, Ursino N, Masi F, Hullebusch EDv, et al. A review of nature-based solutions for urban water management in European circular cities: a critical assessment based on case studies and literature. Blue-Green Systems 2020; 2: 112-136.
Panda M, Mazumdar M. Engineering properties of EVA-modified bitumen binder for paving mixes. Journal of Materials in Civil Engineering 1999; 11: 131-137.
Panko JM, Chu J, Kreider ML, Unice KM. Measurement of airborne concentrations of tire and road wear particles in urban and rural areas of France, Japan, and the United States. Atmospheric Environment 2013; 72: 192-199.
Panko JM, Hitchcock KM, Fuller GW, Green D. Evaluation of Tire Wear Contribution to PM2.5 in Urban Environments. Atmosphere 2019; 10: 99.
Parker-Jurd FNF, Napper IE, Abbott GD, Hann S, Thompson RC. Quantifying the release of tyre wear particles to the marine environment via multiple pathways. Marine Pollution Bulletin 2021; 172: 112897.
Paruch AM, Roseth R. Treatment of tunnel wash waters — experiments with organic sorbent materials. Part II: Removal of toxic metals. Journal of Environmental Sciences 2008; 20: 1042-1045.
Persson L, Carney Almroth BM, Collins CD, Cornell S, de Wit CA, Diamond ML, et al. Outside the Safe Operating Space of the Planetary Boundary for Novel Entities. Environmental Science & Technology 2022; 56: 1510-1521.
Peter KT, Tian Z, Wu C, Lin P, White S, Du B, et al. Using High-Resolution Mass Spectrometry to Identify Organic Contaminants Linked to Urban Stormwater Mortality Syndrome in Coho Salmon. Environmental Science & Technology 2018; 52: 10317-10327.
Petersen K, Bæk K, Grung M, Meland S, Ranneklev SB. In vivo and in vitro effects of tunnel wash water and traffic related contaminants on aquatic organisms. Chemosphere 2016; 164: 363-371.
Pettersson TJR. Water quality improvement in a small stormwater detention pond. Water Science and Technology 1998; 38: 115-122.
Pitt R, Field R. Catchbasins and Inserts for the Control of Gross Solids and Conventional Stormwater Pollutants. Critical Transitions in Water and Environmental Resources Management, 2004, pp. 1-10.
Polacco G, Berlincioni S, Biondi D, Stastna J, Zanzotto L. Asphalt modification with different polyethylene-based polymers. European Polymer Journal 2005; 41: 2831-2844.
Polacco G, Muscente A, Biondi D, Santini S. Effect of composition on the properties of SEBS modified asphalts. European Polymer Journal 2006; 42: 1113-1121.
Polymerdatabase. STYRENE-BUTADIENE POLYMERS (SB, SBS) - PROPERTIES AND APPLICATIONS, 2022.

Prochazka D, Bilík M, Prochazková P, Klus J, Pořízka P, Novotný J, et al. Detection of tire tread particles using laser-induced breakdown spectroscopy. Spectrochimica Acta Part B: Atomic Spectroscopy 2015; 108: 1-7.
Provencher DJ, Kögel DT, Lusher DA, Vorkamp DK, Gomiero DA, Peeken DI, et al. An ecosystem-scale litter and microplastic monitoring plan under the Arctic Monitoring and Assessment Programme (AMAP). Arctic Science 2022; 0: null.
Provencher JF, Covernton GA, Moore RC, Horn DA, Conkle JL, Lusher AL. Proceed with caution: The need to raise the publication bar for microplastics research. Science of The Total Environment 2020; 748: 141426.
Rauert C, Charlton N, Okoffo ED, Stanton RS, Agua AR, Pirrung MC, et al. Concentrations of Tire Additive Chemicals and Tire Road Wear Particles in an Australian Urban Tributary. Environmental Science & Technology 2022.
Rauert C, Kaserzon SL, Veal C, Yeh RY, Mueller JF, Thomas KV. The first environmental assessment of hexa(methoxymethyl)melamine and co-occurring cyclic amines in Australian waterways. Science of The Total Environment 2020; 743: 140834.
Rauert C, Rødland ES, Okoffo ED, Reid MJ, Meland S, Thomas KV. Challenges with Quantifying Tire Road Wear Particles: Recognizing the Need for Further Refinement of the ISO Technical Specification. Environmental Science & Technology Letters 2021; 8: 231-236.
Reddy CM, Quinn JG. Environmental Chemistry of Benzothiazoles Derived from Rubber. Environmental Science & Technology 1997; 31: 2847-2853.
Reddy KR, Xie T, Dastgheibi S. Nutrients Removal from Urban Stormwater by Different Filter Materials. Water, Air, & Soil Pollution 2013; 225: 1778.
Redondo-Hasselerharm PE, de Ruijter VN, Mintenig SM, Verschoor A, Koelmans AA. Ingestion and Chronic Effects of Car Tire Tread Particles on Freshwater Benthic Macroinvertebrates. Environmental Science & Technology 2018; 52: 13986-13994.
Rietveld M, Clemens F, Langeveld J. Solids dynamics in gully pots. Urban Water Journal 2020; 17: 669-680.
Rietveld M, Clemens F, Langeveld J. Monitoring and characterising the solids loading dynamics to drainage systems via gully pots. Urban Water Journal 2021; 18: 699-710.
Robinson T, Schulte-Herbrüggen H, Mácsik J, Andersson J. Raingardens for stormwater management: Potential of raingardens in a Nordic climate. In: Trafikverket, editor. Trafikverkets publikationer, Borlänge, 2019, pp. 61.
Rochman CM, Regan F, Thompson RC. On the harmonization of methods for measuring the occurrence, fate and effects of microplastics. Analytical Methods 2017; 9: 1324-1325.
Rockström J, Steffen W, Noone K, Persson Å, Chapin FSI, Lambin E, et al. Planetary boundaries:exploring the safe operating space for humanity. Ecology and Society 2009; 14: 32.
Rogge WF, Hildemann LM, Mazurek MA, Cass GR, Simoneit BR. Sources of fine organic aerosol. 3. Road dust, tire debris, and organometallic brake lining dust: roads as sources and sinks. Environmental Science & Technology 1993; 27: 1892-1904.
Rødland ES, Lind OC, Reid M, Heier LS, Skogsberg E, Snilsberg B, et al. Characterization of Tire and Road Wear Microplastic Particle contamination in a Road Tunnel: from surface to release. Journal of Hazardous Materials 2022 (accepted April 26th).
Rødland ES, Lind OC, Reid MJ, Heier LS, Okoffo ED, Rauert C, et al. Occurrence of tire and road wear particles in urban and peri-urban snowbanks, and their potential environmental implications. Science of The Total Environment 2022a; 824: 153785.
Rødland ES, Samanipour S, Rauert C, Okoffo ED, Reid MJ, Heier LS, et al. A novel method for the quantification of tire and polymer-modified bitumen particles in environmental samples by pyrolysis gas chromatography mass spectroscopy. Journal of Hazardous Materials 2022b; 423: 127092.
Saba RG, Uthus N, Aurstad J. Long-term performance of asphalt surfacings containing polymer modified binders. In 5th Eurasphalt & Eurobitume Congress. , 2012.
Salbu B, Rosseland BO, Oughton DH. Multiple stressors—a challenge for the future. Journal of Environmental Monitoring 2005; 7: 539-539.
Salbu B, Teien HC, Lind OC, Tollefsen KE. Why is the multiple stressor concept of relevance to radioecology? International Journal of Radiation Biology 2019; 95: 1015-1024.

SAPEA. A Scientific Perspective on Microplastics in Nature and Society. In: Academies SAfPbE, editor, Berlin, 2019.
Sarkar B., S. M. Microbial Degradaion of Natural and Synthetic Rubbers. In: M. S, editor. Microbial Bioremediation & Biodegradation. Springer, Singapore, 2020.
Schuler MS, Relyea RA. A Review of the Combined Threats of Road Salts and Heavy Metals to Freshwater Systems. BioScience 2018; 68: 327-335.
Seiwert B, Klöckner P, Wagner S, Reemtsma T. Source-related smart suspect screening in the aqueous environment: search for tire-derived persistent and mobile trace organic contaminants in surface waters. Analytical and bioanalytical chemistry 2020; 412: 4909-4919.
Seiwert B, Nihemaiti M, Troussier M, Weyrauch S, Reemtsma T. Abiotic oxidative transformation of 6-PPD and 6-PPD quinone from tires and occurrence of their products in snow from urban roads and in municipal wastewater. Water Research 2022; 212: 118122.
Sengoz B, Topal A, Isikyakar G. Morphology and image analysis of polymer modified bitumens. Construction and Building Materials 2009; 23: 1986-1992.
Shan S, Zhang Y, Zhao H, Zeng T, Zhao X. Polystyrene nanoplastics penetrate across the blood-brain barrier and induce activation of microglia in the brain of mice. Chemosphere 2022; 298: 134261.
Sheng Y, Liu Y, Wang K, Cizdziel JV, Wu Y, Zhou Y. Ecotoxicological effects of micronized car tire wear particles and their heavy metals on the earthworm (Eisenia fetida) in soil. Science of The Total Environment 2021; 793: 148613.
Sieber R, Kawecki D, Nowack B. Dynamic probabilistic material flow analysis of rubber release from tires into the environment. Environmental Pollution 2020; 258: 113573.
Skocaj M, Filipic M, Petkovic J, Novak S. Titanium dioxide in our everyday life; is it safe? Radiology and oncology 2011; 45: 227-247.
Sommer F, Dietze V, Baum A, Sauer J, Gilge S, Maschowski C, et al. Tire Abrasion as a Major Source of Microplastics in the Environment. Aerosol and Air Quality Research 2018; 18: 2014-2028.
Spies RB, Andresen BD, Rice Jr DW. Benzthiazoles in estuarine sediments as indicators of street runoff. Nature 1987; 327: 697-699.
SSB. Kjørelengder (driving distance). In: Statistisk sentralbyrå (Statistics Norway), 2019.
Steffen W, Richardson K, Rockström J, Cornell SE, Fetzer I, Bennett EM, et al. Planetary boundaries: Guiding human development on a changing planet. Science 2015; 347: 1259855.
Su L, Cai HW, Kolandhasamy P, Wu CX, Rochman CM, Shi HH. Using the Asian clam as an indicator of microplastic pollution in freshwater ecosystems. Environmental Pollution 2018; 234: 347-355.
Sun J, Ho SSH, Niu X, Xu H, Qu L, Shen Z, et al. Explorations of tire and road wear microplastics in road dust PM2.5 at eight megacities in China. Science of The Total Environment 2022; 823: 153717.
Sundt P, S. R, Haugedal TR, Schulze P-E. Norske landbaserte kilder til mikroplast (Norwegian land-based sources to microplastics). MEPEX, Oslo, 2021, pp. 88.
Sundt P, Schulze P-E, Syversen F. Sources of microplastic-pollution to the marine environment, 2014, pp. 86.
Sundt P, Syversen F, Skogesal O, Schulze P-E. Primary microplastic-pollution: Measures and reduction potentials in Norway, 2016, pp. 117.
Team R. RStudio: Integrated Development for R. RStudio, PBC, Boston, MA, 2020.
Thorpe A, Harrison RM. Sources and properties of non-exhaust particulate matter from road traffic: A review. Science of The Total Environment 2008; 400: 270-282.
Tian Z, Gonzalez M, Rideout CA, Zhao HN, Hu X, Wetzel J, et al. 6PPD-Quinone: Revised Toxicity Assessment and Quantification with a Commercial Standard. Environmental Science & Technology Letters 2022; 9: 140-146.
Tian Z, Zhao H, Peter KT, Gonzalez M, Wetzel J, Wu C, et al. A ubiquitous tire rubber–derived chemical induces acute mortality in coho salmon. Science 2021; 371: 185-189.
UN. Transforming our world: the 2030 Agenda for Sustainable Development In: Nations U, editor. 70/1, The United Nations Sustainable Development Summit on 25 September 2015, 2015.

UNEP. Drowning in Plastics – Marine Litter and Plastic Waste Vital Graphics. . In: United Nations Environment Programme (UNEP) SotB, Rotterdam and Stockholm Conventions (BRS) and GRID-Arendal., editor, 2021.
UNEP. Draft resolution: End plastic pollution: Towards an international legally binding instrument (Advance March 2., 2022). In: (UNEP) UNEAotUNEP, editor. United Nations, Nairobi, 2022.
Unice KM, Bare JL, Kreider ML, Panko JM. Experimental methodology for assessing the environmental fate of organic chemicals in polymer matrices using column leaching studies and OECD 308 water/sediment systems: Application to tire and road wear particles. Sci Total Environ 2015; 533: 476-87.
Unice KM, Kreider ML, Panko JM. Use of a Deuterated Internal Standard with Pyrolysis-GC/MS Dimeric Marker Analysis to Quantify Tire Tread Particles in the Environment. International Journal of Environmental Research and Public Health 2012a; 9.
Unice KM, Kreider ML, Panko JM. Use of a Deuterated Internal Standard with Pyrolysis-GC/MS Dimeric Marker Analysis to Quantify Tire Tread Particles in the Environment. International Journal of Environmental Research and Public Health 2012b; 9: 4033-4055.
Unice KM, Kreider ML, Panko JM. Comparison of Tire and Road Wear Particle Concentrations in Sediment for Watersheds in France, Japan, and the United States by Quantitative Pyrolysis GC/MS Analysis. Environmental Science & Technology 2013; 47: 8138-8147.
Unice KM, Weeber MP, Abramson MM, Reid RCD, van Gils JAG, Markus AA, et al. Characterizing export of land-based microplastics to the estuary - Part I: Application of integrated geospatial microplastic transport models to assess tire and road wear particles in the Seine watershed. Science of The Total Environment 2019; 646: 1639-1649.
Varshney S, Gora AH, Siriyappagouder P, Kiron V, Olsvik PA. Toxicological effects of 6PPD and 6PPD quinone in zebrafish larvae. Journal of Hazardous Materials 2022; 424: 127623.
Vegvesen S. Road lengths with polymer-modified bitumen, 2020.
Vijayan A, Österlund H, Magnusson K, Marsalek J, Viklander M. Microplastics pathways in the urban environment: Urban roadside snowbanks. . Nivatech, 2019.
Vijayan A, Österlund H, Marsalek J, Viklander M. Estimating Pollution Loads in Snow Removed from a Port Facility: Snow Pile Sampling Strategies. Water, Air, & Soil Pollution 2021; 232: 75.
Viklander M. Urban snow deposits—pathways of pollutants. Science of The Total Environment 1996; 189-190: 379-384.
Viklander M. Snow quality in the city of Luleå, Sweden — time-variation of lead, zinc, copper and phosphorus. Science of The Total Environment 1998; 216: 103-112.
Viklander M. Substances in Urban Snow. A comparison of the contamination of snow in different parts of the city of Luleå, Sweden. Water, Air, and Soil Pollution 1999; 114: 377-394.
Villarrubia-Gómez P, Cornell SE, Fabres J. Marine plastic pollution as a planetary boundary threat – The drifting piece in the sustainability puzzle. Marine Policy 2018; 96: 213-220.
Vinay Kumar BN, Löschel LA, Imhof HK, Löder MGJ, Laforsch C. Analysis of microplastics of a broad size range in commercially important mussels by combining FTIR and Raman spectroscopy approaches. Environmental Pollution 2021; 269: 116147.
Vogelsang C, Kristiansen T, Singdahl-Larsen C, Buenaventura N, Pakhomova S, Eidsvoll DP, et al. Mikroplastpartikler inn til og ut fra Bekkelaget renseanlegg gjennom ett år. Norwegian insitute for water research, 2020, pp. 158.
Vogelsang C, Lusher AL, Dadkhah ME, Sundvor I, Umar M, Ranneklev SB, et al. Microplastics in road dust – characteristics, pathways and measures, 2018.
Vollertsen J, Stephansen DA, Nielsen AH, Andersen AF, Lockwood A. PROPER - WP 3 - SUSTAINABLE ASSESSMENT OF MEASURES AND TREATMENT SYSTEMS FOR ROAD RUNOFFS. Task 3.1. Literature Review on Blue-Green Treatment Solutions. University of Aalborg, Aalborg, 2019.
Wagner S, Huffer T, Klockner P, Wehrhahn M, Hofmann T, Reemtsma T. Tire wear particles in the aquatic environment - A review on generation, analysis, occurrence, fate and effects. Water Research 2018; 139: 83-100.
Wagner S, Klöckner P, Reemtsma T. Aging of tire and road wear particles in terrestrial and freshwater environments – A review on processes, testing, analysis and impact. Chemosphere 2022; 288: 132467.
Wagner S, Reemtsma T. Things we know and don't know about nanoplastic in the environment. Nature Nanotechnology 2019; 14: 300-301.

Werkenthin M, Kluge B, Wessolek G. Metals in European roadside soils and soil solution – A review. Environmental Pollution 2014; 189: 98-110.
Wickham H, François R, Henry L, Müller K. R package version 0.7.6. dplyr: A Grammar of Data Manipulation., 2018.
Wik A, Dave G. Occurrence and effects of tire wear particles in the environment - A critical review and an initial risk assessment. Environmental Pollution 2009; 157: 1-11.
Wik A, Lycken J, Dave G. Sediment Quality Assessment of Road Runoff Detention Systems in Sweden and the Potential Contribution of Tire Wear. Water, Air, and Soil Pollution 2008; 194: 301-314.
Winston RJ, Hunt WF. Characterizing Runoff from Roads: Particle Size Distributions, Nutrients, and Gross Solids. Journal of Environmental Engineering 2017; 143.
Wright SL, Thompson RC, Galloway TS. The physical impacts of microplastics on marine organisms: A review. Environmental Pollution 2013: 1-10.
Xu J-L, Thomas KV, Luo Z, Gowen AA. FTIR and Raman imaging for microplastics analysis: State of the art, challenges and prospects. TrAC Trends in Analytical Chemistry 2019; 119: 115629.
Youn J-S, Kim Y-M, Siddiqui MZ, Watanabe A, Han S, Jeong S, et al. Quantification of tire wear particles in road dust from industrial and residential areas in Seoul, Korea. Science of The Total Environment 2021; 784: 147177.
Zakaria MP, Takada H, Tsutsumi S, Ohno K, Yamada J, Kouno E, et al. Distribution of polycyclic aromatic hydrocarbons (PAHs) in rivers and estuaries in Malaysia: a widespread input of petrogenic PAHs. Environmental science & technology 2002; 36: 1907-1918.
Zeng EY, Tran K, Young D. Evaluation of potential molecular markers for urban stormwater runoff. Environmental monitoring and assessment 2004; 90: 23-43.
Zhang J, Zhang X, Wu L, Wang T, Zhao J, Zhang Y, et al. Occurrence of benzothiazole and its derivates in tire wear, road dust, and roadside soil. Chemosphere 2018; 201: 310-317.
Aaneby J, Johnsen IV. Prøvetaking og analyser av sideterreng langs vei
Forsvarets Forskningsintitutt (FFI), 2019.

8 Scientific papers

Paper I

Science of the Total Environment 738 (2020) 139352

Contents lists available at ScienceDirect

Science of the Total Environment

journal homepage: www.elsevier.com/locate/scitotenv

Review

Road de-icing salt: Assessment of a potential new source and pathway of microplastics particles from roads

Elisabeth S. Rødland [a,b,*], Elvis D. Okoffo [d], Cassandra Rauert [d], Lene S. Heier [c], Ole Christian Lind [b], Malcolm Reid [a], Kevin V. Thomas [d], Sondre Meland [a,b]

[a] Norwegian Institute for Water Research, Gaustadalléen 21, N-0349 Oslo, Norway
[b] Norwegian University of Life Sciences, Center of Environmental Radioactivity (CERAD CoE), Faculty of Environmental Sciences and Natural Resource Management, P.O. Box 5003, 1433 Ås, Norway
[c] Norwegian Public Roads Administration, Construction, Postboks 1010, N-2605 Lillehammer, Norway
[d] Queensland Alliance for Environmental Health Sciences (QAEHS), The University of Queensland, 20 Cornwall Street, Woolloongabba, 4102, QLD, Australia

HIGHLIGHTS

- Road de-icing salt is potentially a source of microplastic (MP) to the environment
- Rubber-like particles constituted 96% of the total concentration of MPs in road salt
- Eleven different polymers were confirmed present in road salt
- MP release was calculated based on road salt emissions in Norway, Sweden and Denmark
- Compared to other sources of MP from roads, contribution from road salt is negligible

GRAPHICAL ABSTRACT

Illustration of road salt with microplastic particles released onto the roads. Illustrations created using Adobe Illustrator and free vectors from Freepik.

ARTICLE INFO

Article history:
Received 12 March 2020
Received in revised form 8 May 2020
Accepted 9 May 2020
Available online 02 June 2020

Editor: Damia Barcelo

Keywords:
Plastic pollution
Salt
Road
FTIR
Pyrolysis-GC–MS

ABSTRACT

Roads are estimated to be the largest source of microplastic particles in the environment, through release of particles from tires, road markings and polymer-modified bitumen. These are all released through the wear and tear of tires and the road surface. During the winter in cold climates, the road surface may freeze and cause icing on the roads. To improve traffic safety during winter, road salt is used for de-icing. Knowledge of microplastic (MP) contamination in road salt has, until now, been lacking. This is contrary to the increasing number of studies of microplastics in food-grade salt. The objective of this study was to investigate if road salt could be an additional source of microplastics to the environment. Fourier-Transform Infrared spectroscopy (FT-IR) and Pyrolysis gas chromatography mass spectrometry (GC–MS) were employed to identify and quantify the polymer content in four types of road salts, three sea salts and one rock salt. The particle number of MP in sea salts (range 4–240 MP/kg, mean ± s.d. = 35 ± 60 MP/kg) and rock salt (range 4–192 MP/kg, 424 ± 61 MP/kg, respectively) were similar, whereas, MP mass concentrations were higher in sea salts (range 0.1–7650 μg/kg, 442 ± 1466 μg/kg) than in rock salts (1–1100 μg/kg, 322 ± 481 μg/kg). Black rubber-like particles constituted 96% of the total concentration of microplastics and 86% of all particles in terms of number of particles/kg. Black rubber-like particles appeared to be attributable to wear of conveyer belts used in the salt production. Road salt

* Corresponding author at: Norwegian Institute for Water Research, Gaustadalléen 21, N-0349 Oslo, Norway.
E-mail address: elisabeth.rodland@niva.no (E.S. Rødland).

https://doi.org/10.1016/j.scitotenv.2020.139352

contribution to MP on state and county roads in Norway was estimated to 0.15 t/year (0.003% of total road MP release), 0.07 t/year in Sweden (0.008%) and 0.03 t/year in Denmark (0.0004–0.0008%) Thus, microplastics in road salt are a negligible source of microplastics from roads compared to other sources.

Contents

1. Introduction

Microplastic pollution has gained a lot of attention the last few years, with an increasing number of studies detecting microplastic particles (MPs) in all types of environments (GESAMP, 2016). Although there has been a predominant focus on microplastics in marine environments, it has been suggested that the majority of the plastic contamination in the marine ecosystem comes from terrestrial sources (Andrady, 2011; Frias et al., 2016; Rochman, 2018). MPs are particles in the size range of 1 nm to <5 mm (GESAMP, 2016). In Norway, current estimates indicate a total annual emission of 8400 t of microplastic (Sundt et al., 2014), with an annual release of approximately 5500 t (Sundt et al., 2014; Sundt et al., 2016; Vogelsang et al., 2018) originating from the transport sector (Table S7). A significant proportion of this is expected to be able to reach the aquatic environment (Sundt et al., 2014). Car tire particles released from tire wear (TWP) have been proposed as the main source of MP particles generated on roads, with an annual emission of approximately 5000 t (Sundt et al., 2014; Sundt et al., 2016; Vogelsang et al., 2018). Similar assessments in Sweden and Denmark have also concluded that tires are the main source of microplastic particles from roads (Hann et al., 2018; Lassen et al., 2015; Magnusson et al., 2017; Sundt et al., 2014; Sundt et al., 2016). In addition to TWP, road wear particles from road markings (RWP_{RM}) and polymer-modified bitumen (RWP_{PMB}) have been identified as significant sources (Sundt et al., 2014; Sundt et al., 2016; Vogelsang et al., 2018). The yearly emission of RWP_{RM} is estimated to be 100–300 t in Norway, 500 t in Sweden and 700 t in Denmark. The annual emission of RWP_{PMB} is estimated to be 30 t in Norway and 15 t Sweden (Sundt et al., 2014; Sundt et al., 2016; Vogelsang et al., 2018).

Until now, the application of road salt has not been addressed in terms of a source and pathway of microplastics to the environment. In cold climate regions, substantial amounts of road salt (sodium chloride, NaCl) is used for de-icing to maintain traffic safety during winter (Marsalek, 2003), and the amount of road salt used in several countries has increased dramatically since the 1950s (Schuler and Relyea, 2018). In the United States, approximately 1 million tonnes of road salt were applied in the 1950, and by 2017 this had increased with about 95%, to approximately 22 million tonnes of salt per year (Kelly et al., 2019; Schuler and Relyea, 2018, Table S1). Other countries with high road salt consumptions are Canada (7 million tonnes; Environment Canada, 2012) and China (600,000 t, Ke et al., 2013). The basis for this study is the emission of road salt in Norway, Sweden and Denmark, where 320,000 t, 210,000 t and 55,000 t of salt is used every year (Statens vegvesen, 2019a; Trafikverket, 2019; Vejdirektoratet, 2019a). Even though the total road salt consumption differs a lot between countries, so does the total length of their road network, from about 63,000 kilometer (km) in Norway (state and county roads) to 4.3 million km of paved roads in China (Table S1, CIA, 2017; Government of Canada, 2018; Statens vegvesen, 2019b; Trafikverket, 2017; US Department of Transportation, 2017; Vejdirektoratet, 2019b). Adjusting for the length of the road network, the salt consumption in both Norway and the United States is comparable and probably among the highest in the

world, with approximately 5 t of salt per km road (tonnes/km), with Canada on top with a consumption of over 6 t/km per year. In Sweden, the consumption is less than half of Norway and the United States, with about 2 t/km and in Denmark even lower, <1 t/km (Table S1, CIA, 2017; Government of Canada, 2018; Statens vegvesen, 2019b; Trafikverket, 2017; US Department of Transportation, 2017; Vejdirektoratet, 2019b).

Environmental concerns have arisen due to the amount of road salt applied in many countries, and it is now considered a major threat to freshwater systems in countries with temperate climates (Demers, 1992; Fay and Shi, 2012; Findlay and Kelly, 2011; Karraker et al., 2008; Tiwari and Rachlin, 2018). This is mainly due to the increasing salinity concentrations, which result in negative ecological effects on rivers, wetland and lakes, as well as threatening valuable drinking water. Recent studies have shown that food-grade salt can act as carrier for microplastic particles (MPs) (Gündoğdu, 2018; Iniguez et al., 2017; Karami et al., 2017; Kim et al., 2018; Lee et al., 2019; Seth and Shriwastav, 2018; Yang et al., 2015). Hence, the presence of MPs in salt used for de-icing purposes may also contribute to releases of MPs in the environment.

Several studies have identified MPs in both sea salt and rock salt used for food consumption (Gündoğdu, 2018; Iniguez et al., 2017; Karami et al., 2017; Kim et al., 2018; Lee et al., 2019; Seth and Shriwastav, 2018; Yang et al., 2015). The number of MPs found in food grade sea salt varies widely (n.d.–13,629 MP/kg), whereas the variation found for food grade rock salt is smaller (7–462 MP/kg). Sea salt originating from Asia, Oceania, Africa, South America, North America and Europe have been investigated, and in one of the studies (Kim et al., 2018) the number of MPs found in sea salt were significantly correlated to the number of MPs found in both rivers and seawater of areas were the sea salts are produced. The positive correlation between microplastics in sea salt and microplastics found in sea water has been discussed in several other studies (Gündoğdu, 2018; Lee et al., 2019; Seth and Shriwastav, 2018; Yang et al., 2015), as well as how urbanisation and human activities can potentially contaminate the sea salt at the production sites (Gündoğdu, 2018) in order to explain the variation found in the samples. The results of the food-grade studies indicate that sea salt is more contaminated with microplastics compared to rock salt, and that the sea water microplastic contamination can be transferred to sea salt. However, the presence of MPs in rock salts suggests contamination during production, transportation and packaging, indicating that salt also can act as a source of microplastics and not just a pathway of contaminated sea water.

The enormous quantity of road salt applied on roads during winter, together with recent understanding about MPs in food-grade salt therefore raised the question as to whether road salt could be a fourth significant source of MP in the environment from roads. The present study's main objective was to investigate if MP particles are present in road salt, and to estimate the potential emission of these MPs in Norway, Sweden and Denmark.

2. Materials and method

2.1. Sample collection

Salt used for de-icing purposes was provided by GC Rieber (www.gcrieber-salt.no), which is the main salt distributor in Norway and Denmark. The sea salt originated from three different locations in the Mediterranean Sea: Torrevieja in Spain, and Zarziz and Ben Gardene in Tunisia (Fig. 1). One site of rock salt, originating from Bernburg, Germany, was also included in the study to be able to compare rock salt with the sea salt. The samples from Zarziz, Ben Gardene and Bernburg were between 2 and 5 kg, and were sampled directly from the salt piles at the GC Rieber storage unit at Sjursøya in Oslo, Norway. The salt from Torrevieja was pre-packed as a food-grade salt for commercial sales in a 2-kg polyethylene (PE) bag, packed in Oslo (the polymer type of the bag was tested in this study, see SI). The Torrvieja salt is the same salt used for road purposes. The salt from different locations was stored separately to avoid mixing.

2.2. Sample treatment

Sub-samples were taken from each of the salt sample bags, adding up to 250 g of salt. This was inserted in a 1000 mL bottle. Three technical replicates were taken from each salt sample. The subsampling took place in a sterile cabinet using a metal spoon to collect subsamples from different areas in the sample to total 250 g. To dissolve the salt, 1000 mL of filtered reverse osmosis (RO) water (0.22 μm membrane filters) was added to each bottle and the bottles were incubated at 60 °C and 100 rpm for 24 h. All bottles and equipment used in the laboratory analyses were rinsed with filtered RO water three times before use. To be able to identify any MPs present in the salt samples, the samples were filtered under vacuum onto glass fibre filters (Whatman GF/D, pore size 2.7 μm). For the sample prepared for Pyrolysis GC–MS, one technical replicate of 250 g of salt was taken from the sample and dissolved in 1000 mL filtered RO-water. Then a subsample of 500 mL of dissolved salt was filtered onto GF-filters (Whatman GF/A, 25 mm diameter, 1.6 μm pore size). All filters were placed in sealed petri dishes and dried at room temperature for at least one week.

2.3. Visual analysis and FTIR

The filters were examined using a stereomicroscope with Infinity 1-3C camera and INFINITY ANALYSE and CAPTURE software v6.5.6 to take pictures and to measure size (length, width and depth) of all particles found. For this study, the upper size limit is 5 mm (GESAMP, 2016) and lowest size limits are set by the pore size of the filters used for the Fourier-Transformed Infra-Red Spectrometry (FTIR)-analysis and the Pyrolysis gas chromatography mass spectrometry (GC–MS) (2.7 μm and 1.6 μm, respectively). Colour and morphology were also described for each particle. The categories for morphology were fibres, fibre bundles, fragments, spheres, pellets, foams, films and beads (Lusher et al., 2017; Rochman et al., 2019).

All particles considered by the visual inspection in stereomicroscope to be possible polymers were analysed using Fourier-Transformed Infra-Red Spectrometry (FTIR). The largest fragments (>200 μm) were analysed with single point measurement Attenuated Total Reflectance - Fourier Transformed Infra-Red Spectrometry (ATR-FT-IR) using a Cary 630 FT-IR Spectrometer from Agilent. Smaller particles (59–200 μm, longest axis) and all fibres were analysed with a FT-IR diamond compression cell in μ-transmission using a Spotlight 400 FT-IR Imaging system from Perkin Elmer. The particles were analysed with the full wavelength of the FT-IR (4000–600 cm^{-1}) and resolution of 4 cm^{-1}. The results were compared to the available libraries on each instrument. On the ATR-FT-IR, the results were compared to the Agilent Polymer Handheld ATR Library and the Elastomer O-ring and Seal Handheld ATR Library. On the FT-IR, the results were compared to the reference database from Primpke et al. (2018), the Perkin Elmer ATR Polymer Library and three inhouse reference libraries for rubbers, reference polymers and non-plastic particles. The spectra of all analysed particles were manually inspected. According to the methodology of Lusher et al. (2013) and recommended by the MSFD Technical Subgroup on Marine Litter (2013), only matches of 0.7 or above should be accepted. In this study we have included also matches between 0.7 and 0.6, as we have manually inspected all spectra.

2.4. Pyrolysis GC–MS

There were a large number of particles with rubber-like properties in the samples which could not be analysed using FTIR. Therefore, salt from the site where these particles were most abundant (Ben Gardene) were re-analysed using Pyrolysis GC–MS. The Pyrolysis GC–MS analysis was

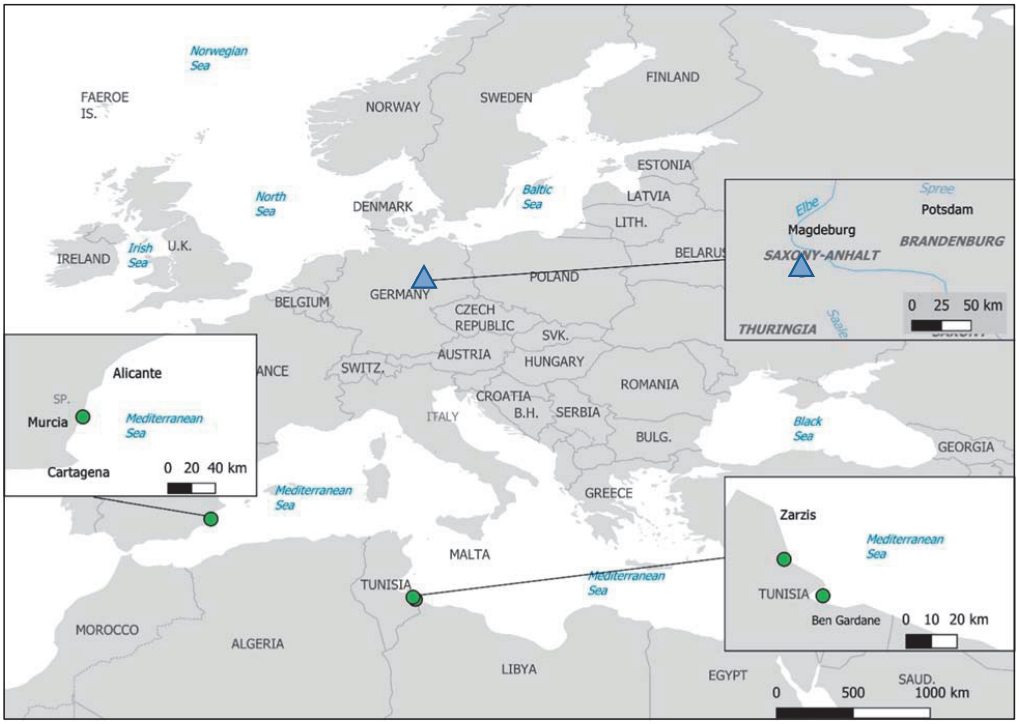

Fig. 1. Map over salt production sites Torrvieja (Spain), Zarziz and Ben Gardene (Tunisia) and Bernburg (Germany), created in QGis (Natural Earth Package).

carried out using a multi-shot micro-furnace pyrolyzer (EGA/PY-3030D) with an auto-shot sampler (AS-1020E) (both Frontier Lab, Fukushima, Japan) attached to a Shimadzu Gas Chromatography—Mass Spectrometer (GC–MS) - QP2010-Plus (Shimadzu Corporation, Japan) equipped with an Ultra Alloy® 5 capillary column (Frontier Lab). Detailed Pyrolysis GC–MS conditions are summarized in Table 1.

Table 1
Instrumental conditions for Pyrolysis-GC–MS measurements.

Apparatus	Parameters	Settings
Micro-furnace Pyrolyzer Frontier EGA/PY-3030D (Single-Shot analysis)	Pyrolyzer furnace/oven temperature	650 °C
	Pyrolyzer interface temperature	320 °C
	Pyrolysis time	0.20 min (12 s)
Gas chromatogram (GC)	Column	Ultra-Alloy® 5 capillary column (30 m, 0.25 mm I.D., 0.25 μm film thickness) (Frontier Lab)
	Injector port temperature	300 °C
	Column oven temperature program	40 °C (2 min) → (20 °C/min) → 320 °C (14 min)
	Injector mode	Split (split 50:1)
	Carrier gas	Helium, 1.0 mL/min, constant linear velocity
Mass spectrometer (MS)	Ion source temperature	250 °C
	Ionization energy	Electron ionization (EI); 70 eV
	Scan mode/range	Selected ion monitoring (SIM) mode, 40 to 600 *m/z*

To identify and quantify single polymers in samples, specific indicator ions were chosen by pyrolyzing polymer standards. The polymers analysed included PE (Sigma-Aldrich, St. Louis, MO, USA), Poly (methyl-methacrylate) (PMMA: Sigma-Aldrich, St. Louis, MO, USA), Polystyrene (PS: Sigma-Aldrich, St. Louis, MO, USA), Polyvinylchloride (PVC: Sigma-Aldrich, St. Louis, MO, USA), Polypropylene (PP: NIVA, Oslo, Norway), Polyethylene terephthalate (PET: Goodfellow, Cambridge, UK) and Polycarbonate (PC: NIVA, Oslo, Norway), as described and identified according to Okoffo et al. (2020), and also Styrene butadiene rubber (SBR) (SBR1500: Polymer Source, Quebec, Canada) (Table 2). For all polymers except for SBR, external calibration curves, ranging from 0.1 to 100 μg and having $R^2 \geq 0.95$, were obtained by extracting polymer standards with pressurized liquid extraction (PLE) (ASE 350, Dionex, Sunyvale, CA) using dichloromethane (DCM) at 180 °C and 1500 psi, with a heat and static-time of 5 min using three extraction cycles. The final extract was analysed in an 80 μL pyrolysis cup (PY1-EC80F, Eco-Cup LF, Frontier Laboratories, Japan). For further PLE details and discussion including extraction parameters, recoveries and application, see Okoffo et al. (2020). For SBR, the external calibration curve ranging from 0.1 to 100 μg having $R^2 = 0.99$, was made in chloroform (Table 3), following the method described in the ISO method (ISO/TS 21396:2017, 2017).

To analyse for plastics, the 1.6 μm glass fibre filters used for the filtration of the samples were cut into three pieces with a pre-cleaned (with acetone and DCM) stainless steel scalpel, rolled and inserted into three pyrolysis cups for Pyrolysis-GC–MS analysis. Deuterated polystyrene (PS-d5; 216 μg/mL in DCM) and deuterated Poly(1,4-butadiene-d6) (7.6 mg/mL in chloroform) (both from Polymer Source, Inc., Quebec, Canada) were used as internal standards with 10 μL added directly to the calibration standards and samples in the cups, allowing the solvent to subsequently evaporate at room temperature.

Table 2
Selected plastic indicator compounds. Italics and bold values used for calibration and quantification.

Plastic	Pyrolysis product	Indicator ions (*m/z*)	Molecular ion (*m/z*)	Retention time (min)	Calibration range (μg/cup)	LOD (μg/kg)	LOQ (μg/kg)	Linearity (R^2)
Polypropylene (PP)	2,4-Dimethyl-1-heptene	70, 83, ***126***	126	4.53	0.2–100	0.90	2.72	0.98
Polystyrene (PS)	5-Hexene-1,3,5-triyltribenzene (styrene trimer)	***91***, 117, 194, 312	312	15.80	0.1–100	0.61	1.84	0.97
Poly-(methyl methacrylate) (PMMA)	Methyl methacrylate	69, ***100***, 89	100	2.95	0.4–100	1.58	4.80	0.99
Polyethylene terephthalate (PET)	Vinyl benzoate	***105***, 77, 148, 51	148	7.61	0.3–100	1.42	4.31	0.99
Polycarbonate (PC)	Bisphenol A (BA)	***213***, 119, 91, 165, 228	228	14.52	0.5–100	1.90	5.74	0.95
Polyethylene (PE)	1-Decene (C10)	***83***, 97, 111, 140	140	6.22	0.2–100	0.93	2.83	0.97
Polyvinyl chloride (PVC)	Benzene	***78***, 74, 52	78	2.44	0.4–100	1.98	6.00	0.96
Styrene butadiene rubber (SBR)	4-Vinylcyclohexene	*39*, ***54***, *79*, *108*	108	4.36	0.1–100	1.71	5.18	0.99
Internal standard								
Polystyrene-d5	Styrene-d5	***109***, 82, 54, 107		5.10				
Poly(1,4-butadiene-d6)		***60***, *120*, 42, 86		4.28				

2.5. Concentration calculations

Length, width and depth of each particle were used to calculate the volume of the particle. This has been done in a few studies before, in order to obtain the concentrations of particles (Hermabessiere et al., 2018; Kim et al., 2018; Simon et al., 2018). For some particles, the depth was difficult to measure in the microscope due to the small size and irregular shape of the particle (fragments). For these particles, the depth was determined by width/2. Previous studies have assumed that the ratio between the depth and the width is the same as the ratio between the width and the length of a particle (Simon et al., 2018). Using the same approach, we determined the mean ratio of width and length for all MP fragments found in the salt sample to be 0.4 ± 0.4. For simplification purposes, we have assumed that all fragments have a depth which corresponds to 50% of the width of the particle. For the particles with confirmed polymer matches, the volume of the particle and the density of the polymer type was used to calculate mass of each particle.

2.6. Quality control and quality assurance

To avoid contamination in the process of sample treatment to analysis, a clean, enclosed lab designed for microplastic analysis was used throughout the study. Lint removal were used on the cotton laboratory coats before working in the lab, and all glassware and equipment were washed and rinsed with filtered RO-water. For each day of sample filtration (2.5 days), control samples (1000 mL filtered RO water in 1000 mL bottles) were filtered ($n = 3$ for days 1 and 2, $n = 2$ for third day).

As we have chosen to only focus on polymer particles found in road salt, i.e. excluding the natural and semisynthetic particles, only the confirmed polymers (match >0.6) is used to calculate the Limit of Detection (LOD) and the Limit of Quantification (LOQ). LOD and LOQ are indictors used to explain the detectable limits of the method (i.e. the lowest concentration that is detectable) and the concentrations that can be quantified in samples, respectively. These two indictors are used in instrumental analysis of organic compounds, especially when using GCMS to report the detectable and quantifiable limits. For the samples analysed with visual inspection and FT-IR, we calculated the LOD and LOQ using the mean number of particles (μx) and the standard deviation (σx) in the following equations:

$$LOD = \mu x + (\sigma x * 3) \quad (1)$$

$$LOQ = \mu x + (\sigma x * 10) \quad (2)$$

For the samples analysed with Pyrolysis GC–MS, the LOD and LOQ for each polymer was calculated by multiplying the standard deviation (σx) of 7 replicate injections of the lowest calibration standard spiked on a 1.6 μm glass fibre filter with 3.3 and 10 respectively. LOD and LOQ values were then divided by the weight (kg) of sample (Table 3).

$$LOD = \sigma x * 3.3 \quad (3)$$

$$LOQ = \sigma x * 10 \quad (4)$$

Each Pyrolysis GC–MS run featured a calibration standard check and a blank (clean pyrolysis cup) every ten sample injections. Instrument blanks (no pyrolysis cup) were run between each batch of samples to avoid cross contamination, and a quality control and quality assurance sample (QAQC) sample was injected at the beginning and end of each run.

Table 3
Comparison between polymer concentrations found in the sample from Ben Gardene using calculated mass of each particle and using Pyrolysis GC–MS for bulk concentration, MP per kilo (μg/kg). Polymer types: polyethylene terephthalate (PET), polyethylene (PE), polyvinyl chloride (PVC), polypropylene (PP), Poly(methyl methacrylate) (PMMA), Polycarbonate (PC) and Styrene Butadiene Rubber (SBR).

Site	Polymer	Estimated (visual + FT-IR) μg/kg ± s.d.	Measured (Pyrolysis GC–MS) μg/kg
Ben Gardene	PS	Not detected	6.0
Ben Gardene	PP	Not detected	13.8
Ben Gardene	PET	126.4 ± 173.3	105.5
Ben Gardene	BRP (PVC/SBR)	4463.6 ± 2759.7	–
Ben Gardene	PVC	–	1754.3
Ben Gardene	SBR	–	87.3
Ben Gardene	PE	116.8	302.3
Ben Gardene	PMMA	Not detected	Not detected
Ben Gardene	PC	Not detected	Not detected

2.7. Emissions of MPs in road salt

To compare the emission of MPs from road salt to the emissions of RAMP in Norway, Sweden and Denmark, the mean calculated concentrations of microplastics for each salt type (sea salt or rock salt) was multiplied with the amount of road salt released in each country. The amount and type of road salt used in Norway, Sweden and Denmark differs greatly. The amount of salt used is mainly dependent on the weather conditions of each winter season and might therefore fluctuate between years. However, the trend for the past 15 years shows an increase in the salt consumption on state and county roads in Norway (Fig. 2). According to the Norwegian Public Roads Administration (Statens vegvesen, 2019a), both the change in weather conditions (increased number of days with temperatures fluctuating around 0 °C), and the expansion of road networks is responsible for this increase. In Sweden, the salt consumption has followed a negative trend since 2007 compared to the amount used in 2003–2006, and for the last 4 years Sweden has used close to half the amount of road salt that was used on state and county roads in Norway. In Denmark, only data from 2011 to 2018 was available. Compared to Norway and Sweden, the salt consumption in Denmark is considerably lower.

2.8. Statistical analysis

The descriptive statistical analysis of the data was conducted in RStudio 1.2.5001 (RStudio, 2019), using the ggplot-package (Wickham, 2009) for graphic display of the dataset. The multivariate statistical analysis of this study includes a constrained redundancy analysis (RDA) and was conducted in Canoco 5.12 (Braak and Šmilauer, 2018). RDA was used to assess any differences in amount and composition of MPs between sites and salt type. The data used for these tests were number of particles for each polymer type found in the samples, and percentage of concentration of each polymer found in the samples. The explanatory variables (categorical variables) were sample sites and the two salt types: sea salt and rock salt. All data was log transformed prior to the RDA and Monte Carlo permutation test (4999 permutations) were used for all tests. A probability (p) value of 0.05 was applied to all statistical tests.

3. Results

3.1. Quality control and quality assurance

In total, 8 fibres were found in the blank control samples and no fragments. All fibres were checked with the FT-IR and 5 fibres had a confirmed match with the database: two cellulose, two viscose wool and one polyethylene terephthalate (PET). Only the confirmed PET fibre is used to calculate LOD and LOQ: the mean number of fibres (μx) was 0.1 with 0.4 as the standard deviation (σx), which gives a LOD of 1.3 and LOQ = 4.1. The calculated mean concentration of microplastic particles in the blank control samples were 0.07 μg (with 0.2 as the standard deviation) which gives LOD = 0.7 μg and LOQ = 2.1 μg. All samples were filtered on the same day as the control sample with the PET fibre is corrected for the mean PET value, which included all the samples from Torrevieja.

The LOD for the pyrolysis method was between 0.61 and 1.98 μg/kg, and the LOQ was between 1.84 and 6 μg/kg. The value for each polymer is listed in Table 2.

3.2. Identification of MPs with FT-IR

In total, 608 particles were identified as potential microplastics following visual identification. Of these, 374 were classified as fragments, 230 as fibres, and 2 as spheres. For the fragments, particles ≥59 μm were analysed with FT-IR. All non-black fragments ($n = 51$) were analysed, and 27 of these were confirmed to be microplastics and 3

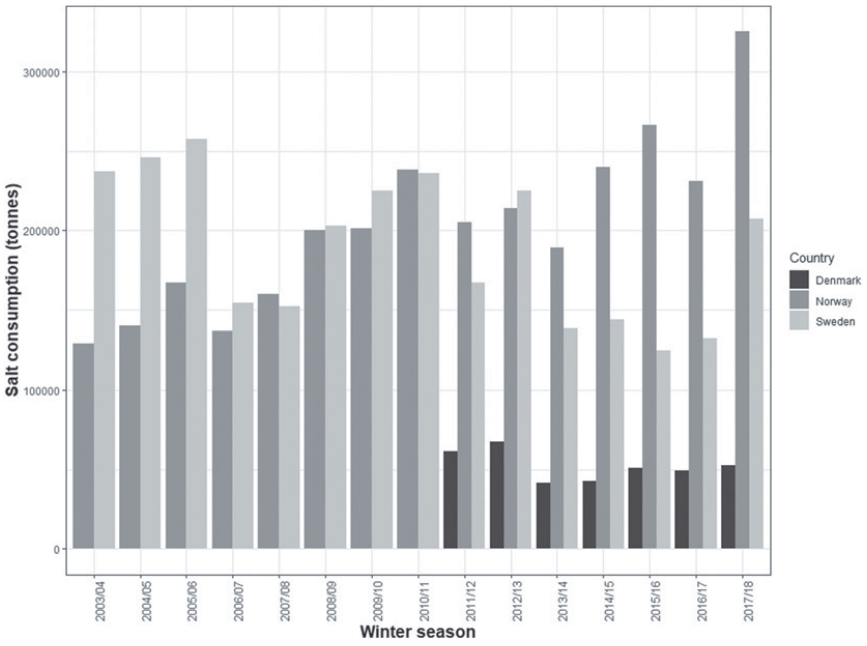

Fig. 2. The amount of road salt (tonnes) used on state and county roads in Norway (Statens vegvesen, 2019a, 2019b), Sweden (Trafikverket, 2019) and Denmark (Vejdirektoratet, 2019a, 2019b) from the winter season of 2003/04 to 2017/2018.

confirmed to be from natural sources (linen and viscose). Nitrile butadiene (NR, 22%) and PET (18%) were the most abundant non-black fragments. A total of 21 non-black fragments were unidentified or had a low match score (<0.6 match) with the database.

The most abundant particle group in the samples were black fragments, collectively named "black rubbery particles" (BRP, $n = 319$). They could all be placed in two morphology-groups, square-like or elongated (Fig. 3) and there was no visible difference between BRP from different salt sites. All had a "rubbery" response to pressure with the forceps and did not crumble or disintegrate, and therefore suspected to be made of polymeric material. Of the 319 B.P. found in the samples combined, 57 B.P. were subjected to FT-IR analysis. Out of these 57, only 20 particles had a match to the database (>0.6); the spectra obtained matched that of reference tire samples - spectra showing the full absorbance of the Germanium crystal due to high carbon black content in tires. However, this result only shows us that the particle has a high carbon black content and does not confirm that they are all tire particles. The remaining 37 B.P. that were tested, could not be identified with respect to polymer type. Tires can contain different polymers, such as Styrene Butadiene Rubber (SBR), Butadiene Rubber (BR) and natural rubber, and tire particles are therefore included in the term microplastic. However, most of the particles found in this study did not seem to match the shape of tire particles reported from other studies (Kreider et al., 2010). Another source of black material with high content of carbon black was suggested, namely conveyer belts. Conveyer belts used in mining, for transporting material on site, are made of Polyvinyl chloride (PVC) (Van and Ter, 1990). To confirm that these numerous black particles could originate from conveyer belts, a new sub-sample of salt from Ben Gardene was analysed using Pyrolysis GC–MS.

Of the fibres detected, 194 were analysed by FT-IR. Unfortunately, 34 fibres were either lost during the transfer from filter paper to diamond compression cell or too small to be transferred. A total of 87 fibres had a confirmed database match (match > 0.6). Of these, 11 were confirmed to be microplastics, and 74 fibres were confirmed to be of natural material (cellulose = 68, wool = 5, cotton = 1) and 9 of semisynthetic material (viscose). 98 fibres were either unidentifiable or had a low match score with the database (match < 0.6). The two spheres were also analysed using FT-IR and had no confirmed match with the database for any material.

3.3. Identification of MPs with Pyrolysis GC–MS

The presence of PVC in the samples from Ben Gardene was confirmed using Pyrolysis GC–MS. While PMMA and PC was not detected in the sample, the other 6 polymers where all above the detection limit and confirmed to be present in the road salt from Ben Gardene. Polyvinyl chloride accounted for 77% of the total polymer content found in the sample, followed by PE (13%), PET (5%), SBR (4%), PP (0.6%) and PS (0.3%). The presence of 4% SBR indicates that some of the BRP found in the salt samples were likely tire particles, at least in the samples from Ben Gardene. However, since we did not manage to distinguish between them in the visual analysis, we will for this study keep the term BRP as a combined group of PVC and SBR.

3.4. Particle measurements

The length of fragments, measured at the longest axis, ranged from 21 μm to 2849 μm (215 ± 229 μm) for all samples, and most of the fragments were smaller than 200 μm (62%) and only 1% were larger than 1000 μm. The length of fibres ranged from 126 μm to 4800 μm (mean ± s.d. = 1266 μm ± 1197 μm) in all salt samples (4). A large proportion of the fibres (45%) were longer than 1000 μm and in total only 14% were smaller than 200 μm.

The mass of both fragments and fibres was calculated from the volume of each particle and density of the polymer type that was

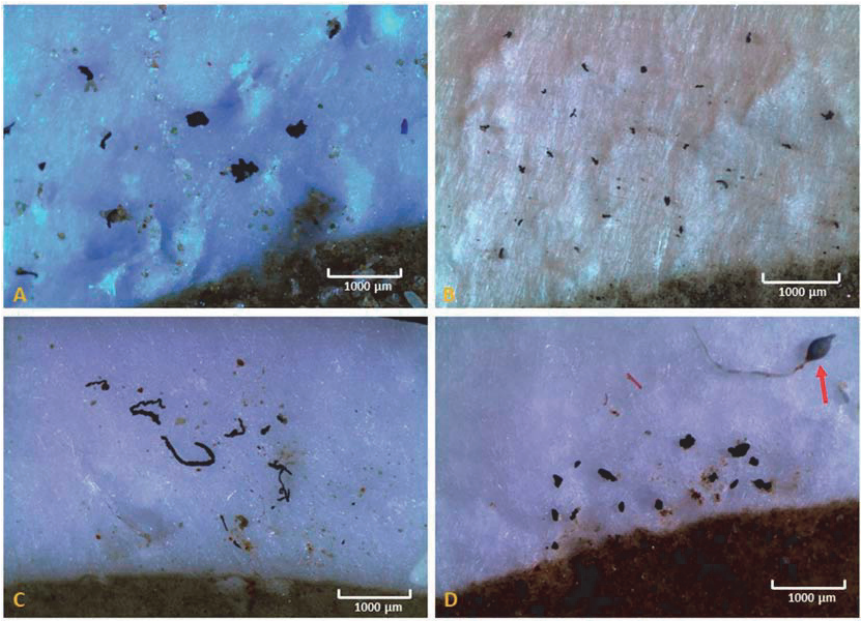

Fig. 3. Examples of black rubber-like particles (BRP) from samples A) Ben Gardene, B) Torrvieja, C) Zarziz and D) Rock salt from Bernburg, Germany. Image D also displays one of the two spheres found in the samples (highlighted with a red arrow). Images are taken with Infinity 1-3C camera and processed with INFINITY ANALYSE and CAPTURE software (v6.5.6). (For interpretation of the references to colour in this figure legend, the reader is referred to the web version of this article.)

confirmed for each, following the description of Subsection 2.5. The mass of fragments ranged from 0.03 μg to 550 μg (11 ± 38 μg), with as much as 78% of all fragments being <10 μg. Comparing the average values of both length and mass for all particles to the median values, it is quite clear that the sizes of MPs found in this study is skewed (Fig. 4), with a few large particles and most of them smaller than 200 μm and with mass lower than 50 μg. The concentrations of fibres ranged from 0.03 μg to 80 μg (5 ± 15 μg) in all samples. More than half of the fibres (52%) were <1 μg and 45% were between 1 and 10 μg.

The calculation of the masses was controlled by comparing the results with the measured concentration using the Pyrolysis GC–MS from the Ben Gardene site (Table 3). At Ben Gardene, only PET and PEE particles were confirmed using FT-IR and the estimated concentration based on the particles detected was 126 ± 173 μg/kg and 117 μg/kg, respectively. The largest group detected in the Ben Gardene sample was the BRP. If we assume that the BRP are PVC-particles from conveyer belts, as suggested in Subsection 3.2, the estimated concentration of BRPs is 4464 ± 2760 μg/kg. Using Pyrolysis GC–MS, the concentration of PET, PVC, PE and SBR was measured to be 106 μg/kg, 1754 μg/kg, 302 μg/kg and 87 μg/kg, respectively. The presence of SBR in the samples suggests that some of the particles in the BRP group are tire particles and not PVC-particles. According to previous studies, the polymer content (both synthetic and natural) in tires is between 40 and 60% (Wik and Dave, 2009) and includes SBR, Polybutadiene, Polyisoprene, Chloroprene, natural rubber and other rubbers (Grigoratos and Martini, 2014; Wagner et al., 2018). The average SBR content of tires, combining car and truck tires, is 11.3% (Eisentraut et al., 2018). Assuming a 11.3% SBR content in tires, the total tire particle concentration in the sample is 773 μg/kg. The visual analysis cannot differentiate between the possible conveyer belt particles and the tire particles, so using only visual techniques both particle types would be mixed. If we also combine the concentration for PVC and the calculated tire concentration based on the measured SBR concentration (using 11.3% SBR/tire) from the pyrolysis, the concentration of these two would add up to 2527 μg/kg salt, which is within the range of concentration found for BRP using the visual analysis and concentration calculations.

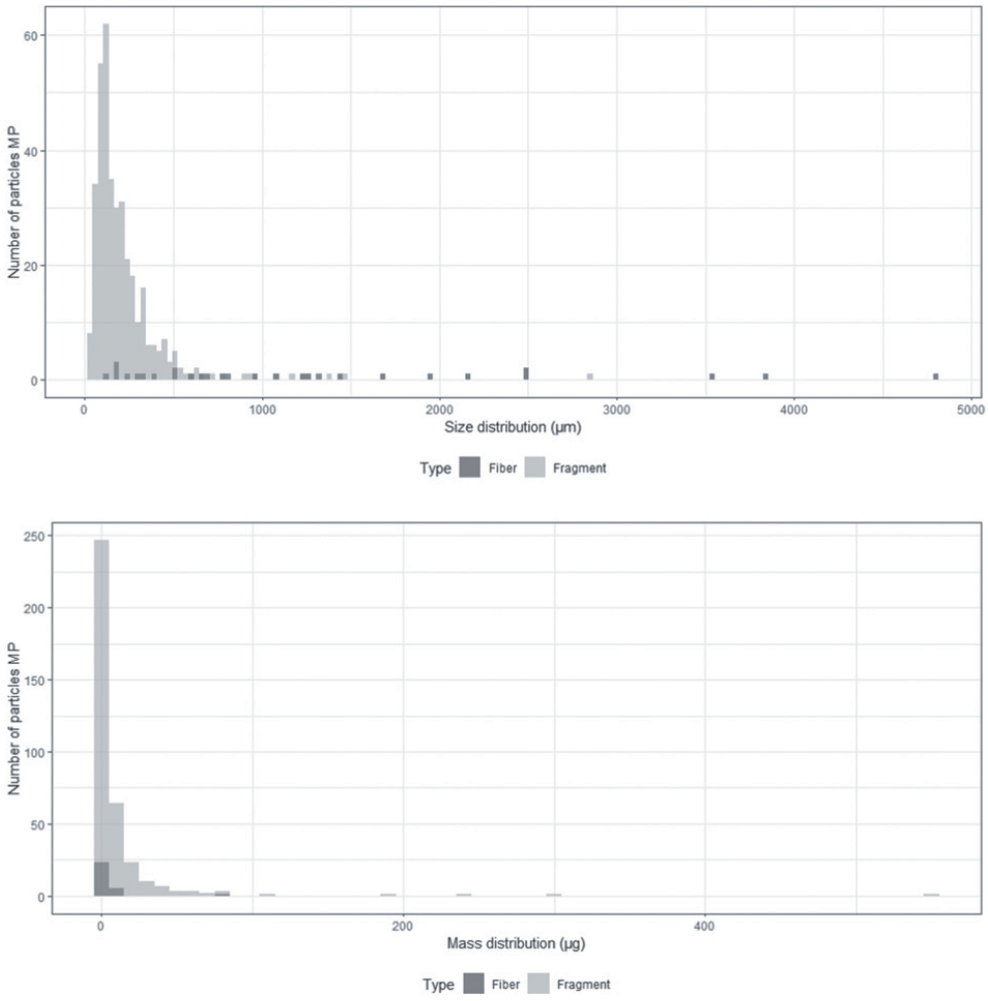

Fig. 4. Bar plot showing size (above) and the mass (below) distribution of all MPs found in the salt samples combined. Fibres and fragments are separated.

3.5. Comparison of MPs between salt production sites

The number of MPs found varied between samples, from 32 to 252 MP/kg (mean ± s.d. = 132 ± 63 MP/kg; n = 12, Table S2). The concentration of microplastic particles varied between samples from 1.5 to 3987 μg/kg (mean ± s.d. = 595 ± 1129; n = 12, Table S3). Fragments were the most abundant type of particles in the samples, with 24–240 fragments per sample (mean ± s.d. = 122 ± 64 MP/kg; n = 12) compared to 4–16 fibres per sample (mean ± s.d. 10 = ±3 MP/kg). Comparing the concentrations per sample, the highest concentrations were also identified from the fragments, with an average of 1359 μg/kg (s.d. ± 2251 μg/kg) compared to 49 μg/kg (s.d. ± 93 μg/kg) for the fibres.

The samples from Ben Gardene contained a relatively high amount of fragments (mean ± s.d. = 4503 ± 2725 μg/kg; 195 MP/kg ± 41) compared to all the other sites: Torrevieja (mean ± s.d. = 173 ± 103 μg/kg; 107 MP/kg ± 20), Zarziz (mean ± s.d. = 24 ± 31 μg/kg; 52 n/kg ± 33) and Bernburg (mean ± s.d. = 735 ± 503 μg/kg; 136 MP/kg ± 60) (Fig. 5, Tables S4 & S5). For all sites, the number of fibres found per sample was considerably lower than the number of fragments. Torrevieja had the highest number of fibres (mean ± s.d. = 13 ± 3 MP/kg, n = 3) compared to Zarziz (mean ± s.d. = 11 ± 2 MP/kg), Ben Gardene (mean ± s.d. = 9 ± 2 MP/kg), and Bernburg (mean ± s.d. = 8 ± 5 MP/kg), although all sites were quite similar in number of fibres found. However, when we use the concentration data, the concentration of fibres from the Ben Gardene site (mean ± s.d. = 128 ± 172 μg/kg, n = 3) had four times higher concentration than Torrevieja (mean ± s.d. = 32 ± 6 μg/kg), five times higher than the Bernburg (mean ± s.d. = 24 ± 6 μg/kg) and 64 times higher concentration than Zarziz (mean ± s.d. = 2 ± 1 μg/kg).

3.6. Comparison between salt types

When comparing the types of road salt, the results indicate that sea salts have a higher concentration of MPs (442 ± 1466 μg/kg), and a larger variation in the samples compared to the rock salt (322 ± 481 μg/kg). However, the rock salts have the highest number of particles (61 ± 76 MP/kg) compared to the sea salts (35 ± 60 MP/kg). All data are summarized in Tables S1–S2.

The polymers identified differed between the samples. However, the most abundant particle-type found in all four sites were the BRP, which we have confirmed to consist of PVC and SBR (Fig. S4, Tables S4 & S5). These were both the most numerous particles, as well as highest in concentration, and in fact accounted for 96% of the total MP (MP/kg) found in the samples combined, with confirmed PET at a second place (3%) and the rest accounts for 1% combined (Acryl A, Epoxy Resin ER, Ethylene Propylene EP, PEE, PVC (non-black), High-density Polyethylene (HDPE), Nitrile butadiene (NR), Polyurethane (PUR) acrylic resin, Polypropylene (PP)). Even though the BRP were the most abundant group at all sites, they were clearly found in the highest concentration at Ben Gardene (13,391 μg/kg; 580 MP/kg) and at Bernburg (2196 μg/kg; 400 MP/kg) (Fig. 6). The only other polymer found at all sites were PET fibres. Other detected polymers had greater variation between sites. One of the sites, Zarziz, had considerably more diverse particles than the others, with three different fibre polymers (A, PEE, PET) and six different fragment polymers (EP, NR, PET, PP, PVC and BRP) found.

The polymer type composition in the various salts appeared slightly different. However, using sampling sites as categorical variables in an RDA on both number of particles (pseudo-F = 2.0, $p > 0.05$) and % concentration data (pseudo-F = 2.1, $p > 0.05$) revealed no statistically significant difference in composition between sites (Fig. 7, Figs. S5 & S6). For the number of particles and concentration data, the sites explained 33% and 23.3% of the observed variation, respectively. The distance in the RDA between the two sites Ben Gardene and Bernburg is considerably lower when using concentration data compared to number of particles in 3a. There was, however, no significant difference found between the two salt types; sea salt and rock salt (MP/kg, pseudo-F = 0.9, $p > 0.05$; MP g/kg, pseudo-F = 0.7, $p > 0.05$, see Figs. S5 & S6).

3.7. Estimation of MP release from road salt

For the calculations of MP release from road salt, the latest dataset from 2017/2018 is used. In this period, Norway used 320,000 t (Fig. 2) (Statens vegvesen, 2019a), distributed on about 50% sea salt produced in the Mediterranean and 50% rock salt produced in salt mines in Germany. Sweden only used rock salt on their state and county roads, and for the season 2017/2018, close to 210,000 t of salt was used (Trafikverket, 2019). In Denmark, 55,000 t of salt were used in the whole of 2018, and only sea salt from the Mediterranean was used (Vejdirektoratet, 2019a). The average concentration of MPs in the sea salt was 442.1 μg/kg salt and the average number of particles was 35.1 MP/kg. The average concentration of MPs in the rock salt was 321.8 μg/kg and the average number of particles was 60.5 MP/kg. Even though

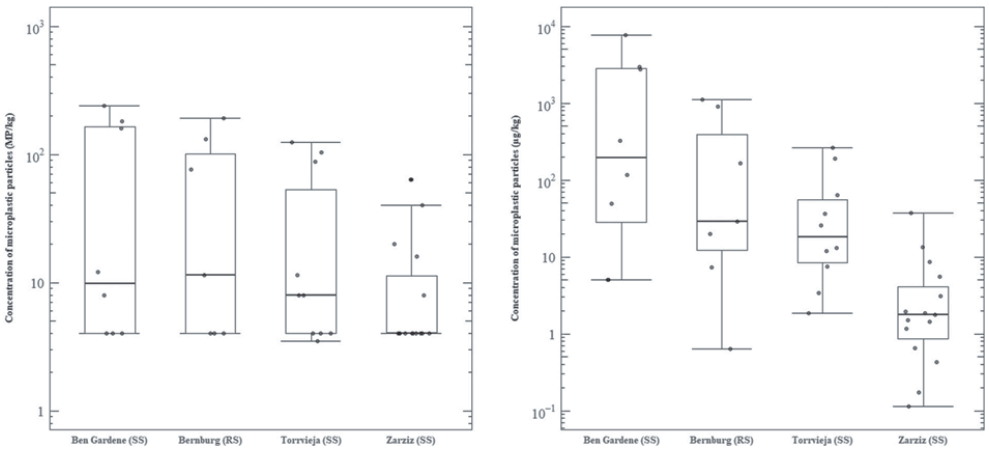

Fig. 5. Box plot showing the spread of microplastic particles found throughout the samples analysed, depicted in number of MP per kilo salt (MP/kg) at left and concentrations per kilo salt (μg/kg) at right. Grey dots are single measurements. The y-axes are logarithmic.

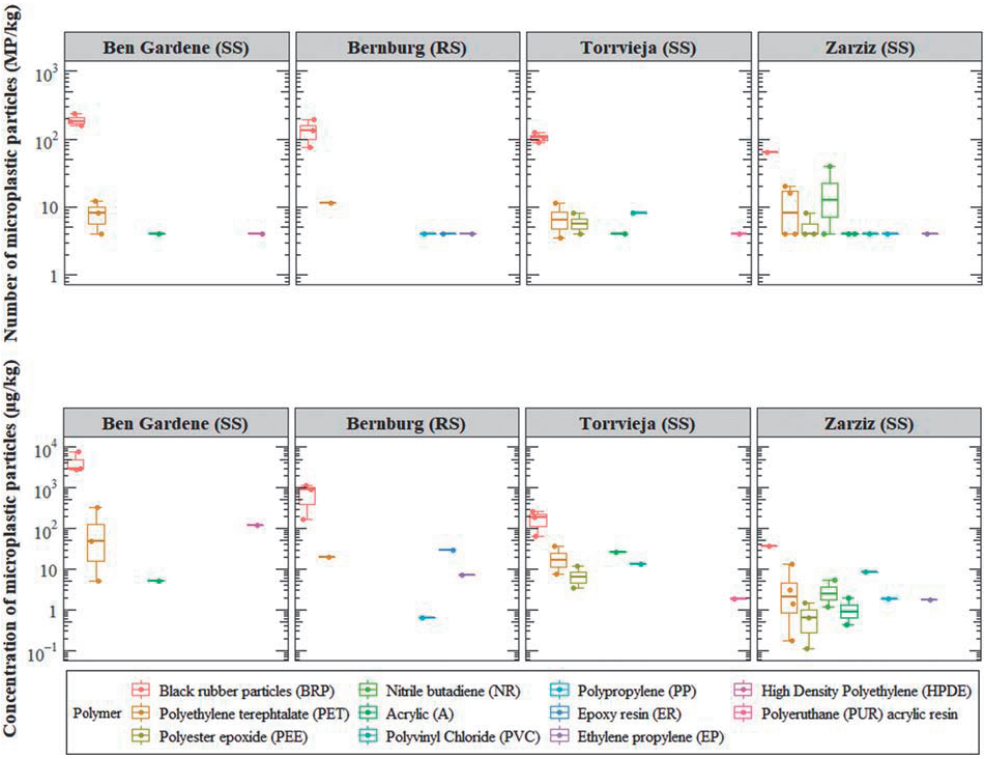

Fig. 6. Box-plot showing the distribution of microplastic fibres and fragments per kilo salt found at each site, by polymer type (above) and the mean concentration of microplastic fibres and fragments found at each site, by polymer type (below). Polymer types: Black rubbery particles, polyethylene terephthalate (PET), acryl (A), epoxy resin (ER), ethylene propylene (EP), polyester epoxide (PEE), polyvinyl chloride (PVC, non-black particles), high-density polyethylene (HDPE), nitrile butadiene (NR), polyurethane (PUR) acrylic resin, polypropylene (PP).

the statistical analysis using multivariate tools showed no significant difference between the rock salt and sea salt in this study with regards to microplastic particles, the salt types for this calculation are taken into consideration. From this analysis we estimate that road salt used on state and county roads contributes to a total of 0.15 t of MPs per year (tonnes/year) in Norway, which is 0.23 grams per kilometre road (g/km). This is equivalent to 0.003% of the total release of RAMP. In Sweden and Denmark, the release of MPs from road salt is 0.07 t/year (0.07 g/km) and 0.03 t/year (0.04 g/km), respectively. This is equivalent to 0.008% of RAMP in Sweden and 0.0004–0.0008% of RAMP in Denmark. Summary of the calculations are presented in the supporting information (Table S4).

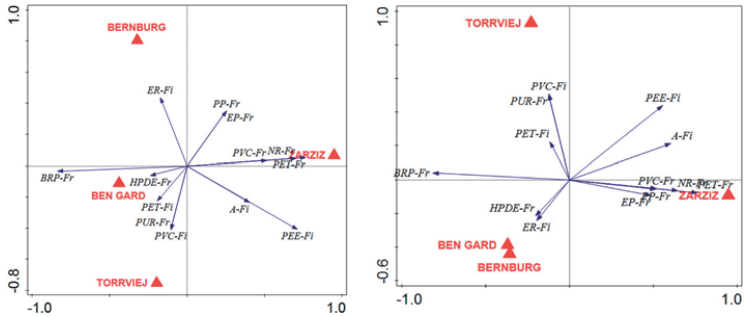

Fig. 7. The figure shows the constrained RDA plot of the variation of polymer types (arrows; Black rubber particles (BRP), Polyethylene terephthalate (PET), Polyester epoxide (PEE), Nitrile butadiene (NR), Acrylic (A), Polyvinyl chloride (PVC), Polypropylene (PP), Epoxy resin (ER), Ethylene propylene (EP). Fi = fibres and Fr = fragments) when using "sample sites" as the explanatory variable (triangular shapes; Torrevieja, Zarziz, Ben Gardene and Bernburg). In the left plot, the number of particles per polymers is used and in right plot, the concentration of polymers (% of total) is used. The arrow points in the direction of steepest increase of the polymer type. A sharp angle between the arrows indicate positive correlation, while arrows going in opposite direction indicate negative correlation. Angle close to 90 degrees indicate no correlation.

4. Discussion

4.1. Road de-icing salt compared to RAMP

Based on the results in the present study, road salt seems to be a negligible source of road-related microplastic pollution compared to other main sources, and especially compared to the contribution from car tires. It is, however, important to underline that the estimation of total RAMP emissions in Norway (Sundt et al., 2014; Sundt et al., 2016; Vogelsang et al., 2018) is based on the total annual distance travelled for different vehicle types, and does not distinguish between state, county, municipal or other roads (Vogelsang et al., 2018). In Sweden, the RAMP emissions are for roads open to the public only (Magnusson et al., 2017), meaning that they are excluding all private roads from their calculations. For Denmark there is no information on what types of roads they have included in the emission calculations (Lassen et al., 2015). This study, on the other hand, has calculated the emission of MPs from road salt emitted from state and county roads only. Although a large proportion of the road network that uses road salt will be either state or county roads, there are also municipal roads, especially in larger cities like Oslo and Stockholm, where road salt is widely used. There might also be other roads where winter and road conditions require that road salt is used to ensure traffic safety. Additionally, road salt (e.g. $CaCl_2$ or $MgCl_2$) is also applied on gravel roads in summer to prevent air dust during dry weather conditions. However, these numbers are difficult to obtain, as there are different road owners and no common reporting platform for road salt use. In Norway, state and county roads combined have a total length of 62,923 km, municipal roads of 44,048 km and private roads 100,384 km (Statens vegvesen, 2019b). Many smaller roads, both county and municipal, are not salted during winter as other winter maintenance measures are preferred (e.g. the roads are just ploughed and sanded). It should be clearly stated that the emission calculation is associated with relatively large uncertainties. These arise because it is based on calculated concentrations, a small sample size compared to the total salt emission, as well as a varying salt consumption per year. In addition, the salt used in this study comes from only one salt importer. Even though they are one of the major importers of salt to all three countries, there may also be other salt importers using other salt production sites. Future studies should aim to investigate road salt from other sources and calculate the emission of microplastic particles from road salt in other countries, especially countries with high road salt emissions such as USA, Canada and China.

4.2. Black rubbery particles

In the present work, we suggest that the sources of BRPs are conveyer belts, which are used at all salt production sites included in this study (Rieber, 2019). The belts are in general made of thermoplastic materials with carbon black added for durability. There are probably several different thermoplastics used in conveyer belts, determined by the different applications of the conveyer belt and the manufacturers. However, according to a U.S. patent (Van and Ter, 1990) from 1990, conveyer belts used within mining industries use PVC. No specific information on the types of conveyer belts used at the salt production sites could be obtained. However, since rock salt originates from salt mines it is likely that the conveyer belts used in salt production is of similar type to those used for other mining activities. Upon visual examination using microscope and forceps, the BRPs identified in rock salt did not differ from the ones found in sea salt (Fig. 3), which supports the assumption that they originate from the same material. Since we also found a presence of SBR in the Ben Gardene sample, it is a possibility that some of the BRP could come from tire wear, as well as both trucks, lorries, tractors and other vehicles may be used at production sites of both sea salt and rock salt. Even though they did not display similar characteristic shape as tire particles in other studies (Kreider et al., 2010), they might also be made of different types of tires and not subjected to the harsh road climate in which other tire particles are assumed to be infused with road wear particles.

4.3. Comparison with other studies

In total, the number of particles found for both sea salt and rock salt were comparable to some studies on food-grade salt, although a large variation in number of MPs is reported in the different studies (Table S5). In this study, sea salt was found to have 35 ± 60 MP/kg, ranging from 32 to 252 MP/kg. In the food-grade salt studies, the number of MPs found differ between n.d. MP/kg and 16,329 MP/kg. One of the food-grade salt studies also included Spanish sea salts from the Mediterranean (Iniguez et al., 2017). In this study, the number of MPs from the Mediterranean samples ranged from 60 to 280 MP/kg. Two brands of sea salt were collected from Murcia, which is close to Torrevieja. The mean number of MPs from Murcia was 280 ± 3 MP/kg and 105 ± 7 MP/kg. In comparison, the mean number of MPs found for the Torrevieja site in our study was 36 ± 49 MP/kg. The mean number of MPs in rock salt in the present study was 61 ± 76 MP/kg. Our result corresponds well to the results found for food-grade rock salt, which was 38 ± 55 MP/kg (Kim et al., 2018) and 12 ± 1 MP/kg (Gündoğdu, 2018). Only two other studies reported concentrations of microplastic particles in sea salt. However, they represent sea salt from different oceans. The concentrations varied between n.d. and 46.5 mg/kg salt (Kim et al., 2018; Seth and Shriwastav, 2018). The Mediterranean Sea salts ranged from 0.5–2.4 mg/kg, which corresponds well to the findings of this study (442 ± 1466 μg/kg). Although the results of the present study are comparable to previous salt studies, the fact that different methods have been used, both in preparation and analysis, needs to be addressed. As for a large proportion of microplastic studies, the lack of consistency in methodologies or standardisation is an obvious issue of concern. In the food-grade salt studies, the pore size used to retain the MPs after dissolving the salts differed between 0.2 and 5 μm for all studies except one where they used the pore size 149 μm (Karami et al., 2017), thus excluding all particles <149 μm from their samples. The reason for this is not sufficiently explained and as this study also reported a very low range of MPs (n.d.–10 MP/kg), the pore size used is an obvious issue when comparing studies. For the other studies where pore sizes of 0.2–5 μm were applied, a consistent use of the same pore size would be beneficial when comparing results. However, they have all used pore sizes that will retain particles that are at least 5 μm in size, and using visual techniques such as microscopes, FT-IR (Iniguez et al., 2017; Kim et al., 2018; Lee et al., 2019; Seth and Shriwastav, 2018; Yang et al., 2015) or Raman spectroscopy (Gündoğdu, 2018; Karami et al., 2017), the lower limit of detection depends on the lower limit of the analysis. One of the food-grade salt studies (Renzi and Blašković, 2018) was excluded from comparison with our results because they did not apply chemical analysis of the polymer content to confirm the presence of MPs, and they reported the largest variation in the salt studies (20–19,820 MP/kg).

The main difference between production of food grade salt and road salt, is that the food grade salt goes through a double washing process at the production site whereas the road salt is only subjected to a single washing process (Rieber, 2019). None of the other salt studies have reported the presence of "black rubbery particles", large concentrations of PVC or tire particles/SBR. As our study shows such a high abundance, we can only hypothesize why it was not identified in other studies. One reason might be the extra washing step that is used for food grade salts. There might also be other refining steps when processing salt for the food market, compared to salt used for industrial purpose.

Considering all MPs except the BRPs, road salt is considerably less contaminated compared to both sea salts and rock salts used for food. A suggested reason for this finding might be that the road salt used for this study has never been packaged and came directly from bulk samples at the importer's storage site. The Torrevieja-sample had also been transported in bulk like the other salts in the study, but we

received it in a plastic bag-package meant for commercial sale, packed in Norway. This bag was made of PE (see Figs. S1–S3), and no PE was found in the salts from Torrevieja. We can therefore disregard that the microplastics in the Torrevieja-samples came directly from the packaging. In comparison to our samples, most food grade salts are packed in bulk bags for shipment and then repacked in smaller packages for different salt brands (Rieber, 2019). Such bulk bags (for example "Flexible intermediate bulk container, FIBC") are commonly made from woven polyethylene PE or PP (Diffpack, 2020), which might explain why both PE and PP fibres are found in high numbers in the salt used for food (Gündoğdu, 2018; Iniguez et al., 2017; Karami et al., 2017; Kim et al., 2018; Lee et al., 2019; Seth and Shriwastav, 2018; Yang et al., 2015), and less in the road salt. PET is commonly used in packaging, as well as one of the most used synthetic fibres in the textile industry, thus it is not surprising that PET was the second most abundant polymer found in the road salt samples, after BRP. PET is also found in high abundance in the studies of food-grade salt (Gündoğdu, 2018; Iniguez et al., 2017; Karami et al., 2017; Kim et al., 2018; Seth and Shriwastav, 2018; Yang et al., 2015).

It has been suggested that PET is more abundant than other polymer-types in food-grade salt due to its higher density (1.34–1.39 g/cm^3) (Bråte et al., 2017) compared to PE (Low density PE: 0.92 g/cm^3, High density PE: 0.95 g/cm^3) (Polymer Science, 2020) and PP (Bråte et al., 2017) (0.90–0.92 g/cm^3), causing PET to more easily follow the salt during the production process (Iniguez et al., 2017; Yang et al., 2015). In the present study, BRP were the most abundant particle. Using the results from the Pyrolysis GC–MS, we can assume that most of the BRPs are made of PVC, as PVC was found to be the polymer with the largest mass in the Ben Gardene sample. As we stated in this study, most BRPs are of PVC, they would have a density of 1.160–1.3 g/cm^3 (Bråte et al., 2017), with a high carbon black content (1.8–2.1 g/cm^3) (INCHEM, 2017). It is likely that these particles will have a higher density than the other polymers found, and therefore be accumulated with the salt. Each brand of salt might also have different purification processes for their salt before it is packaged and released to the food market. The road salt is commonly transported in bulk containers, using conveyer belts up until the very last step of the transportation. This might explain why we find so much of these black rubber particles in this study compared to none being detected in the previous salt studies.

4.4. Limitations of the methodology

In the present study the lowest limit of detection is related to the lowest sizes of particles that could be handled with forceps and transferred to either ATR-FTIR or μFTIR windows. Using the longest axis of the particles as the length, the smallest detected particle that was possible to transfer to the FT-IR compression cell and get a match score (>0.6) from was 59 μm long (and 37 μm wide). However, particles as small as 21 μm (longest axis) were detected on filters and included in this dataset, as it had matching morphology to BRP. So, for this study and the methods used, it was not possible to detect particles below 21 μm, although there might be particles <21 μm present. In this study, GF-filters with pore size 1.6 μm was used. However, for the analysis using visual methods, the pore size used has less of an impact as long as it is lower than the smallest particle size possible to detect on the filter papers and measure using the FTIR. For the Pyrolysis GC–MS on the other hand, the pore size used can have a larger impact on the results. Using Pyrolysis GC–MS makes it possible to detect even small amounts of polymers if the mass of these particles in total is above the LOQ for the Pyrolysis GC–MS method. This is demonstrated in our sample from Ben Gardene where we found low concentrations of PS and PP in the sample via GC–MS but did not detect particles via the visual analysis. We were also able to detect and measure the concentration of SBR in the sample, which corresponds to some of the BRP being tire particles. On the other side, if we do have a number of very small particles of a specified polymer in the sample and a few quite large particles (<5 mm) of the same polymer, the presence of the small particles will be masked in the total amount of polymers and likely not contribute that much to the total mass. This also means that the information on sizes will be lost. This can be adjusted using filters with different pore sizes as well as sieves to separate the sample in size fractions. This will contribute to more data on the mass of polymers related to size fractions, which may be of value, and should be considered in future studies. The use of Pyrolysis GC–MS also allows for the detection of nanoplastics if the filters with appropriate pore sizes to retain particles in the nanoscale are used and if the measurements are above the LOQ.

As shown in this study, the mass of polymers found using visual techniques and concentration calculation corresponded well to the mass found using Pyrolysis GC–MS. In the visual analysis, three groups of polymers where detected; BRP (suspected PVC), PET and PE. This complies with results from the Pyrolysis GC–MS where PVC, PET and PE had the highest, second highest and third highest concentration in the sample, respectively. This validates that visual analysis together with FT-IR can be used to calculate concentrations of different polymers from a sample, not just the number of particles. However, this is of course limited to what the FT-IR can analyse, and as shown in this study, particles with a high carbon black content can prove difficult to analyse via FTIR.

5. Conclusions

The concentration of MP in rock salt and sea salt used for de-icing of winter roads was low. The estimated annual release of MPs from road de-icing salt is considerably lower than the estimated release coming from other known MP sources in Norway. Based on the current study, the application of road salt for de-icing of winter roads is a negligible source of microplastic to the environment. It is likely that the MPs found in sea salt are due to both contaminated sea water and contamination through processing. This needs to be further investigated in order to reduce the contamination of salts used for road purposes. As only one rock salt site was included in this study, we propose that future studies on road salt should include different rock salt sites for comparison with the sea salt, as well as include data for municipal roads in new estimates. We also suggest that future studies should include more detailed analysis of the "black rubbery particles", for example by employing Pyrolysis GC–MS, as well as employing Pyrolysis GC–MS in a wider scale to investigate the presence of small microplastics and nanoplastics in the salt samples.

Declaration of competing interest

The authors declare that they have no known competing financial interests or personal relationships that could have appeared to influence the work reported in this paper.

Acknowledgements

We would like to thank Rachel Hurley and Nina Buenaventura (NIVA) for guidance on visual analysis and FTIR. We would also like to thank Amy Lusher and Emelie Skogsberg (NIVA) for valuable comments to the manuscript.

Funding sources

This work was funded in collaboration between the Norwegian Institute for Water Research (NIVA) and the NordFoU-project REHIRUP, consisting of the Norwegian Public Roads Administration, the Swedish Transport Administration and the Danish Road Directorate. Part of the

work is also supported by the Research Council of Norway through its Centres of Excellence funding scheme, project number 223268/F50.

Author contributions

The manuscript was written through contributions of all authors. All authors have given approval to the final version of the manuscript.

Appendix A. Supplementary data

Supplementary data to this article can be found online at https://doi.org/10.1016/j.scitotenv.2020.139352.

References

Andrady, A.L., 2011. Microplastics in the marine environment. Mar. Pollut. Bull. 62, 1596–1605.

Braak, CJFt, Šmilauer, P., 2018. Canoco Reference Manual and User's Guide: Software for Ordination (Version 5.10). Biometris, Wageningen University & Research, Wageningen.

Bråte, I.L.N., Huwer, B., Thomas, K.V., Eidsvoll, D.P., Halsband, C., Almroth, B.C., et al., 2017. Micro-and Macro-plastics in Marine Species From Nordic Waters. Nordic council of Ministry Report.

CIA, 2017. Statistics of road network. https://www.cia.gov/library/publications/the-world-factbook/fields/385.html.

Demers, C.L., 1992. Effects of road deicing salt on aquatic invertebrates in four Adirondack streams. Chemical Deicers and the Environment. Lewis Publishers, Boca Raton, Florida, USA, pp. 245–251.

Diffpack, 2020. FIBC.

Eisentraut, P., Dümichen, E., Ruhl, A.S., Jekel, M., Albrecht, M., Gehde, M., et al., 2018. Two birds with one stone—fast and simultaneous analysis of microplastics: microparticles derived from thermoplastics and tire wear. Environ. Sci. Technol. Lett. 5, 608–613.

Environment Canada, 2012. Five-year Review of Progress: Code of Practice for the Environmental Management of Road Salts (Report published March 31, 2012).

Fay, L., Shi, X., 2012. Environmental impacts of chemicals for snow and ice control: state of the knowledge. Water Air Soil Pollut. 223, 2751–2770.

Findlay, S.E.G., Kelly, V.R., 2011. Emerging indirect and long-term road salt effects onecosystems. Ann. N. Y. Acad. Sci. 58–68.

Frias, J.P.G.L., Gago, J., Otero, V., Sobral, P., 2016. Microplastics in coastal sediments from southern Portuguese shelf waters. Mar. Environ. Res. 114, 24–30.

GESAMP, 2016. Sources, fate and effects of microplastics in the marine environment: part two of a global assessment. Joint Group of Experts on the Scientific Aspects of Marine Environmental Protection, p. 220.

Government of Canada, 2018. Statistics of road network. https://www.tc.gc.ca/eng/policy/transportation-canada-2018.html#item-10.

Grigoratos, T., Martini, G., 2014. Non-exhaust traffic related emissions. Brake and tyre wear PM. JRC Science and Policy Reports, p. 53.

Gündoğdu, S., 2018. Contamination of table salts from Turkey with microplastics. Food Addit. Contam. Part A 35, 1006–1014.

Hann, S., Sherrington, C., Jamieson, O., Hickman, M., Bapasola, A., 2018. In: Sherrington, C. (Ed.), Investigating Options for Reducing Releases in the Aquatic Environment of Microplastics Emitted by Products. Eunomia.

Hermabessiere, L., Himber, C., Boricaud, B., Kazour, M., Amara, R., Cassone, A.-L., et al., 2018. Optimization, performance, and application of a pyrolysis-GC/MS method for the identification of microplastics. Anal. Bioanal. Chem. 410, 6663–6676.

INCHEM, 2017. Carbon Black. 2020. European Commission.

Iniguez, M.E., Conesa, J.A., Fullana, A., 2017. Microplastics in Spanish table salt. Sci. Rep. 7.

ISO/TS 21396:2017, 2017. Rubber — Determination of Mass Concentration of Tire and Road Wear Particles (TRWP) in Soil and Sediments — Pyrolysis-GC/MS Method. International Organization for Standardization, Genève, Switzerland.

Karami, A., Golieskardi, A., Choo, C.K., Larat, V., Galloway, T.S., Salamatinia, B., 2017. The presence of microplastics in commercial salts from different countries. Sci. Rep. 7.

Karraker, N.E., Gibbs, J.P., Vonesh, J.R., 2008. Impacts of road deicing salt on the demography of vernal pool-breeding amphibians. Ecol. Appl. 18, 724–734.

Ke, C., Li, Z., Liang, Y., Tao, W., Du, M., 2013. Impacts of chloride de-icing salt on bulk soils, fungi, and bacterial populations surrounding the plant rhizosphere. Appl. Soil Ecol. 72, 69–78.

Kelly, V.R., Findlay, S.E.G., Weathers, K.C., 2019. Road Salt: The Problem, the Solution, and How to Get There. Cary Institute of Ecosystem Studies (Report. 16 pages).

Kim, J.-S., Lee, H.-J., Kim, S.-K., Kim, H.-J., 2018. Global pattern of microplastics (MPs) in commercial food-grade salts: sea salt as an indicator of seawater MP pollution. Environ. Sci. Technol. 52, 12819–12828.

Kreider, M.L., Panko, J.M., McAtee, B.L., Sweet, L.I., Finley, B.L., 2010. Physical and chemical characterization of tire-related particles: comparison of particles generated using different methodologies. Sci. Total Environ. 408, 652–659.

Lassen, C., Hansen, S.F., Magnusson, K., Hartmann, N.B., Rehne Jensen, P., Nielsen, T.G., et al., 2015. Microplastics: Occurrence, Effects and Sources of Releases to the Environment in Denmark. Danish Environmental Protection Agency.

Lee, H., Kunz, A., Shim, W.J., Walther, B.A., 2019. Microplastic contamination of table salts from Taiwan, including a global review. Sci. Rep. 9, 10145.

Lusher, A.L., McHugh, M., Thompson, R.C., 2013. Occurrence of microplastics in the gastrointestinal tract of pelagic and demersal fish from the English Channel. Mar. Pollut. Bull. 67, 94–99.

Lusher, A.L., Welden, N.A., Sobral, P., Cole, M., 2017. Sampling, isolating and identifying microplastics ingested by fish and invertebrates. Anal. Methods 9, 1346–1360.

Magnusson, K., Eliasson, K., Fråne, A., Haikonen, K., Hultén, J., Olshammar, M., et al., 2017. Swedish Sources and Pathways for Microplastics to the Marine Environment: A Review of Existing Data. IVL Swedish Environmental Research Institute.

Marsalek, J., 2003. Road salts in urban stormwater: an emerging issue in stormwater management in cold climates. Water Sci. Technol. 48, 61–70.

MSFD Technical Subgroup on Marine Litter, 2013. Guidance on Monitoring of Marine Litter in European Seas European Commission. Joint Research Centre, Institute for Environment and Sustainability.

Okoffo, E.D., Ribeiro, F., O'Brien, J.W., O'Brien, S., Tscharke, B.J., Gallen, M., et al., 2020. Identification and quantification of selected plastics in biosolids by pressurized liquid extraction combined with double-shot pyrolysis gas chromatography–mass spectrometry. Sci. Total Environ. 715, 136924.

Polymer Science, 2020. Polymer properties database. URL. http://www.polymerdatabase.com.

Primpke, S., Wirth, M., Lorenz, C., Gerdts, G., 2018. Reference database design for the automated analysis of microplastic samples based on Fourier transform infrared (FTIR) spectroscopy. Anal. Bioanal. Chem. 410, 5131–5141. https://doi.org/10.1007/s00216-018-1156-x.

Renzi, M., Blašković, A., 2018. Litter & microplastics features in table salts from marine origin: Italian versus Croatian brands. Mar. Pollut. Bull. 135, 62–68.

Rieber, G., 2019. Personal Communication on the Different Salt Production Sites and Practices Used for Road Salt.

Rochman, C.M., 2018. Microplastics research—from sink to source. Science 360, 28–29.

Rochman, C.M., Brookson, C., Bikker, J., Djuric, N., Earn, A., Bucci, K., et al., 2019. Rethinking microplastics as a diverse contaminant suite. Environ. Toxicol. Chem. 38, 703–711.

RStudio, 2019. RStudio: Integrated Development for R. RStudio, Inc, Boston, MA.

Schuler, M.S., Relyea, R.A., May 2018. A review of the combined threats of road salts and heavy metals to freshwater systems. BioScience 68 (5), 327–335. https://doi.org/10.1093/biosci/biy018.

Seth, C.K., Shriwastav, A., 2018. Contamination of Indian sea salts with microplastics and a potential prevention strategy. Environ. Sci. Pollut. Res. 25, 30122–30131.

Simon, M., van Alst, N., Vollertsen, J., 2018. Quantification of microplastic mass and removal rates at wastewater treatment plants applying focal plane Array (FPA)-based Fourier transform infrared (FT-IR) imaging. Water Res. 142, 1–9.

Statens vegvesen, 2019a. Hvor mye salt brukes i Norge? Updated January 2019. https://www.vegvesen.no/fag/veg+og+gate/drift+og+vedlikehold/Vinterdrift/salting/sporsmal-og-svar/hvor-mye-salt.

Statens vegvesen, 2019b. Road statistics from the road map applications Vegkart. https://vegkart.atlas.vegvesen.no/, Accessed date: 8 May 2020.

Sundt, P., Schulze, P.-E., Syversen, F., 2014. Sources of Microplastic-pollution to the Marine Environment. p. 86.

Sundt, P., Syversen, F., Skogesal, O., Schulze, P.-E., 2016. Primary Microplastic-pollution: Measures and Reduction Potentials in Norway. p. 117.

Tiwari, A., Rachlin, J.W., 2018. A review of road salt ecological impacts. Northeast. Nat. 25, 123–142, 20.

Trafikverket, 2017. Statistics over Swedish road network. https://www.trafikverket.se/resa-och-trafik/vag/Sveriges-vagnat/.

Trafikverket, 2019. Vägverkets saltförbrukning säsongerna 1976/77–2017/18.

US Department of Transportation, 2017. Statistics of road network. https://www.fhwa.dot.gov/policyinformation/statistics/2016/hm12.cfm.

Van, C., Ter, B., 1990. Conveyor Belt of PVC Provided with a Compound Layer of Reinforcing Material and a Process of Weaving Said Reinforcing Layer, United States.

Vejdirektoratet, 2019a. Saltforbrug og antal udkald på statvejnettet. p. 2019.

Vejdirektoratet, 2019b. Statistics over Danish road network. https://www.dst.dk/da/Statistik/emner/geografi-miljoe-og-energi/infrastruktur/vejnet.

Vogelsang, C., Lusher, A.L., Dadkhah, M.E., Sundvor, I., Umar, M., Ranneklev, S.B., et al., 2018. Microplastics in Road Dust – Characteristics, Pathways and Measures.

Wagner, S., Huffer, T., Klockner, P., Wehrhahn, M., Hofmann, T., Reemtsma, T., 2018. Tire wear particles in the aquatic environment - a review on generation, analysis, occurrence, fate and effects. Water Res. 139, 83–100.

Wickham, H., 2009. ggplot2: Elegant Graphics for Data Analysis. Springer, New York.

Wik, A., Dave, G., 2009. Occurrence and effects of tire wear particles in the environment - a critical review and an initial risk assessment. Environ. Pollut. 157, 1–11.

Yang, D.Q., Shi, H.H., Li, L., Li, J.N., Jabeen, K., Kolandhasamy, P., 2015. Microplastic pollution in table salts from China. Environ. Sci. Technol. 49, 13622–13627.

Supporting Information

Road de-icing salt: assessment of a potential new source and pathway of microplastics particles from roads

Elisabeth S Rødland,[1,2*] Elvis D Okoffo,[4] Cassandra Rauert,[4] Lene S Heier,[3] Ole Christian Lind,[2] Malcolm Reid[1], Kevin V Thomas,[4] and Sondre Meland [1, 2]

[1]*Norwegian Institute for Water Research, Gaustadalléen 21, N-0349 Oslo, Norway.*

[2]*Norwegian University of Life Sciences, Center of Environmental Radioactivity (CERAD CoE), Faculty of Environmental Sciences and Natural Resource Management, P.O. Box 5003, 1433 Ås, Norway*

[3]*Norwegian Public Roads Administration Construction, Postboks 1010, N-2605 Lillehammer, Norway.*

[4]*Queensland Alliance for Environmental Health Sciences (QAEHS), The University of Queensland, 20 Cornwall Street, Woolloongabba, 4102 QLD, Australia.*

Correspondence and requests for materials should be addressed to E.R. (email: elisabeth.rodland@niva.no)

The Supporting Information contains 17 pages, 6 tables and 6 figures.

SI-1 List of Abbreviations

µg/kg	Micrograms of microplastic particles per kilo
µm	Micrometer
µx	Mean number of particles (used for LOD and LOQ)
σx	Standard deviation (used for used for LOD and LOQ)
g/km	Grams per kilometre road
Km	Kilometre
s.d.	Standard deviation
ATR-FT-IR	Attenuated Total Reflectance - Fourier Transformed Infra-Red Spectrometry
A	Acrylic
BR	Butadiene Rubber
BRP	Black rubber-like particles
CaCl2	Calcium chloride
MgCl2	Magnesium chloride
DCM	Dichloromethane
EP	Ethylene propylene
ER	Epoxy resin
FT-IR	Fourier-Transform Infrared spectroscopy
GC-MS	Gas chromatography mass spectrometry
HPDE	High Density Polyethylene
LOD	Limit of Detection
LOQ	Limit of Quantification
MP	Microplastic
MP/kg	Number of microplastic particles per kilo
NaCl	Sodium chloride

NR	Nitrile rubber
P	Probability
PC	Polycarbonate
PE	Polyethylene
PEE	Polyester epoxide
PET	Polyethylene terephthalate
PLE	Pressurized liquid extraction
PMMA	Poly-(methyl methacrylate)
PP	Polypropylene
PS	Polystyrene
PS-d5	Polystyrene-d5
PUR	Polyeruthane acrylic resin
PVC	Polyvinyl chloride
QAQC	Quality control and quality assurance
RAMP	Road-associated microplastic particles
RDA	Redundancy analysis
RO	Reverse osmosis
RS	Rock salt
RWPPMB	Road wear particles polymer-modified bitumen
RWPRM	Road wear particles from road marking
SBR	Styrene butadiene rubber
SS	Sea salt
TWP	Tire wear particles

SI-2 Salt consumption and road network

Table S1. Summary of the total length of road network and salt consumption of Norway, Sweden, Denmark and comparable countries. The length of roads given corresponds to the roads used to quantify the salt consumption. There may be a larger total road network in each country, which is not stated in this table.

Country	Norway	Sweden	Denmark	USA	Canada	China
Km road network	62 900	98 500	74 800	4 112 543	1 130 000	4 338 600
Type of road	State and county	State and county	Total road network	Total urban and rural (paved)	Public roads	Total (paved)
Total salt consumption (tonnes/year)	320000	210000	55 000	22 000 000	7 000 000	600 000
Salt (tonnes) per km road	5.1	2.1	0.7	5.3	6.2	0.1
References road network	Statens vegvesen 2019a	Trafikverket, 2017	Vejdirektoratet 2019a	US Department of Transportation, 2017	Government of Canada, 2018	CIA, 2017
Reference salt consumption	Statens vegvesen, 2019b	Trafikverket, 2017	Vejdirektoratet 2019b	Kelly et al., 2019	Environment Canada, 2012	Ke et al., 2013

SI-2 Torrvieja sample bag

The sample bag that the Torrvieja salt sample came from was tested with single point measurement Attenuated Total Reflectance - Fourier Transformed Infra-Red Spectrometry (ATR-FT-IR) using a Cary 630 FTIR Spectrometer from Agilent. Three subsamples of the same bag were tested (Figure S1-S3) and all confirmed that the bag is made of Polyethylene (Poly-E), with a library search match >0.7 for all subsamples.

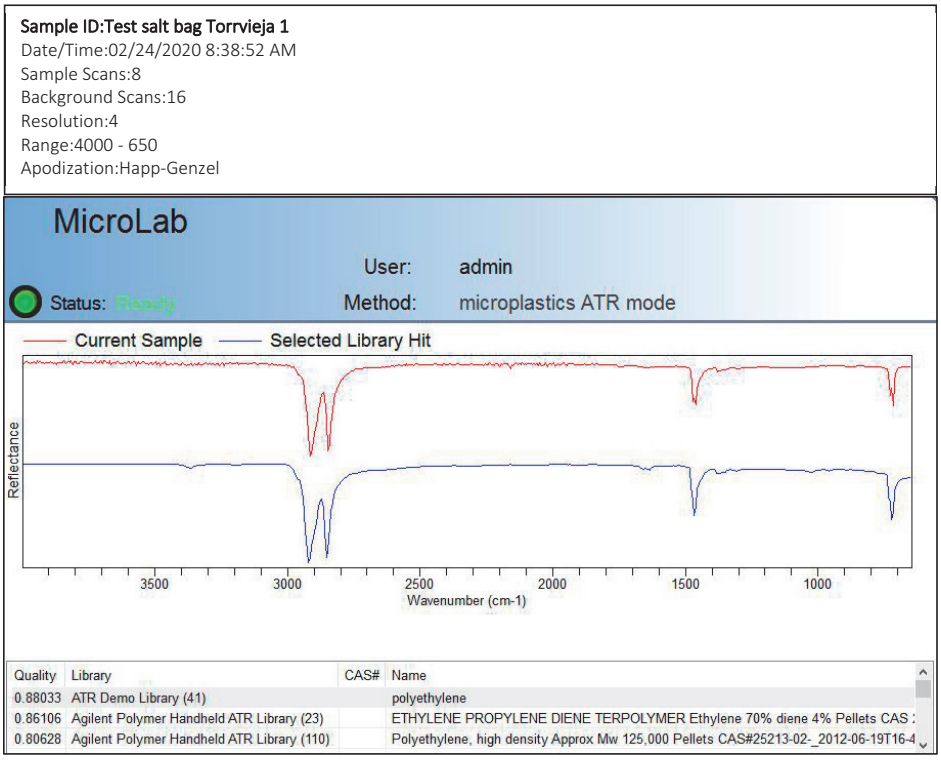

Figure S1 Results from analysing the plastic salt bag from Torrvieja with ATR-FT-IR (Match >0.7 with Poly-E) – subsample 1

Sample ID:Test salt bag Torrvieja 3
Date/Time:02/24/2020 9:03:09 AM
Sample Scans:8
Background Scans:16
Resolution:4
Range:4000 - 650
Apodization:Happ-Genzel

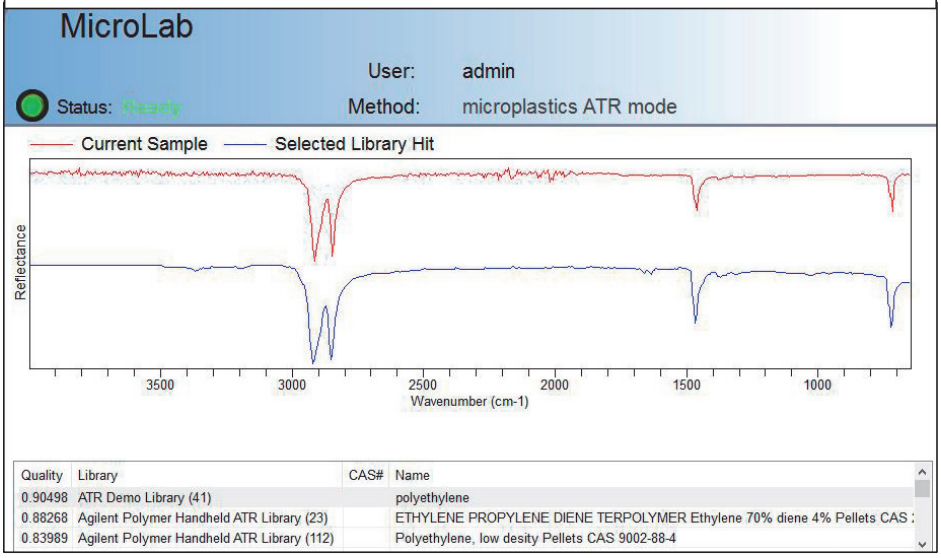

Quality	Library	CAS#	Name
0.90498	ATR Demo Library (41)		polyethylene
0.88268	Agilent Polymer Handheld ATR Library (23)		ETHYLENE PROPYLENE DIENE TERPOLYMER Ethylene 70% diene 4% Pellets CAS :
0.83989	Agilent Polymer Handheld ATR Library (112)		Polyethylene, low desity Pellets CAS 9002-88-4

Figure S2 Results from analysing the plastic salt bag from Torrvieja with ATR-FT-IR (Match >0.7 with Poly-E) – subsample 2

Sample ID:Test salt bag Torrvieja 2
Date/Time:02/24/2020 8:41:40 AM
Sample Scans:8
Background Scans:16
Resolution:4
Range:4000 - 650
Apodization:Happ-Genzel

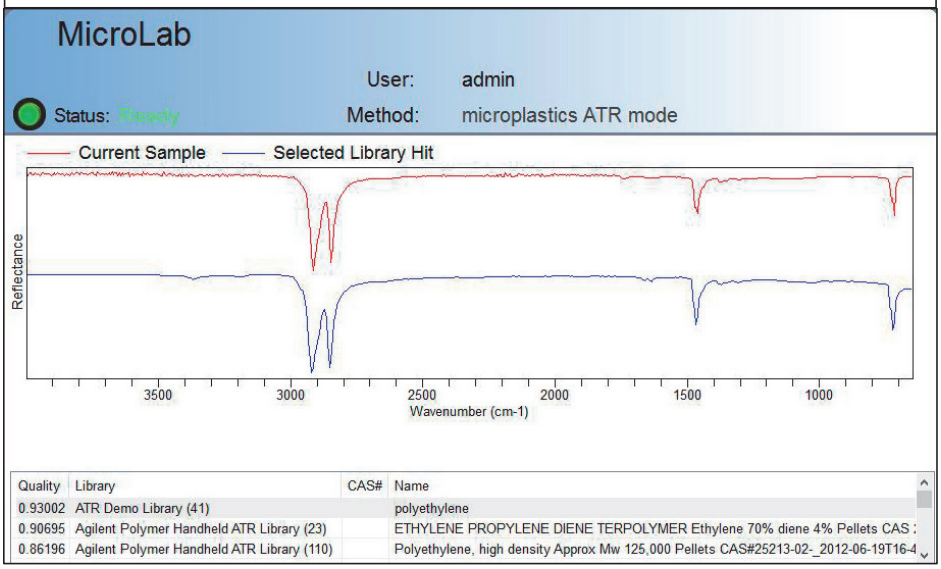

Quality	Library	CAS#	Name
0.93002	ATR Demo Library (41)		polyethylene
0.90695	Agilent Polymer Handheld ATR Library (23)		ETHYLENE PROPYLENE DIENE TERPOLYMER Ethylene 70% diene 4% Pellets CAS :
0.86196	Agilent Polymer Handheld ATR Library (110)		Polyethylene, high density Approx Mw 125,000 Pellets CAS#25213-02-_2012-06-19T16-4

Figure S3 Results from analysing the plastic salt bag from Torrvieja with ATR-FT-IR (Match >0.7 with Poly-E) – subsample 3

SI-3 Mass and size distribution of all MPs found in the salt samples

Tables S1-S4 summarizes the microplastic particles found in the salt samples, differentiated by number of particles per kilo salt (MP/kg), concentration of polymers per kilo salt (µg/kg), number of particles per kilo (MP/kg) for different polymers and concentration of polymers per kilo salt (µg/kg) for different polymers.

Table S2. Summary of the microplastic particles found in total and between sites, separated by fibre and fragment, in number of MPs per kilo (MP/kg)

Site	Type	Mean	s.d.	Median	Min.	Max.	N
All	All	132	63	126	32	252	12
All	Fibre	10	3	12	4	16	11
All	Fragment	122	64	116	24	240	12
Sea salts	All	35	60	4	4	240	33
Rock salt	All	61	76	12	4	192	7
Ben Gardene	All	77	99	10	4	240	3
Germany	All	61	76	12	4	192	3
Torrvieja	All	36	49	8	4	124	3
Zarziz	All	12.5	17	4	4	64	3
Ben Gardene	Fragment	195	41	184	160	240	3
Germany	Fragment	136	60	136	76	196	3
Torrvieja	Fragment	107	20	104	88	128	3
Zarziz	Fragment	52	33	44	24	88	3
Ben Gardene	Fibre	9	2	8	8	12	3
Germany	Fibre	8	5	8	4	12	2
Torrvieja	Fibre	13	3	12	12	16	3
Zarziz	Fibre	11	2	12	8	12	3

Table S3. Summary of the microplastic particles found in total and between sites, separated by fibre and fragment, in concentration of MP per kilo (µg /kg)

Site	Type	Mean	s.d.	Median	Min.	Max.	N
All	All	595.5	1129.2	103.2	1.5	3986.8	12
All	Fibers	48.8	93.0	25.0	1.1	324.9	11
All	Fragment	1358.7	2251.4	228.3	4.9	7648.7	12
Sea salts	All	442.1	1466.2	7.5	0.1	7648.7	33
Rock salt	All	321.8	480.7	28.6	0.6	1122.4	7
Ben Gardene	All	1736.5	2699.3	220.9	5.0	7648.7	3
Germany	All	321.8	480.7	28.6	0.6	1122.4	3
Torrvieja	All	61.8	90.9	19.3	1.8	264.9	3
Zarziz	All	5.3	9.6	1.8	0.1	37.5	3
Ben Gardene	Fragment	4502.6	2724.8	2956.4	2902.5	7648.7	3
Germany	Fragment	734.6	502.9	914.1	166.6	1123.0	3
Torrvieja	Fragment	173.4	102.5	189.9	63.7	266.7	3
Zarziz	Fragment	24.2	31.4	7.4	4.9	60.5	3
Ben Gardene	Fibre	128.1	171.6	49.4	10.0	324.9	3
Germany	Fibre	24.4	6.0	24.4	20.1	28.6	2
Torrvieja	Fibre	32.5	6.5	36.1	25.0	36.4	3
Zarziz	Fibre	2.1	0.9	2.2	1.1	2.9	3

Table S4. Summary of all polymer types found for each site, separated by fibre and fragment, in number of MPs per kilo (MP/kg). Polymer types: Black rubbery particles (BRP), polyethylene terephthalate (PET), acryl (A), epoxy resin (ER), ethylene propylene (EP), polyester epoxide (PEE), polyvinyl chloride (PVC, non-black particles), high-density polyethylene (HPDE), nitrile butadiene (NR), polyeruthane (PUR) acrylic resin, polypropylene (PP).

Site	Type	Polymer	Mean	s.d	Median	Min	Max	N
Ben Gardene	Fibre	A	4		4	4	4	1
Ben Gardene	Fibre	PET	8	4	8	4	12	3
Germany	Fibre	ER	4		4	4	4	1
Germany	Fibre	PET	12		12	12	12	1
Torrvieja	Fibre	A	4		4	4	4	1
Torrvieja	Fibre	PEE	6	3	6	4	8	2
Torrvieja	Fibre	PET	8	6	8	4	12	2
Torrvieja	Fibre	PVC	8		8	8	8	1
Zarziz	Fibre	A	4	0	4	4	4	2
Zarziz	Fibre	PE	5	2	4	4	8	3
Zarziz	Fibre	PET	4	0	4	4	4	2
Ben Gardene	Fragment	BRP	193	42	180	160	240	3
Ben Gardene	Fragment	HPDE	4		4	4	4	1
Germany	Fragment	BRP	133	58	132	76	192	3
Germany	Fragment	EP	4		4	4	4	1
Germany	Fragment	PP	4		4	4	4	1
Torrvieja	Fragment	BRP	105	18	104	88	124	3
Torrvieja	Fragment	PUR	4		4	4	4	1
Zarziz	Fragment	BRP	64		64	64	64	1
Zarziz	Fragment	EP	4		4	4	4	1
Zarziz	Fragment	NR	22	25	22	4	40	2
Zarziz	Fragment	PET	18	3	18	16	20	2
Zarziz	Fragment	PP	4		4	4	4	1
Zarziz	Fragment	PVC	4		4	4	4	1

Table S5. Summary of all polymer types found for each site, separated by fibre and fragment, in concentration of MP per kilo (µg /kg). Polymer types: Black rubbery particles (BRP), polyethylene terephthalate (PET), acryl (A), epoxy resin (ER), ethylene propylene (EP), polyesterepoxide (PEE), polyvinyl chloride (PVC, non-black particles), high-density polyethylene (HPDE), nitrile butadiene (NR), polyeruthane (PUR) acrylic resin, polypropylene (PP).

Site	Type	Polymer	Mean	s.d	Median	Min	Max	N
Ben Gardene	Fibre	A	5.0		5.0	5.0	5.0	1
Ben Gardene	Fibre	PET	126.4	173.3	49.4	5.0	324.9	3
Germany	Fibre	ER	28.6		28.6	28.6	28.6	1
Germany	Fibre	PET	20.1		20.1	20.1	20.1	1
Torrvieja	Fibre	A	25.5		25.5	25.5	25.5	1
Torrvieja	Fibre	PEE	7.7	6.1	7.7	3.4	11.9	2
Torrvieja	Fibre	PET	21.8	20.2	21.8	7.5	36.1	2
Torrvieja	Fibre	PVC	13.1		13.1	13.1	13.1	1
Zarziz	Fibre	A	1.2	1.1	1.2	0.4	1.9	2
Zarziz	Fibre	PE	0.8	0.7	0.7	0.1	1.5	3
Zarziz	Fibre	PET	0.8	0.9	0.8	0.2	1.4	2
Ben Gardene	Fragment	BRP	4463.6	2759.7	2956.4	2785.7	7648.7	3
Ben Gardene	Fragment	HPDE	116.8		116.8	116.8	116.8	1
Germany	Fragment	BRP	731.9	501.3	906.8	166.6	1122.4	3
Germany	Fragment	EP	7.3		7.3	7.3	7.3	1
Germany	Fragment	PP	0.6		0.6	0.6	0.6	1
Torrvieja	Fragment	BRP	172.8	101.7	189.9	63.7	264.9	3
Torrvieja	Fragment	PUR	1.8		1.8	1.8	1.8	1
Zarziz	Fragment	BRP	37.5		37.5	37.5	37.5	1
Zarziz	Fragment	EP	1.8		1.8	1.8	1.8	1
Zarziz	Fragment	NR	3.3	3.1	3.3	1.2	5.5	2
Zarziz	Fragment	PET	8.2	7.2	8.2	3.1	13.2	2
Zarziz	Fragment	PP	1.9		1.9	1.9	1.9	1
Zarziz	Fragment	PVC	8.6		8.6	8.6	8.6	1

SI-4 Distribution of polymers in all samples combined, by number of microplastic particles per kilo salt (MP/kg) and by concentration per kilo salt (µg/kg)

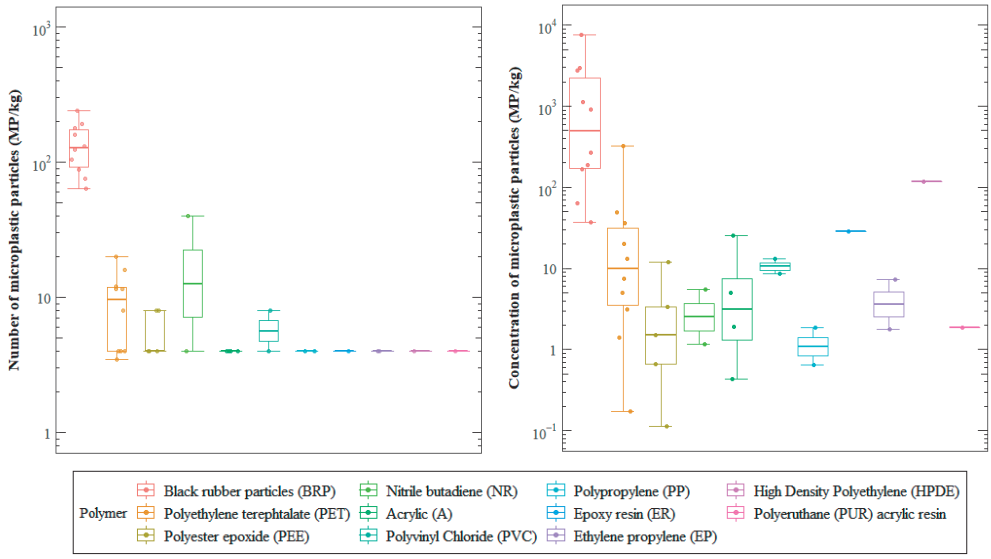

Figure S4 The total polymer distribution for all samples combined, in number of microplastic particles (MP/kg) and concentration of microplastic particles (µg/kg)

SI-5 Multivariate statistics

Figures S5-S6 shows the results of doing RDA analysis on the concentration of polymers and the number of particles from each type of polymers with the salt type (sea salt or rock salt) as the explanatory factor.

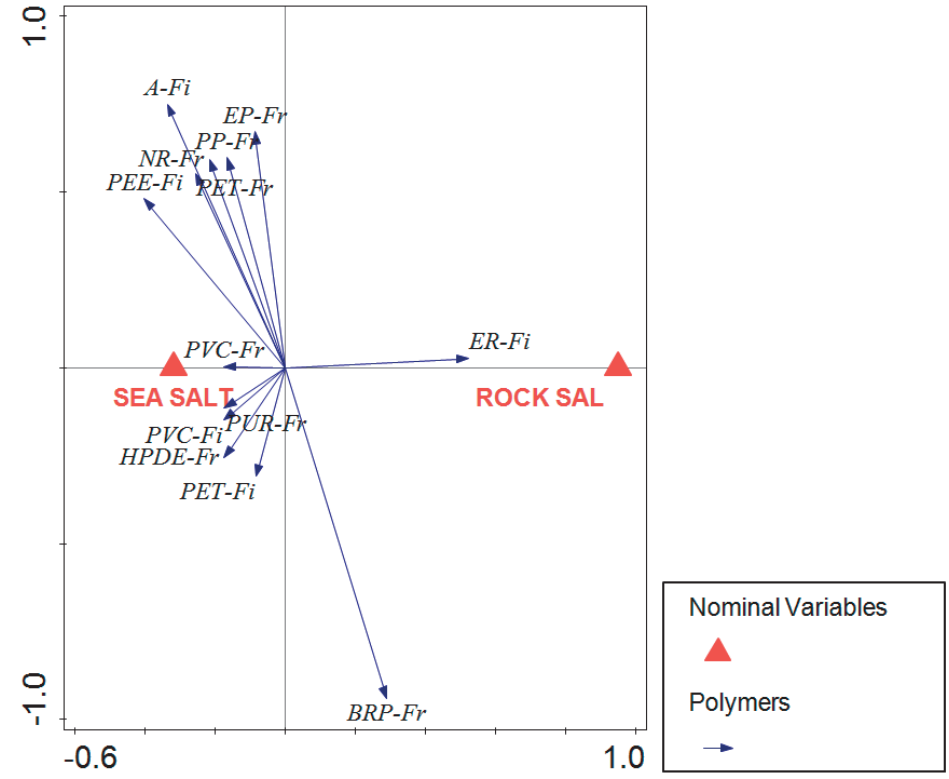

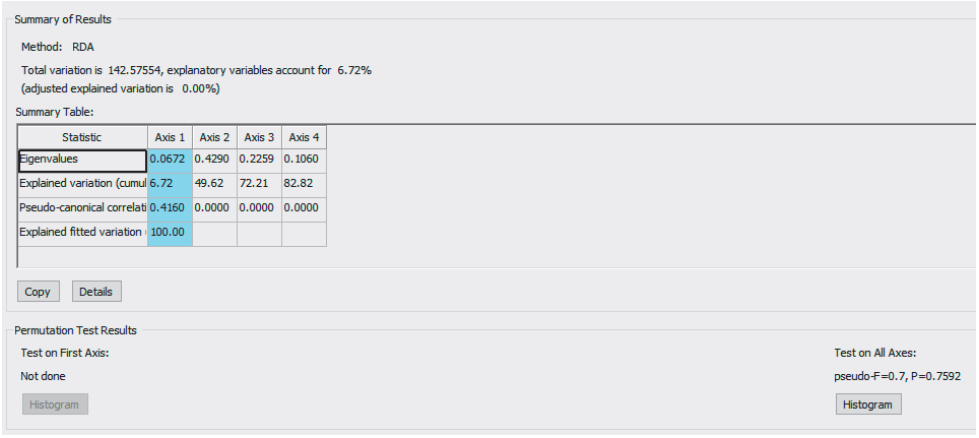

Summary of Results

Method: RDA

Total variation is 142.57554, explanatory variables account for 6.72%
(adjusted explained variation is 0.00%)

Summary Table:

Statistic	Axis 1	Axis 2	Axis 3	Axis 4
Eigenvalues	0.0672	0.4290	0.2259	0.1060
Explained variation (cumul	6.72	49.62	72.21	82.82
Pseudo-canonical correlati	0.4160	0.0000	0.0000	0.0000
Explained fitted variation	100.00			

Copy Details

Permutation Test Results

Test on First Axis:
Not done
Histogram

Test on All Axes:
pseudo-F=0.7, P=0.7592
Histogram

Figure S5. RDA plot and output: Concentration of Polymer ~ salt types

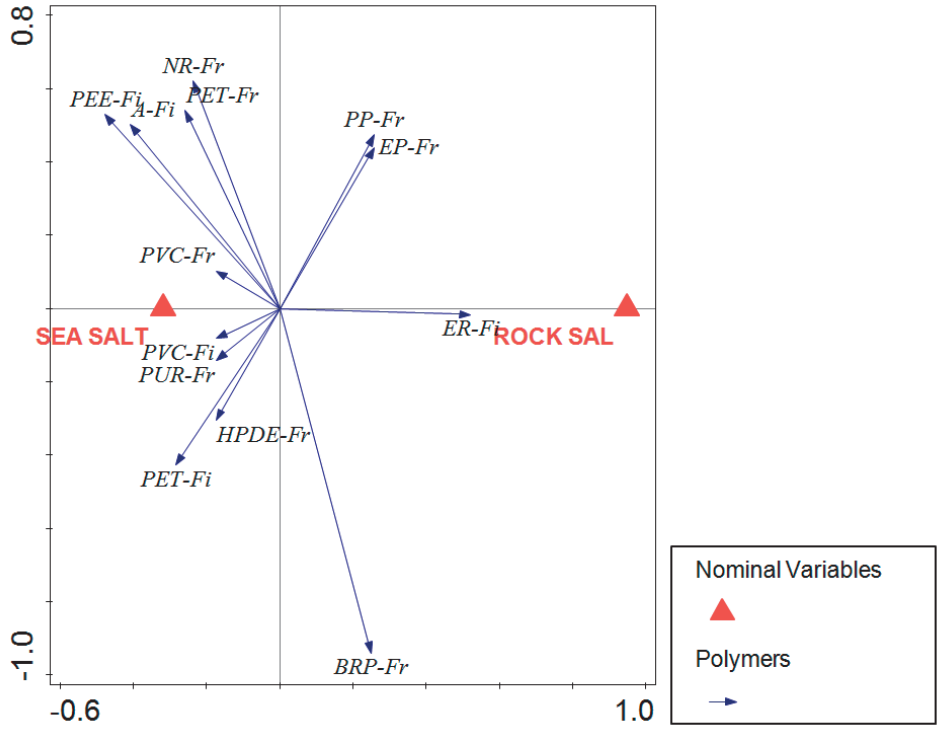

Summary of Results

Method: RDA

Total variation is 121.39898, explanatory variables account for 8.57%
(adjusted explained variation is 0.00%)

Summary Table:

Statistic	Axis 1	Axis 2	Axis 3	Axis 4
Eigenvalues	0.0857	0.4506	0.1550	0.0948
Explained variation (cumul	8.57	53.63	69.12	78.61
Pseudo-canonical correlati	0.5442	0.0000	0.0000	0.0000
Explained fitted variation	100.00			

Copy Details

Permutation Test Results

Test on First Axis:

Not done

Histogram

Test on All Axes:

pseudo-F=0.9, P=0.7592

Histogram

Figure S6. RDA plot and output: Number of particles per Polymer ~salt types

SI-6 Summarized table of microplastic particles in salt studies

Table S6. Number of particles per kilo salt (MP/kg) identified in salt studies. N= number of salt types tested. N/A = not applicable. N.d. = not detected.

Origin	Pore size of filters used, µm	Range (MP/kg)	Range (mg/kg)	N	References
		Sea salt			
Mediterranean Sea	2.7	4-240	0.0001-7.6	3	Present study
Atlantic Ocean	5	50-150	N/A	7	Iniguez et al. (2017)
Mediterranean Sea	5	60-280	N/A	9	Iniguez et al. (20179
North Pacific Ocean	2.7	0 - 1674	n.d. - 73	18	Kim et al. (2018)
South Pacific Ocean	2.7	46 – 13 629	0.1 – 46.5	2	Kim et al. (2018)
North Atlantic	2.7	0 - 136	n.d. – 1.9	3	Kim et al. (2018)
South Atlantic	2.7	24	0.5	1	Kim et al. (2018)
Mediterranean Sea	2.7	4 -30	0.5-2.4	2	Kim et al. (2018)
Black Sea	2.7	12	3.7	1	Kim et al. (2018)
South Pacific Ocean	149	1-9	N/A	2	Karami et al. (2017)
North Atlantic Ocean	149	0-10	N/A	9	Karami et al. (2017)
North Pacific Ocean	149	0-1	N/A	2	Karami et al. (2017)
South Atlantic Ocean	149	1	N/A	1	Karami et al. (2017)
North Pacific Ocean	5	550-681	N/A	5	Yang et al. (2015)
Unknown (Turkish produced)	0.2	16-84	N/A	5	Gündoğdu (2018)
Unknown (sold in Taiwan)	5	2.5 - 20	N/A	10	Lee et al. (2019)
North Pacific Ocean	0.45	56-103	0.065	8	Seth and Shriwastav (2018)
		Rock salt			
Germany	2.7	24-240	0.0006-1.1	1	Present study
China, the Philippines, Bulgaria, Italy, Hungary, Germany, United States	2.7	28-462	N/A	9	Kim et al. (2018)
China	5	7-204	N/A	5	Yang et al. (2015)
Unknown (Turkish produced)	0.2	9-16	N/A	5	Gündoğdu (2018)
Unknown (sold in Taiwan)	5	12.5	N/A	1	Lee et al. (2019)

SI-7 Summary of RAMP and road salt

Table S7. Summary table of the estimated release of RAMP, Road salt consumption of 2017/18 and calculated release of MPs from road salt in Norway, Sweden and Denmark. Calculated MP release per km road uses length of road network from Table S1.

Estimated release of RAMP	Norway	Sweden	Denmark
Total (tonnes) per year	4368 - 5348	8193	4310 - 7290
TWP (tonnes) per year	4250 - 5000	7 674	4 200 -6 600
RWP_{RM} (tonnes) per year	90 - 320	504	110 – 690
RWP_{PMB} (tonnes) per year	28	15	-
References	(Sundt et al., 2014; Sundt et al., 2016; Vogelsang et al., 2018)	(Magnusson et al., 2017)	(Lassen et al., 2015)
Road salt consumption 2017/18	Norway	Sweden	Denmark
Sea salt (tonnes) per year	150 000		55 000
Rock salt (tonnes) per year	170 000	210 000	
Total (tonnes) per year	320 000	210 000	55 000
References	(Statens vegvesen, 2019)	(Trafikverket, 2019)	(Vejdirektoratet, 2019)
Calculated release of MP from road salt	Norway	Sweden	Denmark
Sea salt (tonnes) per year	0.09		0.03
Rock salt (tonnes) per year	0.06	0.07	
Total (tonnes) per year	0.15	0.07	0.03
Total (g) per km road	0.23	0.07	0.04
Contribution to total RAMP %	0.003	0.008	0.0004-0.0008

References

CIA, 2017. Statistics of Road network. https://www.cia.gov/library/publications/the-world-factbook/fields/385.html

Environment Canada, 2012. Five-year Review of Progress: Code of Practice for the Environmental Management of Road Salts. Report published March 31. 2012.

Government of Canada, 2018. Statistics of road network. https://www.tc.gc.ca/eng/policy/transportation-canada-2018.html#item-10

Lassen C, Hansen SF, Magnusson K, Hartmann NB, Rehne Jensen P, Nielsen TG, et al. Microplastics: Occurrence, effects and sources of releases to the environment in Denmark. Danish Environmental Protection Agency, 2015.

Magnusson K, Eliasson K, Fråne A, Haikonen K, Hultén J, Olshammar M, et al. Swedish sources and pathways for microplastics to the marine environment: A review of existing data. IVL Swedish Environmental Research Institute, 2017.

Statens vegvesen, 2019a. Hvor mye salt brukes i Norge? Updated January 2019. https://www.vegvesen.no/fag/veg+og+gate/drift+og+vedlikehold/Vinterdrift/salting/sporsmal-og-svar/hvor-mye-salt

Statens vegvesen. 2019b. Road statistics from the road map applications Vegkart. Accessed 08. may 2020. https://vegkart.atlas.vegvesen.no/

Sundt P, Schulze P-E, Syversen F. Sources of microplastic-pollution to the marine environment, 2014, pp. 86.

Sundt P, Syversen F, Skogesal O, Schulze P-E. Primary microplastic-pollution: Measures and reduction potentials in Norway, 2016, pp. 117.

Trafikverket, 2017. Statistics over Swedish road network. https://www.trafikverket.se/resa-och-trafik/vag/Sveriges-vagnat/

Trafikverket, 2019. Vägverkets saltförbrukning säsongerna 1976/77-2017/18.

US Department of Transportation, 2017. Statistics of road network. https://www.fhwa.dot.gov/policyinformation/statistics/2016/hm12.cfm

Vejdirektoratet, 2019b. Statistics over Danish road network. https://www.dst.dk/da/Statistik/emner/geografi-miljoe-og-energi/infrastruktur/vejnet

Vogelsang C, Lusher AL, Dadkhah ME, Sundvor I, Umar M, Ranneklev SB, et al. Microplastics in road dust – characteristics, pathways and measures, 2018.

Paper II

Journal of Hazardous Materials 423 (2022) 127092

Contents lists available at ScienceDirect

Journal of Hazardous Materials

journal homepage: www.elsevier.com/locate/jhazmat

Research Paper

A novel method for the quantification of tire and polymer-modified bitumen particles in environmental samples by pyrolysis gas chromatography mass spectroscopy

Elisabeth S. Rødland [a,b,*], Saer Samanipour [a,c,d], Cassandra Rauert [d], Elvis D. Okoffo [d], Malcom J. Reid [a], Lene S. Heier [e], Ole Christian Lind [b], Kevin V. Thomas [d], Sondre Meland [a,b]

[a] Norwegian Institute for Water Research, Økernveien 94, 0579 Oslo, Norway
[b] Norwegian University of Life Sciences, Center of Excellence in Environmental Radioactivity (CERAD), Faculty of Environmental Sciences and Natural Resource Management, P.O. Box 5003, 1433 Ås, Norway
[c] Faculty of Science, Van't Hoff Institute for Molecular Sciences, University of Amsterdam, Science Park, 904 GD Amsterdam, the Netherlands
[d] Queensland Alliance for Environmental Health Sciences (QAEHS), The University of Queensland, 20 Cornwall Street, Woolloongabba, 4102 QLD, Australia
[e] Norwegian Public Roads Administration, Construction, Postboks 1010, N-2605 Lillehammer, Norway

ARTICLE INFO

Editor: Dr. R Teresa

Keywords:
Microplastics
Tire wear particles
Rubber particles
Road particles
Pyrolysis GC/MS

ABSTRACT

Tire and road wear particles may constitute the largest source of microplastic particles into the environment. Quantification of these particles are associated with large uncertainties which are in part due to inadequate analytical methods. New methodology is presented in this work to improve the analysis of tire and road wear particles using pyrolysis gas chromatography mass spectrometry. Pyrolysis gas chromatography mass spectrometry of styrene butadiene styrene, a component of polymer-modified bitumen used on road asphalt, produces pyrolysis products identical to those of styrene butadiene rubber and butadiene rubber, which are used in tires. The proposed method uses multiple marker compounds to measure the combined mass of these rubbers in samples and includes an improved step of calculating the amount of tire and road based on the measured rubber content and site-specific traffic data. The method provides good recoveries of 83–92% for a simple matrix (tire) and 88–104% for a complex matrix (road sediment). The validated method was applied to urban snow, road-side soil and gully-pot sediment samples. Concentrations of tire particles in these samples ranged from 0.1 to 17.7 mg/mL (snow) to 0.6–68.3 mg/g (soil/sediment). The concentration of polymer-modified bitumen ranged from 0.03 to 0.42 mg/mL (snow) to 1.3–18.1 mg/g (soil/sediment).

1. Introduction

Tire and road wear particles (TRWP) are estimated to be the largest single source of synthetic polymer particles in the microscopic size range (1 μm - 1 mm), to the environment (Boucher et al., 2020; Knight et al., 2020), often referred to as microplastic particles. A large number of studies have been published on microplastic particles over the last years, however, there is still a lack of standardization and harmonization on how to analyze, quantify and report these findings (Lusher et al., 2021). Compared to the more conventional plastic types such as polyethylene terephthalate (PET) or polystyrene (PS) which are widely used in a large variety of products, the data on concentrations of TRWP in environmental samples is very limited (Baensch-Baltruschat et al., 2020). Measurements of TRWP in such samples have been hampered by inadequate analytical methodology. The most commonly applied analytical method for microplastics today is visual analysis coupled to a chemical analysis step, such as Fourier transform infrared spectroscopy (FTIR). However, as tire particles contain black pigment (carbon black), the infrared light is absorbed and FTIR analysis is unable to identify the rubber content (Baensch-Baltruschat et al., 2020). A recent study has also demonstrated the potential for under-reporting of microplastics when only visual techniques such as FTIR are applied (Ribeiro et al., 2021).

Thermal methods, such as pyrolysis gas chromatography mass spectrometry (Py-GC/MS) (Unice et al., 2012; ISO, 2017a, 2017b, 2017c; Goßmann et al., 2021) and thermal extraction and desorption gas chromatography mass spectroscopy (TED GC/MS) (Eisentraut et al., 2018; Klöckner et al., 2019) are becoming more common, as these

* Corresponding author at: Norwegian Institute for Water Research, Økernveien 94, 0579 Oslo, Norway.

https://doi.org/10.1016/j.jhazmat.2021.127092
Received 14 July 2021; Received in revised form 27 August 2021; Accepted 29 August 2021
Available online 2 September 2021

methods use the products of the thermal decomposition as markers to identify and quantify polymers and rubbers. Such methods can be used to potentially a) identify specific tire and asphalt markers present in TRWP and b) based on those numbers, assess the amount of rubber released into the environment.

A recent study raised questions over the selection of markers used for quantifying tire rubber and how these are extrapolated to a derivation of tire-mass (Rauert et al., 2021). This included the use of 4-vinylcyclohexene (4-VCH) as a marker as specified in the ISO technical specifications for soil and sediments (ISO, 2017a) and for air (ISO, 2017c). In Rauert et al. (2021), two additional pyrolysis marker compounds were tested, the SB hybrid dimer and SBB hybrid trimer. Both showed a large and inconsistent variability in the calculated %rubber content in analyzed reference tires (n = 39) and were not recommended as viable single markers. This is contradictory to studies by Eisentraut et al. (2018) and Goßmann et al. (2021) which suggested using SB dimer for the quantification of SBR in personal vehicle tires.

Tires contain a wide range of substances, such as rubber materials, fillers, softeners, vulcanization agents and other additives (Baensch-Baltruschat et al., 2020; Sommer et al., 2018). Each type and brand of tires contain different amounts of these components. Thus, tires are a complex mixture to analyze. Two main types of rubber can be found in tires; natural rubber (NR, polyisoprene) and synthetic rubbers, which includes styrene butadiene rubber (SBR) and butadiene rubber (BR). Previous studies have reported that the total percentage of rubber in tire tread is 50% (w/w), of which SBR+BR contribute 44% in personal vehicle tires (PV), and NR contributes 45% in heavy vehicle tires (HV) (Unice et al., 2012). The rest of the tire consists of additional rubbers and other components, as described by Sommer et al. (2018). Another study has reported that PV tires has a total rubber content of 41%, in which SBR contributes 30% and BR 20% (Grigoratos and Martini, 2014). Thus, the total contribution of SBR+BR would be 20% (12 +8% of the tire mass). Other studies have reported smaller contributions of SBR+BR in PV tires, e.g. 20–30% of the total mass of the tire, with a 60:40 ratio between SBR and BR (Vogelsang et al., 2018). Another study used the global market share of rubber in PV tires to state that tires contain 11% SBR (Eisentraut et al., 2018). For heavy vehicles, previous studies have reported that HV tires contain mainly NR, even up to 100% NR. However, this has been disputed in the recent study of Rauert et al. (2021), which showed that SBR and BR products were present in all HV tires and even in higher concentration than some of the PV tires. The use of the NR component to measure the amount of tire has also been shown to be difficult, as the thermal decomposition of NR and plant material both will result in the presence of dipentene (polyisoprene) in an environmental sample (Eisentraut et al., 2018). SBR contains both a styrene and a butadiene component and can be formulated either as solution styrene butadiene rubber (SSBR) or emulsion styrene butadiene rubber (ESBR). SBR can also have a wide range of styrene content (16–45%) according to different polymer manufacturers (SI-1 Table S1). Tires made with SSBR are especially subject to variable styrene content as the solution process is difficult to perform consistently (ANON, 1996). A lack of knowledge on the variability of SBR+BR and NR content in both PV and HV tires is a challenge for quantifying TRWP in samples and need to be addressed.

Another potential source of microplastic particles to the environment is polymer-modified bitumen (PMB) (Vogelsang et al., 2018; Sundt et al., 2014) used in road asphalt. PMB usually constitutes 5% of the total road asphalt and is only used in the top layer of the road surface. Several countries including Australia, China, Denmark, Norway, Russia, Sweden and the United Kingdom (ANON, 2018), add PMB to their road surfaces to increase resistance to cracking and deformation (rutting) of the road surface (S. et al., 2012). In Norway, the annual release of microplastics from roads is estimated to be approximately 5000 metric tons (mt), in which PMB asphalt and tires are estimated to contribute 28 mt and 4500 mt, respectively (Vogelsang et al., 2018; Sundt et al., 2014, 2016). PMB can be manufactured using different polymers, such as styrene butadiene styrene (SBS), styrene ethylene butadiene styrene (SEBS), low-density polyethylene (LDPE), ethylene vinyl acetate (EVA), polypropylene (PP) and styrene isoprene styrene (SIS) (Polacco et al., 2005, 2006; Giavarini et al., 1996; Panda and Mazumdar, 1999; Sengoz et al., 2009; M et al., 2003; Chen et al., 2002). In Norway, PMB asphalt makes up approximately 6% (3282 km) of the total state and county road network (Vegvesen, 2020; Kjørelengder, 2019), however, it is used mainly in and around the largest cities and on roads where the traffic densities and speed is the highest. Thus, there is a potentially important source of rubber associated with PMB asphalt. SBS is the only polymer used in Norway, contributing 5% of the mass of PMB (NVF, 2013).

The SBS used for PMB bitumen is a block copolymer, made of blocks of polystyrene and polybutadiene (ANON, 2021), with a styrene content of 30% (w/w). When pyrolyzed at the same temperatures, SBR and SBS form the same pyrolysis products, but at different intensities (Tsuge et al., 2011). This is due to the different ratio of styrene and butadiene in the two polymers. For all pyrolysis products related to butadiene rubber, BR (Tsuge et al., 2011) will also produce the same pyrolysis products as SBR and SBS. As recently discussed in Rauert et al. (2021), the marker compounds and the conversion from rubber to tire described in current Py-GC/MS methodologies do not account for variability in tire composition of synthetic rubber. These methods also incorrectly assume that the SBR pyrolysis products are selective. This study aims to address these challenges.

Our study is aimed at quantifying the total mass of SBR+BR+SBS in environmental samples using pyrolysis products previously not explored as markers for SBR and SBS, as well as combining multiple pyrolysis products for the quantification in order to compensate for individual differences between types of tires. Further, the total mass of SBR+BR+SBS is used to calculate the mass of tire and PMB in a sample using different calculation approaches based on available traffic data and the measured SBR+BR content in reference tires relevant for the sample locations and sample time. The non-specificity of the SBR and SBS pyrolysis products in tire and environmental samples was also tested and can be found in supplementary Information (SI-10).

2. Experimental details

2.1. Chemicals and reference material

The reference standard SBR used in this study was SBR-1500 (Polymer Source Inc., Canada), a non-vulcanized SBR with 23.5% styrene content. The reference standard SBS polymer was Kraton D, a standard SBS (30% styrene) added to PMB in Norway and provided by the bitumen company Nynas AB (Drammen, Norway). Deuterated poly(1,4-butadiene-d6) (d6-PB, Polymer Source, Inc., Quebec, Canada) was used as an internal standard, as described in the method by Unice et al. (2012), ISO (2017a, 2017b). All standards were dissolved in chloroform ($CHCl_3$, Sigma Aldrich). SBR and SBS were prepared in three different concentrations: 100 μg/mL, 500 μg/mL and 1000 μg/mL, and d6-PB was prepared at 2.5 mg/mL.

2.2. Sample collection and processing

Reference tire samples were collected from 31 unused tires using knives with disposable ceramic blades (Slice TM), or with taping knives (Ironside TM), using separate blades for each tire. The tire samples were donated from two major tire manufacturers, Bridgestone and Continental, and one tire import company, Starco Norge. Various environmental samples (snow, soil, gully-pot sediment) were collected from sites with high average annual daily traffic (AADT), and where PMB-asphalt was applied. Snow samples were collected in February (2019) at two sites; Skullerud (SK, Oslo, Norway, 71 250 AADT, 59°51'39.5"N 10°49'51.7"E) and Storo (ST, Oslo, Norway (50 950 AADT, 59°56'37.6"N 10°46'47.2"E). Snow cores were collected at 0 m, 1 m and 3 m distance from the road at Skullerud and 0 m from the road at Storo.

The length of the snow cores for each sample were measured and then packed in zip-lock bags (made of polyethylene, PE) and kept in freezer (−20 °C) until processing. The frozen snow sample was weighed and then melted in the zip-lock bag in room temperature. The volume of melt water was recorded and then transferred to pre-cleaned glass beakers using 1 mm sieves to remove large items. The samples were stirred by hand-shaking the beakers for 20 s before 16 mL subsamples were transferred to glass jars, that had been pretreated in the muffle furnace (Nabertherm, Germany) at 550 °C in order to remove any contamination. The subsamples were frozen (−20 °C, 24H) and freeze dried (3–4 days, Leybold Heraeus Lyovac GT2). Dried snow material was then put directly into the pyrolysis cup by weight. Soil samples (SK-sed) from Skullerud (Oslo, Norway, 71 250 AADT, 59°51'39.5"N 10°49'51.7"E) were sampled August 27th and 28th (2018). They were collected as mixture samples at 0–1.5 m, 1.5–3 m and 3–4.5 m distance from the road, using Multi-increment sampling (MIS, > 30 subsamples of > 0.5 kg for each sample location). The samples were sieved with 1 mm sieves and placed in small glass jars (pre-treated in muffle furnace) for storage. The samples were then put directly into the pyrolysis cup by weight. Gully-pot sediment sample (SF) were sampled from the Smestad tunnel (Oslo, Norway, 44 060 AADT, 59°56'10.4"N 10°40'47.7"E). The gully-pot samples were collected from three different gully-pots inside the tunnel, collected during two tunnel wash events (5th of November 2018 and 21st of April 2020). The sediment samples were taken using a small Van Veen grab sampler and collected in disposable aluminum foil baking pans. Subsamples were collected with a pre-cleaned metal spoon (RO-water) and stored in small glass jars (pre-treated in muffle furnace). The glass jars were then frozen and freeze-dried as described for the snow samples. Dried sediment material was then put directly into the pyrolysis cup by weight. All samples were analyzed in triplicates (technical replicates) except for SK-0 m, which was analyzed in nine replicates and the (2018) samples of SF, which were single samples.

The proposed method focuses on samples where it is expected to find high concentrations of road contamination, low concentration of other synthetic polymers than tire and PMB-rubber, and low concentration of organic matter. This includes tunnel wash water, road-runoff, road dust, gully-pot sediments and in some cases also road-side soil. When analyzing these samples, it is recommended as a cost-benefit measure to analyze samples directly, either on glass-fiber filters or as freeze-dried material. However, if it is expected that the concentrations of tire and PMB in the sample are low and/or it is expected to find higher concentrations of other polymers or organic matter, it is recommended to include different steps of pre-treatment to minimize influence on pyrolysis marker compounds from competing sources. Such steps should be customized to each sample based on sample type and sampling location. For example, if analyzing urban road dust from larger cities, it could be expected that the samples also contain a large proportion of microplastics that is not related to tire and PMB, such as PET and PVC (O'Brien et al., 2021). In these cases, density separation (Klöckner et al., 2019) targeting the tire and PMB fractions could be applied. For samples with high concentrations of organic matter, the organic matter can cause large background noise. This will make it more difficult to analyze low concentrations of tire and PMB, as well as influencing the marker compounds for tire and PMB with competing sources. To reduce the interference from organic matter, treatment with hydrogen peroxide (H_2O_2) or Fenton's reagent could then be applied (Hurley et al., 2018). Another option would be to use a thermal desorption step to remove volatile compounds before pyrolyzing the sample (Okoffo et al., 2020a).

2.3. Pyrolysis gas chromatography-mass spectrometry

Samples were analyzed with a multi-shot pyrolyzer (EGA/PY-3030D) equipped with an auto-shot sampler (AS-1020E) (Frontier lab Ltd., Fukushima, Japan) coupled to a GC/MS (5977B MSD with 8860 GC, Agilent Technologies Inc., CA, USA). Samples were weighed (1–14 mg d.w. for environmental samples and 0.05–0.15 mg for tire samples) into each pyrolysis cup. All samples were analyzed in triplicates. Internal standard (d6-PB) was added to the cup and the pyrolysis cup was placed in the auto-sampler of the pyrolysis unit. Blank samples were analyzed to assess potential contamination during sample preparation. These included empty pyrolysis-cups, cups with internal standard (10 μL) and cups with chloroform (30 μL) + internal standard (10 μL). Cups used for Pyrolysis GC/MS were new. Blank runs (with no cups) were performed between successive batches to avoid carry-over between samples. Standard solution samples of 25–30 μg SBR were included as quality control samples (QC) and analyzed in between sample runs.

The samples were pyrolyzed with single-shot mode at 700 °C for 0.2 min (12 s). Injections were made using a 50:1 split and with a pyrolyzer interface temperature at 300 °C. Further details on the Py-GC/MS setup are given in SI-2 Tables S3–3.

2.4. Total SBR+BR+SBS quantification

To mitigate the issue associated with the chemical complexity of tires and the inadequate availability of standards for the identification of the individual components, a total SBR, BR, and SBS concentration approach was adopted. For this purpose, the total ion chromatogram (TIC) of both SBR1500 and SBS was thoroughly investigated by manual inspection, employing MZmine 2 (Pluskal et al., 2010). The peaks that showed the least difference in peak height between SBR and SBS, were selected and investigated further as potential markers. Using different combination of possible markers, the best fit for quantifying both SBR and SBS in the same sample was determined by the marker combinations with the lowest standard deviation when applied to SBR1500 + SBS. The selected markers consisted of *m/z* 78 Da for *benzene, m/z* 118 Da for *α-methylstyrene*, *m/z* 117 Da for *ethylstyrene* and *m/z* 91 Da for *butadiene trimer* (first trimer in the TIC) (SI Table S2). A set of calibration curves were prepared for three different ratios of SBR and SBS (20:80, 40:60 and 80:20). Masses of 1 μg, 2 μg, 5 μg, 25 μg, 100 μg and 150 μg, were inserted into pyrolysis cups (n = 3) and spiked with 25 μg d6-PB as internal standard. The summarized peak height of all marker compounds is normalized against the peak height of d6-PB and then plotted against the mass of SBR+SBS at each calibration level to form the calibration curve ($R = 0.99$, $p < 0.05$, Fig. S1).

2.5. Calculation of tire and PMB

The concentration of tire and PMB in the sample is calculated via a set of equations based on the available data in each case. The flow chart presented in Fig. 1 explains which equations to use in different scenarios.

The first step in the calculation process is to determine if PMB particles are expected in the sample. If so, the next step is to determine if traffic data for the sample location can be collected. The traffic data needed is the annual average daily traffic (AADT), the ratio between personal vehicles (PV) and heavy vehicles (HV) for each road stretch and the use of studded tires or non-studded tires. The second input are sets of emission factors (EF) for tire and road wear. Emission factors are representative values that relates a quantity of a pollutant to a specific activity that leads to the release of this pollutant (Agency, 2021). For example, by measuring the tire loss in mass from driving a personal vehicle in different conditions such as highway and urban driving, previous studies have derived the mass of tire particles (mg) per kilometer driven by a personal vehicle (v/km). For tire wear, the proposed emission factors from Klein et al. (2017) were used. For highway driving, the EFs for personal vehicles (PV) is 0.104 g per vehicle kilometer driven (g/vkm) and 0.668 g/vkm for heavy vehicles (HV). For urban driving, the EFs are higher; 0.132 g/vkm for PV and 0.850 g/vkm for HV (Table S5). For road wear, the central bureau for statistics in the Netherlands (Anon, 1998), reported EFs for low density vehicles (personal vehicles, PV) at 7.9 g/vkm and for high density vehicles (heavy vehicles, HV) at 38 g/vkm. Roughly 5 times higher emissions are

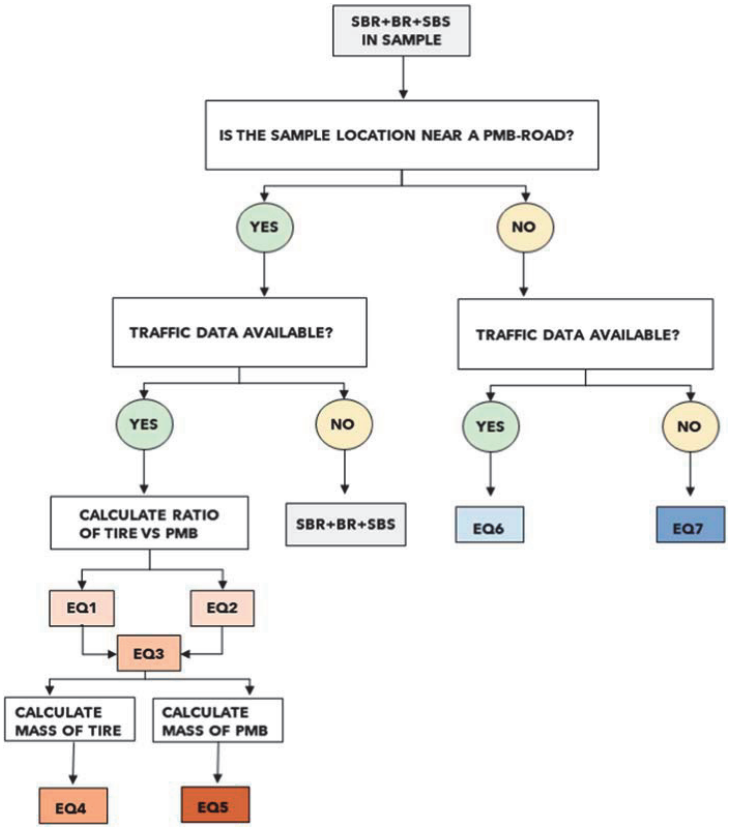

Fig. 1. Flowchart guiding the selection of the most appropriate calculation (equation) dependent on the scenario and available data.

expected from HV compared to PV. In Norway, the use of studded tires is extensive, thus a lot of the work on road wear has been focused on the use of studded tires. The term SPS is used for "specific studded tire road wear", which is estimated to be 5–10 g/vkm for PV (NVF, 2013) and roughly 5 times higher for HV. In the national estimations of PMB, Vogelsang et al. (2018) used 7.5 g/vkm as the EF for road wear. However, the use of studded tires varies in different locations due to climate and legislation. The correct percentage of studded tires at each location needs to be applied in order to calculate the emission of road wear at a specific site. For this study, three levels of EFs for road wear with studded tires (5, 7.5 and 10 g/vkm) were used in order to reflect the variation in EFs reported by different studies It is assumed that the road wear from non-studded tires is insignificant when compared to studded tires (Sörme and Lagerkvist, 2002). For non-studded tires, the Norwegian Public Roads Administration reports that the road wear from non-studded winter tires and summer tires are 40 times lower than the wear from studded tires (Snilsberg, 2020). This corresponds to similar values reported from New Zealand, where road wear EFs for non-studded tires (PV) are reported to be 0.44 g/vkm when the asphalt has 50% bitumen and 0.09 g/vkm for 10% bitumen (Kennedy et al., 2002). The EFs are therefore corrected for the ratio of studded tires used at the sample location (Table SI-5). With this information, it is possible to estimate the mass of tires and PMB produced over a given time at any site (Eq. 1, based on road specific tread emission from Vogelsang et al. (2018). These estimates are used to determine the expected ratio between tire and PMB, which then gives the expected ratio between SBR+BR and SBS in a sample.

$$EM_T = (L_r * N_{v,\ r,\ t} * ((R_{PV} * EFT_{PV}) + (R_{HV} * EFT_{HV})) \quad (1)$$

$$EM_A = L_r * N_{v,\ r,\ t} * (((R_{PV-st} * EFA_{PV-st}) + (R_{PV-nst} * EFA_{PV-nst}) * R_{PV}) + ((R_{HV-st} * EFA_{HV-st}) + (R_{HV-nst} * EFA_{PV-nst}) * R_{HV})) \quad (2)$$

Where:

EM_T is estimated mass of tire in a sample (mg);

EM_A is the estimated mass of asphalt in a sample (mg);

L_r is the length of the particular road stretch r (km);

$N_{v,r,t}$ is the number of vehicles that have travelled the particular road stretch r during the given time period t;

EFT_{PV} is the emission factor for personal vehicle tires (mg/vkm);

EFT_{HV} is the emission factor for heavy vehicle tires (mg/vkm);

R_{PV} is the ratio of personal vehicles at the sampling location;

R_{HV} is the ratio of heavy vehicles at the sampling location;

EFA_{PV-st} is the emission factor for asphalt based on studded personal vehicle tires (mg/vkm);

EFA_{PV-nst} is the emission factor for asphalt based on non-studded personal vehicle tires (mg/vkm);

EFA_{HV-st} is the emission factor for asphalt based on studded heavy vehicle tires (mg/vkm);

EFA_{PV-nst} is the emission factor for asphalt based on non-studded heavy vehicle tires (mg/vkm);

R_{PV-st} is the ratio of personal vehicles (PV) with studded tires at the sampling location, compared to all PV vehicles;

R_{PV} is the ratio of personal vehicles (PV) at the sampling location compared to all vehicles;

R_{HV-st} is the ratio of heavy vehicles (HV) with studded tires at the sampling location, compared to all HV vehicles;

R_{HV} is the ratio of heavy vehicles (HV) at the sampling location, compared to all vehicles.

As the asphalt contains 5% bitumen and the bitumen contains 5% SBS, the estimated mass of SBS in the sample is found by applying the conversion factor (CF_{SBS}) of 0.0025 to the mass of asphalt. The mean SBR+BR concentration of reference tires (PV and HV combined, $SBR+BR_{RT}$) is used to convert the estimated mass of tires to estimated mass of SBR+BR. The ratio of SBS can then be established for each sample location by the following Eq. 3.

$$R_{SBS} = \frac{(EM_A * CF_{SBS})}{(EM_T * SBR + BR_{RT}) + (EM_A * CF_{SBS})} \quad (3)$$

where

R_{SBS} is the estimated ratio of SBS from the total SBR+BR+SBS concentration;

EM_A is estimated mass of asphalt in a sample (mg);

CF_{SBS} is the conversion factor for asphalt to SBS (0.0025);

EM_T is estimated mass of tire in a sample (mg);

$SBR + BR_{RT}$ is the measured SBR+BR concentration in reference tires (μg/mg).

Using the estimated ratio of SBS for each sample location, the expected mass of tire (M_T) and PMB (M_{PMB}) in that sample can be calculated, using Eqs. 4 and 5. The variables S_{PV} and S_{HV} are the mean mass of SBR+BR measured in personal vehicle (PV) tires and heavy vehicle (HV) tires, respectively. These values are obtained from analyzing the reference tire samples.

$$M_T = \frac{M_S - (M_S * R_{SBS}) * Sc}{(S_{PV} * R_{PV}) + (S_{HV} * R_{HV})} \quad (4)$$

$$M_{PMB} = \frac{(M_S * R_{SBS})}{C_{PMB}} \quad (5)$$

where

M_T is the mass of tire in a sample (mg);

M_{PMB} is the mass of PMB in a sample (μg);

M_S is the mass of SBR+BR+SBS in a sample (μg);

R_{SBS} is the estimated ratio of SBS from the total SBR+BR+SBS concentration for each location;

Sc is the conversion factor for styrene content in standards vs tires;

S_{PV} is the mass of SBR+BR in personal vehicle tires (μg/mg);

R_{PV} is the ratio of personal vehicles at the sampling location;

$S_{HV}$is the mass of SBR+BR in heavy vehicle tires (μg/mg);

R_{HV} is the ratio of heavy vehicles at the sampling location;

C_{PMB} is the conversion factor for SBS to PMB, based on the percentage SBS in PMB (0.05).

The variable Sc is applied if the styrene content of the standards used for the calibration curve differs from the expected styrene content in tires. The styrene content differs between different types of tires, based on the ratio of SBR to BR, as well as the type of SBR used in each tire (Table S1). SBR has on average 27.4% styrene and BR has 0% styrene. According to Unice et al. (2012), the average ratio of SBR to BR is 65–35%, which means that most tires will have a styrene content of 17.8% (0.274 × 0.65 = 0.178). SBS used in PMB has an average styrene content of 30%. For each environmental sample location, the expected styrene content of the sample can be calculated using the ratio of SBS (R_{SBS}, Eq. 5). As an example, the R_{SBS} at Skullerud is 5.4%. This means that in the samples from Skullerud, the expected the styrene content from tire and PMB together will be 19.4%.

(0.178 + (0.30*0.054) = 0.194). The calibration curve used in this method contains on average 27% styrene (Table SI-4). To correct for this difference, the correction factor (Sc) is calculated as: (1–0.27) / (1–0.194) = 0.91 for Skullerud samples. This approach is then applied to all sample locations to correct for styrene differences.

Using Eqs. 4 and 5, the mass of tire and PMB in the sample will be obtained from the measured SBR+BR+SBS values. As both the ratio of SBS in PMB bitumen (Vogelsang et al., 2018; NVF, 2013; Anon, 1998) and the SBR+BR mass in PV and HV tires display a large variation of values (Rauert et al., 2021), only applying the mean value of SBS and SBR+BR to calculate PMB and tire would lead to large uncertainties. As an attempt to deal with this, a Monte Carlo prediction model (100,000 simulations, Crystal Ball in Excel (Oracle)) is used to calculate the predicted mean value of tire and PMB and predicted standard deviation. The Monte Carlo simulation predicts what the tire and PMB values in the sample will be based on the SBR+BR values found in the reference tires of this study and the emission factors for road wear, as described above.

If the sample is expected to contain PMB-particles, but no traffic data is available, then it will not be possible to apply Eqs. 1–5. For these locations, reporting the combined concentration of SBR+BR+SBS will give information on the amount of rubber present in the sample, although the separation between the rubber types will not be possible.

If the sample is collected near a location where PMB is not applied to the asphalt, then it can be expected that SBS is not present in the sample, thus the four chosen markers will give the total mass of SBR+BR. Simplified versions of Eq. 4 can then be applied to obtain the mass of tire in the sample. If traffic data for the location is obtained, then Eq. 6 is applied. If there is no traffic data available, Eq. 7 can be applied. For this approach, a calibration curve based on SBR1500 alone can be applied and the Sc is calculated based on the styrene content of SBR1500 and tires alone.

$$M_T = \frac{M_{SB} * Sc}{(S_{PV} * R_{PV}) + (S_{HV} * R_{HV})} \quad (6)$$

$$M_T = \frac{M_{SB} * Sc}{S_V} \quad (7)$$

where

M_T is the mass of tire in a sample (mg);

M_{SB} is the mass of SBR+BR in a sample (μg);

Sc conversion factor for styrene content in standards vs tires;

S_{PV} is the mass of SBR+BR in personal vehicle tires (μg/mg);

R_{PV} is the ratio of personal vehicles at the sampling location;

$S_{HV}$is the mass of SBR+BR in heavy vehicle tires (μg/mg);

R_{HV} is the ratio of heavy vehicles at the sampling location;

$S_V$is the average mass of SBR+BR in vehicle tires (μg/mg).

2.6. Statistical analysis

The statistical analysis and modelling were performed using RStudio 1.3.1093 (Team, 2020), R version 4.0.4 (2021–02–15). Following packages were used for the analysis: ggplot-package (Lai et al., 2016) (gplot2_3.3.3).

The uncertainty analysis was performed by using Excel Monte-Carlo Add-In Crystal Ball (Team, 2021). Using the crystal ball applications, both Eqs. 4,5 and 6 were simulated 100'000 times, and the application provides statistics for the simulation in order to obtain the mean value and standard deviation of each analyzed sample.

3. Results and discussion

3.1. Total concentration of SBR+BR+SBS

3.1.1. Accuracy and precision of the method

None of the marker compounds were detected in any of the blank cups or the solvent blanks tested. The limit of detection (LOD, 3xS/N) for the four markers was between 1 and 2 μg of SBR+SBS (SI-6, Table S6)

and the limit of quantification (LOQ, 10xS/N) was between 1 and 5 μg.

Method accuracy (%) was determined via standard addition of SBR and SBS (alone and in combination) into environmental samples and one tire reference sample. Accuracy was 85–151% (SI-7, Tables S7-S10). The calculation of recovery is explained in SI-7. Poorer precision was observed in the lowest concentrations approaching the LOQ, which is expected. This is due to observed heterogeneity in concentrations of SBR+BR in the tire itself, and due to signal-noise levels approaching the LOD (Vogelsang et al., 2018).

3.1.2. Concentration of SBR+BR+SBS in reference tires

SBS is not present in the reference tires as confirmed by one of the largest tire manufacturers (Bridgestone and Rødland, 2020). Thus, the results from using the SBR+BR+SBS-method on pure tire samples can be considered to contain only SBR and BR. The concentration of SBR+BR measured in the reference tires using the mixture markers showed a large range of values (115–682 μg/mg, n = 31), with an average SBR+BR concentration of 319 ± 127 μg/mg (average ± standard deviation) for all tires (Table 1, Fig. 2). However, to demonstrate that the proposed marker combinations are more suitable for the Norwegian reference tires than previously proposed markers (4-VCH, SB dimer, SBB trimer), all reference tires have been quantified using different markers. As seen in Table 1, the % standard deviation (standard deviation compared to the average value), shows that the variation in SBR+BR concentrations is lower when using the proposed mixture of *benzene, α-methylstyrene, ethylstyrene* and *butadiene trimer* for quantification compared to the other markers. This is supported by several studies, showing that the use of multiple markers can give more reliable results, and are less impacted by possible interference compared to single markers (Okoffo et al., 2020b; Ribeiro et al., 2020; Brereton, 2007).

The reference tires can also be grouped in two major groups; by car type (PV vs. HV) and by season (summer vs winter, all-year), however, none of these groups were significantly different to each other (see SI-8 for boxplot and statistical analysis). When calculating the mass of tires based on the measured mass of SBR+BR, both Eqs. 4 and 6 is designed to use SBR+BR values for PV and HV tires for the seasonality relevant for the samples. For example, for snow samples, the PV and HV values for winter tires were applied. Using Eq. 7, the average SBR+BR for all tires can be applied.

All the proposed markers (*benzene*, *α-methylstyrene, ethylstyrene and butadiene trimer*) displayed higher variability in the HV tires compared to the PV tires. The marker *benzene* is the most stable marker for both types of tires, showing a st.d. of 22% in PV and 44% in HV (SI Table S10). The marker *α-methylstyrene* is the least stable marker, with a 96% standard variation across all tires, which illustrates the difficulty of measuring different tires with different rubber contents. However, *α-methylstyrene* has the lowest percentage standard deviation when used in a combination of SBR and SBS, thus it is needed for environmental samples where it is expected to find tires and PMB-particles in a mixture. For all the sample types included in the study, the contribution ratio (%) of each marker is tested using Kruskal-Wallis test (Table S11). The results show that the ratios of *benzene, α-methylstyrene, ethylstyrene* and *butadiene trimer* were significantly different between the sample types tested (SI Fig. S6). Samples that contain a balanced mixture of SBR and SBS have a lower percentage of *benzene* and higher percentage of *α-methylstyrene* and *ethylstyrene*. Looking at the average *benzene* percentage, the gully-pot samples from Smestad were slightly lower compared to the snow samples and the soil samples. Gully-pots are expected to only retain minor fractions of tire particles and mainly particles above 50 μm (Vogelsang et al., 2018). The knowledge on PMB-particles is limited, however, as these contain a very small fraction of rubber (5%) and mainly mineral components, it should be expected that PMB particles have a higher density than tire particles. It is therefore more likely that a larger fraction of PMB compared to tire particles are retained in gully-pots. This could potentially explain the difference in the *benzene* percentage observed for the Smestad gully-pot samples, as the PMB particles would contribute to a higher percentage of the styrene-related markers. As described in chapter 2.2, the present proposed method is optimized for samples where it is expected that SBR+BR+SBS are the main microplastic component. For example, a recent study by Goßmann et al. (2021) showed that TWP was the main microplastic component of road dust, with 5 g/kg TWP compared to just 0.3 g/kg of other microplastics components (d.w.). Additional method preparation steps including density separation (Klöckner et al., 2019) may be required if samples are expected to contain significant amounts of interfering polymer types, such as polyvinyl chloride (PVC), polyethylene terephthalate (PET), acrylonitrile-butadiene-styrene copolymer (ABS) and polystyrene (PS). PVC and PET share benzene as a pyrolysis product, while ABS and PS will produce *α-methylstyrene* which are also produced by TRWP pyrolysis.

Although there are significant differences between marker ratios of different sample types, the average contribution of each marker is stable and can be used to verify that the samples are not substantially influenced by compounds other than SBR, BR and SBS. Differences in the marker ratios can in fact contribute to better understanding of the samples, and additionally to determine whether additional sample preparation steps are needed or not, and finally to have an assumption of how influenced the sample is from SBS.

3.2. Calculation of Tire and PMB in environmental samples

The use of the calculation method (Eqs. 4 and 5) is demonstrated on the environmental samples analyzed, Skullerud snow (SK), Skullerud soil (SK-sed) and Smestad tunnel gully-pot sediment (SF) (Table 2). The SBR+BR+SBS concentration for each individual sample can be found in Table S9-S10. The SK and SF samples were collected during winter, so the winter tire concentrations (PV, HV) were applied. For the SK-sed samples, the average SBR+BR for summer and winter tires combined was applied. Using the Monte Carlo simulations, the average predicted tire and PMB concentration in each sample was calculated. It needs to be pointed out that the calculation will not be able to predict how the actual transport pattern between tire and PMB might change with distance, due to differences in size or density. This calculation assumes that the ratio between tire and PMB is constant at all distances analyzed in this study. The assumptions apply for the SK and SK-sed samples. The highest concentration of tire particles was found in gully-pot samples (SF). One of the gully-pots (SF1) was sampled both in 2018 and 2020, and the concentrations found in 2020 were significantly higher (66.3 ± 184 mg/g, predicted average ± standard deviation using 100,000 Monte Carlo simulations), compared to 2018 (12.2 ± 33.8 mg/

Table 1
The table compares the average concentration and % standard deviation of SBR+BR in reference tires (n = 31) using the mixture markers (benzene + α-methylstyrene+ ethylstyrene + butadiene trimer), the 4-vinylcyclohexene (4-VCH), the SB dimer and the SBB trimer for quantification.

	benzene + α-methylstyrene + ethylstyrene + butadiene trimer (μg/mg)	4-VCH (μg/mg)	SB (μg/mg)	SBB (μg/mg)
PV mean	311.1	93.6	364.1	193.9
PV std. %	26.5	44.8	68.0	66.7
HV mean	329.5	144.9	335.5	266.4
HV std. %	51.0	62.1	89.8	92.8
All tires mean	319.1	116.0	351.6	225.6
All tires std. %	39.7	61.8	77.1	85.3

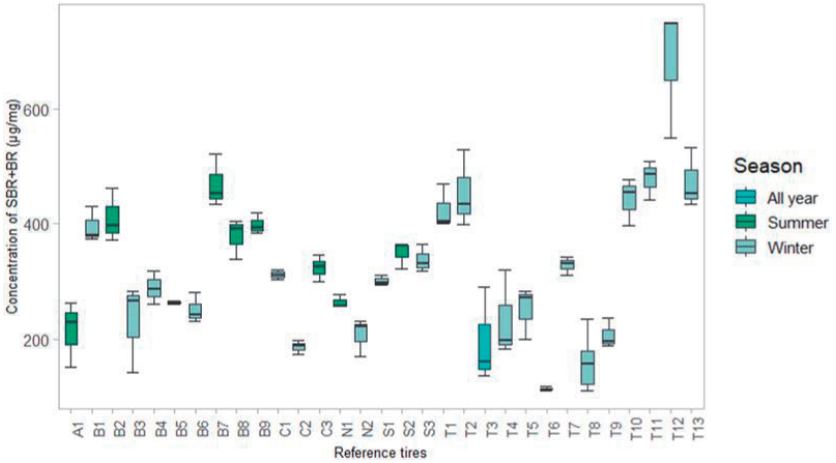

Fig. 2. Concentration of SBR+BR (µg/mg) in reference tires. Tires A1-S3 are personal vehicle tires (PV) and T1 to T13 are heavy vehicle tires, all analysed in triplicates? (n = 3). Type of tire is depicted by color.

Table 2
The table summarizes the results from using Eq. 4, where the input variables R_{SBS}, S_{PV} and S_{HV} (in yellow) have a distribution assumption fitted to the values and the variables M_S, S_C, R_{PV} and R_T (in white) are constant. The output value M_T (in blue) is then predicted with 100,000 Monte Carlo simulations, which gives an average M_T and the standard deviation for each sample. The average M_T and standard deviation for all SK and SF samples is calculated based on the predicted average M_T.

	Output values	Input variables							Predicted values	
Sample	M_T (mg/g, mg/mL)	M_S (µg/g, µg/mL)	R_{SBS}	S_C	S_{PV} (µg/mg)	S_{HV} (µg/mg)	R_{PV}	R_{HV}	Average M_T (mg/g, mg/mL)	Standard deviation (mg/g, mg/mL)
SK-0m	1.7	494.7	0.054	1.00	278.6	318.0	0.88	0.12	1.7	3.6
SK-1m	1.6	490.3	0.054	1.00	278.6	318.0	0.88	0.12	1.7	3.6
SK-3m	0.10	30.0	0.054	1.00	278.6	318.0	0.88	0.12	0.11	0.22
SK-sed-0m	4.9	1614.2	0.054	1.00	311.1	329.5	0.88	0.12	4.9	0.04
SK-sed-1.5m	4.8	1601.2	0.054	1.00	311.1	329.5	0.88	0.12	4.8	0.04
SK-sed-3m	3.7	1211.8	0.054	1.00	311.1	329.5	0.88	0.12	3.7	0.03
SF1-2018	10.7	3351.8	0.048	1.00	278.6	318.0	0.92	0.08	12.2	33.8
SF1-2020	62.9	18606.3	0.048	1.00	278.6	318.0	0.92	0.08	66.3	184.0
SF2-2020	5.6	1664.5	0.048	1.00	278.6	318.0	0.92	0.08	5.9	16.5
SF3-2020	8.7	2564.7	0.048	1.00	278.6	318.0	0.92	0.08	9.1	25.4

g). The main reason for this could be the time of sampling, as the 2018 samples were collected in November, just before the winter season and the 2020 samples were collected in April, just after the winter season. As winter tires, both studded and non-studded are used in Oslo, it is expected to find higher concentrations of tire and road wear particles after the winter season compared to before. The concentration of tire found in the other two gully-pots were significantly lower than SF1 (Table 2). The reason for these differences may be that the gully-pots have not been emptied at the same time, or SF1 received more tire and PMB-particles, being the gully-pot closest to the tunnel inlet. The concentrations of tire found in the SK-sed soil at 0 and 1.5 m distance from the road were similar (4.9 ± 0.04 and 4.8 ± 0.04 mg/g). At 3 m distance, the predicted tire concentration was lower (3.7 ± 0.03 mg/g). Same concentrations were found for both 0 m and 1 m distance from the road in the SK snow samples (1.7 ± 3.6 mg/mL). At 3 m distance, a significantly lower predicted concentration was found (0.11 ± 0.22 mg/mL). The results using the Monte Carlo simulations also show that there is a large standard deviation in the predicted concentrations. This is related to the large variations of SBR+BR-values found in the reference tires, as explained in chapter 3.2.2. A comparison of the SF gully-pot sediment and the SK-sed soil samples shows that the retention found in the roadside soil is comparable to the retention in gully-pots. This confirms that soil retention could be an important step in retaining tire particles from further dispersion from the road system. The results found in this study are comparable to other studies using Py-GC/MS methods to measure the amount of tire particles in environmental samples. Previous studies have reported findings of 9100 µg/g of TRWP in roadside soil (average value, range 200–20,000 µg/g d.w.) (Unice et al., 2013). However, the method applied by Unice et al. assumes that a TRWP particle contains 50% tire tread and 50% minerals (or other road components), as well as a fixed 25% rubber content in all tire tread particles. A recent study by Klöckner et al. (2021) reported a possible 75% tire tread in the TRWP in their study, showing that a fixed 50% tread content does not apply to all TRWPs. As the proposed method presented here calculates tire tread and PMB concentrations separately, and not TRWP, comparisons with other studies need to take this into account. No comparable gully-pot samples

analysed with Py-GC/MS were found. However, three studies using TED-GC-MS have analyzed sludge samples from road treatment systems and found between 16 and 150 mg/g TRWP, based on 50% tread content (Eisentraut et al., 2018; Klöckner et al., 2019). Mengistu et al. (2021) studied gully-pot sediments in Norway using simultaneous thermal analysis (STA), Fourier transform infra-red (FTIR) and parallel factor analysis (PARAFAC). Concentrations of tire particles were found to be between 1 and 150 mg/g (Mengistu et al., 2021), which is comparable to the present study. However, as the sampling sites in the study by Mengistu et al. (2021) were from municipality roads with a substantially lower AADT (417 – 2608 AADT) compared to the Smestad tunnel (44 060 AADT), it was presumed that the gully-pot sediments would show a larger difference in tire concentrations compared to what was found. This potentially confirms the importance of emptying the gully-pots for sediment regularly. The gully pots in tunnels are frequently emptied as part of the regular tunnel cleaning, while gully pots along smaller roads may accumulate sediment for longer periods before emptying, or even not emptied at all (Lindholm, 2015). The concentrations found in the gully-pots confirms that tire particles are retained in gully-pots and that high concentrations of tire particles can be found along roads with both low and high traffic densities. It also shows that the concentrations found are comparable to other road treatment systems, thus the potential of gully-pots as simple retention measures for TRWP should be further explored. Unfortunately, there is no information available on the presence of any PMB bitumen in the sample sites used for comparison. If PMB bitumen is used at these locations, this present study shows that the concentrations of TRWP reported are likely overestimations due to the presence of SBS in road samples.

Furthermore, the use of the PMB calculation (Eq. 5), gives the average predicted mass of PMB (M_{PMB}) (Table 3), based on the expected ratio of SBS for each location. Being a ratio based on the SBR+BR+SBS concentration, the results from the PMB calculations are proportional to the results of the tire calculations, so the variations within and between sites described for tire particles will be the same and therefore not described in detail here. All calculations can be found in Table 3 and supplementary (S15).

3.3. Method Potentials and limitations

The presented method shows great potential in measuring the total mass of SBR+BR+SBS in environmental samples, and subsequently the possibility to calculate the mass of both tire and PMB particles in these samples. The method can be applied to samples with or without the presence of PMB, and it can be used with or without traffic data input for samples without PMB. This flexibility makes it a novel and robust method which can be applied to most sample sites and most relevant road matrices, such as soil, sediment and snow as demonstrated by this study. It should also be applicable to other relevant matrices such as road dust, road-runoff and tunnel wash water, and should be explored further in future studies. The presented method proposes to use reference tires that are relevant for each study, i.e. considering geographically and seasonal differences. Alternatively, a large sample set of tires from across the globe and for different purposes such as winter or summer, may be useful in order to compare measurements from different studies. A reference database may also contribute to understand the variability in tires caused by the different geometric isomers that SBR can exist in. Studies have shown that the marker compound VCH is affected by the ratio of the different butadiene isomers present (Choi, 2002; Choi and Kwon, 2014, 2020), and it is a possibility that such a variation would also occur in other SBR-related marker compounds.

The preferred pathway for this method (Fig. 1) is dependent on the availability of high-resolution traffic data for each location where samples are collected, such as AADT, ratio of PV and HV, ratio of studded tires and the polymer type used for PMB. As this data may be difficult to obtain in some countries, modified equations to apply where traffic data is lacking, is provided. Some countries also use rubber granulate from discarded tires in the polymer-modified asphalt (Bouman et al., 2020) instead of adding single polymers to the bitumen. In these cases, the tire contribution from the PMB will be added to the total tire concentration for the location, as it will not be possible to distinguish between the two sources of tire. There are currently no studies available that have measured the contribution of tire particles from rubber granulate PMBs, or if the road abrasion factors will be the same for PMB asphalt with tire and SBS. This should be addressed in future studies.

4. Conclusions

The present study aimed to improve the methods for determining concentration data of tire and road wear particles in environmental samples. Opposed to the current methods (ISO, 2017a, 2017b), the present method utilised multiple pyrolysis marker components to both determine the content of tires as well as the so far neglected content of polymer-modified bitumen in road wear. Quantification with the combined pyrolysis marker components proposed in this study (*benzene,*

Table 3
The table summarizes the results from using Eq. 5, where the input variables R_{SBS} (in yellow) have a distribution assumption fitted to the values and the variables M_S and C_{PMB} (in white) are constant. The output value M_{PMB} (in blue) is then predicted with 100 000 Monte Carlo simulations, which gives an average M_{PMB} and the standard deviation for each sample. The average M_{PMB} and standard deviation for all SK and SF samples is calculated based on the predicted average M_{PMB}.

	Output values	Input variables			Predicted values	
Sample	M_{PMB} (mg/g, mg/mL)	M_S (µg/g, µg/mL)	R_{SBS}	C_{PMB}	Average M_{PMB} (mg/g, mg/mL)	Standard deviation (mg/g, mg/mL)
SK-0m	0.53	494.7	0.054	1.00	0.54	0.085
SK-1m	0.53	490.3	0.054	1.00	0.54	0.084
SK-3m	0.032	30.0	0.054	1.00	0.033	0.0051
SK-sed-0m	1.7	1614.2	0.054	1.00	1.8	0.28
SK-sed-1.5m	1.7	1601.2	0.054	1.00	1.8	0.27
SK-sed-3m	1.3	1211.8	0.054	1.00	1.3	0.21
SF1-2018	3.2	3351.8	0.048	1.00	3.3	0.53
SF1-2020	17.7	18606.3	0.048	1.00	18.1	2.9
SF2-2020	1.6	1664.5	0.048	1.00	1.6	0.26
SF3-2020	2.4	2564.7	0.048	1.00	2.5	0.40

α-methylstyrene, *ethylstyrene* and *butadiene trimer)* showed high recovery percentages (83–104%) in the performed tests and displayed lower variability in reference tires than previously proposed markers. The presented method has also a new and improved step of calculating the amount of tire and road wear in a sample based on the measured rubber content and site-specific traffic data for each location. Using site-specific data may in many situations be more useful for local road and environmental management compared to using global statistics and tire values from different parts of the world. Tires have been shown to have a large variation in content, likely to accommodate for different driving styles and weather conditions found in different parts of the world. Our study shows that there are large differences between different brands and/or types of tires. Using fixed rubber concentrations to calculate the mass of tires in environmental samples, as commonly used in previous methods, is therefore contributing to large uncertainties. These uncertainties are important to communicate when presenting results of tire concentrations in environmental samples. Our study proposes to combine large datasets of tires with a Monte Carlo prediction simulation. Predicting the possible tire values based on the variation in rubber content gives us a predicted mean value and a predicted standard deviation of that mean. This both decreases uncertainty as well as communicates that tires are a difficult matrix to measure. Also, using locally adapted values could give higher resolution data which is relevant both for environmental research and for planning measures in current and future road projects.

CRediT authorship contribution statement

Elisabeth S. Rødland: Conceptualization, Methodology, Data curation, Formal analysis, Visualization, Writing – original draft, Writing – review & editing. **Saer Samanipour**: Methodology, Data curation, Formal analysis, Writing – original draft, Writing – review & editing. **Cassandra Rauert:** Investigation, Writing – original draft, Writing – review & editing. **Elvis Okoffo**: Writing – original draft, Writing – review & editing. **Malcolm Reid**: Conceptualization, Writing – original draft, Validation, Writing – review & editing. **Lene Heier:** Conceptualization, Writing – original draft, Writing – review & editing. **Ole Christian Lind:** Conceptualization, Writing – original draft, Writing – review & editing. **Kevin Thomas:** Writing – original draft, Writing – review & editing. **Sondre Meland:** Conceptualization, Writing – original draft, Writing – review & editing, Funding acquisition, Project administration.

Declaration of Competing Interest

The authors declare that they have no known competing financial interests or personal relationships that could have appeared to influence the work reported in this paper.

Acknowledgements

A sincere thank you to Alfhild Kringstad (NIVA) for all help related to the lab work, especially with the GC/MS and interpretations and José Antonio Baz Lomba (NIVA) for reading through the manuscript. This work was funded in collaboration between the Norwegian Institute for Water Research (NIVA) (funded by the Norwegian Research Council, grant number 160016) and the NordFoU-project REHIRUP (grant number 604133). Part of the work is also supported by the Norwegian University of Life Sciences (NMBU) and the Centre for Environmental Radioactivity (CERAD) through the Norwegian Reseach Council's Centres of Excellence funding scheme (project number 223268/F50). The Queensland Alliance for Environmental Health Sciences, The University of Queensland, gratefully acknowledges the financial support of the Queensland Department of Health.

Appendix A. Supporting information

Supplementary data associated with this article can be found in the online version at doi:10.1016/j.jhazmat.2021.127092.

References

Agency, U.S. E.P. , 2021. Basic Information of Air Emissions Factors and Quantification. https://www.epa.gov/air-emissions-factors-and-quantification/basic-information-air-emissions-factors-and-quantification#About%20Emissions%20Factors. (17 August 2021).
Anon , 1998. CBS Central Bureau for Statistics: Methodiekbeschrijving van de berekeing van de emissies door mobiele bronnen inNederland. In het kader van het Emissiejaarrapport. Cited in Klimont et al. (2002).
ANON , 1996. CIWMB Effects of waste tires, waste tire facilities, and waste tire projects on the environment; California, USA.
NVF, 2013. Trender innen belegningsbransjen i Norden: Belegningstrender i Norge; Nordiskt Vägforum, Utvalg for Belegninger,: 2013; p 61.
ANON (EAPA), 2018. E. A. P. A. Heavy duty surfaces the arguments for SMA. Technical review.
ANON , 2021. Kraton SBS in Polymer-modofied bitumen. https://kraton.com/products/paving/AsphaltBinder.php. (26.04.2021),
M, Y.B., Müller, A.J., Rodriguez, Y., 2003. Use of rheological compatibility criteria to study SBS modified asphalts. J. Appl. Polym. Sci. 90 (7), 1772–1782.
Baensch-Baltruschat, B., Kocher, B., Stock, F., Reifferscheid, G., 2020. Tyre and road wear particles (TRWP) - A review of generation, properties, emissions, human health risk, ecotoxicity, and fate in the environment. Sci. Total Environ. 733, 137823.
Boucher, J., Billard, G., Simeone, E., Sousa, J., 2020. The marine plastic footprint; 2831720281; IUCN.
Bouman, E. Meland, S., Furuseth, I.S., Tarrasón, L. , 2020. Feasibility study for asphalt rubber pavements in Norway. 'Rubber Road' feasibility study.; NILU.
Brereton, R.G., 2007. Applied Chemometrics for Scientists.
Bridgestone, 2020. Confirmation that SBS is not used in tires. In Rødland, E. , Ed.
Chen, J.S., Liao, M.C., Tsai, H.H., 2002. Evaluation and optimization of the engineering properties of polymer-modified asphalt. Pract. Fail. Anal. 2 (3), 75–83.
Choi, S.-S., 2002. Characteristics of the pyrolysis patterns of styrene-butadiene rubbers with differing microstructures. J. Anal. Appl. Pyrolysis 62 (2), 319–330.
Choi, S.-S., Kwon, H.-M., 2014. Analytical method for determination of butadiene and styrene contents of styrene-butadiene rubber vulcanizates without pretreatment using pyrolysis-gas chromatography/mass spectrometry. Polym. Test. 38, 87–90.
Choi, S.-S., Kwon, H.-M., 2020. Considering factors on determination of microstructures of SBR vulcanizates using pyrolytic analysis. Polym. Test. 89, 106572.
Eisentraut, P., Dümichen, E., Ruhl, A.S., Jekel, M., Albrecht, M., Gehde, M., Braun, U., 2018. Two birds with one stone—fast and simultaneous analysis of microplastics: microparticles derived from thermoplastics and tire wear. Environ. Sci. Technol. Lett. 5 (10), 608–613.
Giavarini, C., De Filippis, P., Santarelli, M.L., Scarsella, M., 1996. Production of stable polypropylene-modified bitumens. Fuel 75 (6), 681–686.
Goßmann, I., Halbach, M., Scholz-Böttcher, B.M., 2021. Car and truck tire wear particles in complex environmental samples - a quantitative comparison with "traditional" microplastic polymer mass loads. Sci. Total Environ. 773, 145667.
Grigoratos, T., Martini, G., 2014. Non-exhaust traffic related emissions. Brake and tyre wear PM. JRC Sci. Policy Rep. 53.
Hurley, R.R., Lusher, A.L., Olsen, M., Nizzetto, L., 2018. Validation of a method for extracting microplastics from complex, organic-rich, environmental matrices. Environ. Sci. Technol. 52 (13), 7409–7417.
ISO, 2017a. ISO/TS 21396: Rubber — determination of mass concentration of tire and road wear particles (TRWP) in soil and sediments — Pyrolysis-GC/MS method. In International Organization for Standardization, Genève, Switzerland.
ISO, 2017b. ISO/TS 20593: Ambient air — determination of the mass concentration of tire and road wear particles (TRWP) — Pyrolysis- GC-MS method. In International Organization for Standardization, Geneve, Switzerland.
ISO, 2017c. ISO/TS 20593: Ambient air — determination of the mass concentration of tire and road wear particles (TRWP) - Pyrolysis-GC-MS method. In International Organization for Standardization, Geneve, Switzerland.
Kennedy, K. Gadd, J., Moncrieff, I. Emission factors for contaminants released by motor vehicles in New Zealand'; Prepared for the New Zealand Ministry of Transport and Infrastructure Auckland. 2002.
(SSB), S. s., Kjørelengder , 2019. (driving distance).
Klein, J., Molnár-in 't Veld, H., Geilenkirchen, G., Hulskotte, J., Ligterink, N., Dellaert, S., d. B, R., 2017. Methods for calculating transport emissions in the Netherlands 2017.; Force on Transportation of the Dutch Pollutant Release and Transfer Register. PBL Netherlands Environmental Assessment Agency, p. 75.
Klöckner, P., Reemtsma, T., Eisentraut, P., Braun, U., Ruhl, A.S., Wagner, S., 2019. Tire and road wear particles in road environment – quantification and assessment of particle dynamics by Zn determination after density separation. Chemosphere 222, 714–721.
Klöckner, P., Seiwert, B., Weyrauch, S., Escher, B.I., Reemtsma, T., Wagner, S., 2021. Comprehensive characterization of tire and road wear particles in highway tunnel road dust by use of size and density fractionation. Chemosphere 279, 130530.
Knight, L.J., Parker-Jurd, F.N., Al-Sid-Cheikh, M., Thompson, R.C., 2020. Tyre wear particles: an abundant yet widely unreported microplastic? Environ. Sci. Pollut. Res. 27, 18345–18354.

Lai, F.Y., O'Brien, J., Bruno, R., Hall, W., Prichard, J., Kirkbride, P., Gartner, C., Thai, P., Carter, S., Lloyd, B., Burns, L., Mueller, J., 2016. Spatial variations in the consumption of illicit stimulant drugs across Australia: a nationwide application of wastewater-based epidemiology. Sci. Total Environ. 568, 810–818.

Lindholm, O., 2015. Forurensingstilførsler fra veg og betydningen av å tømme sandfang. VANN 01, 93–100.

Lusher, A.L., Hurley, R., Arp, H.P.H., Booth, A.M., Bråte, I.L.N., Gabrielsen, G.W., Gomiero, A., Gomes, T., Grøsvik, B.E., Green, N., Haave, M., Hallanger, I.G., Halsband, C., Herzke, D., Joner, E.J., Kögel, T., Rakkestad, K., Ranneklev, S.B., Wagner, M., Olsen, M., 2021. Moving forward in microplastic research: a Norwegian perspective. Environ. Int. 157, 106794.

Mengistu, D., Heistad, A., Coutris, C., 2021. Tire wear particles concentrations in gully pot sediments. Sci. Total Environ. 769, 144785.

O'Brien, S., Okoffo, E.D., Rauert, C., O'Brien, J.W., Ribeiro, F., Burrows, S.D., Toapanta, T., Wang, X., Thomas, K.V., 2021. Quantification of selected microplastics in Australian urban road dust. J. Hazard Mater. 416, 125811.

Okoffo, E.D., Ribeiro, F., O'Brien, J.W., O'Brien, S., Tscharke, B.J., Gallen, M., Samanipour, S., Mueller, J.F., Thomas, K.V., 2020a. Identification and quantification of selected plastics in biosolids by pressurized liquid extraction combined with double-shot pyrolysis gas chromatography–mass spectrometry. Sci. Total Environ. 715, 136924.

Okoffo, E.D., Tscharke, B.J., O'Brien, J.W., O'Brien, S., Ribeiro, F., Burrows, S.D., Choi, P.M., Wang, X., Mueller, J.F., Thomas, K.V., 2020b. Release of plastics to Australian land from biosolids end-use. Environ. Sci. Technol. 54 (23), 15132–15141.

Panda, M., Mazumdar, M., 1999. Engineering properties of EVA-modified bitumen binder for paving mixes. J. Mater. Civ. Eng. 11 (2), 131–137.

Pluskal, T., Castillo, S., Villar-Briones, A., Orešič, M. , 2010. MZmine 2: Modular framework for processing, visualizing, and analyzing mass spectrometry-based molecular profile data, BMC Bioinformatics, PMID: 20650010.

Polacco, G., Berlincioni, S., Biondi, D., Stastna, J., Zanzotto, L., 2005. Asphalt modification with different polyethylene-based polymers. Eur. Polym. J. 41 (12), 2831–2844.

Polacco, G., Muscente, A., Biondi, D., Santini, S., 2006. Effect of composition on the properties of SEBS modified asphalts. Eur. Polym. J. 42 (5), 1113–1121.

Rauert, C., Rødland, E.S., Okoffo, E.D., Reid, M.J., Meland, S., Thomas, K.V., 2021. Challenges with quantifying tire road wear particles: recognizing the need for further refinement of the ISO technical specification. Environ. Sci. Technol. Lett. 8 (3), 231–236.

Ribeiro, F., Okoffo, E.D., O'Brien, J.W., Fraissinet-Tachet, S., O'Brien, S., Gallen, M., Samanipour, S., Kaserzon, S., Mueller, J.F., Galloway, T., Thomas, K.V., 2020. Quantitative analysis of selected plastics in high-commercial-value australian seafood by pyrolysis gas chromatography mass spectrometry. Environ. Sci. Technol. 54 (15), 9408–9417.

Ribeiro, F., Okoffo, E.D., O'Brien, J.W., O'Brien, S., Harris, J.M., Samanipour, S., Kaserzon, S., Mueller, J.F., Galloway, T., Thomas, K.V., 2021. Out of sight but not out of mind: size fractionation of plastics bioaccumulated by field deployed oysters. J. Hazard. Mater. Lett. 2, 100021.

Saba, R.G., Uthus, N., Aurstad, J., 2012. Long-term performance of asphalt surfacings containing polymer modified binders. In 5th Eurasphalt & Eurobitume Congress.

Sengoz, B., Topal, A., Isikyakar, G., 2009. Morphology and image analysis of polymer modified bitumens. Constr. Build. Mater. 23 (5), 1986–1992.

Snilsberg, B., 2020. In: Rødland, E. (Ed.), Road Wear From Studded and Non-Studded Tires.

Sommer, F., Dietze, V., Baum, A., Sauer, J., Gilge, S., Maschowski, C., Giere, R., 2018. Tire Abrasion as a major source of microplastics in the environment. Aerosol Air Qual. Res. 18 (8), 2014–2028.

Sörme, L., Lagerkvist, R., 2002. Sources of heavy metals in urban wastewater in Stockholm. Sci. Total Environ. 298 (1–3), 131–145.

Sundt, P., Schulze, P.-E., Syversen, F., 2014. Sources of microplastic-pollution to the marine environment; p 86.

Sundt, P., Syversen, F., Skogesal, O., Schulze, P.-E., 2016. Primary microplastic-pollution: Measures and reduction potentials in Norway; p 117.

Team, E.I. D. , 2021. Orcle Crystal Ball, 11.1.2.4.850; Oracøe.

Team, R., 2020. RStudio: Integrated Development for R. RStudio. PBC, Boston, MA.

Tsuge, S., Ohtani, H., Watanabe, C., 2011. Pyrolysis-GC/MS Data Book of Synthetic Polymers: Pyrograms, Thermograms and MS of Pyrolyzates. Elsevier.

Unice, K.M., Kreider, M.L., Panko, J.M., 2012. Use of a deuterated internal standard with pyrolysis-GC/MS dimeric marker analysis to quantify tire tread particles in the environment. Int. J. Environ. Res. Public Health 9 (11), 4033–4055.

Unice, K.M., Kreider, M.L., Panko, J.M., 2013. Comparison of tire and road wear particle concentrations in sediment for watersheds in France, Japan, and the United States by quantitative pyrolysis GC/MS analysis. Environ. Sci. Technol. 47 (15), 8138–8147.

Vegvesen, S., 2020. Road lengths with polymer-modified bitumen.

Vogelsang, C., Lusher, A.L., Dadkhah, M.E., Sundvor, I., Umar, M., Ranneklev, S.B., Eidsvoll, D., Meland, S., 2018. Microplastics in road dust – characteristics, pathways and measures.

A Novel Method for Quantification of Tire and Polymer-modified Bitumen Particles in Environmental Samples by Pyrolysis Gas Chromatography Mass Spectroscopy

Elisabeth S. Rødland[1,2], Saer Samanipour[1,3,4], Cassandra Rauert[4], Elvis D. Okoffo[4], Malcom J. Reid[1], Lene S. Heier[5], Ole Christian Lind[2], Kevin V. Thomas[4], Sondre Meland[1,2]

[1]Norwegian Institute for Water Research, Gaustadalléen 21, NO-0349 Oslo, Norway
[2]Norwegian University of Life Sciences, Center of Excellence in Environmental Radioactivity (CERAD), Faculty of Environmental Sciences and Natural Resource Management, P.O. Box 5003, 1433 Ås, Norway
[3]Faculty of Science, Van't Hoff Institute for Molecular Sciences, University of Amsterdam, Science Park, 904 GD Amsterdam, the Netherlands
[4]Queensland Alliance for Environmental Health Sciences (QAEHS), The University of Queensland, 20 Cornwall Street, Woolloongabba, 4102 QLD, Australia.
[5]Norwegian Public Roads Administration Construction, Postboks 1010, N-2605 Lillehammer, Norway

SI-1 Styrene content of tires

Table S1. Styrene content reported for different tires, information found in datasheets for each tire listed at the Producers websites.

Type of SBR	Product code	Producer	% styrene	% styrene	
SSBR	SOL 527OH	KUMHO Petrochemcial	21	21	
	SOL C6450SL	KUMHO Petrochemcial	35	35	
	SOL 6360SL	KUMHO Petrochemcial	33	33	
	SOL C6270L	KUMHO Petrochemcial	25	25	
	SOL 6270SL	KUMHO Petrochemcial	25	25	
	SOL 6270M	KUMHO Petrochemcial	25	25	
	SSBR-2560	SIBUR International	23-27	25	Average
	SSBR-2560 TDAE	SIBUR International	20-30	25	Average
	SSBR-4040 TDAE	SIBUR International	35-45	40	Average
	SSBR-3750 TDAE	SIBUR International	35-40	37.5	Average
	SSBR-3755 TDAE	SIBUR International	35-40	40	Average
	SLF 30H41	Goodyear	30	30	
	SLF33H23	Goodyear	33	33	
	SLF 16S42	Goodyear	16	16	
	SLF 18B10	Goodyear	18	18	
ESBR	SBR1500	SIBUR International	23.5	23.5	
	Emulprene 1778	Dynasol	22.5-24.5	23.5	Average
	Emulprene 1732	Dynasol	30.5-33.5	32	Average
	Emulprene 1723	Dynasol	22.5-24.5	23.5	Average
	Emulprene 1712	Dynasol	22.5-24.5	23.5	Average
	Emulprene 1502CR	Dynasol	22.5-24.5	23.5	Average
	Emulprene 1502	Dynasol	22.5-24.5	23.5	Average
	Emulprene 1500	Dynasol	22.5-24.5	23.5	Average
	Emulsil 4793T	Dynasol	35.5-37.5	36.5	Average
	Emulsil 4773T	Dynasol	35.5-37.5	36.5	Average
	Emulsil 4773R	Dynasol	35.5-37.5	36.5	Average
	Emulsil 1671	Dynasol	22.5-24.5	23.5	Average
	Emulblack 3651	Dynasol	22.5-24.5	23.5	Average
	Emulblack 1848	Dynasol	22.5-24.5	23.5	Average
	Emulblack 1848K	Dynasol	22.5-24.5	23.5	Average
	Emulblack 1608	Dynasol	22.5-24.5	23.5	Average
	Emulblack 1606R	Dynasol	22.5-24.5	23.5	Average
			Average	27.4	

SI-2 Pyrolysis GC-MS details

Table S2. Marker compounds used to quantify SBR+BR+SBS. Italics and bold values used for calibration and quantification

Polymer	Pyrolysis product	Indicator ions (m/z)	Retention Time (mins)	Highest peak intensity
Styrene butadiene rubber (SBR)/Styrene butadiene styrene (SBS)	Benzene	51, 67, **78**	2.7	SBR
	α-methylstyrene	78, 91, **118**	9.5	SBS
	Ethylstyrene	77, 91, **117**	11.7	SBS
	Butadiene trimer A	65, **91**, 146	14.6	SBR
	Styrene monomer	104	7.2	SBS
Internal standard	Poly(1,4-butadiene-$_d$6)	***60***, 120, 42, 86	5.3	

Table S3. Instrumental conditions for Pyrolysis-GC-MS measurements

Apparatus	Parameters	Settings
Micro-furnace Pyrolyzer Frontier EGA/PY-3030D (Single-Shot analysis)	Pyrolyzer furnace/oven temperature	700 °C
	Pyrolyzer interface temperature	300 °C
	Pyrolysis time	0.20 min (12 seconds)
Gas chromatogram (GC)	Column	Ultra-Alloy® 5 capillary column (30 m, 0.25 mm I.D., 0.25 µm film thickness) (Frontier Lab)
	Injector port temperature	300 °C
	Column oven temperature program	50 °C (2 min) → (5 °C /min) → 160 °C (24 min) → (15 °C /min) → 300 °C (9 min)
	Injector mode	Split (split 50:1)
	Carrier gas	Helium, 1.0 mL/min, constant linear velocity
Mass spectrometer (MS)	Ion source temperature	230 °C
	Ionization energy	Electron ionization (EI); 70 eV
	Scan mode/range	Selected ion monitoring (TIC) mode, 45 to 350 m/z

SI-3 Styrene content

Table S4. The average styrene content in the calibration curve based on the styrene content of SBR1500 (23.5 %) and Kraton SBS (30%) is calculated.

SBR %	SBS %	SBR	SBS	SBR:SBS
20	80	4.7	24	28.7
40	60	9.4	18	27.4
80	20	18.8	6	24.8
			Average	**27.0**

SI-4 Emission factor

For this study, three levels of EFs for road wear with studded tires (5, 7.5 and 10 g/vkm) were used in order to reflect the variation in EFs reported by different studies. As there are currently no studies of road wear emission factors for Norway, the currently available emission factors provided by studies from other countries are utilized in this study. Three levels of EFs were found: 5, 7.5 and 10 g/vkm, for personal vehicles with studded tires. For heavy vehicles, it is suggested that the road wear is 5 times that of personal vehicles. As described in section 2.5, the road wear from non-studded winter tires and summer tires are 40 times lower than the wear from studded tires[1]. The EFs are therefore corrected for the ratio of studded tires used at the sample location (Table SI-5). For each level, the amount of SBS was calculated from each of them based on the percentage of SBS added to PMB and the percentage of PMB added to asphalt. Then a Monte Carlo simulation (Crystal Ball in Excel) is applied to calculate the expected SBS level present based three levels of SBS (personal vehicles + heavy vehicles for each level

Table S5. Emission factors of asphalt and tire

Type	EF	Level	$EFA_{PV\text{-}st}$ (g/vkm)	$EFA_{PV\text{-}nst}$ (g/vkm)	$EFA_{HV\text{-}st}$ (g/vkm)	$EFA_{HV\text{-}nst}$ (g/vkm)
Asphalt	EFA	1	5	0.125	25	0.625
		2	7.5	0.188	37.5	0.938
		3	10	0.25	50	1.25
			EFT_{PV}	EFT_{HV}		
Tire	EFT	Highway	0.104	0.668		
		Urban	0.132	0.850		

SI-5 Calibration curve Total concentration SBR+BR+SBS

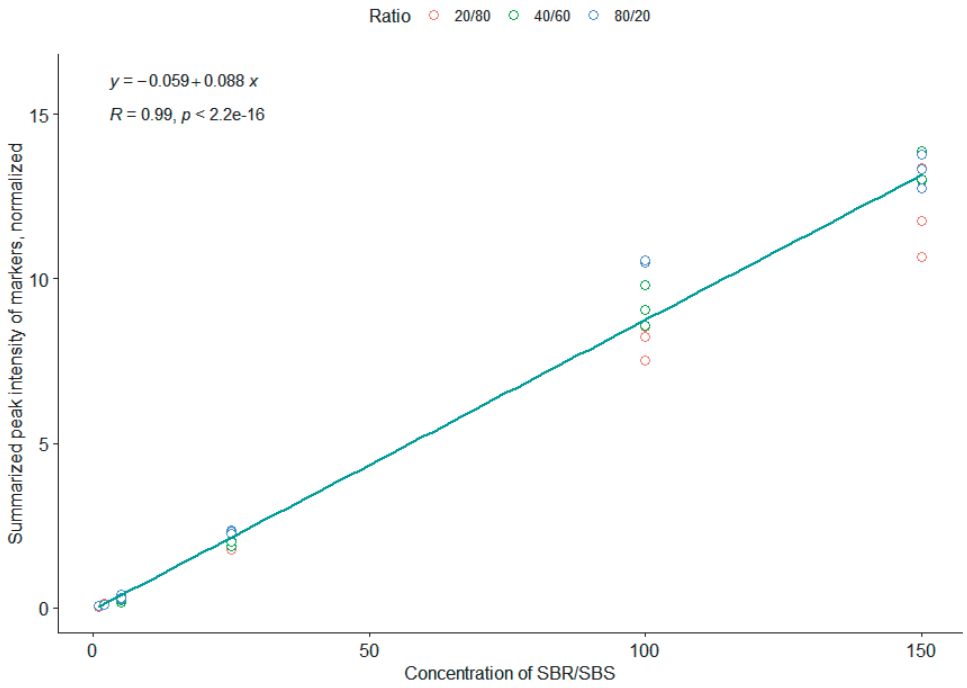

Figure S1. Calibration curve for mixture calibration of SBR and SBS. Calibration points 1 µg, 2µg, 25 µg, 100 µg and 150 µg. Three ratios of SBR:SBS (20:80, 40:60, 80:20) and three replicates for each ratio at all calibration points.

SI-6 LOD and LOQ

Table S6. LOD and LOQ values for the 4 markers of the final method. Noise level is established by the average noise level of 8 values of 1 µg to 3 µg SBR+SBS.

Markers	Noise level (N)	LOD (3xN)	LOQ (10xN)
m/z 78	720	1 µg	1 µg
m/z 118	600	1 µg	5 µg
m/z 117	425	2 µg	5 µg
m/z 91	620	2 µg	5 µg

SI-7 Method validation

Accuracy

The recovery for each sample is calculated by the following steps: 1) calculate the concentration of SBR+SBS in the sample (µg/mg), 2) subtract the expected average concentration of tire in the sample , 3) multiply this with the weight added to the sample, 4) divide it with the amount of spiked standard solution (µg) and 5) multiply with 100 to obtain the percentage value.

Table S7. Method validation testing the recovery (%) for standard solutions of SBR, SBS and mixt samples of SBR+SBS. Mix-samples have a given ratio of SBR:SBS.

Sample	Measured concentration of SBR+BR+SBS (µg/sample)	Expected concentration of SBR+BR+SBS (µg/sample)	Accuracy %
Mix 1-A (20:80)	1.5	1	149.8
Mix 1-D (40:60)	1.5	1	150.7
Mix 1-G (80:20)	1.4	1	143.6
Mix 4-A (20:80)	21.2	25	84.6
Mix 4-D (40:60)	25.8	25	103.3
Mix 4-G (80:20)	27.3	25	109.2
SBR_25ug	28.9	25	115.8
SBR_30ug-A	32.8	30	87.8
SBR_30ug-B	35.4	30	109.2
SBR_30ug-C	37.5	30	117.9
SBS_25ug	22.0	25	87.8
SBS_30ug-A	26.1	30	109.2
SBS_30ug-B	21.1	30	117.9
SBS_30ug-C	23.5	30	125.1

Table S8. Method validation testing the standard error of prediction (%), with tire samples, spiked with standard solutions of SBR+SBS (40:60 ratio SBR:SBS)

Sample	SBR/SBS (µg/ sample)	Weight of sample (mg)	Spiking SBR/SBS total µg	Total SBR/SBS (µg/mg)	SBR/SBS without average tire particle	SBR/SBS (µg/mg) in cup without average tire particle	Recovery %	Mean recovery %
C2-1	27.1	0.133		203.4				
C2-2	25.1	0.144		174.6				
C2-3	23.9	0.128		186.3				
C2-4	21.1	0.124		170				
C2-5	24.1	0.137		175.6				
C2-6	24.4	0.129		189.4				
C2-13_spiked10	42.2	0.150	10	281.9	98.7	14.8	147.8	
C2-14_spiked10	24.0	0.098	10	243.7	60.4	5.9	59.4	
C2-15_spiked10	36.0	0.134	10	265.2	82.0	11.0	109.8	
C2-16_spiked10	25.4	0.113	10	224.4	41.2	4.7	46.6	
C2-17_spiked10	30.7	0.122	10	252.6	69.4	8.4	84.4	
C2-18_spiked10	24.6	0.109	10	226.9	43.7	4.7	47.4	82.6
C2-7_spiked50	72.5	0.126	50	577.1	393.9	49.5	99.0	
C2-8_spiked50	61.9	0.120	50	516.0	332.7	39.9	79.9	
C2-9_spiked50	72.5	0.111	50	656.5	473.2	52.3	104.6	
C2-10_spiked50	60.6	0.099	50	610.0	426.7	42.4	84.8	
C2-11_spiked50	67.4	0.102	50	663.7	480.5	48.8	97.6	
C2-12_spiked50	61.0	0.096	50	633.6	450.4	43.4	86.7	92.1
C2-19_spiked130	139.1	0.146	130	950.1	766.9	112.3	86.4	
C2-20_spiked130	132.4	0.104	130	1269.3	1086.1	113.3	87.1	
C2-21_spiked130	139.3	0.109	130	1282.3	1099.1	119.4	91.8	
C2-22_spiked130	145.3	0.114	130	1269.7	1086.5	124.3	95.6	
C2-23_spiked130	143.7	0.135	130	1064.0	880.7	119.0	91.5	
C2-24_spiked130	140.4	0.107	130	1308.4	1125.2	120.7	92.9	90.9
Average % recovery								88.5

Table S9. Method validation testing the standard error of prediction (%), with environmental samples, spiked with standard solutions of SBR+SBS (40:60 ratio SBR:SBS)

Sample	SBR+SBS (µg/ sample) measured in the sample	Weight of sample (mg)	Mass of SBR (µg) spiked	Mass of SBS (µg) spiked	Total mass of SBR+SBS (µg) spiked	SBR+SBS (µg/mg) with spiked level removed	Recovery %	Mean recovery %
SK-0m-1	7.7	1.2				6.5		
SK-0m-2	8.1	1.1				7.6		
SK-0m-3	14.6	1.5				10.0		
SK-0m-4	41.3	5.0				8.3		
SK-0m-5	35.6	5.0				7.1		
SK-0m-6	36.5	4.6				8.0		
SK-0m - spiked 50µg-1	54.9	1.0	20	30	50	55.6	94.1	
SK-0m - spiked 50µg-2	60.3	1.0	20	30	50	61.7	105.2	
SK-0m - spiked 50µg-3	57.4	1.1	20	30	50	52.6	97.5	
SK-0m - spiked 50µg-4	75.1	4.7	20	30	50	15.9	75.6	
SK-0m - spiked 50µg-5	73.8	5.2	20	30	50	14.2	65.6	
SK-0m - spiked 50µg-6	83.1	4.8	20	30	50	17.3	90.4	88.1
SF1-2018-1	3.0	1.0				3.2		
SF1-2018-2	3.7	1.0				3.8		
SF1-2018-3	3.7	1.2				3.1		
SF1 - spiked 50µg-1	60.8	0.9	20	30	50	64.5	115.2	
SF1 - spiked 50µg-2	52.5	0.9	20	30	50	56.1	98.8	
SF1 - spiked 50µg-3	51.9	1.1	20	30	50	48.7	96.7	103.6

Table S10. Statistics of the peak height of each pyrolysis product (marker) suggested for this method (Benzene, α-methylstyrene, ethylstyrene, Butadiene trimer) and the sum of these four markers, compared to the peak height of the 4-Vinylcyclohexene marker. All peak heights are normalized against the internal standard (d-PB) and the mass of the sample: in SBR standard solutions (1-150 µg), in SBR+SBS standard solutions (1-150 µg, ratio 20:80, 40:60, 80:20 SBR:SBS) and reference tires (mass 0.05-0.165 mg).

Sample	Statistics	4-Vinylcyclohexene	Benzene	α-methylstyrene	ethylstyrene	Butadiene trimer	SUM
SBR standard solution	Average	0.0205	0.0689	0.0118	0.00200	0.00638	0.0890
	Median	0.0180	0.0659	0.0100	0.00199	0.00736	0.0847
	Standard deviation	0.0053	0.024	0.0062	0.00030	0.0021	0.028
	% Standard deviation	26.0	34.3	53.1	14.9	32.7	31.6
SBR+SBS standard solution	Average	0.0173	0.0631	0.0193	0.00412	0.00244	0.0890
	Median	0.0166	0.0618	0.0195	0.00415	0.00240	0.0879
	Standard deviation	0.00450	0.00935	0.00167	0.000414	0.000442	0.00971
	% Standard deviation	25.9	14.8	8.6	10.0	18.2	10.9
Tires All	Average	2.64	21.8	3.16	0.512	1.47	27.0
	Median	2.66	21.8	1.92	0.483	1.02	27.0
	Standard deviation	1.59	7.51	3.02	0.206	0.993	9.92
	% Standard deviation	60.2	34.4	95.8	40.3	67.3	36.8
Tires Personal Vehicle PV	Average	2.20	20.9	3.70	0.526	1.60	26.7
	Median	2.01	21.1	2.06	0.473	1.23	26.7
	Standard deviation	1.05	4.64	3.61	0.235	1.03	7.30
	% Standard deviation	48.0	22.2	97.5	44.8	64.2	27.3
Tires Heavy Vehicle HV	Average	3.20	23.0	2.45	0.494	1.31	27.3
	Median	3.83	23.5	1.92	0.519	0.928	27.4
	Standard deviation	1.95	10.0	1.85	0.162	0.934	12.6
	% Standard deviation	61.0	43.5	75.5	32.8	71.2	46.3

Table S11. Ratio (%) of the four markers *Benzene, α-methylstyrene, ethylstyrene* and *Butadiene trimer* in different samples.

Sample type	Benzene	α-methylstyrene	ethylstyrene	Butadiene trimer
SBR+SBS (n=18)	71 ± 4	17 ± 5	4 ± 1	7 ± 4
SBR	77 ± 3	12 ± 3	2 ± 1	8 ± 4
SBS	66 ± 5	19 ± 5	8 ± 1	8 ± 2
Reference tires (n=31)	82 ± 10	10 ± 8	2 ± 0	5 ± 3
Skullerud snow (SK) (n=3)	82 ± 2	13 ± 1	2 ± 0	4 ± 0
Skullerud soil (SK-SED) (n=3)	87 ± 3	9 ± 3	2 ± 1	1 ± 1
Smestad gully pot (SF) (n=6)	79 ± 3	15 ± 2	2 ± 0	4 ± 0
P-value Kruskal-Wallis	P<0.05	P<0.05	P<0.05	P<0.05

Kruskal-wallis tests results

Benzene by Type: Kruskal-Wallis chi-squared = 105.48, df = 6, p-value < 2.2e-16
methylstyrene by Type: Kruskal-Wallis chi-squared = 72.442, df = 6, p-value = 1.289e-13
ethylstyrene by Type: Kruskal-Wallis chi-squared = 155.45, df = 6, p-value < 2.2e-16
Butadiene by Type:Kruskal-Wallis chi-squared = 62.594, df = 6, p-value = 1.335e-11

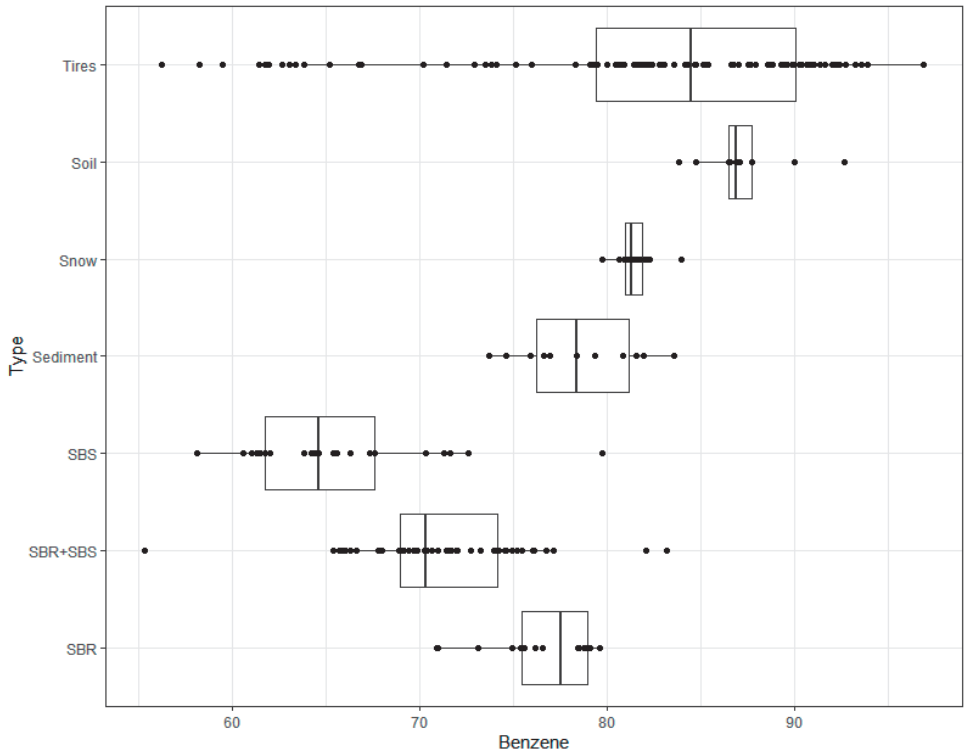

Figure S2. The figure shows the variation in the percentage of *Benzene* in all samples tested (tire, soil, snow, sediment, SBS standard, SBR standard, SBR+SBS mixture standard), compared to the total signal of all four marker compounds.

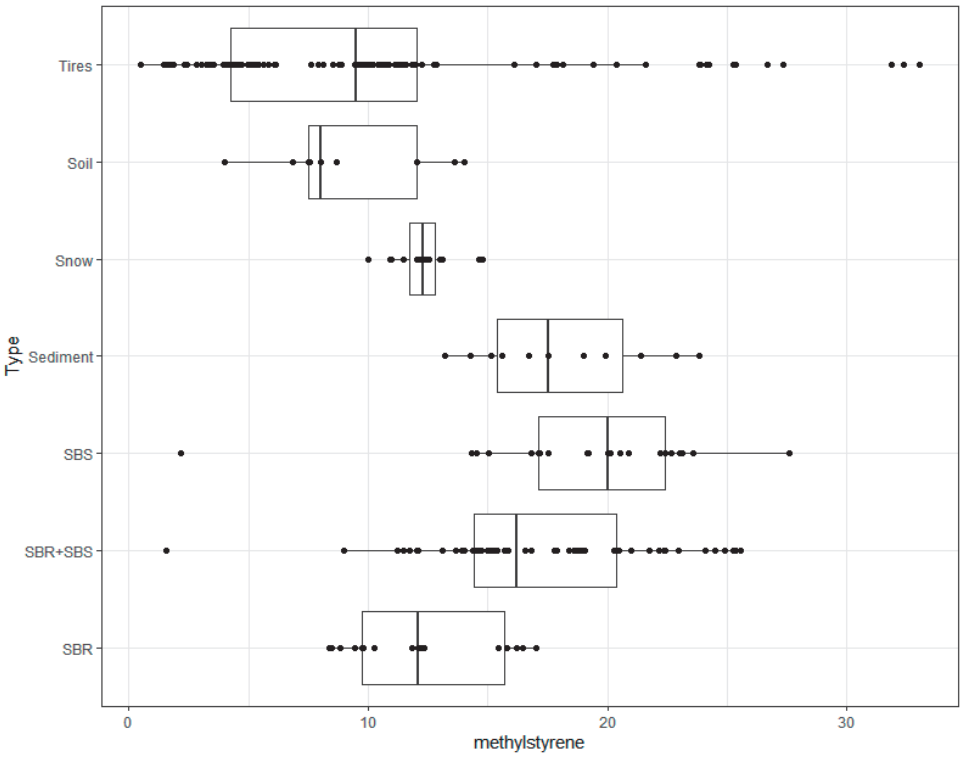

Figure S3. The figure shows the variation in the percentage of *α-methylstyrene* in all samples tested (tire, soil, snow, sediment, SBS standard, SBR standard, SBR+SBS mixture standard), compared to the total signal of all four marker compounds.

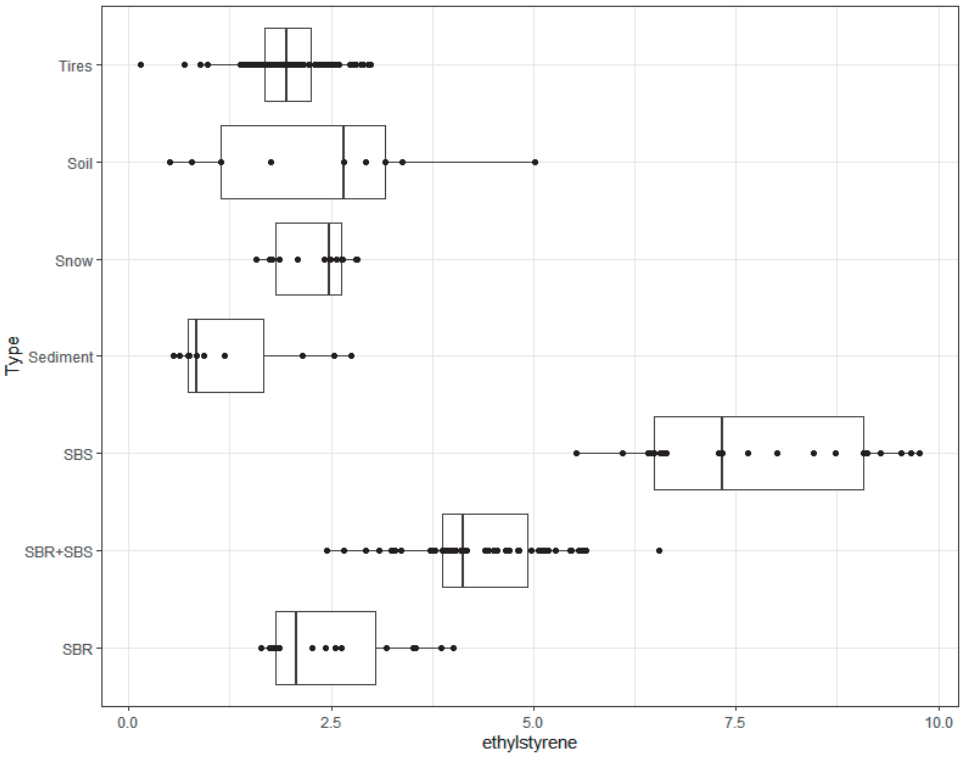

Figure S4. The figure shows the variation in the percentage of *ethylstyrene* in all samples tested (tire, soil, snow, sediment, SBS standard, SBR standard, SBR+SBS mixture standard), compared to the total signal of all four marker compounds.

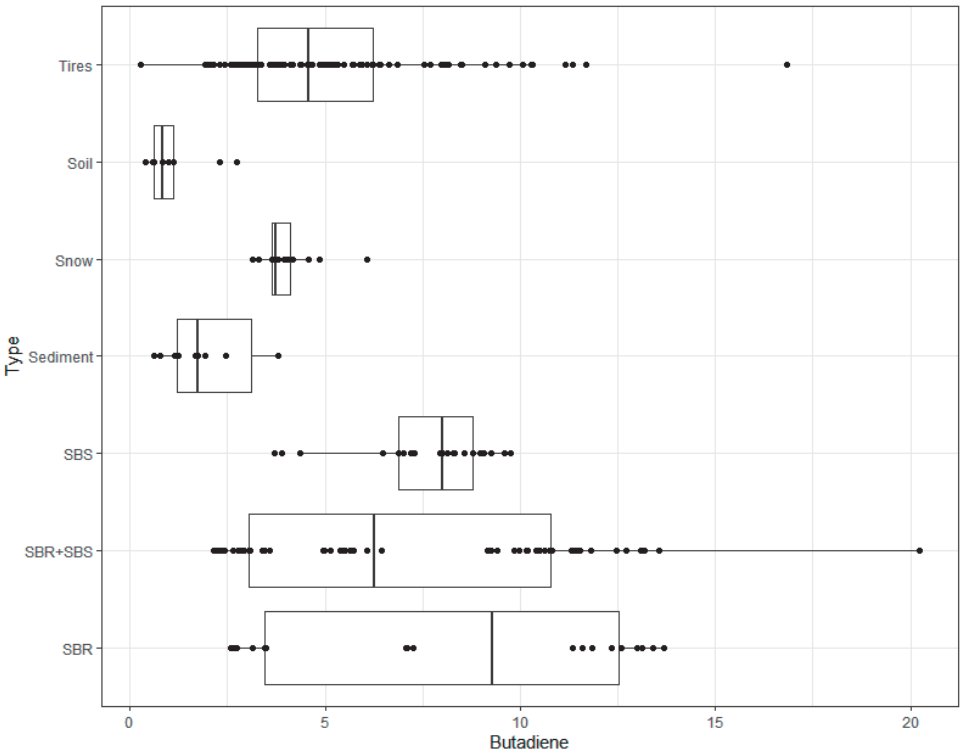

Figure S5. The figure shows the variation in the percentage of *Butadiene* in all samples tested (tire, soil, snow, sediment, SBS standard, SBR standard, SBR+SBS mixture standard), compared to the total signal of all four marker compounds.

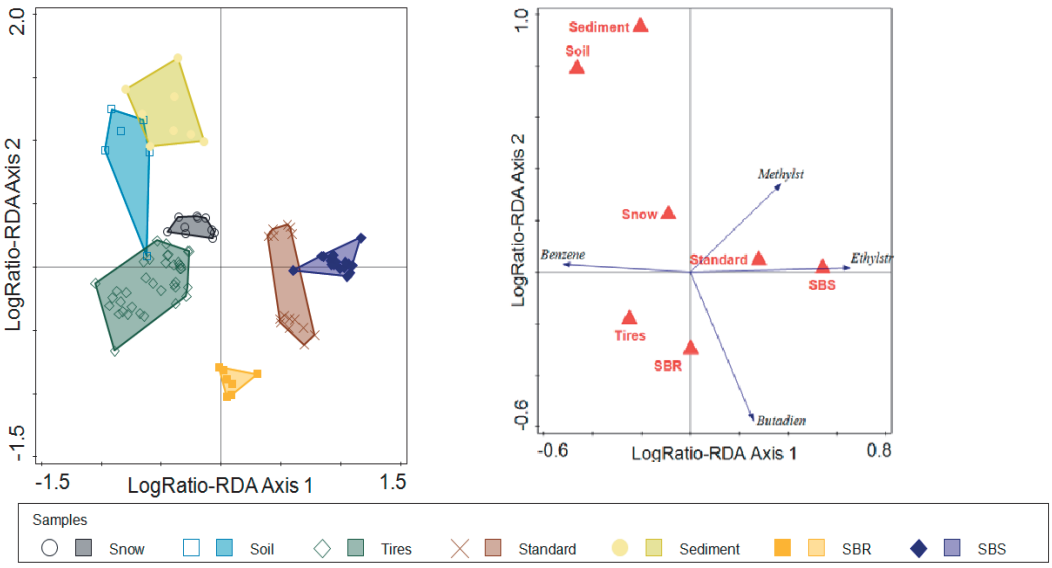

Figure S6. The figure shows an Aitchison-weighted-log-ratio-RDA analysis (P<0.05) of the ratio of the marker compounds in different environmental samples; snow (SK), Soil (SK-SED), tires, Standard (SBR+SBS standard), Sediment (SF), SBR (standard) and SBS (standard).

SI-8 Reference tires

Statistical testing

All statistical tests on the reference tire data were performed on log-transformed data, where the expectations of normal distribution were met (Shapiro-Wilk test of residuals from ANOVA, $P > 0.05$). As the dataset only had one all year-tire, this tire was excluded from the statistical testing. For the group "Season", the Levenes' test proved that the variance was equal and a two-sample t-test assuming equal variance was performed. The P-value for SBR ~ Season was 0.068, thus no significant difference was detected between the two seasonal groups of tires,

summer and winter tires. For the group "Vehicle type", the Levenes' test proved that the variance was not equal, and the Welch's two-sample t-test was performed. The P-value for SBR ~Vehicle type was 0.91, thus no significant difference was detected between the two vehicle groups.

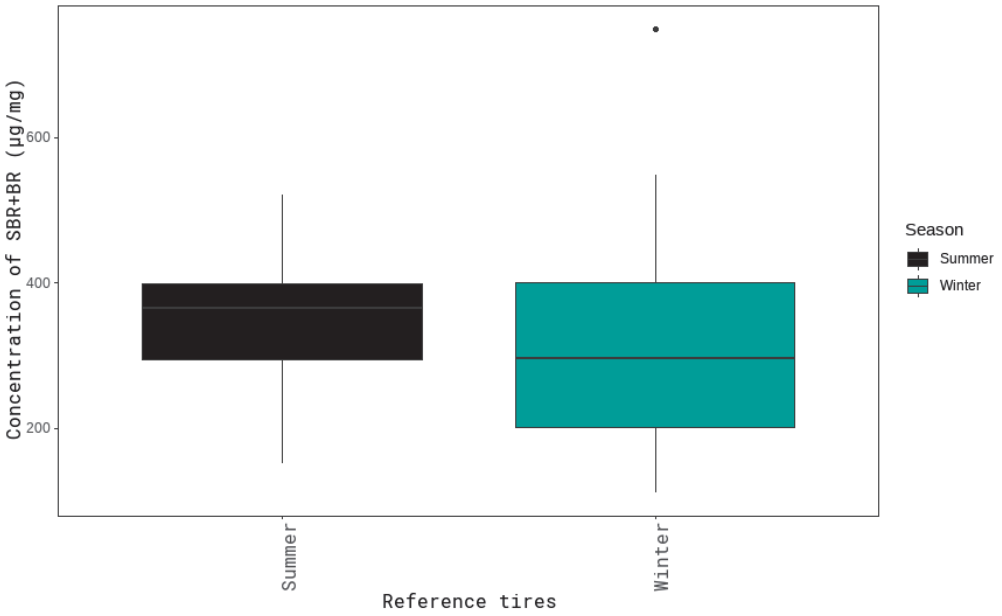

Figure S7. Concentration of SBR+BR (µg/mg) in reference tires, grouped by season. The group "Summer" includes eight different tires and the group "Winter" includes 23 different tires. All analysed in replicates (n=3). Type of tire is depicted in colors.

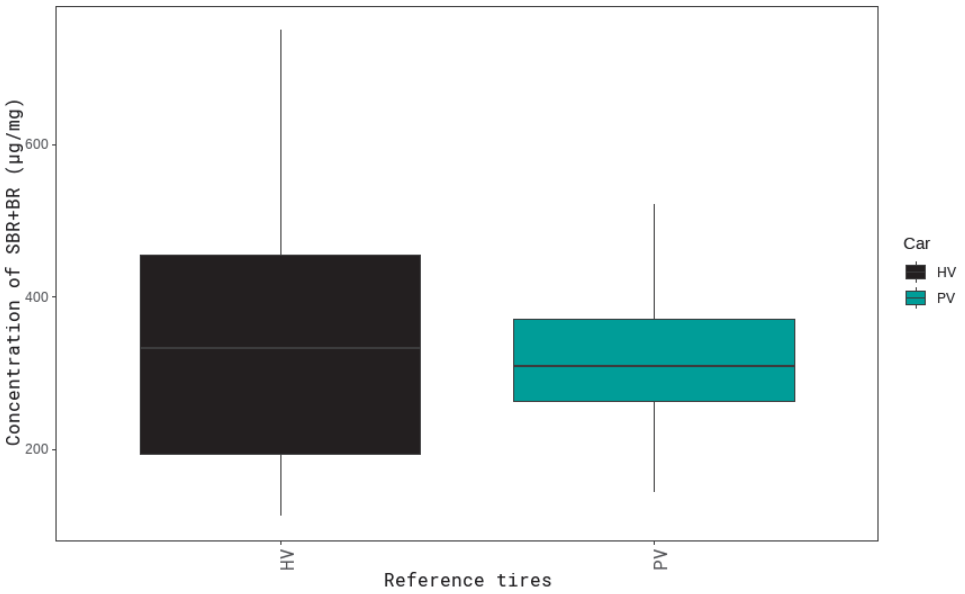

Figure S8. Concentration of SBR+BR (µg/mg) in reference tires, grouped by vehicle type. The group "HV" includes 13 different heavy vehicle tires. The group "PV" includes 18 different personal vehicle tires. All analysed in replicates (n=3). Type of tire is depicted in colors.

Table S12. Overview of tire samples used in the study and the measured concentration of SBR+BR in each tire sample.

SAMPLES	TIRE TYPE				CONCENTRATIONS			
	Brand	Car type	Season	Studs	SBR+BR (µg/sample)	Weight sample (mg)	SBR+BR (µg/mg)	Mean SBR+BR (µg/mg)
A1-A	ATLAS	PV	Summer	N-S	19.06	0.072	264.7	
A1-B	ATLAS	PV	Summer	N-S	17.65	0.1158	152.4	
A1-C	ATLAS	PV	Summer	N-S	16.68	0.0726	229.8	215.6
B1-A	BRIDGESTONE	PV	Winter	N-S	35.23	0.0939	375.2	
B1-B	BRIDGESTONE	PV	Winter	N-S	44.37	0.1029	431.2	
B1-C	BRIDGESTONE	PV	Winter	N-S	38.13	0.1	381.3	395.9
B2-A	BRIDGESTONE	PV	Summer	N-S	38.78	0.0976	397.3	
B2-B	BRIDGESTONE	PV	Summer	N-S	43.97	0.0951	462.4	
B2-C	BRIDGESTONE	PV	Summer	N-S	24.19	0.0649	372.8	410.8
B3-A	BRIDGESTONE	PV	Winter	S	15.09	0.1055	143.0	
B3-B	BRIDGESTONE	PV	Winter	S	34.78	0.1223	284.4	
B3-C	BRIDGESTONE	PV	Winter	S	35.57	0.1329	267.7	231.7
B4-A	BRIDGESTONE	PV	Winter	N-S	22.97	0.0796	288.6	
B4-B	BRIDGESTONE	PV	Winter	N-S	13.17	0.0502	262.3	
B4-C	BRIDGESTONE	PV	Winter	N-S	16.03	0.0502	319.4	290.1
B5-A	BRIDGESTONE	PV	Winter	N-S	20.77	0.0784	264.9	
B5-B	BRIDGESTONE	PV	Winter	N-S	19.83	0.074	268.0	
B5-C	BRIDGESTONE	PV	Winter	N-S	26.00	0.099	262.7	265.2
B6-A	BRIDGESTONE	PV	Winter	S	20.37	0.0839	242.8	
B6-B	BRIDGESTONE	PV	Winter	S	31.53	0.1117	282.3	
B6-C	BRIDGESTONE	PV	Winter	S	21.11	0.091	232.0	252.4
B7-A	BRIDGESTONE	PV	Summer	N-S	30.92	0.0713	433.7	
B7-B	BRIDGESTONE	PV	Summer	N-S	44.48	0.0981	453.5	
B7-C	BRIDGESTONE	PV	Summer	N-S	67.45	0.1296	520.5	469.2
B8-A	BRIDGESTONE	PV	Summer	N-S	32.76	0.0963	340.2	
B8-B	BRIDGESTONE	PV	Summer	N-S	30.56	0.0779	392.3	
B8-C	BRIDGESTONE	PV	Summer	N-S	39.05	0.0964	405.1	379.2
B9-A	BRIDGESTONE	PV	Summer	N-S	26.57	0.0676	393.1	
B9-B	BRIDGESTONE	PV	Summer	N-S	24.09	0.0628	383.7	
B9-C	BRIDGESTONE	PV	Summer	N-S	41.79	0.0998	418.8	398.5
C1-A	CONTINENTAL	PV	Winter	S	32.02	0.1024	312.7	
C1-B	CONTINENTAL	PV	Winter	S	44.68	0.1466	304.8	
C1-C	CONTINENTAL	PV	Winter	S	36.14	0.1123	321.8	313.1
C2-A	CONTINENTAL	PV	Winter	N-S	12.20	0.0645	189.2	
C2-B	CONTINENTAL	PV	Winter	N-S	10.38	0.0523	198.5	
C2-C	CONTINENTAL	PV	Winter	N-S	8.92	0.0511	174.6	187.4
C3-A	CONTINENTAL	PV	Summer	N-S	25.22	0.084	300.2	
C3-B	CONTINENTAL	PV	Summer	N-S	37.10	0.1136	326.6	

C3-C	CONTINENTAL	PV	Summer	N-S	38.85	0.1119	347.2	324.7
N1-A	NOKIAN	PV	Summer	N-S	25.35	0.0978	259.2	
N1-B	NOKIAN	PV	Summer	N-S	34.18	0.1228	278.4	
N1-C	NOKIAN	PV	Summer	N-S	18.35	0.0712	257.7	265.1
N2-A	NOKIAN	PV	Winter	N-S	23.17	0.1351	171.5	
N2-B	NOKIAN	PV	Winter	N-S	21.63	0.097	223.0	
N2-C	NOKIAN	PV	Winter	N-S	20.43	0.088	232.2	208.9
S1-A	YOKOHAMA	PV	Winter	N-S	21.65	0.0724	299.1	
S1-B	YOKOHAMA	PV	Winter	N-S	40.67	0.1301	312.6	
S1-C	YOKOHAMA	PV	Winter	N-S	32.50	0.11	295.5	302.4
S2-A	KUMHO	PV	Summer	N-S	21.89	0.0677	323.4	
S2-B	KUMHO	PV	Summer	N-S	40.50	0.1113	363.9	
S2-C	KUMHO	PV	Summer	N-S	33.48	0.0918	364.7	350.7
S3-A	KUMHO	PV	Winter	N-S	29.37	0.0921	318.9	
S3-B	KUMHO	PV	Winter	N-S	50.67	0.1386	365.6	
S3-C	KUMHO	PV	Winter	N-S	48.83	0.1467	332.9	339.1
T1-A	BRIDGESTONE	HV	Winter	N-S	26.12	0.0653	400.0	
T1-B	BRIDGESTONE	HV	Winter	N-S	26.10	0.0556	469.4	
T1-C	BRIDGESTONE	HV	Winter	N-S	21.12	0.0522	404.6	424.6
T2-A	BRIDGESTONE	HV	Winter	N-S	42.37	0.0887	477.7	
T2-B	BRIDGESTONE	HV	Winter	N-S	59.52	0.1309	454.7	
T2-C	BRIDGESTONE	HV	Winter	N-S	37.20	0.0937	397.0	443.1
T3-A	BRIDGESTONE	HV	All-year	N-S	59.19	0.1166	507.6	
T3-B	BRIDGESTONE	HV	All-year	N-S	48.34	0.1096	441.1	
T3-C	BRIDGESTONE	HV	All-year	N-S	43.24	0.089	485.8	478.2
T4-A	BRIDGESTONE	HV	Winter	N-S	40.90	0.0869	548.3	
T4-B	BRIDGESTONE	HV	Winter	N-S	67.50	0.1129	749.1	
T4-C	BRIDGESTONE	HV	Winter	N-S	49.30	0.1176	748.1	681.8
T5-A	BRIDGESTONE	HV	Winter	N-S	51.37	0.0966	531.8	
T5-B	BRIDGESTONE	HV	Winter	N-S	36.42	0.0803	453.5	
T5-C	BRIDGESTONE	HV	Winter	N-S	38.75	0.0892	434.4	473.3
T6-A	BRIDGESTONE	HV	Winter	N-S	32.40	0.0746	434.3	
T6-B	BRIDGESTONE	HV	Winter	N-S	47.63	0.0901	528.6	
T6-C	BRIDGESTONE	HV	Winter	N-S	26.34	0.0659	399.7	454.2
T7-A	BRIDGESTONE	HV	Winter	N-S	39.01	0.1339	291.3	
T7-B	BRIDGESTONE	HV	Winter	N-S	16.48	0.1198	137.6	
T7-C	BRIDGESTONE	HV	Winter	N-S	23.97	0.1478	162.1	197.0
T8-A	BRIDGESTONE	HV	Winter	N-S	27.47	0.1487	184.7	
T8-B	BRIDGESTONE	HV	Winter	N-S	17.64	0.0886	199.1	
T8-C	BRIDGESTONE	HV	Winter	N-S	29.96	0.0935	320.4	234.7
T8-D	BRIDGESTONE	HV	Winter	N-S	46.71	0.1645	284.0	
T8-E	BRIDGESTONE	HV	Winter	N-S	26.56	0.1319	201.4	
T8-F	BRIDGESTONE	HV	Winter	N-S	44.51	0.1634	272.4	252.6
T9-A	BRIDGESTONE	HV	Winter	N-S	16.66	0.1468	113.5	
T9-B	BRIDGESTONE	HV	Winter	N-S	18.65	0.1571	118.7	

T9-C	BRIDGESTONE	HV	Winter	N-S	18.53	0.165	112.3	114.8
T10-A	BRIDGESTONE	HV	Winter	N-S	49.21	0.1573	312.9	
T10-B	BRIDGESTONE	HV	Winter	N-S	34.18	0.0996	343.1	
T10-C	BRIDGESTONE	HV	Winter	N-S	42.87	0.129	332.3	329.4
T11-A	BRIDGESTONE	HV	Winter	N-S	16.30	0.1182	137.9	
T11-B	BRIDGESTONE	HV	Winter	N-S	14.78	0.1246	118.6	
T11-C	BRIDGESTONE	HV	Winter	N-S	8.07	0.0721	112.0	122.8
T12-A	CONTINENTAL	HV	Winter	N-S	14.10	0.078	180.8	
T12-B	CONTINENTAL	HV	Winter	N-S	17.45	0.0984	177.3	
T12-C	CONTINENTAL	HV	Winter	N-S	33.30	0.1415	235.3	197.8
T13-A	CONTINENTAL	HV	Winter	N-S	16.21	0.0853	190.0	
T13-B	CONTINENTAL	HV	Winter	N-S	21.53	0.1097	196.3	
T13-C	CONTINENTAL	HV	Winter	N-S	16.43	0.0691	237.8	208.0

Table S13. Summary statistics for SBR+BR concentration in reference tires

Car	Season	Studs	Average	St.dev	Median	Min	Max	N
HV	All	All	329.4704	167.9238	316.6181	111.9838	749.1487	42
PV	All	All	311.1063	82.44017	308.6877	143.0467	520.4553	54
HV	All year	All	197.0157	82.61152	162.1452	137.5569	291.345	3
HV	Winter	All	339.6592	169.0378	332.3168	111.9838	749.1487	39
PV	Summer	All	351.7186	83.80793	364.3001	152.3822	520.4553	24
PV	Winter	All	278.6165	66.28292	283.3496	143.0467	431.2067	30
HV	All year	N-S	197.0157	82.61152	162.1452	137.5569	291.345	3
HV	Winter	N-S	339.6592	169.0378	332.3168	111.9838	749.1487	39
PV	Summer	N-S	351.7186	83.80793	364.3001	152.3822	520.4553	24
PV	Winter	N-S	284.1422	71.08127	288.5971	171.4966	431.2067	21
PV	Winter	S	265.7234	55.024	282.2939	143.0467	321.8333	9

SI-9 Results for all environmental samples

Table S14. Results of testing the multimarker method on environmental samples (SK, SK-SED and SF), by µg/sample and µg/mg of sample material.

Sample	SBR/SBS (µg/sample)	Weight of sample (mg)	Total SBR/SBS (µg/mg)
SK-0m-7	40.78	3.9647	10.28
SK-0m-8	49.72	3.9903	12.46
SK-0m-9	58.56	5.0749	11.54
SK-1m-1	35.25	3.1733	11.11
SK-1m-2	43.98	3.6385	12.09
SK-1m-3	85.90	5.3141	16.17
SK-3m-1	10.22	1.6157	6.32
SK-3m-2	28.54	3.5642	8.01
SK-3m-3	22.72	3.2357	7.02
SK-SED-1-1A	5.62	3.06	1.8
SK-SED-1-1B	13.85	8.21	1.7
SK-SED-1-1C	5.78	3.56	1.6
SK-SED-1-2A	9.75	9.71	1.0
SK-SED-1-2B	12.82	11.29	1.1
SK-SED-1-2C	13.29	6.98	1.9
SK-SED-1-3A	14.49	8.31	1.7
SK-SED-1-3B	14.85	9.56	1.6
SK-SED-1-3C	18.30	14.26	1.3
SF1-2020-1	65.55	3.4	19.0
SF1-2020-2	63.62	3.4	18.7
SF1-2020-3	86.62	4.8	18.1
SF2-2020-1	19.14	9.2	2.1
SF2-2020-2	11.77	11.1	1.1
SF2-2020-3	23.54	12.8	1.8
SF3-2020-1	42.55	11.6	3.7
SF3-2020-2	16.97	9.9	1.7
SF3-2020-3	30.77	13.3	2.3

Calibration curve formula for SK-SED and SF (2020) samples:

$y=0.0878x-0.064$

Calibration curve formula for SK and SF (2018) samples:

$y = 0.0881x - 0.0591$

TableS15. Environmental samples for method demonstration

Samples	Sample type	Not normalized, NN					Normalized				SUM N	Concentration of SBR/SBS (µg/sample)	Weight of sample (mg)	Concentration of SBR/SBS (mg/kg)
		m/z 78	m/z 118	m/z 117	m/z 91	m/z 60	m/z 78	m/z 118	m/z 117	m/z 91				
210226_SK-SED-1-1A	SK soil 0m	3.18E+05	5.11E+04	1.89E+03	4.18E+03	1.03E+06	0.308	0.063	0.002	0.005	0.379	5.04	3.06	1648.15
210226_SK-SED-1-1B	SK soil 0m	8.14E+05	1.36E+05	1.11E+04	9.58E+03	8.06E+05	0.788	0.143	0.012	0.010	0.953	11.58	8.21	1410.89
210226_SK-SED-1-1C	SK soil 0m	3.31E+05	4.60E+04	2.99E+03	2.33E+03	9.50E+05	0.321	0.062	0.004	0.003	0.390	5.17	3.56	1452.38
210226_SK-SED-1-2A	SK soil 1.5m	5.71E+05	5.29E+04	2.09E+04	1.51E+04	7.41E+05	0.553	0.087	0.035	0.025	0.700	8.70	9.71	895.82
210226_SK-SED-1-2B	SK soil 1.5m	7.47E+05	7.42E+04	2.89E+04	7.25E+03	6.05E+05	0.723	0.103	0.040	0.010	0.877	10.71	11.29	948.84
210226_SK-SED-1-2C	SK soil 1.5m	8.29E+05	6.97E+04	1.62E+04	5.71E+03	7.20E+05	0.803	0.064	0.015	0.005	0.887	10.83	6.98	1551.13
210226_SK-SED-1-3A	SK soil 3m	9.26E+05	7.24E+04	2.80E+04	2.89E+04	1.09E+06	0.896	0.064	0.025	0.026	1.011	12.24	8.31	1473.38
210226_SK-SED-1-3B	SK soil 3m	9.94E+05	4.29E+04	3.14E+04	4.19E+03	1.13E+06	0.963	0.038	0.028	0.004	1.032	12.49	9.56	1306.25
210226_SK-SED-1-3C	SK soil 3m	1.18E+06	1.01E+05	6.79E+04	8.06E+03	1.13E+06	1.139	0.114	0.077	0.009	1.340	15.99	14.26	1121.04
210305_SF1-3-1	SF-1-2020 rep1	3.82E+06	1.09E+06	4.50E+04	9.43E+04	8.86E+05	4.309	1.226	0.051	0.106	5.691	65.55	3.45	19003.27
210305_SF1-3-2	SF-1-2020 rep2	3.57E+06	1.11E+06	4.50E+04	1.19E+05	8.76E+05	4.073	1.262	0.051	0.135	5.522	63.62	3.40	18723.52
210305_SF1-3-3	SF-1-2020 rep3	4.21E+06	1.09E+06	6.45E+04	1.05E+05	7.24E+05	5.806	1.500	0.089	0.146	7.541	86.62	4.79	18092.16
210305_SF2-3-1	SF-2-2020 rep1	1.17E+06	3.26E+05	1.11E+04	1.89E+04	9.43E+05	1.239	0.346	0.012	0.020	1.617	19.14	9.17	2087.82
210305_SF2-3-2	SF-2-2020 rep2	7.89E+05	2.52E+05	7.97E+03	8.01E+03	1.09E+06	0.723	0.231	0.007	0.007	0.969	11.77	11.10	1059.97
210305_SF2-3-3	SF-2-2020 rep3	1.21E+06	2.92E+05	1.30E+04	2.66E+04	7.68E+05	1.570	0.381	0.017	0.035	2.003	23.54	12.76	1845.58
210305_SF3-3-1	SF-3-2020 rep1	1.71E+06	3.52E+05	1.17E+04	2.43E+04	5.72E+05	2.995	0.614	0.020	0.042	3.672	42.55	11.59	3671.21
210305_SF3-3-2	SF-3-2020 rep2	1.19E+06	2.26E+05	1.05E+04	2.44E+04	1.02E+06	1.169	0.223	0.010	0.024	1.426	16.97	9.88	1717.50
210305_SF3-3-3	SF-3-2020 rep3	1.63E+06	2.95E+05	1.23E+04	1.20E+04	7.38E+05	2.205	0.400	0.017	0.016	2.638	30.77	13.35	2305.30
200626_SF1	SF-1-2018 rep1	4.50E+05	2.70E+04	5.10E+03	7.60E+03	2.10E+05	2.143	0.129	0.024	0.036	2.332	27.14	0.95	28493.09
200626_SF2	SF-1-2018 rep2	4.50E+05	3.10E+04	5.50E+03	8.80E+03	2.30E+05	1.957	0.135	0.024	0.038	2.153	25.11	0.97	25963.40
200626_SF3	SF-1-2018 rep3	3.90E+05	2.60E+04	4.80E+03	8.60E+03	2.10E+05	1.857	0.124	0.023	0.041	2.045	23.88	1.17	20344.51
200626_SK1	SK-0m Rep1	1.30E+05	1.70E+04	2.70E+03	5.10E+03	2.50E+05	0.520	0.068	0.011	0.020	0.619	7.70	1.18	6513.71
200626_SK2	SK-0m Rep2	1.30E+05	1.90E+04	3.30E+03	5.80E+03	2.40E+05	0.542	0.079	0.014	0.024	0.659	8.15	1.07	7635.77
200626_SK3	SK-0m Rep3	2.20E+05	3.50E+04	4.70E+03	9.90E+03	2.20E+05	1.000	0.159	0.021	0.045	1.225	14.58	1.47	9952.66
200626_SK4	SK-0m Rep4	6.00E+05	1.10E+05	1.40E+04	2.80E+04	2.10E+05	2.857	0.524	0.067	0.133	3.581	41.32	4.98	8297.31

200626_SK5	SK-0m Rep5	5.40E+05	1.00E+05	1.20E+04	2.50E+04	2.20E+05	2.455	0.455	0.055	0.114	3.077	35.60	5.02	7092.65
200626_SK6	SK-0m Rep6	5.70E+05	9.10E+04	1.10E+04	2.30E+04	2.20E+05	2.591	0.414	0.050	0.105	3.159	36.53	4.57	7989.69
200826_SK0-1	SK-0m Rep7	4.30E+05	6.50E+04	1.40E+04	2.10E+04	1.50E+05	2.867	0.433	0.093	0.140	3.533	40.78	3.96	10284.96
200826_SK0-2	SK-0m Rep8	4.90E+05	7.60E+04	1.60E+04	2.30E+04	1.40E+05	3.500	0.543	0.114	0.164	4.321	49.72	3.99	12460.78
200826_SK0-3	SK-0m Rep9	5.80E+05	8.80E+04	2.00E+04	2.60E+04	1.40E+05	4.143	0.629	0.143	0.186	5.100	58.56	5.07	11539.06
1200826_SK1-1	SK-1m Rep1	3.70E+05	5.60E+04	1.20E+04	1.90E+04	1.50E+05	2.467	0.373	0.080	0.127	3.047	35.25	3.17	11109.17
1200826_SK1-2	SK-1m Rep2	4.00E+05	6.20E+04	1.40E+04	2.00E+04	1.30E+05	3.077	0.477	0.108	0.154	3.815	43.98	3.64	12086.92
1200826_SK1-3	SK-1m Rep3	6.80E+05	1.00E+05	2.00E+04	2.60E+04	1.10E+05	6.182	0.909	0.182	0.236	7.509	85.90	5.31	16165.40
1200826_SK3-1	SK-3m Rep1	1.30E+05	1.60E+04	4.10E+03	9.70E+03	1.90E+05	0.684	0.084	0.022	0.051	0.841	10.22	1.62	6323.82
1200826_SK3-2	SK-3m Rep2	3.20E+05	4.50E+04	9.80E+03	1.80E+04	1.60E+05	2.000	0.281	0.061	0.113	2.455	28.54	3.56	8006.53
1200826_SK3-3	SK-3m Rep3	2.70E+05	3.60E+04	8.20E+03	1.60E+04	1.70E+05	1.588	0.212	0.048	0.094	1.942	22.72	3.24	7021.04

SI-10 Description of Approach I

Our first approach was to separate between SBR and SBS using multiple markers (SI-2, Table S2) with the maximum difference in intensity between them, e.g. two markers where SBR had the largest intensity and two markers where SBS had the largest intensity. Different pyrolysis temperatures were tested (350°C, 400°C, 450°C, 500°C, 550°C, 700°C, Figures S9-S17), however, none of the temperatures revealed any distinct pyrolysis products that could be used to distinguish between SBR and SBS. Therefore, the following separation attempts were performed with 700°C, as used in the study by Fabbri[2]. Using the relationship between the markers found in the standard solutions of SBR and SBS would reflect the ratio of each of the compounds in a sample. This approach was used to create a Partial Least Square (PLS) model (Figures S18-19). The model showed a clear separation between SBR and SBS in a mixture sample (Figure S20). When testing this approach on real environmental samples, however, the model failed to successfully predict tires and displayed the tire samples far outside the model score domain (Figure S21). Further investigations of the samples and the ratios of markers showed that real tires are far more complex and likely contain different types of SBR, with different ratios of styrene and butadiene (Table S1) as well as different isomers of butadiene, as discussed in Rauert et al.[3]. The different isomers of the butadiene monomer have been shown to contribute to different masses of the marker compound 4-vinylcyclohexene (4-VCH)[4]. The same impact may be expected in other marker compounds related to the butadiene isomers. If the composition of

these isomers in tires and the SBR1500 standard differ, the concentrations found using the SBR1500 to create the calibration curves will result in variable sample concentrations. As the recipes for specific tires are kept as trade secrets, a larger investigation of both reference tires and different SBR standards might be useful[5, 6].

Multivariate modeling

We tested the feasibility of using multivariate statistical approaches to distinguish the contribution of SBR, SBS, and their mixtures in complex environmental samples. To assess the applicability of the approach we generated a training set that was used for the model development and validation, while we employed the real samples for the model testing. Additionally, we generated the calibration curves for the quantification of the total SBR, BR, and SBS.

The training set for the multivariate method was generated by adding the standards directly into pyrolysis cups and allowing solvents to evaporate at room temperature. The training set consisted of individual polymers having masses of 0.1μg, 1μg, 5μg,10μg, 25μg, 75 μg, and 100 μg analyzed in triplicate – and mixtures of SBR and SBS in seven different ratios with a total mass of 50 μg (SBR:SBS ratios: 90:10, 80:20, 70:30, 50:50, 30:70, 20:80, 10:90), also analyzed in triplicates.

Statistical analysis

All the chromatograms were converted to CDF format employing the MassHunter GC/MS Translator[7] software package implemented via Agilent MassHunter. Ten replicate injections of SBR and SBS were used for the selection of the most relevant fragments. The potentially relevant fragments were selected by the manual

inspection of the total ion chromatograms (TIC) of those injections, employing MZmine 2[8]. The spectra of the TIC peaks/markers that distinguished the SBR samples from SBS samples were extracted as CSV files.

The Principal Component Analysis (PCA) was used for the selection of the most relevant fragments in distinguishing SBR and SBS standards from each other. For each potential marker/TIC-peak, the spectra of three scans with the highest peak intensity were extracted and aligned with a unit mass resolution to generate a matrix used for the data analysis. In order to remove the noise in the aligned spectra, the m/z values that were not present in all three scans and the three replicates were removed. The noise removed matrix was used in the next step for PCA. The PCA was performed on the mean-centered data for identification of the m/z values that were describing the variance in the data. Singular value decomposition[9] was used for the PCA, given its robustness in explaining the variance in the data. The PCA model with minimum number of components and explained variance of larger than 60% was selected as the final model. The fragments that had a contribution larger than 15% in the loading space were considered the most relevant fragments and were used for the multivariate calibration model.

For the distinction of SBR, SBS, and their mixtures from each other, we generated a multivariate classification model between the previously selected fragments (via PCA) and their identity (i.e. label). This model was generated employing Partial Least Square discrimination analysis (PLS-DA)[10]. The PLS-DA model was initialized with total possible components (i.e. the number of fragments - 2 = 5). The components that explained less than 1% of variance in the data were removed from

the initialized model. In the next stage of the model validation the remaining components were removed one at the time from the one with the lowest level of variance explained until the resulting model was different from the initialize model in a statistically significant way. Finally, the model with the least number of components (in this case 3) went through 5 folds of cross-validation to assess the impact of the random events on the model performance. The statistical analysis and modelling were performed using Matlab 2015R[11].

Results

The total ion chromatograms (TIC) of SBR, SBS standards, and blanks were manually inspected to identify the markers, which were present in all the replicates and showed a statistically significant difference between SBR and SBS with a $p < 0.05$ (Figure S9-17). The PCA showed a clear separation of SBR and SBS replicates in the first PC (Figure S11), explaining 96% of variance in the data, while the PC2 was mainly associated to the observed variance amongst replicates (2%). Based on the loading values for each m/z value, seven extracted ion chromatogram (XIC) peaks were selected, given their contribution to explaining the variance in the data.

The selected fragments were then used for generation of PLS-DA model (Figure S18). The data generated for the individual solutions and the mixtures were combined, resulting in 72 total measurements and 7 variables (i.e. fragments) in x-block and three categories in the y-block. The markers that appeared to be the most significant ones in distinguishing the three categories (SBR, SBS and mix) from each other were 1,3-butadiene (*m/z* 54 Da), benzene (*m/z* 78 Da), α-methylstyrene (*m/z*

118 Da) and m-ethylstyrene (*m/z* 117 Da). Details on the marker compounds is found in Table S16.

Table S16. Marker compounds investigated in Approach I. Italics and bold values used for calibration and quantification

Polymer	Pyrolysis product	Indicator ions (m/z)	Retention Time (mins)	Highest peak intensity
Styrene butadiene rubber (SBR)/Styrene butadiene styrene (SBS)	1,3 Polybutadiene	39, **53,** 54	1.8	SBR
	4-Vinylcyclohexene	54, 79, 108	5.7	SBR
	Benzene	51, 67, **78**	2.7	SBR
	α-methylstyrene	78, 91, **118**	9.5	SBS
	M-ethylstyrene	77, 91, **117**	11.7	SBS
	Butadiene trimer A	65, **91**, 146	14.6	SBR
	Styrene monomer	104	7.2	SBS
Internal standard	Poly(1,4-butadiene-$_d$6)	***60***, 120, 42, 86	5.3	

Chromatograms of SBR and SBS by different temperatures

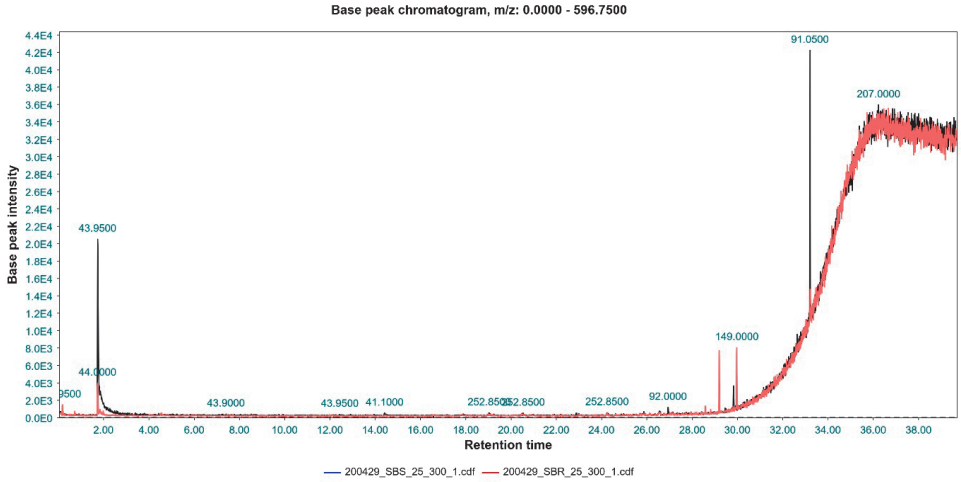

Figure S9. Chromatogram of SBR and SBS, 25 µg, 300°C

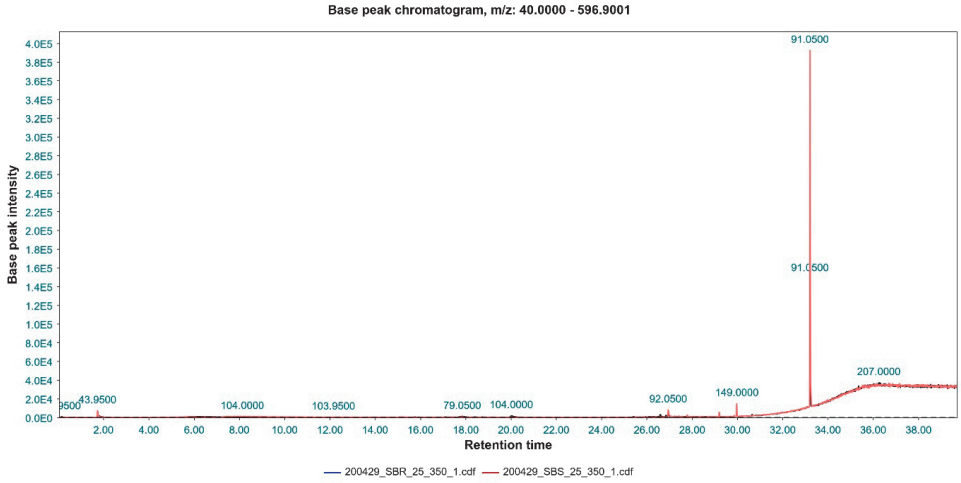

Figure S10. Chromatogram of SBR and SBS, 25 µg, 350°C

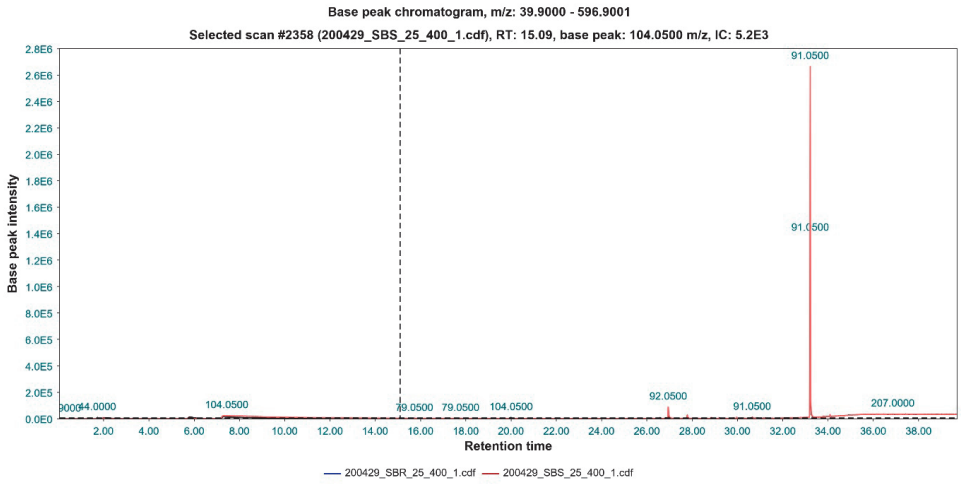

Figure S11. Chromatogram of SBR and SBS, 25 µg, 400°C

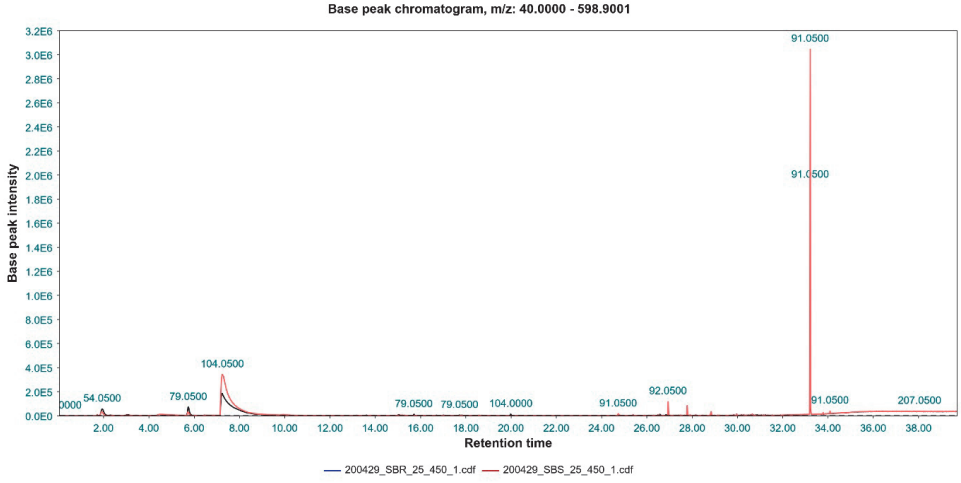

Figure S12. Chromatogram of SBR and SBS, 25 µg, 450°C

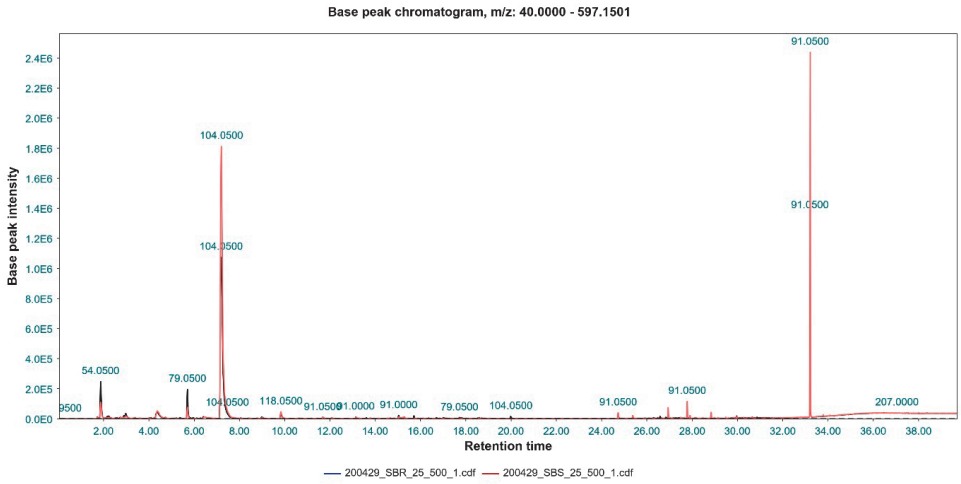

Figure S13. Chromatogram of SBR and SBS, 25 µg, 500°C

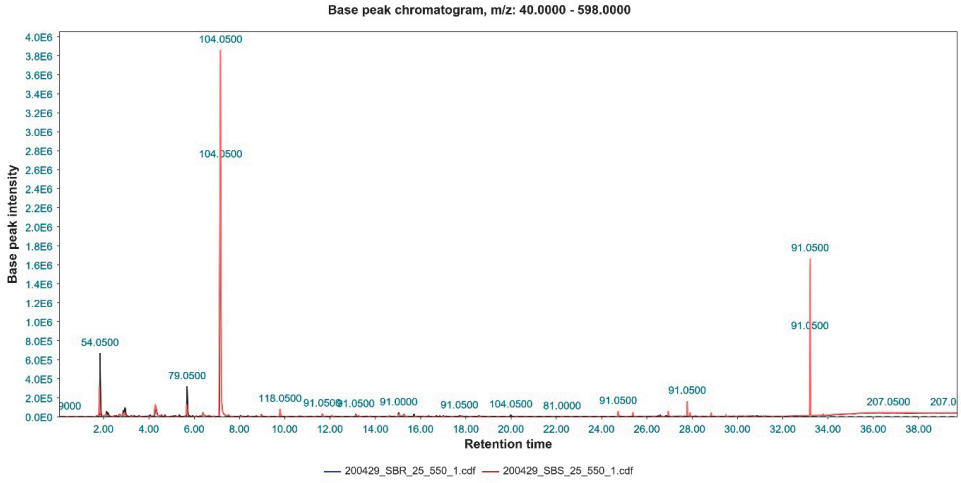

Figure S14. Chromatogram of SBR and SBS, 25 µg, 550°C

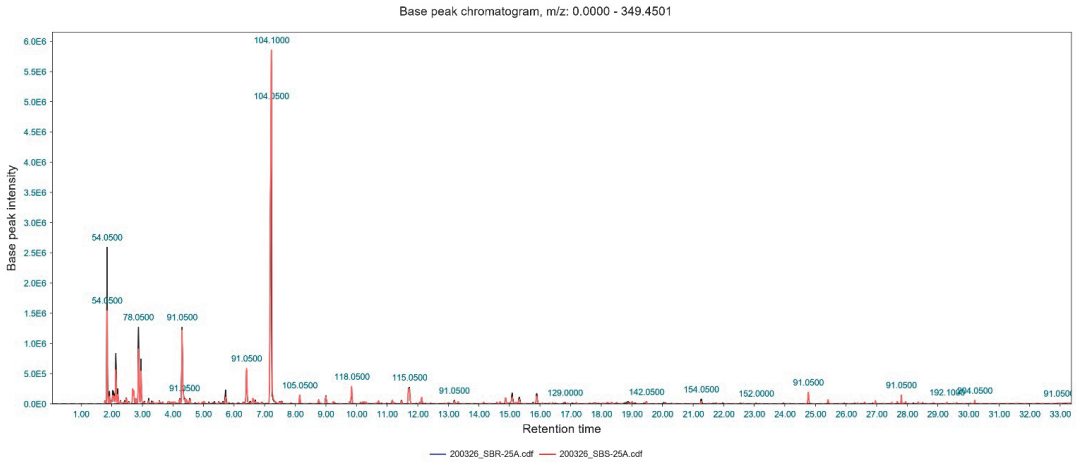

Figure S15. Chromatogram of SBR and SBS, 25 µg, 700°C

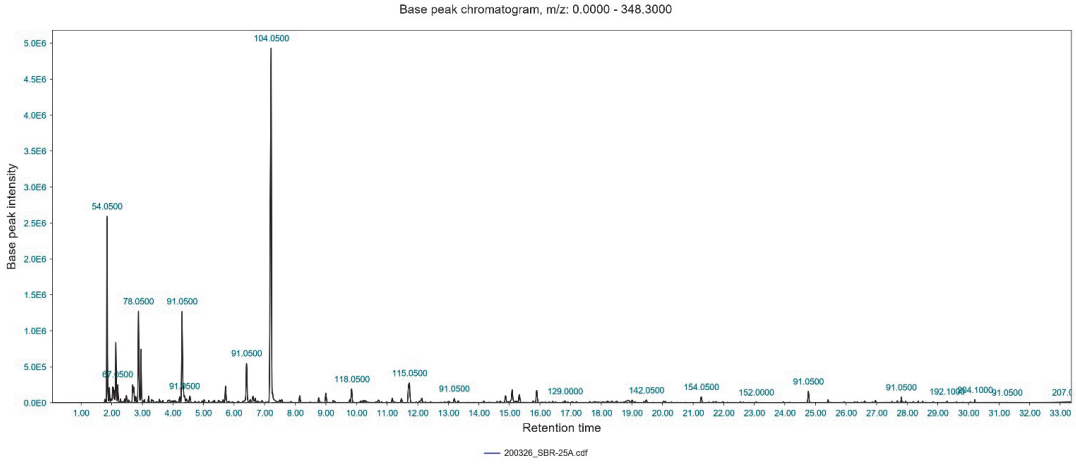

Figure S16. Chromatogram of SBR, 25 µg, 700°C

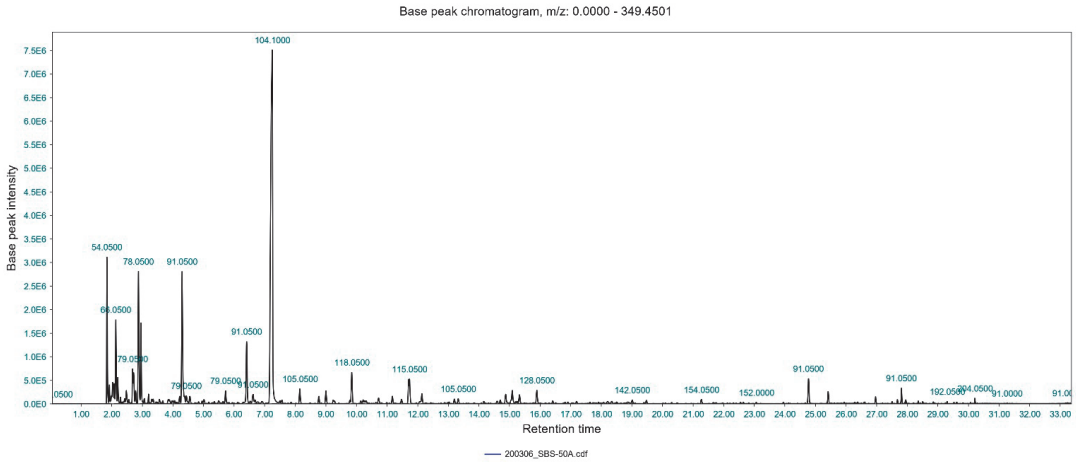

Figure S17. Chromatogram of SBS, 25 µg, 700°C

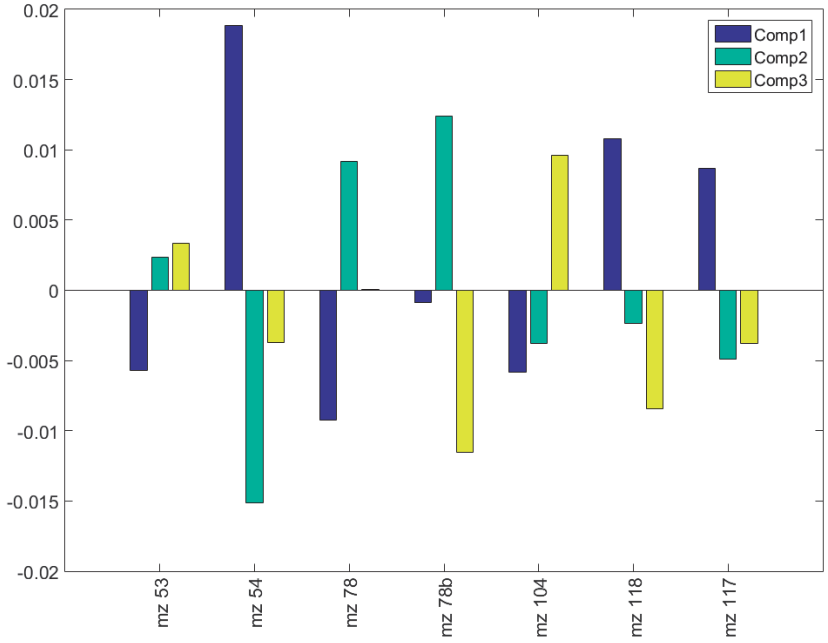

Figure S18. The coefficients of the three component PLS-DA model.

When testing the validated model with real environmental samples, the generated scores by the model for tires appeared outside of the model score domain (Figure S21). The environmental samples used where snow samples from Storo (ST, February 2019) and tunnel wash water (T04, November 2018). The snow sample was taken 0m from the road (ST) in Oslo, Norway (50 950 AADT, 59°56'37.6"N 10°46'47.2"E), using a snow corer. The snow was further weighed, melted and sieved through 1 mm sieves to remove large items. The sample was then stirred by hand-shaking the beaker for 20 seconds before 16 mL subsamples were transferred to a glass jar, that had been pretreated in the muffle furnace (Nabertherm, Germany) at 550˚C in order to remove any contamination. The subsample was frozen (-20C, 24H) and freeze dried (3-4 days, Leybold Heraeus Lyovac GT2). Dried snow material was then put directly into the pyrolysis cup by weight. The tunnel wash water was collected directly in the pump basin where wash water passes before being directed into a sedimentation pond. The tunnel wash water (approximately 50 mL) was filtered onto glass fiber filters (Whatman GF-F, 25mm).

Further investigation of the signal generated by the real tires versus the mixtures of SBR and SBS, and the ratios of the fragments indicated the inadequacy of the SBR and SBS standards for the analysis of tires. The observed differences between the standards and real tires were attributed to the fact that during the production of tires, the ratios of styrene and butadiene varies depending on the production process (Table S1) while these ratios are constant in the standards. This implies that these standards are not representative of the tire composition and therefore cannot

be used for the quantification of tires in environmental samples, when dealing with mixtures of SBR and SBS.

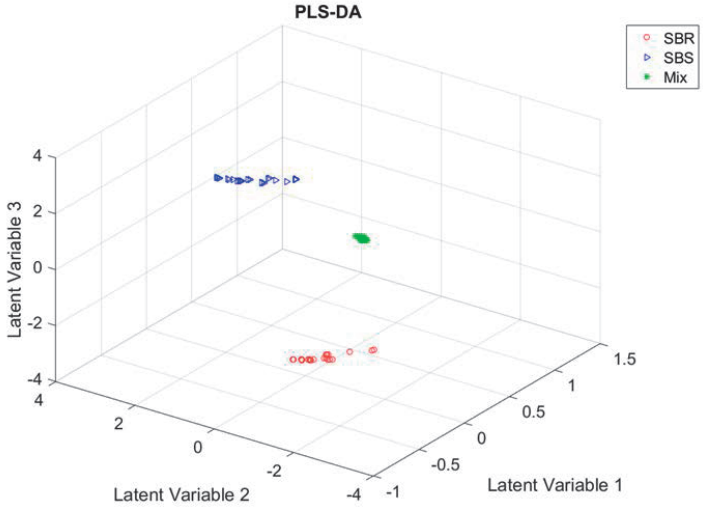

Figure S19. The 3D score plot of the PLS-DA model for the y-block for the training set. Each cluster represent a different set of samples.

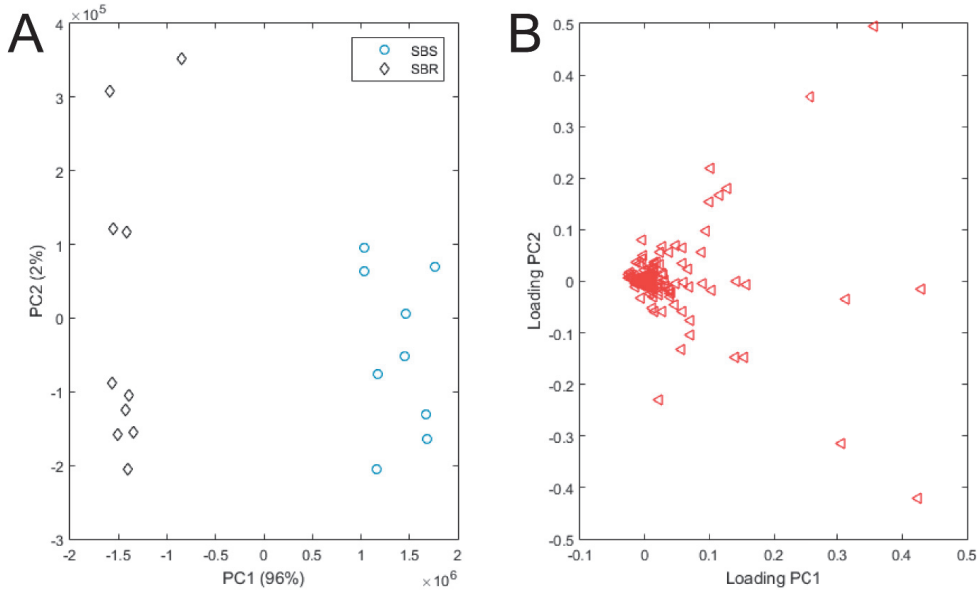

Figure S20. Depicts a) the PCA score plots for the first two PCs and b) loadings associated with those PCs.

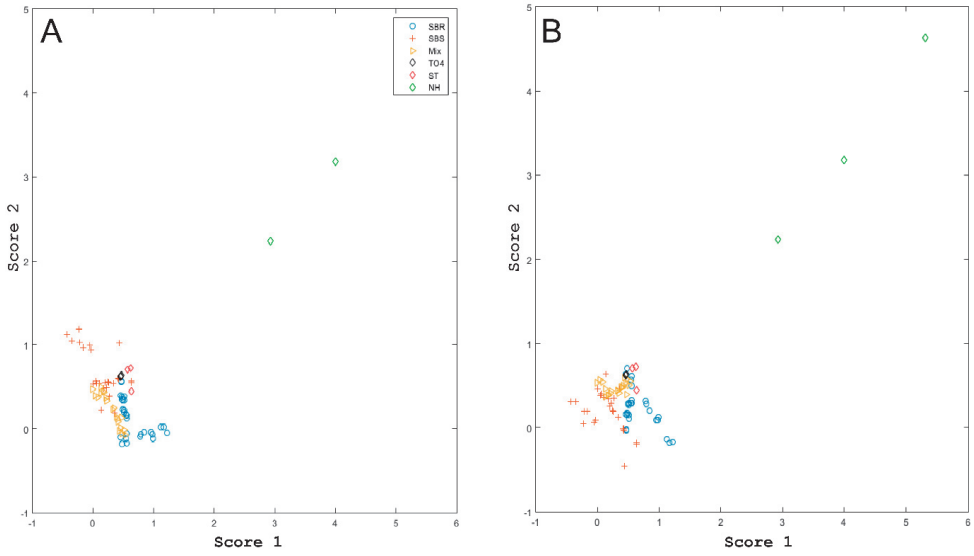

Figure S21. Separation of samples using PLS-DA model. A) between the first two latent variables and B) score values for the first and third latent variables (I.e. component).

References

1. Snilsberg, B., Road wear from studded and non-studded tires. In Rødland, E., Ed. 2020.
2. Fabbri, D., Use of pyrolysis-gas chromatography/mass spectrometry to study environmental pollution caused by synthetic polymers: a case study: the Ravenna Lagoon. *Journal of Analytical and Applied Pyrolysis* **2001,** *58*, 361-370.
3. Rauert, C.; Rødland, E. S.; Okoffo, E. D.; Reid, M. J.; Meland, S.; Thomas, K. V., Challenges with Quantifying Tire Road Wear Particles: Recognizing the Need for Further Refinement of the ISO Technical Specification. *Environ Sci Tech Let* **2021,** *8*, (3), 231-236.
4. Choi, S.-S., Characteristics of the pyrolysis patterns of styrene-butadiene rubbers with differing microstructures. *Journal of Analytical and Applied Pyrolysis* **2002,** *62*, (2), 319-330.
5. Choi, S.-S.; Kwon, H.-M., Analytical method for determination of butadiene and styrene contents of styrene-butadiene rubber vulcanizates without pretreatment using pyrolysis-gas chromatography/mass spectrometry. *Polymer Testing* **2014,** *38*, 87-90.
6. Choi, S.-S.; Kwon, H.-M., Considering factors on determination of microstructures of SBR vulcanizates using pyrolytic analysis. *Polymer Testing* **2020,** *89*.
7. Agilent *MassHunter GC/MS Translator*, 2019.
8. Pluskal, T.; Castillo, S.; Villar-Briones, A.; Orešič, M. *MZmine 2: Modular framework for processing, visualizing, and analyzing mass spectrometry-based molecular profile data, BMC Bioinformatics*, PMID: 20650010; 2010.
9. Samanipour, S.; Kaserzon, S.; Vijayasarathy, S.; Jiang, H.; Choi, P.; Reid, M. J.; Mueller, J. F.; Thomas, K. V., Machine learning combined with non-targeted LC-HRMS analysis for a risk warning system of chemical hazards in drinking water: A proof of concept. *Talanta* **2019,** *195*, 426-432.
10. de Jong, S., SIMPLS: An alternative approach to partial least squares regression. *Chemometrics and Intelligent Laboratory Systems* **1993,** *18*, (3), 251-263.
11. MATLAB The MathWorks Inc.: Natick, Massachusetts:, 2015.

Paper III

Science of the Total Environment 824 (2022) 153785

Contents lists available at ScienceDirect

Science of the Total Environment

journal homepage: www.elsevier.com/locate/scitotenv

Occurrence of tire and road wear particles in urban and peri-urban snowbanks, and their potential environmental implications

Elisabeth S. Rødland [a,b,*], Ole Christian Lind [b], Malcolm J. Reid [a], Lene S. Heier [c], Elvis D. Okoffo [d], Cassandra Rauert [d], Kevin V. Thomas [d], Sondre Meland [a,b]

[a] Norwegian Institute for Water Research, Økernveien 94, NO-0579 Oslo, Norway
[b] Norwegian University of Life Sciences, Faculty of Environmental Sciences and Natural Resource Management, P.O. Box 5003, NO-1432 Ås, Norway
[c] Norwegian Public Roads Administration, Construction, Postboks 1010, N-2605 Lillehammer, Norway
[d] Queensland Alliance for Environmental Health Sciences (QAEHS), The University of Queensland, 20 Cornwall Street, Woolloongabba, 4102, QLD, Australia

HIGHLIGHTS

- TRWP is estimated to be one of the largest sources of MP to the environment.
- Mass data of TRWP are limited and not before presented for roadside snow.
- Roadside snow from various road types were analysed with Pyr-GC/MS.
- Concentrations of TRWP showed large variations between and within road types.
- Speed and AADT explained the main variation observed.

GRAPHICAL ABSTRACT

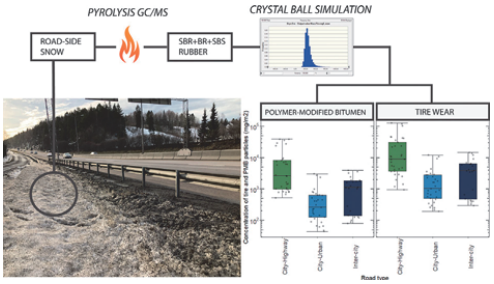

ARTICLE INFO

Article history:
Received 10 December 2021
Received in revised form 17 January 2022
Accepted 6 February 2022
Available online 16 February 2022

Editor: Pavlos Kassomenos

Keywords:
Road pollution
Snow
Tire particles
Bitumen particles
Microplastic
Pyrolysis GC/MS

ABSTRACT

According to estimates put forward in multiple studies, tire and road wear particles are one of the largest sources to microplastic contamination in the environment. There are large uncertainties associated with local emissions and transport of tire and road wear particles into environmental compartments, highlighting an urgent need to provide more data on inventories and fluxes of these particles. To our knowledge, the present paper is the first published data on mass concentrations and snow mass load of tire and polymer-modified road wear particles in snow. Roadside snow and meltwater from three different types of roads (peri-urban, urban highway and urban) were analysed by Pyrolysis Gas Chromatography Mass Spectrometry. Tire particle mass concentrations in snow (76.0–14,500 mg/L meltwater), and snow mass loads (222–109,000 mg/m^2) varied widely. The concentration ranges of polymer-modified particles were 14.8–9550 mg/L and 50.0–28,800 mg/m^2 in snow and meltwater, respectively. Comparing the levels of tire and PMB particles to the total mass of particles, showed that tire and PMB-particles combined only contribute to 5.7% (meltwater) and 5.2% (mass load) of the total mass concentration of particles. The large variation between sites in the study was investigated using redundancy analysis of the possible explanatory variables. Contradictory to previous road studies, speed limit was found to be one of the most important variables explaining the variation in mass concentrations, and not Annual Average Daily Traffic. All identified variables explained 69% and 66%, for meltwater and mass load concentrations, respectively. The results show that roadside snow contain total suspended solids in concentrations far exceeding release limits of tunnel and road runoff, as well as tire particles in concentrations comparable to levels previously reported to cause toxicity effects in organisms. These findings strongly indicate that roadside snow should be treated before release into the environment.

* Corresponding author.
E-mail address: elisabeth.rodland@niva.no (E.S. Rødland).

http://dx.doi.org/10.1016/j.scitotenv.2022.153785

1. Introduction

Estimates suggest that tire and road wear particles (TRWP) emissions constitute one of the largest contributors to microplastics pollution (Boucher et al., 2020; Knight et al., 2020). The estimated release of synthetic rubber (Styrene Butadiene Rubber, SBR, and Butadiene Rubber, BR) from tire wear particles (TWP) varies in different countries. In Norway, the estimated release of microplastics from terrestrial sources is 19,000 t/year, where tire wear and road dust is estimated to contribute with 40% of the total estimated release (Sundt et al., 2021). In some countries, such as Australia, China, Denmark, Norway, Russia, Sweden and the United Kingdom (EAPA, 2018), it is common to add polymers to the bitumen of road asphalt in order to increase resistance to cracking and deformation (rutting) of the road surface (R.G. et al., 2012). This type of bitumen is referred to as polymer-modified bitumen (PMB). Various polymers are used for this purpose, such as styrene butadiene styrene (SBS), styrene ethylene butadiene styrene (SEBS), low-density polyethylene (LDPE), ethylene vinyl acetate (EVA), polypropylene (PP) and styrene isoprene styrene (SIS) (Chen et al., 2002; Giavarini et al., 1996; M. et al., 2003; Panda and Mazumdar, 1999; Polacco et al., 2005; Polacco et al., 2006; Sengoz et al., 2009). In Norway, only SBS rubber is used for the PMB asphalt (NVF, 2013; Rødland et al., 2022). The abrasion of the road surface and the release of road particles are estimated to be heavily impacted by the ratio of personal vehicles (PV) versus heavy vehicles (HV), as well as the use of studded winter tires (Rødland et al., 2022). The release of road abrasion particles from studded PV is estimated to be between 5 and 10 g per vehicle kilometer driven (g/vkm) for stone mastic asphalt (SMA) and between 15 and 20 g/vkm for asphalt concrete (AC) (SI-4 Table S3) (Bakløkk et al., 1997; Horvli, 1996; Snilsberg et al., 2016). The estimated road abrasion for studded HV tires is roughly 5 times the value for PV, and the abrasion from non-studded winter tires and summer tires are expected to be 40 times lower compared to studded tires (Snilsberg, 2008). The use of studded tires in Norway is extensive, covering over 80% of all vehicles in the northern part of Norway during winter. However, in the eastern part of Norway, where winters are considered milder and traffic density is high, the overall percentage in 2017 was approximately 20% (Reitan et al., 2017). The percentage of studded tires used in Oslo in 2019 was 8.6% for PV and 1.6% for HV (Rosland, 2020). Emitted TWP and PMB particles can be mixed with other road particles (such as mineral and organic matter). These are referred to as TRWP and are released to different environmental compartments through various pathways, such as road runoff, tunnel wash water, dry and wet atmospheric deposition and snow accumulation. Despite great efforts to improve analytical methods in recent years, especially developing new markers and methods for Pyrolysis GC/MS, analytical challenges still contribute to uncertainties associated with TRWP data on inventory and fluxes in the environment (Miller et al., 2021; Rauert et al., 2021; Rødland et al., 2022; Wagner et al., 2021). There are currently several different analytical methods for quantifying TWP in the environment (Chae et al., 2021; Goßmann et al., 2021; ISO, 2017a; ISO, 2017b; Klöckner et al., 2021; Parker-Jurd et al., 2021), however, only one method includes the presence of PMB-particles together with tire wear particles (Rødland et al., 2022).

The TRWP contain a large variety of chemicals, and a recent study identified 214 different organic chemicals in tires, in which 145 were classified as leachable (Müller et al., 2022). About 60% of the leachables were classified as mobile compounds, indicating a large potential for transport in the environment (Müller et al., 2022). Examples of tire-derived chemicals that have been found to be harmful to organisms are benzothiazoles, N-1,3-dimethylbutyl-N 0-phenyl-*p*-phenylenediamine (6-PPD), 1,3-diphenylguanidine (DPG) and different polycyclic aromatic hydrocarbons (PAHs) (Halsband et al., 2020; Seiwert et al., 2020; Tian et al., 2021; Unice et al., 2015).

The number of studies of road contamination in snow are limited, but those that are published have reported high levels of heavy metals, polycyclic aromatic hydrocarbons (PAHs), salt and overall particulate material in roadside snow (Moghadas et al., 2015; Vijayan et al., 2021; Viklander, 1999). Using snow as the target matrix is useful both for showing the concentration levels accumulating over a short-time window, and as a potential extreme pulsed contaminant release event when the snow melts during spring. Previous studies have looked at the number of road-related rubber particles in different snow samples and reported between 190 and 193,000 particles/L in melted snow (Bergmann et al., 2019; Vijayan et al., 2019), however no studies have so far, to the best of our knowledge, measured the mass concentrations of TRWP in snow samples. The overall objective of the present study was to provide new knowledge on the concentration levels of TRWP rubbers along roads, and the potential impact on the environment if measures are not taken. The objective was further divided into three goals. The first was to assess the concentrations of tire and PMB particles in roadside snow and compare the levels to other road-related releases such as road runoff. The second goal was to utilize the accumulation of TRWP rubber in snowbanks to explore the impact of traffic variables such as Average Annual Daily Traffic (AADT) and speed limit on the accumulation. The third goal was to assess the potential environmental impact of tire and PMB particles from roadside snow.

2. Materials and method

2.1. Sample collection and processing

Snow samples were collected from several sites in three areas around the City of Oslo, Norway, on 26th and 27th of February 2019. There are no weather stations present for all locations, so the Hovin weather station covering the city of Oslo is used for weather data (Yr, 2019). The weather in the end of January 2019 was warm, up to 14 °C on January 30th and the whole month had low precipitation (2.8 mm). In February, the weather fluctuated more, with a cold period (−9.9 °C up to 4.8 °C) with higher precipitation (6.9 mm) from 1st to 12th of February. Then there was a warmer period (−1.4 °C to 10.2 °C) from the 13th of February until the first sampling day on the 26th of February with 4.1 mm of precipitation. Three sampling sites were along a peri-urban highway (Inter-city Highway) outside of Oslo; Holstad (HO), Vinterbro (VI) and Skullerud (SK). An additional four sites were along the City Highway (Bryn (BR), Storo (ST), Ullevål stadion (US) and Lysaker (LY)), and the final four sites were in the area in the inner city (City Urban; Tøyen (TØ), Carl Berner (CB), Ila (IL) and Frogner (FR)) (Fig. 1, SI-1 Table S1). The three road types are associated with different driving styles. The Inter-city Highway has a higher speed limit (80 km/h) and is associated with long-distance driving. The City Highway has a speed limit of 70 km/h and includes areas with more braking and accelerating (crossings, roundabouts) compared to the Inter-city Highway. The urban city roads are associated with an urban driving style, including lower speed limits (40–50 km/h) and frequent braking and accelerating (traffic lights, crossings, roundabouts, zebra crossings). All sites within each area were chosen to provide a spatial dispersion. They also represent different AADT level within the area, based on data collected from (Vegkart, 2019) (SI-1 Table S1). A city-reference snow sample was taken from a lawn area in the centre of the Tøyen Botanical garden, approximately 60 m from the closest urban road and on a hilltop. The winter maintenance for all sites are similar. In general, snow from all three site groups are pushed to the sides by snow ploughs where there is available space. In the City Urban sites where space for snow storage is limited, the snow is transported to a melting facility in the harbour when needed (BYM, 2021; NPRA, 2022). Road-deicing salts (mainly NaCl and $MgCl_2$) are also used on all the roads in this study when the temperatures fluctuate around 0 °C.

The samples were collected using a metal snow corer (inner diameter 4.2 cm) in snowbanks at 0 m (0–1 m), 1 m (1–2 m) and 3 (3–4 m) m from the road. At each site, 5 cores were taken within a 1 m square at random. Some sites had low snow depth, at which 10 cores were sampled to obtain a representative snow volume. All snow cores were measured for length. The 5–10 cores from each site were then mixed together in one bag per site (ziplock, polyethylene (PE) bag). The mixed samples were stored in a freezer (−20 °C) until processing and chemical analysis. The

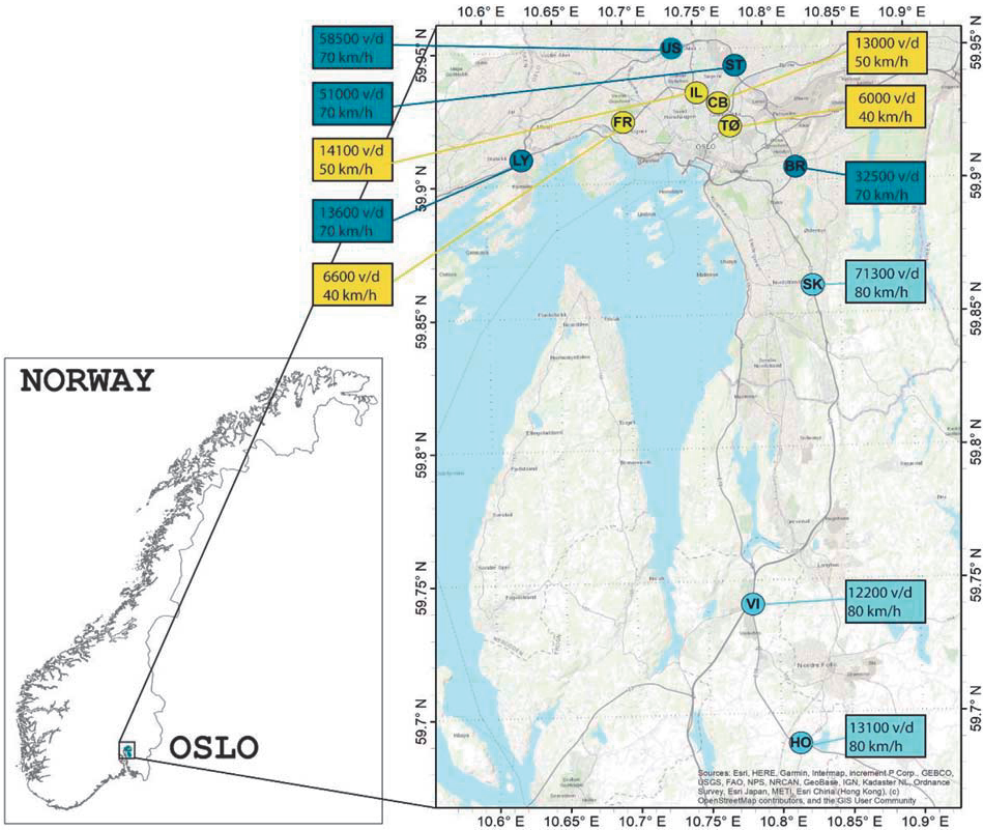

Fig. 1. Map of the sampling locations: Inter-city Highway: Holstad (HO), Vinterbro (VI), Skullerud (SK). City Highway: Bryn (BR), Storo (ST), Ullevål stadion (US), Lysaker (LY). City Urban: Frogner (FR), Ila (IL), Carl Berner (CB), Tøyen (TØ).

frozen snow samples were weighed and then melted in the zip-lock bag at room temperature. The volume of melt water was recorded and then transferred to pre-cleaned glass beakers using 1 mm sieves to remove large items. The samples were stirred by handshaking for 20 s before 16 mL sub-samples were transferred to glass jars. These jars had been pre-treated in the muffle furnace (Nabertherm, Germany) at 550 °C in order to remove any contamination from other polymer particles that could interfere with the analysis results. Contamination could include polyvinyl chloride (PVC), polyethylene terephthalate (PET), acrylonitrile-butadiene-styrene copolymer (ABS) and Polystyrene (PS) (Rødland et al., 2022). The sub-samples were frozen (−20C, 24H) and freeze dried (3–4 days, Leybold Heraeus Lyovac GT2). Dried snow material were weighed directly into the pyrolysis cups for analysis.

2.2. Pyrolysis GC–MS

Samples were analysed with a Multi-Shot Pyrolyzer (EGA/PY-3030D) equipped with an Auto-Shot Sampler (AS-1020E) (Frontier lab Ltd., Fukushima, Japan) coupled to gas chromatography mass spectrometer (GC/MS) (5977B MSD with 8860 GC, Agilent Technologies Inc., CA, USA). Samples were pyrolyzed with single-shot mode at 700 °C for 0.2 min (12 s). Injections were made using a 50:1 split and with a pyrolyzer interface temperature at 300 °C. The pyrolysis method followed Rødland et al. (2022), and uses the combined peak heights of four selected markers normalized against an internal standard (deuterated Polybutadiene, d6-PB). The selected markers consisted of *m/z* 78 Da for *benzene*, *m/z* 118 Da for *α-methylstyrene*, *m/z* 117 Da for *ethylstyrene* and *m/z* 91 Da for *butadiene trimer* (first trimer in the TIC) (SI-2 Table 2).

The calibration curve was created with three different ratios of SBR and SBS (20:80, 40:60 and 80:20). Total mass of SBR + SBS of 1 μg, 2 μg, 5 μg, 25 μg, 100 μg and 150 μg, were inserted into pyrolysis cups (n = 3) and spiked with 25 μg d6-PB as internal standard. The normalized sum peak of all marker compounds is plotted against the mass of SBR + SBS at each calibration level to form the calibration curve ($R = 0.99$, $p = 2.2 \times 10^{-16}$, Supplementary Information (SI) Fig. S1).

2.3. Meltwater concentrations vs mass load calculations

The rubber concentrations (SBR + BR + SBS) in samples were analysed as meltwater concentrations in mg/L. Tire and PMB results for acute release through meltwater were reported as mg/L concentrations. In addition to meltwater concentrations, values were converted to mass load (ML) concentrations, in mg/m^2. The ML conversion is a useful tool when comparing measured contaminant concentrations in snow from various sites, where the snow has been frozen and thawed at different times. This has been previously applied in studies of road-related contaminants in snow (Boom and Marsalek, 1988; Moghadas et al., 2015; Reinosdotter and Viklander, 2005; Viklander, 1997).

The conversion from mg/L to ML can be done using the following equation according to Moghadas et al. (2015):

$$ML = K * Cs * SWE \quad (1)$$

where *ML* is the mass load of the given pollutant per square meter of a snow deposit (mg/m^2);

K is a unit conversion coefficient (0.1 to convert from cm snow cores to m);

Cs is the pollutant concentration C in the melted snow sample s (mg/L);

SWE is the snow water equivalent of the sample (cm), calculated from the measured snow core height (cm) multiplied with the snow density (g/cm^3) for each snow sample.

A calculation example for ML is given is SI-5 and all snow core sample data can be found in SI-10.

2.4. Calculation of tire and PMB particles

The concentration of SBR + BR + SBS per cup (μg/cup) was calculated with the added weight of dried snow material (mg) to give the concentration of SBR + BR + SBS μg/mg dried snow material. The amount of dried snow from each sample was related to the volume of melted snow (mL) for each sample, and then upscaled to give the concentration of SBR + BR + SBS mg/L per sample. The concentration of SBR + BR + SBS in meltwater (mg/L) was used to calculate the concentration of tire particles and PMB particles in the sample. The calculation is described in detail in Rødland et al. (2022). This method utilizes emission factors (EFs) for tire wear (Klein et al., 2017) and for road wear (Bakløkk et al., 1997; Horvli, 1996; Snilsberg, 2008; Snilsberg et al., 2016) to find the expected ratio of tire to PMB in each sample (SI-4 Tables S3 and S4). The EFs for road wear is adjusted to include the ratio of studded tires used for both personal and heavy vehicles at each site. Then the SBR + BR + SBS values are used to calculate the concentration of tires (M_T) and PMB (M_{PMB}) separately by applying the following Eqs. (2)–(5). A calculation example can be found in the Supplementary (SI-5)

$$M_T = \frac{M_S - (M_S * R_{SBS}) * Sc}{(S_{PV} * R_{PV}) + (S_{HV} * R_{HV})} \quad (2)$$

$$M_{PMB} = \frac{(M_S * R_{SBS})}{C_{PMB}} \quad (3)$$

where

M_T is the mass of tire in a sample (mg);

M_{PMB} is the mass of PMB in a sample (μg);

M_S is the mass of SBR + BR + SBS in a sample (μg);

R_{SBS} is the estimated ratio of SBS from the total SBR + BR + SBS concentration for each location;

Sc is the conversion factor for styrene content in standards vs tires;

S_{PV} is the mass of SBR + BR in personal vehicle tires (μg/mg);

R_{PV} is the ratio of personal vehicles at the sampling location;

$S_{HV}$is the mass of SBR + BR in heavy vehicle tires (μg/mg);

R_{HV} is the ratio of heavy vehicles at the sampling location;

C_{PMB} is the conversion factor for SBS to PMB, based on the percentage SBS in PMB (0.05).

The mass of SBR + BR in personal vehicles and heavy vehicles were obtained by analysis of reference tires representing the Norwegian tire use as reported in Rødland et al. (2022). The equations were performed using the Excel Add-in package Crystal Ball, where 100,000 Monte Carlo simulations were applied. This gives the predicted statistics of the tire and PMB concentrations from each sample. For this study, the mean, median, standard deviation, minimum, maximum, and the 10th, 25th, 75th and 90th percentiles for both tire and PMB concentrations were reported. The results using meltwater were converted to ML (mg/m^2) after simulation and both results are presented to facilitate comparison with previous work.

2.5. Statistical analysis

The statistical analysis of the data was conducted in RStudio 1.3.109 (Team, 2020), R version 4.0.4 (2021-02-15), specifically using the ggplot2-package (Lai et al., 2016) (gplot2_3.3.3), the car-package (Fox and Weisberg, 2019) and the dplyr-package (Wickham et al., 2018) for creating boxplot graphs, linear regression and for performing Analysis of Variance (ANOVA). The uncertainty analysis of tire and PMB calculation was performed by using Excel Monte-Carlo Add-In Crystal Ball, as described in Section 2.2.

2.5.1. Univariate statistics

All ANOVAs were performed on log-transformed data. The assumption of normal distribution of residuals was tested using Andersen-Darling normality test. If the assumption of normality was not met, ANOVA was still applied when number of samples (n) in each group were >15. The assumption of equal variance was tested using Levene's Test of Homogeneity of Variance. Whenever this assumption was not met, Welch's one-way ANOVA was used. The statistically significant level was set to $p = 0.05$.

Linear regression was used to assess the relationship between total suspended solids (TSS) and total concentration of rubbers for both meltwater and mass loads concentrations. The residuals of the regression model were checked for normality using Andersen Darling Normality test. If assumption of normality was not met, the linearity was tested using assumption free Redundancy analysis (RDA), with rubber concentration as response variable and TSS concentration as the explanatory variable.

2.5.2. Multivariate statistics

To assess the relationship between the response variables (SBR + BR + SBS concentrations in meltwater and mass load) and explanatory variables (traffic variables, road type and distance from the road), multivariate statistical analyses were conducted by using Canoco 5.12 (Ter Braak and Smilauer, 2018). Redundancy analysis (RDA) was used to explore the observed variation in the concentration of SBR + BR + SBS using the explanatory variables. Different variants of RDA were performed. Both the meltwater (mg/L) and massload (mg/m^2) data was log-transformed by the default transformation setting in Canoco. First, a constrained RDA with all variables were performed to explore the total variation explained by all identified variables. Second, RDA with forward selection were tested, where the explanatory variables contributing the most to the variation can be selected until there are no more variation to explain. In the forward selection mode, both the simple effects (the effect of each independent variable) and the constrained effects (the effect of the variable considering the other variables) were tested. The significance level in the RDA is derived by Monte Carlo permutation tests (9999 permutations performed). For all tests, $p < 0.05$ is set as the level of significance.

3. Results

3.1. Concentrations of SBR + BR + SBS rubber in snow

The reference sample location was chosen as a site close to one of the sample locations in Urban city to be relevant and to show possible background concentration in snow further away from a road. The SBR + BR + SBS concentration found in the reference sample was 8.9 mg/L in meltwater concentration and 3.2 mg/m^2 in mass load concentration. As the location is approximately 60 m distance from the nearest busy road, it is not possible to calculate the tire and PMB contribution to the SBR + BR + SBS concentrations. The concentrations of total suspended solids (TSS) in the reference snow were 556 mg/L and 198 mg/m^2.

All samples were analysed in triplicates and the standard deviation (in percentage) ranged from 3 to 34%, with an average of 15% s.d. The concentrations varied largely between different sites, road types and distance from

the road (Fig. 2, SI-7 Table S8). The lowest concentration of SBR + BR + SBS was detected at Frogner 0 m, for both meltwater and mass load concentrations (32 ± 5.9 mg/L, 119 ± 22 mg/m^2). The highest concentration for meltwater was found at Lysaker 0 m (4438 ± 191 mg/L) and the highest for mass load at Storo 0 m (29,686 ± 2949 mg/m^2). The City Highway sites had the largest mean concentrations of SBR + BR + SBS rubber for both meltwater (1290 ± 1510 mg/L) and mass load (6224 ± 8565 mg/m2), the Inter-city Highway sites had the second-highest (284 ± 222 mg/L, 1173 ± 1112 mg/m^2) and the City Urban sites had the lowest mean concentrations (124 ± 153 mg/L, 574 ± 760 mg/m^2) (Fig. 2, SI Table S3).

The difference in concentrations between the three road types were significant (ANOVA) for both meltwater ($p < 0.0001$) and mass load ($p < 0.0001$). For the concentrations in meltwater, there was a significant difference between all pairs of road types (City Urban - City Highway $p < 0.0001$; Inter-city highway – City Highway $p < 0.0001$; Intercity Highway – City urban $p < 0.0001$). For the concentrations in mass loads, only the difference between City Urban and City Highway ($p < 0.0001$) and Inter-city Highway and City Highway ($p < 0.0001$) were significant. Within the City-Highway and the City-Urban sites, the mean concentrations both in meltwater and mass loads showed that the presence of SBR + BR + SBS rubbers are highest at 0 m distance from the road and decreases towards 3 m distance (Fig. 3, SI-7 Table S8,). However, this decreasing pattern was not found to be significant (ANOVA, $p > 0.05$) when using the distance as categorical variable. In the Inter-City samples, the sites at 1 m distance had a higher mean and median concentration of rubbers compared to the samples at 0 m and 3 m (SI Table S8, Fig. 3), and the difference between 3 m and 1 m was found to be significant for both mass load ($p = 0.0131$) and meltwater ($p < 0.0001$) concentrations. For concentrations in meltwater, also the difference between 3 m and 0 m was found to be significant ($p < 0.0001$). Overall, when combining all snow samples analysed, the difference between the samples collected at 0 m, 1 m and 3 m was statistically significant both for values in meltwater ($p = 0.00056$), and for mass load ($p = 0.00157$). However, the difference was only significant between the 3 m and 0 m (meltwater $p = 0.0012$; mass load $p = 0.0024$) and between 3 m and 1 m (meltwater $p = 0.0040$; mass load $p = 0.012$) (Fig. 2).

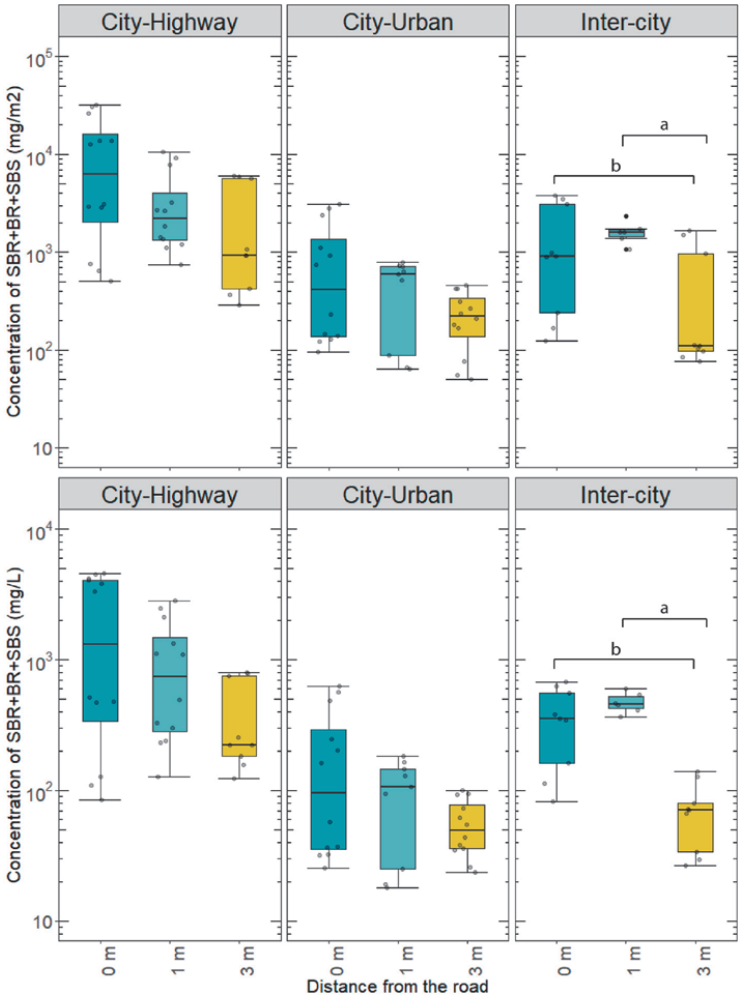

Fig. 2. Concentration of SBR + BR + SBS in meltwater (mg/L, below) and mass load (mg/m^2, above) at distances 0 m, 1 m and 3 m distance from the road The difference is significant ($p < 0.05$) between Inter City 1 m and 3 m (a) and between Inter City 0 m and 3 m (b).

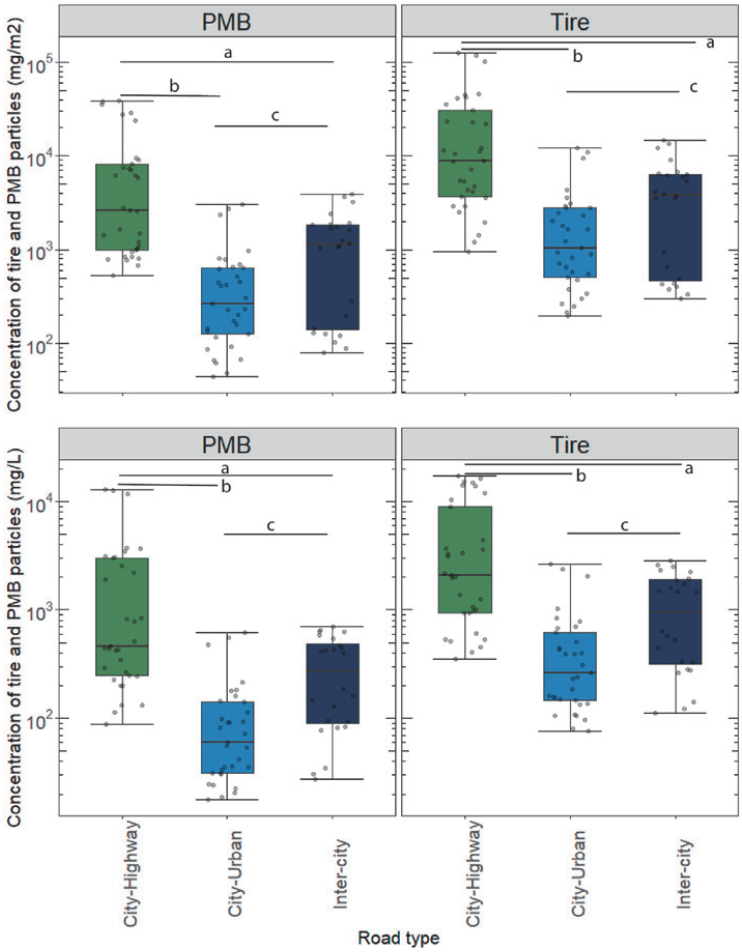

Fig. 3. Concentration of tire and PMB particles for all distances (0, 1 and 3 m) pooled, in mass load (mg/m^2, above) and meltwater (mg/L, below). The difference is significant ($p < 0.05$) between Inter-city and City highway (a), between City Highway and City Urban (b) and between City Urban and Inter City (c).

3.2. Concentrations of tire and PMB in snowbanks

The calculation from SBR + BR + SBS concentrations to tire and PMB concentration are reported in SI-6 Tables S6 and S7, and all concentration data is summarized in Table S8. The concentration of tire particles in meltwater varied from 76.0 mg/L (Tøyen 1 m) to 14,500 mg/L (Lysaker 0 m), with an average of 2090 ± 3700 mg/L for all sites (Fig. 3, Table S8). The PMB concentration ranged from 14.8 (Tøyen 1 m) to 9550 (Lysaker 0 m) mg/L, with an average concentration of 731 ± 1810 mg/L (Fig. 3, Table S8). The concentration of tire particles in mass load varied from 222 mg/m^2 (Ila 3 m) to 109,000 mg/m^2 (Storo 0 m), with an average of 10,600 ± 2200 mg/m^2. For PMB, the concentration in mass load varied from 45.0 mg/m^2 (Ila 3 m) to 28,800 mg/m^2(Lysaker 0 m), with an average of 2960 ± 6410 mg/m^2. The three road groups show a large spread in concentrations of tire and PMB and the variation between the groups are statistically significant (ANOVA: Meltwater $p < 0.0001$, massload: $p < 0.0001$). The City Highway sites show slightly higher concentrations of both tire and PMB for meltwater and for mass loads. The difference in concentration of tire and PMB between 0 m, 1 m and 3 m distance is also significant for both meltwater ($p < 0.0001$) and for mass load ($p < 0.0001$).

3.3. Total concentrations of particles

The total mass of particles (TSS) in the samples were calculated based on the total weight of particles (<1 mm) per L melted snow. The concentration of TSS varied between 1810 and 355,000 mg/L, with an average of 49,700 ± 76,800 mg/L for meltwater and 6340 to 2,810,000 mg/m^2 for mass loads, with an average of 247,000 ± 516,000 mg/m^2 (SI-7 Table S8). Comparing the levels of tire and PMB particles to the total mass of particles (W_{Tire}/W_{TSS}, W_{PMB}/W_{TSS}) showed that tire and PMB-particles only contribute 5.7% of the particles for the meltwater concentrations and 5.2% of the particles for the mass load concentrations.

A linear relationship was found between the total particle concentrations and the synthetic rubber concentrations. The model of SBR + BR + SBS (log-transformed) ~ TSS (log-transformed) in mass load concentration (Fig. 4) did not have normally distributed residuals, and an assumption free Redundancy Analysis (RDA) was performed. With TSS as the explanatory

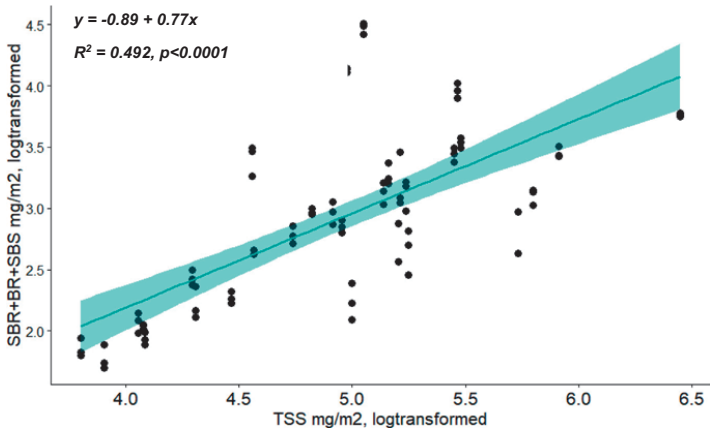

Fig. 4. Assumption-free linear regression of TSS (mg/m^2, log transformed) and rubber (SBR + BR + SBS, mg/m^2, log transformed) performed by RDA, $R^2 = 0.492$ ($p < 0.0001$) and $y = -89 + 0.77x$.

variable, 49% of the variation in SBR + BR + SBS concentration (mg/m^2) was explained ($p < 0.0001$). For concentrations in meltwater (mg/L), the residuals of the linear regression model were normally distributed; $R^2 = 0.48$ ($p < 0.0001$, SI-8 Fig. S2).

3.4. Relationship between SBR + BR + SBS, traffic features and road type

To assess any relationship between tire and PMB particles, road type and traffic features, the concentration of SBR + BR + SBS was applied instead of estimated tire and PMB particles. Tire and PMB are calculated using AADT, which consequently exclude AADT to be used as an independent explanatory variable. Thus, using the total concentration of these rubbers will allow the exploration of all traffic variables, including AADT.

The explanatory variables explored were site *Group* (Inter-city Highway, City Highway and City Urban), *AADT* (total), *PV%, HV%, STUD%* (studded tires %), *Speed limit, STOP-GO* (areas with acceleration/braking), *Distance* from the road (0, 1 and 3 m) and the interaction between *AADT x Speed limit*. Using an assumption free multiple linear regression with RDA on all explanatory variables, 69% of the variation found for concentrations in meltwater could be explained ($p = 0.0001$). For the concentrations in mass loads, 66% could be explained by the identified explanatory factors ($p = 0.0001$). (SI-9 Table S8). Exploring the variation using only the traffic variables and distance (removing road groups) lowered the percentage explained to 50% ($p = 0.0001$) for meltwater and 47% mass load concentrations ($p = 0.0001$). The Simple (i.e. the unique effect of each explanatory variable) and conditional effect (i.e. the unique effect of each explanatory variable after considering already chosen explanatory variable(s)) of each explanatory variable are presented in SI-9 Table S8. For meltwater concentrations, the statistically significant variables that explain the observed variation in SBR + BR + SBS concentrations are *Group-City-Highway* (34%), *Group-City-urban(30%)*, *Speed limit (22%)*, *distance (15%)*, *AADT*speed limit (12%)* and *AADT (12%)*. For mass loads, the variables responsible were slightly different. *Group-City-Highway* was still the main explanatory variable (34%), followed by *Group-City-Urban (23%)*, *Speed limit (16%)*, *AADT (14%)*, *AADT*Speed limit (14%)* and *Distance (13%)*. The significance of *Speed limit* was reduced for concentrations in mass loads compared to meltwater. The weather in Oslo before the snow was collected was fluctuating a lot, with both dry periods and precipitation, as well as both very cold and very warm temperatures (Yr, 2019). Even though the weather was not monitored for each exact sample location, the weather data available indicates that the sampled snow represents several melt and freeze episodes. This is also supported by the density data (SI-10), where the density varies between 31.5 and 72.2 g/m^3. In the calculation of mass load concentrations, density of the snow sample is one of the key parameters. Therefore, density is accounted for when applying the RDA analysis on mass load concentrations but not for the meltwater concentrations. The correlation (R^2 adjusted, RDA) between density and the SBR + BR + SBS concentration in meltwater was 36% and by including density as a variable together with the other identified variables mentioned above, the variation explained increased to 74% for meltwater.

4. Discussion

4.1. Meltwater concentrations vs. mass loads

Snowpacks are continuously affected by freezing and thawing processes which vary in time and space. Consequently, the occurrence of contaminants in roadside snow may also vary greatly in both time and space which makes it difficult to compare concentration data between different sites. Hence, previous studies on contaminants in roadside snow (Moghadas et al., 2015; Vijayan et al., 2021; Viklander, 1998) have presented results as concentrations in mass load to overcome this issue. Considering the environmental impact, meltwater concentrations are potentially more relevant. Most tire and PMB particles in snow will be transported to the environment in meltwater during the snowmelt periods. Meltwater concentrations are also more comparable to other studies of tire and road particles in other environmental matrices. A snowpack is by no means a homogenous sample matrix, especially when considering particle pollution. However, using sampling strategies where multiple samples are collected and combined to represent a larger area (multi-incremental sampling), as applied in the present study, could be important to obtain representative samples. Such strategies have been suggested in previous studies of snow (Vijayan et al., 2021) as well as for roadside soil sampling (Johnsen and Aaneby, 2019).

4.2. Tire and PMB particle concentrations in snow

The SBR + BR + SBS concentrations in meltwater and mass load in the reference snow sample were very low compared to the roadside snow samples, only 1.5% and 0.11% of the average concentration of SBR + BR + SBS in roadside snow. Despite the low concentrations, quantifiable concentrations of rubbers were found in the reference site at such a distance from nearby roads. The rubbers may originate from atmospheric deposition from nearby roads. In the review of TRWP release in Germany, Wagner et al. (2018) estimated that 10% of the total tire wear mass on highways are deposited from the atmosphere. It is also a possibility that some of these

rubbers originate from small maintenance vehicles used in the park, although no information on the use of these vehicles in the park could be obtained.

The ratio of tire vs PMB particle based on the calculated ratio of SBS (RSBS) varied between the sites, however, for all sites except Lysaker, the mean calculated percentage of SBS was between 3.7 and 4.7%.For Lysaker, the only site with asphalt concrete surface layer, the mean calculated SBS percentage was 10.8%. The increased road wear for sites with concrete asphalt compared to the sites with stone mastic asphalt is supported by the fact that Lysaker had the highest concentration of SBR + BR + SBS in meltwater and the second highest for mass load concentrations, although the traffic density (AADT) at Lysaker is only 13,600 v/day compared to between 14,000 and 71,000 v/day at Ila, Bryn, Storo, Ullevål stadion and Skullerud. Our data support the notion that the type of road surface does have an important impact on the release of road abrasion particles and the total release of rubber particles from roads with polymer-modified bitumen.

A limited number of relevant studies of tire wear and road wear particles in the environment, and additionally that different analytical approaches have been used, makes it difficult to have a direct comparison of our results with earlier findings. Only one study in which tire wear material concentrations were quantified in roadside snow could be identified. Using Benzothiazole (BT) as the marker, Bauman and Ismeier measured tire and PMB particle concentrations of 563 mg/L (Baumann and Ismeier, 1998). However, BTs may not be a reliable marker for tire wear studies since the concentration of different BTs varies between different tires and as they have shown the ability to transform during different environmental conditions (Asheim, 2018; Bye and Johnson, 2019; Zhang et al., 2018).

In the lack of other snow-studies, tire wear particles in road runoff are the most relevant environmental matrices to compare with. The current available data show that tire particles are found in the range of 3–180 mg/L in road run-off (Baumann and Ismeier, 1998; Kumata et al., 2000; Kumata et al., 1997; Kumata et al., 2002; Parker-Jurd et al., 2021; Reddy and Quinn, 1997; Wik and Dave, 2009). The results found for meltwater snow in the present study are significantly higher (76.0–14,500 mg/L), suggesting that snowpacks accumulate tire wear over time and potentially poses a higher acute release risk to the environment compared to road runoff. Similar trends were found for metals and PAHs in snow during melting in previous studies (Viklander, 1996).

4.3. Total particle concentrations

Total particle concentrations have been reported for a range of environmental samples, such as roadside snow (5–12,700 mg/L: Moghadas et al. (2015), Viklander (1999), tunnel wash water (8–31,000 mg/L, Meland and Rødland (2018), Hallberg et al. (2014))) and sedimentation pond effluent (<15 mg/L, Hallberg et al. (2014)). Compared to previous studies, the total particle concentrations found for the roadside snow in this study are significantly higher, from 1800 to 355,000 mg/L in meltwater and 6340 to 2,810,000 mg/m^2. The variable AADT might be a reason for the large variations found for TSS in these studies, as the AADT for snow-sites in our study are between 6000 and 71,250 vehicles (v)/day, compared to 1500–20,000 v/day in the studies of Moghadas et al. (2015). The TSS values found in tunnel wash water in Norway, where the AADT varied between 1550 and 77,000 v/day, were in fact more comparable to the values found for roadside snow in this study. The relationship found between TSS and SBR + BR + SBS concentrations suggests that there is scope to predict tire and PMB concentrations based on the measured TSS. This also suggest that historical TSS data may be used to estimate the presence of tire and PMB particles in previous studies, where the tire and PMB concentrations have not been analysed specifically.

4.4. Exploring the variations

There are several possible explanatory variables that impact the variation in rubber content in the roadside snow. Exploring all the identified traffic variables as well as deposition as a function of distance from the road, explained 50% of the variation for meltwater and 46% for mass load concentrations. However, adding the road groups as a variable increased the overall explanation to 69% for meltwater and 66% for mass loads.

Previous studies of road-related pollution have also explored the possible explanatory variables for other contaminants. Especially *AADT* has been proposed as one of the main drivers behind the variation of road-related pollutants in roadside snow (Li et al., 2014; Moghadas et al., 2015; Viklander, 1999), roadside soil (Werkenthin et al., 2014) as well as in road dust (Gunawardena et al., 2015) and in tunnel wash water (Meland and Rødland, 2018), as increased number of vehicles causes increased abrasion on tires and road surface as well as increased release of other pollutants related to vehicles. The results of our study suggest that *AADT* is less important compared to the road location (*Group*), followed by speed limit and distance from the road. The high impact found for the road group locations could also be explained by the physical difference between these roads, where both City Highway and City Urban are urban roads with numerous traffic lights, crossings, roundabouts and other obstacles. Another possible explanation for the high impact of road groups could be different snow handling and road maintenance for the different road groups. As described in Viklander (1998) the snow handling procedures can have an substantial impact on the concentrations of road-related contaminants in mass load of snow. The impact of snow handling could also have an impact on the meltwater vs. mass load concentrations, as mass loads take into consideration the density of the snowpack as a measure of melting and packing. Our study, however, indicates the opposite, as the variables explained the variation slightly better for meltwater concentrations compared to mass load concentrations. Another aspect not explored in this present study is how atmospheric deposition from nearby roads have impacted the study sites. As shown in this study, SBR + BR + SBS rubbers were detected even at 60 m distance from the nearest road, suggesting that tire and/or PMB particles can be transported for relatively long distances.

Previous studies have reported that urban driving styles with increased braking and accelerating results in higher emission factors for tire wear than highway driving (Dannis, 1974; LeMaitre et al., 1998; Luhana et al., 2004; Stalnaker et al., 1996), as summarized in Vogelsang et al. (2018). Increasing speed has been found to cause increasing abrasion in tires in previous studies (Li et al., 2011) as higher speed will cause higher friction between tire and the road surface as well as generate higher temperatures in the tire tread, adding to the abrasion of the tires. As for tires, driving speed has also been found to impact the road pavement abrasion, as demonstrated for increasing PM_{10} concentrations with increasing driving speed from driving simulators (Gustafsson et al., 2009). Higher speed may also cause smaller tire and road particles to be deposited further away from the roadsides due to suspension and splash and spray as well as being caused by increased speed (Gustafsson et al., 2009). This could explain why the mean and median concentrations of SBR + BR + SBS in both meltwater and mass loads are higher at 1 m distance compared to 0 m distance in the Inter-City Highway sites, where also the highest speed limits are found. It should, however, be underlined that the speed limit used for the analysis in this study is the official speed limit on each site and not the actual average driving speed of the vehicles, as this information was not available. In future studies, atmospheric deposition, monitoring of real-time driving speed and driving behavior, the use of different driving lanes for specific vehicle types and impact of different snow handling procedures should be investigated further.

4.5. Environmental impact

The high concentrations of total particles, tire and PMB-particles present in roadside snow suggests that melting snow could pose a potential threat to the environment. The meltwater from large accumulations of snow should be considered for treatment before release into the aquatic environment. There are currently no limits set for the release of tire and PMB-particles from roads, or for other road-related matrices such as road and

tunnel runoff. The current legislation in Norway demands that a permit for release is applied for and granted if there is a release of pollutants that can have an environmental impact (Pollution Control Act, 1987), such as for the release of tunnel wash water. For TSS, there is limit value set for release of TSS in general, however, in most permits given to road runoff release in Norway, the limit for TSS to freshwater recipients is 100 mg/L and to marine recipients 400 mg/L (Rødland and Helgadottir, 2018). Thus, the TSS values in the range of 1800–355,000 mg/L observed for snowpacks in the present work are far exceeding these limit values set for road and tunnel runoff. The specific impact on the environment from TRWP is still being studied. The current published research on tire toxicity are performed on different types of artificially generated tire particles, tire leachates and/or environmental samples such as runoff sediments, which makes comparisons difficult (Baensch-Baltruschat et al., 2020; Rødland, 2019). The recently discovered acute toxicity of 6-PPD-quinone, a transformation product coming from the tire antiozonant chemical 6-PPD, on both juvenile and adult coho salmon (*Oncorhynchus kisutch*) (McIntyre et al., 2021; Tian et al., 2021) has gained significant attention by both the research community and regulators. Acute toxicity was found for adult coho salmon exposed to tire leachates of 320 mg/L tire particles (1.3–1.8 μg/L 6PPD-quinone). However, the observed acute toxicity found for coho salmon might be species-specific, as recent studies have found no acute toxicity for other organisms or even other salmon species tested (chum salmon, *Oncorhynchus keta*) (Hiki et al., 2021; McIntyre et al., 2021). As the concentrations of tire particles found for roadside snow (76–19,000 mg/L) is within the range where toxic effects on some organisms have been confirmed by previous studies (Gualtieri et al., 2005; Khan et al., 2019; McIntyre et al., 2021; Panko et al., 2013; Tian et al., 2021), it is possible that toxic effects could be observed if meltwater is released directly into a recipient, and especially smaller recipients with lower dilution capacity. Müller et al. (2022) showed that less than 20% of the organic chemical in tires had leached completely by 28 days in water, suggesting that tire particles left in an aquatic environment will continue to leach out chemicals over time unless they are removed. However, as the current knowledge on tire toxicity lacks standardization and there are no published studies on the toxicity of PMB-particles, more research is needed to address the possible environmental impact of TRWP into the environment.

5. Conclusions

The present study is the first study on mass concentrations of both tire and PMB particles in roadside snow. The study also contributes to the understanding of which traffic-related processes can be attributed to the production of these particles alongside different roads. The results show that the concentrations of tire particles along roads vary widely at over three orders of magnitude in meltwater (76–14,500 mg/L). The results also show that the total concentration of particles (1800–355,000 mg/L) in roadside snow far exceeds the limits for TSS set for other types of road-related runoff such as tunnel wash water. This shows that roadside snow in peri-urban and urban environments are highly polluted and thus, should be treated before meltwater runoff is released into the environment. The large concentration differences relate to the difference in road surface and traffic variables identified for the different sites. The high concentration of TSS and rubbers at Lysaker is in agreement with previous estimates that concrete asphalt surface layers contribute three times more road abrasion compared those with stone mastic asphalt. The main traffic variables driving the variation was found to be speed limit and AADT, where speed limit was found to be the most important variable explaining the variation in both meltwater and mass load concentrations. This is contradictory to previous road runoff studies, where AADT has been reported as the main explanatory variable. Increased speed causes higher friction between tire and the road surface, which generates higher temperatures in the tire tread and consequently increased tire abrasion. For the PMB, the road surface abrasion also increases with driving speed due to the increased friction with tires. Higher speed is also related to increased suspension and splash and spray-effect, which can cause smaller tire and PMB particles to be deposited further away from the roadsides. Increased AADT generates more abrasion on the road surface due to the increased number of vehicles, as well as the release of tire abrasion particles due to increased number of tires passing the area. Part of the variation was also found to be related to the road type of each site, e.g. urban city road (municipality road), peri-urban highway road (state road) and inter-city highway road (state road). Within each road type, the sites include variable AADT, speed limit and areas of braking and acceleration. There is, however, also a variation explained by the road groups that could not be assigned to any known traffic variable. This suggests that there may be other variables that impact the production of tire and PMB particles that are yet to be explored, such as the importance of different snow handling procedures and winter maintenance. This should be prioritized for future research.

CRediT authorship contribution statement

Elisabeth Rødland: Conceptualization, Methodology, Investigation, Formal analysis, Writing – Original Draft, Writing - Reviewing and Editing, Visualization. **Ole Christian Lind:** Conceptualization, Writing - Reviewing and Editing. **Malcolm J. Reid:** Conceptualization, Writing - Reviewing and Editing. **Lene S. Heier:** Conceptualization, Writing - Reviewing and Editing. **Elvis D. Okoffo:** Investigation, Writing - Reviewing and Editing. **Cassandra Rauert:** Investigation, Writing - Reviewing and Editing. **Kevin V. Thomas:** Writing - Reviewing and Editing. **Sondre Meland:** Conceptualization, Writing - Reviewing and Editing, Formal analysis, Project administration.

Declaration of competing interest

The authors declare that they have no known competing financial interests or personal relationships that could have appeared to influence the work reported in this paper.

Acknowledgements

A sincere thank you to Ashenafi Seifu Gragne (NIVA) for contributing the map of locations for this publication. This work was funded in collaboration between the Norwegian Institute for Water Research (NIVA) (funded by the Research Council of Norway, grant number 160016) and the NordFoU-project REHIRUP (grant number 604133). Part of the work is also supported by the Norwegian University of Life Sciences (NMBU) and the Centre for Environmental Radioactivity (CERAD) through the Research Council of Norway's Centres of Excellence funding scheme (project number 223268/F50). The Queensland Alliance for Environmental Health Sciences, The University of Queensland, gratefully acknowledges the financial support of the Queensland Department of Health.

Appendix A. Supplementary data

Supplementary data to this article can be found online at https://doi.org/10.1016/j.scitotenv.2022.153785.

References

Act PC, 1987. Concerning Protection Against Pollution And Concerning Waste.
Asheim, J. Benzotriazoles, 2018. Benzothiazoles And Inorganic Elements as Markers of Road Pollution Sources in a Sub-Arctic Urban Setting (Trondheim, Norway), p. 125.
Baensch-Baltruschat, B., Kocher, B., Stock, F., Reifferscheid, G., 2020. Tyre and road wear particles (TRWP) - a review of generation, properties, emissions, human health risk, ecotoxicity, and fate in the environment. Sci. Total Environ. 733, 137823.
Bakløkk, L., Horvli, I., Myran, T., 1997. Piggdekkslitasje og støvutvikling. Status-Litteraturstudie. SINTEF Bygg og miljøteknikk, Avdeling Vegteknikk.
Baumann, W., Ismeier, M., 1998. Emissionen beim bestimmungsgemässen Gebrauch von Reifen. Kautschuk und Gummi, Kunststoffe. 51, pp. 182–186.
Bergmann, M., Mützel, S., Primpke, S., Tekman, M.B., Trachsel, J., Gerdts, G., 2019. White and wonderful? Microplastics prevail in snow from the Alps to the Arctic. Sci. Adv. 5, eaax1157.
Boom, A., Marsalek, J., 1988. Accumulation of polycyclic aromatic hydrocarbons (PAHs) in an urban snowpack. Sci. Total Environ. 74, 133–148.

Boucher, J., Billard, G., Simeone, E., Sousa, J.T., 2020. The Marine Plastic Footprint. IUCN, Gland, Switzerland.

Bye, N., Johnson, J.P., 2019. Assessment of Tire Wear Emission in a Road Tunnel, Using Benzothiazoles as Tracer in Tunnel Wash Water. orwegian University of Life Sciences Master of Science.

BYM, 2021. In: Rødland, E. (Ed.), Snow Handling on Municipality Roads in Oslo, Norway. Oslo Municipality Master of Science

Chae, E., Jung, U., Choi, S.-S., 2021. Quantification of tire tread wear particles in microparticles produced on the road using oleamide as a novel marker. Environ. Pollut. 288, 117811.

Chen, J.S., Liao, M.C., Tsai, H.H., 2002. Evaluation and optimization of the engineering properties of polymer-modified asphalt. Pract. Fail. Anal. 2, 75–83.

Dannis, M.L., 1974. Rubber dust from the normal wear of tires. Rub. Chem. Technol. 47, 1011–1037.

EAPA EAPA, 2018. Heavy Duty Surfaces the Arguments for SMA. Technical review, Brussels, Belgium.

Fox, J., Weisberg, S.A., 2019. n R Companion to Applied Regression. Sage, Thousand Oaks CA.

Giavarini, C., De Filippis, P., Santarelli, M.L., Scarsella, M., 1996. Production of stable polypropylene-modified bitumens. Fuel 75, 681–686.

Goßmann, I., Halbach, M., Scholz-Böttcher, B.M., 2021. Car and truck tire wear particles in complex environmental samples – a quantitative comparison with "traditional" microplastic polymer mass loads. Sci. Total Environ. 773, 145667.

Gualtieri, M., Andrioletti, M., Vismara, C., Milani, M., Camatini, M., 2005. Toxicity of tire debris leachates. Environ. Int. 31, 723–730.

Gunawardena, J., Ziyath, A.M., Egodawatta, P., Ayoko, G.A., Goonetilleke, A., 2015. Sources and transport pathways of common heavy metals to urban road surfaces. Ecol. Eng. 77, 98–102.

Gustafsson, M., Blomqvist, G., Gudmundsson, A., Dahl, A., Jonsson, P., Swietlicki, E., 2009. Factors influencing PM10 emissions from road pavement wear. Atmos. Environ. 43, 4699–4702.

Hallberg, M., Renman, G., Byman, L., Svenstam, G., Norling, M., 2014. Treatment of tunnel wash water and implications for its disposal. Water Sci. Technol. 69, 2029–2035.

Halsband, C., Sørensen, L., Booth, A.M., Herzke, D., 2020. Car tire crumb rubber: does leaching produce a toxic chemical cocktail in coastal marine systems? Front. Environ. Sci. 8.

Hiki, K., Asahina, K., Kato, K., Yamagishi, T., Omagari, R., Iwasaki, Y., et al., 2021. Acute toxicity of a tire rubber-derived chemical, 6PPD quinone, to freshwater fish and crustacean species. Environ.Sci.Technol.Lett. 8, 779–784.

Horvli, I. Generelt, 1996. Dekketyper, egenskaper og bruksområder, EVU-kurs Asfaltdekker 2003. Notat 949, March 1996. Institutt for bygg, anlegg og transport, NTNU.

ISO, 2017a. ISO/TS 20593: Ambient Air - Determination of the Mass Concentration of Tire And Road Wear Particles (TRWP) - Pyrolysis-GC-MS Method. International Organization for Standardization, Geneve, Switzerland.

ISO, 2017b. ISO/TS 21396: Rubber — Determination of Mass Concentration of Tire And Road Wear Particles (TRWP) in Soil And Sediments — Pyrolysis-GC/MS Method. International Organization for Standardization, Genève, Switzerland.

Johnsen, A.V., Aaneby, J., 2019. Prøvetakingsstrategi – prøvetaking av masser langs vei Forsvarets Forskningsinstitutt (FFI), p. 41.

Khan, F.R., Halle, L.L., Palmqvist, A., 2019. Acute and long-term toxicity of micronized car tire wear particles to Hyalella azteca. Aquat. Toxicol. 213, 105216.

Klein, J., Molnár-in 't Veld, H., Geilenkirchen, G., Hulskotte, J., Ligterink, N., Dellaert, S., 2017. Methods for calculating transport emissions in the Netherlands. Force on Transportation of the Dutch Pollutant Release And Transfer Register. PBL Netherlands Environmental Assessment Agency, p. 75.

Klöckner, P., Seiwert, B., Wagner, S., Reemtsma, T., 2021. Organic markers of tire and road wear particles in sediments and soils: transformation products of major antiozonants as promising candidates. Environ.Sci.Technol. 55, 11723–11732.

Knight, L.J., Parker-Jurd, F.N.F., Al-Sid-Cheikh, M., Thompson, R.C., 2020. Tyre wear particles: an abundant yet widely unreported microplastic? Environ. Sci. Pollut. Res. Int. 27, 18345–18354.

Kumata, H., Takada, H., Ogura, N., 1997. 2-(4-Morpholinyl)benzothiazole as an indicator of tire-wear particles and road dust in the urban environment. Molecular Markers in Environmental Geochemistry. 671. American Chemical Society, pp. 291–305.

Kumata, H., Sanada, Y., Takada, H., Ueno, T., 2000. Historical trends of N-Cyclohexyl-2-benzothiazolamine, 2-(4-morpholinyl)benzothiazole, and other anthropogenic contaminants in the urban reservoir sediment core. Environ.Sci.Technol. 34, 246–253.

Kumata, H., Yamada, J., Masuda, K., Takada, H., Sato, Y., Sakurai, T., et al., 2002. Benzothiazolamines as tire-derived molecular markers: sorptive behavior in street runoff and application to source apportioning. Environ.Sci.Technol. 36, 702–708.

Lai, F.Y., O'Brien, J., Bruno, R., Hall, W., Prichard, J., Kirkbride, P., et al., 2016. Spatial variations in the consumption of illicit stimulant drugs across Australia: a nationwide application of wastewater-based epidemiology. Sci. Total Environ. 568, 810–818.

LeMaitre, O., Süssner, M., Zarak, C., 1998. Evaluation of tyre wear performance. SAE technical paper series. International congress and Exposition, Detroit, Michigan 1998 (980256).

Li, Y., Zuo, S., Lei, L., Yang, X., Wu, X., 2011. Analysis of impact factors of tire wear. J. Vib. Control 18, 833–840.

Li, X., Jiang, F., Wang, S., Turdi, M., Zhang, Z., 2014. Spatial distribution and potential sources of trace metals in insoluble particles of snow from Urumqi,China. Environ. Monit. Assess. 187, 4144.

Luhana, L., Sokhi, R., Warner, L., Mao, H., Boulter, P., McCrae, I.S., Wright, J., Osborn, D., 2004. Measurements of non-exhaust particulate matter. Deliverable 8 of the European Commission DG TrEn 5th Framework PARTICULATES (Characterisation of Exhaust Particulate Emissions from Road Vehicles) project.

M., Yb., Müller, A.J., Rodriguez, Y., 2003. Use of rheological compatibility criteria to study SBS modified asphalts. J. Appl. Polym. Sci. 90, 1772–1782.

McIntyre, J.K., Prat, J., Cameron, J., Wetzel, J., Mudrock, E., Peter, K.T., et al., 2021. Treading water: tire wear particle leachate recreates an urban runoff mortality syndrome in coho but not chum salmon. Environ.Sci.Technol. 55, 11767–11774.

Meland, S., Rødland, E., 2018. Pollution in tunnel wash water – a study of 34 road tunnels in Norway. VANN. 01.

Miller, J.V., Maskrey, J.R., Chan, K., Unice, K.M., 2021. Pyrolysis-gas chromatography-mass spectrometry (Py-GC-MS) quantification of tire and road wear particles (TRWP) in environmental matrices: assessing the importance of microstructure in instrument calibration protocols. Anal.Lett. 1–13.

Moghadas, S., Paus, K.H., Muthanna, T.M., Herrmann, I., Marsalek, J., Viklander, M., 2015. Accumulation of traffic-related trace metals in urban winter-long roadside snowbanks. Water Air Soil Pollut. 226, 404.

Müller, K., Hübner, D., Huppertsberg, S., Knepper, T.P., Zahn, D., 2022. Probing the chemical complexity of tires: identification of potential tire-borne water contaminants with high-resolution mass spectrometry. Sci. Total Environ. 802, 149799.

NPRA, 2022. In: Rødland, E. (Ed.), Snow Handling on Oslo State Roads. Norwegian Public Roads Administration.

NVF, 2013. Trender innen belegningsbransjen i Norden: Belegningstrender i Norge. Nordiskt Vägforum, Utvalg for Belegninger, p. 61.

Panda, M., Mazumdar, M., 1999. Engineering properties of EVA-modified bitumen binder for paving mixes. J. Mater. Civ. Eng. 11, 131–137.

Panko, J.M., Kreider, M.L., McAtee, B.L., Marwood, C., 2013. Chronic toxicity of tire and road wear particles to water- and sediment-dwelling organisms. Ecotoxicology 22, 13–21.

Parker-Jurd, F.N.F., Napper, I.E., Abbott, G.D., Hann, S., Thompson, R.C., 2021. Quantifying the release of tyre wear particles to the marine environment via multiple pathways. Mar. Pollut. Bull. 172, 112897.

Polacco, G., Berlincioni, S., Biondi, D., Stastna, J., Zanzotto, L., 2005. Asphalt modification with different polyethylene-based polymers. Eur. Polym. J. 41, 2831–2844.

Polacco, G., Muscente, A., Biondi, D., Santini, S., 2006. Effect of composition on the properties of SEBS modified asphalts. Eur. Polym. J. 42, 1113–1121.

R.G., S., N., U., J., A., 2012. Long-term performance of asphalt surfacings containing polymer modified binders. 5th Eurasphalt & Eurobitume Congress.

Rauert, C., Rødland, E.S., Okoffo, E.D., Reid, M.J., Meland, S., Thomas, K.V., 2021. Challenges with quantifying tire road wear particles: recognizing the need for further refinement of the ISO technical specification. Environ.Sci.Technol.Lett. 8, 231–236.

Reddy, C.M., Quinn, J.G., 1997. Environmental chemistry of benzothiazoles derived from rubber. Environ.Sci.Technol. 31, 2847–2853.

Reinosdotter, K., Viklander, M., 2005. A comparison of snow quality in two Swedish municipalities–Luleå and Sundsvall. Wat. Air Soil Pollut. 167, 3–16.

Reitan, K.M., Snilsberg, B., Lysbakken, K.R., Gryteselv, D., 2017. Road dust and air quality in Trondheim. Maintenance Measures Against Road Dust. Report no 348.

Rødland, E., 2019. Ecotoxic potential of road-associated microplastic particles (RAMP). VANN. 03, pp. 166–183.

Rødland, E., Helgadottir, D., 2018. Tool for assessing pollution from untreated tunnel wash water. VANN 04, 367–376.

Rødland, E.S., Samanipour, S., Rauert, C., Okoffo, E.D., Reid, M.J., Heier, L.S., et al., 2022. A novel method for the quantification of tire and polymer-modified bitumen particles in environmental samples by pyrolysis gas chromatography mass spectroscopy. J. Hazard. Mater. 423, 127092.

Rosland, P., 2020. Piggdekktellinger fra Oslo siden 2015 (Studded-tires Count in Oslo Since 2015).

Seiwert, B., Klöckner, P., Wagner, S., Reemtsma, T., 2020. Source-related smart suspect screening in the aqueous environment: search for tire-derived persistent and mobile trace organic contaminants in surface waters. Anal. Bioanal. Chem. 412, 4909–4919.

Sengoz, B., Topal, A., Isikyakar, G., 2009. Morphology and image analysis of polymer modified bitumens. Constr. Build. Mater. 23, 1986–1992.

Snilsberg, B., 2008. Pavement Wear And Airborne Dust Pollution in Norway-characterization of the Physical and Chemical Properties of Dust Particles. NTNU PhD.

Snilsberg, B., Saba, R.G., Uthus, N., 2016. Asphalt pavement wear by studded tires – effects of aggregate grading and amount of coarse aggregate. 6th Euroasphalt & Eurobitume Congress, Prague Czech Republic.

Stalnaker, D., Turner, J., Parekh, D., Whittle, B., Norton, R., 1996. Indoor simulation of tyre wear: Some case studies. Tyre Sci. Technol. 24, 94–118.

Sundt, P., S, R., Haugedal, T.R., Schulze, P.-E., 2021. Norske landbaserte kilder til mikroplast (Norwegian Land-based Sources to Microplastics). MEPEX, Oslo, p. 88.

Team R, 2020. RStudio: Integrated Development for R. RStudio, PBC, Boston, MA.

Ter Braak, C.J.F., Smilauer, P., 2018. CANOCO Reference Manual and Canodraw for Windows User's Guide: Software for Canonical Community Ordination (Version 5.12.5). CANOCO.

Tian, Z., Zhao, H., Peter, K.T., Gonzalez, M., Wetzel, J., Wu, C., et al., 2021. A ubiquitous tire rubber–derived chemical induces acute mortality in coho salmon. Science 371, 185–189.

Unice, K.M., Bare, J.L., Kreider, M.L., Panko, J.M., 2015. Experimental methodology for assessing the environmental fate of organic chemicals in polymer matrices using column leaching studies and OECD 308 water/sediment systems: application to tire and road wear particles. Sci. Total Environ. 533, 476–487.

Vegkart - online map-based database of traffic data for Norwegian Public Roads A dministration.

Vijayan, A., Österlund, H., Magnusson, K., Marsalek, J., Viklander, M., 2019. Microplastics Pathways in the Urban Environment: Urban Roadside Snowbanks. Nivatech.

Vijayan, A., Österlund, H., Marsalek, J., Viklander, M., 2021. Estimating pollution loads in snow removed from a port facility: snow pile sampling strategies. Water Air Soil Pollut. 232, 75.

Viklander, M., 1996. Urban snow deposits—pathways of pollutants. Sci. Total Environ. 189–190, 379–384.

Viklander, M, 1997. Snow quality in urban areas, PhD thesis. Division of Sanitary Engineering, Luleå University of Technology, Luleå, Sweden.

Viklander, M., 1998. Snow quality in the city of Luleå, Sweden — time-variation of lead, zinc, copper and phosphorus. Sci. Total Environ. 216, 103–112.

Viklander, M., 1999. Substances in urban snow. A comparison of the contamination of snow in different parts of the city of Luleå,Sweden. Water Air Soil Pollut. 114, 377–394.
Vogelsang, C., Lusher, A.L., Dadkhah, M.E., Sundvor, I., Umar, M., Ranneklev, S.B., 2018. Microplastics in road dust – characteristics, pathways and measures.
Wagner, S., Huffer, T., Klockner, P., Wehrhahn, M., Hofmann, T., Reemtsma, T., 2018. Tire wear particles in the aquatic environment - a review on generation, analysis, occurrence, fate and effects. Water Res. 139, 83–100.
Wagner, S., Klöckner, P., Reemtsma, T., 2021. Aging of tire and road wear particles in terrestrial and freshwater environments – a review on processes, testing, analysis and impact. Chemosphere 132467.
Werkenthin, M., Kluge, B., Wessolek, G., 2014. Metals in european roadside soils and soil solution – a review. Environ. Pollut. 189, 98–110.
Wickham, H., François, R., Henry, L., Müller, K., 2018. R Package Version 0.7.6. dplyr: A Grammar of Data Manipulation.
Wik, A., Dave, G., 2009. Occurrence and effects of tire wear particles in the environment - a critical review and an initial risk assessment. Environ. Pollut. 157, 1–11.
Yr, 2019. Historical Weather Data for Oslo Hovin Station.
Zhang, J., Zhang, X., Wu, L., Wang, T., Zhao, J., Zhang, Y., et al., 2018. Occurrence of benzothiazole and its derivates in tire wear, road dust, and roadside soil. Chemosphere 201, 310–317.

Supplementary Information

Occurrence of tire and road wear particles in urban and peri-urban snowbanks, and their potential environmental implications

Elisabeth S. Rødland[1,2], Ole Christian Lind[2], Malcolm J. Reid[1], Lene S. Heier[3], Elvis D. Okoffo[4], Cassandra Rauert[4], Kevin V. Thomas[4], Sondre Meland[1,2]

[1]Norwegian Institute for Water Research, Økernveien 94, NO-0579 Oslo, Norway
[2]Norwegian University of Life Sciences, Faculty of Environmental Sciences and Natural Resource Management, P.O. Box 5003, NO-1432 Ås, Norway
[3]Norwegian Public Roads Administration, Construction, Postboks 1010, N-2605 Lillehammer, Norway
[4]Queensland Alliance for Environmental Health Sciences (QAEHS), The University of Queensland, 20 Cornwall Street, Woolloongabba, 4102 QLD, Australia.

SI-1 Sample overview

Table S1. Overview of the traffic data for each location in the study. Data are accurate to the year of sampling (Vegkart, 2019). The table shows the Average Annual Daily Traffic (vehicles/day) in total (AADT TOT) for all locations, as well as AADT for personal vehicles (AADT PV), heavy vehicles (AADT HV), personal vehicles with studded tires (AADT PV WS, 9.8% for all locations) and heavy vehicles with studded tires (AADT HV WS, 2.2 % for all locations) and the speed limit (km/h).

Road type	Site	Code	AADT TOT	AADT PV	AADT HV	AADT PV WS	AADT HV WS	Speed limit
Unit			Vehicles/ day	Vehicles/ day	Vehicles/ day	Vehicles/ day	Vehicles/ day	Km/ hour
Inter-city Highway	Holstad (HO)	IC-1	13080	12034	1046	1386	380	80
	Skullerud (SK)	IC-2	71250	62700	8550	7553	1981	80
	Vinterbro (VI)	IC-3	12240	11261	979	1297	356	80
Mean			32190	28665	3525	3412	906	80
Standard deviation			33830	29478	4352	3586	931	0
City Highway	Bryn (BR)	CH-1	36919	32489	4430	3913	1027	70
	Lysaker (LY)	CHC-2	13565	12480	1085	1438	394	70
	Storo (ST)	CH-3	50950	46365	4586	5401	1465	70
	Ullevål Stadion (US)	CH-4	58518	53251	5267	6203	1683	70
Mean			41011	37365	3646	4347	1181	70
Standard deviation			24068	21825	2244	2551	690	0
City Urban	Carl Berner (CB)	CU-1	13000	12220	780	1378	386	50
	Frogner (FR)	CU-2	6600	6138	462	700	194	40
	Ila (IL)	CU-3	14100	12690	1410	1495	401	50
	Tøyen (TØ)	CU-4	6000	5640	360	636	178	40
Mean			8900	8156	744	944	258	45
Standard deviation			4513	3934	579	479	124	7
	Reference (RF)		-	-	-	-	-	-

SI-2 Pyrolysis markers

Table S2. Marker compounds used to quantify SBR+BR+SBS. Italics and bold values used for calibration and quantification

Polymer	Pyrolysis product	Indicator ions (m/z)	Retention Time (mins)
Styrene butadiene rubber (SBR)/Styrene butadiene styrene (SBS)	Benzene	51, 67, **78**	2.7
	α-methylstyrene	78, 91, **118**	9.5
	Ethylstyrene	77, 91, **117**	11.7
	Butadiene trimer A	65, **91**, 146	14.6
	Styrene monomer	104	7.2
Internal standard	Poly(1,4-butadiene-$_d$6)	***60***, 120, 42, 86	5.3

SI-3 Calibration curve

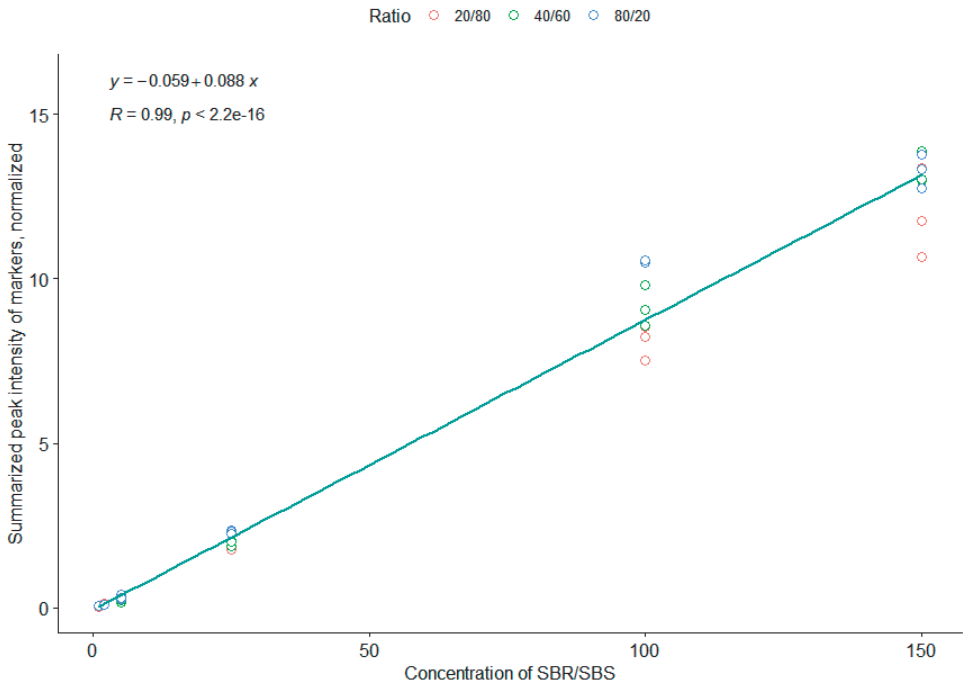

Figure S1. Calibration curve for mixture calibration of SBR and SBS. Calibration points 1 µg, 2µg, 25 µg, 100 µg and 150 µg. Three ratios of SBR:SBS (20:80, 40:60, 80:20) and three replicates for each ratio at all calibration points. The calibration curve was first published in Rødland et al. (2022), as it was created for both studies.

SI-4 Emission factors for road and tire abrasion

Table S3: Road abrasion values for different road surfaces (EFA) for studded personal vehicles (PV-st) and non-studded PV (PVnst), studded heavy vehicles (HV-st) and non-studded HV (HV-nst). Values are modified after reported values for studded PV tires, with reported 5 times higher emission for all HV tires and a 40 times lower emission from non-studded tires (Bakløkk et al., 1997; Horvli, 1996; Snilsberg, 2008; Snilsberg et al., 2016)

Road surface	$EFA_{PV\text{-}st}$ (g/vkm)	$EFA_{HV\text{-}st}$ (g/vkm)	$EFA_{PV\text{-}nst}$ (g/vkm)	$EFA_{HV\text{-}nst}$ (g/vkm)
Stone mastic asphalt (SMA)	5-10	25-50	0.125-0.25	0.625-1.25
Asphalt concrete (AC)	15-20	75-100	0.375-0.5	1.875-2.5
Topeca	<15	<75	<0.375	<1.875
Porpus asphalt	18-25	90-125	0.45-0.625	2.25-3.125
Asphalt concrete with more gravel	15-30	75-150	0.375-0.75	1.875-3.75

Table S4: Emission factors for tires for highway (EFT_H) and urban driving (EFT_U) for personal vehicles (PV) and heavy vehicles (HV), reported by (Klein J. et al., 2017)l

Tire	PV	HV
EFT_H	0.104	0.668
EFT_U	0.132	0.850

Table S5: *Calculating the ratio of SBR+BR to SBS using emission factors reported in tables S3 and S4, and traffic values for each location. All roads are SMA (skeleton mastic asphalt) except for Lysaker, which is CA (concrete asphalt). Driving mode H = highway, U = urban*

Site	AÅDT v/day	PV ratio	HV ratio	Ratio studded tires HV	Ratio studded tires PV	Driving mode	EF-PV tires g/vkm	EF-HV tires g/vkm	EF-PV-ST road g/vkm	EF-HV-ST road g/vkm	EF-PV-NST road g/vkm	EF-HV-NST road g/vkm	SBS g/day	Ratio SBR winter tires	SBR g/day	% SBS	Mean % SBS
Bryn	36919	0.88	0.12	0.106	0.0316	H	0.104	0.668	5-10	25-50	0.125 - 0.25	0.625-1.25	6.75-15.7	0.3	190.1	3.4-7.6	5.37
Carl Berner	13000	0.94	0.06	0.106	0.0316	U	0.132	0.85	5-10	25-50	0.125 - 0.25	0.625-1.25	2.23-5.38	0.3	68.3	3.2-7.3	5.05
Frogner	6600	0.93	0.07	0.106	0.0316	U	0.132	0.85	5-10	25-50	0.125 - 0.25	0.625-1.25	1.15-2.74	0.3	36.1	3.1-7.1	4.90
Holstad	13080	0.92	0.08	0.106	0.0316	H	0.104	0.668	5-10	25-50	0.125 - 0.25	0.625-1.25	2.30-5.46	0.3	58.5	3.8-8.5	5.96
Ila	14100	0.9	0.1	0.106	0.0316	U	0.132	0.85	5-10	25-50	0.125 - 0.25	0.625-1.25	2.53-5.94	0.3	86.2	2.8-6.4	4.50
Skullerud	71250	0.88	0.12	0.106	0.0316	H	0.104	0.668	5-10	25-50	0.125 - 0.25	0.625-1.25	13.0-30.3	0.3	367.0	3.4-7.6	5.37
Storo	50950	0.91	0.09	0.106	0.0316	U	0.132	0.85	5-10	25-50	0.125 - 0.25	0.625-1.25	9.04-21.4	0.3	300.5	2.9-6.6	4.62
Tøyen	6000	0.94	0.06	0.106	0.0316	U	0.132	0.85	5-10	25-50	0.125 - 0.25	0.625-1.25	1.03-2.48	0.3	31.5	3.2-7.3	5.05
Ullevål	58518	0.91	0.09	0.106	0.0316	U	0.132	0.85	5-10	25-50	0.125 - 0.25	0.625-1.25	10.4-24.5	0.3	345.2	2.9-6.6	4.62
Vinterbro	12240	0.92	0.08	0.106	0.0316	H	0.104	0.668	5-10	25-50	0.125 - 0.25	0.625-1.25	2.15-5.11	0.3	54.8	3.8-8.5	5.96
Lysaker	13565	0.92	0.08	0.106	0.0316	H	0.104	0.668	15-20	75-100	0.375-0.500	1.875-2.50	7.14-13.3	0.3	60.7	10.5-17.9	13.51

SI-5 Calculation example from SBR+BR+SBS to tire and PMB concentrations

To demonstrate how the measured value of SBR+BR+SBS is utilized to calculate the concentration of tire and PMB in a sample, a calculation example for Bryn 0m is provided.

1) Calculate the concentration in mass load

All sample data collected for the snow cores needed for these calculations are summarized in SI-10 Table S9. Calculation is based on Moghadas et al. (2015

Equation 1

$$ML = K * Cs * SWE$$

where *ML* is the mass load of the given pollutant per square meter of a snow deposit (mg/m^2);

K is a unit conversion coefficient (0.1 to convert from cm snow cores to m);

Cs is the pollutant concentration C in the melted snow sample s (mg/L);

SWE is the snow water equivalent of the sample (cm), calculated from the measured

snow core height (cm) multiplied with the snow density (g/cm^3) for each snow sample.

Example from Bryn 0m

Snow density = weight of snow sample / volume of snow core

Snow density = 821.1g / 1442.8cm^3

Snow density = 0.57g/cm^3

SWE = snow core height * snow density

SWE = 104.1cm * 0.57g/cm^3

SWE = 59.3cm

$$ML = K * Cs * SWE$$

$$ML = 0.1 * \ 107.3mg/L * 59.3cm$$

2) Calculate the ratio of SBR+BR vs SBS rubber in the sample

The calculations are described in detail in Rødland et al. (2022). Here we use the emission factors available to calculate the expected SBR+BR and SBS values for the specific site based on AADT, percentage of personal (PV) and heavy vehicles (HV), percentage of studded tires. A road length is needed for the emission calculations and this is set to 0.1km for all sites. The calculation is summarized for all sites in SI Tables S6-S7.

Equation 2

$$EM_T = (L_r * N_{v,r,t} * ((R_{PV} * EFT_{PV}) + (R_{HV} * EFT_{HV}))$$

Equation 3

$$EM_A = L_r * N_{v,r,t} * (((R_{PV-st} * EFA_{PV-st}) + (R_{PV-nst} * EFA_{PV-nst}) * R_{PV}) + ((R_{HV-st} * EFA_{HV-st}) + (R_{HV-nst} * EFA_{PV-nst}) * R_{HV}))$$

Where:

EM_T is estimated mass of tire in a sample (mg);

EM_A is the estimated mass of asphalt in a sample (mg);

L_r is the length of the particular road stretch *r* (km);

$N_{v,r,t}$ is the number of vehicles that have travelled the particular road stretch *r* during the given time period *t*;

EFT_{PV} is the emission factor for personal vehicle tires (mg/vkm);

EFT_{HV} is the emission factor for heavy vehicle tires (mg/vkm);

R_{PV} is the ratio of personal vehicles at the sampling location;

R_{HV} is the ratio of heavy vehicles at the sampling location;

EFA_{PV-st} is the emission factor for asphalt based on studded personal vehicle tires (mg/vkm);

EFA_{PV-nst} is the emission factor for asphalt based on non-studded personal vehicle tires (mg/vkm);

EFA_{HV-st} is the emission factor for asphalt based on studded heavy vehicle tires (mg/vkm);

EFA_{PV-nst} is the emission factor for asphalt based on non-studded heavy vehicle tires (mg/vkm);

R_{PV-st} is the ratio of personal vehicles (PV) with studded tires at the sampling location, compared to all PV vehicles;

R_{PV} is the ratio of personal vehicles (PV) at the sampling location compared to all vehicles;

R_{HV-st} is the ratio of heavy vehicles (HV) with studded tires at the sampling location, compared to all HV vehicles;

R_{HV} is the ratio of heavy vehicles (HV) at the sampling location, compared to all vehicles.

Example Bryn (values from Table S5):

Equation 3:

$$EM_T = (L_r * N_{v,r,t} * ((R_{PV} * EFT_{PV}) + (R_{HV} * EFT_{HV}))$$

$$EM_T = 0.1 * 36919 * ((0.88 * 0.104) + (0.12 * 0.668))$$

$$EM_T = 633.83 g/day$$

SBR+BR in Norwegian winter tires (mean value for PV and HV) = 30%

$$SBR+BR = EM_T * 0.3$$

$$SBR+BR = 633.83 * 0.3$$

$$SBR+BR = 190.1 g/day$$

Equation 3

The road wear emission factors are based on the estimated release of 5-10g/vkm for studded PV. As this is a range, we calculate the road wear for three levels: 5, 7.5 and 10g/vkm and then find the average for each site. For HV the release is estimated at 5 x the PV emissions (25g/vkm). For non-studded vehicles, the release for both PV (0.125g/vkm) and HV (0.625g/vkm) are estimated to be 40 times lower than for studded tires.

The calculation below is for the first level, 5g/vkm.

$$EM_A = L_r * N_{v,r,t} * (((R_{PV-st} * EFA_{PV-st}) + (R_{PV-nst} * EFA_{PV-nst}) * R_{PV}) + ((R_{HV-st} * EFA_{HV-st}) + (R_{HV-nst} * EFA_{PV-nst}) * R_{HV}))$$

$$EM_A = 0.1 * 36919 * (((0.0316 * 5) + \big((1 - 0.0316) * 0.125\big) * 0.88) + ((0.106 * 25) + \big((1 - 0.106) * 0.625\big) * 0.12))$$

$$EM_A = 0.1 * 36919 * (((0.0316 * 5) + \big((1 - 0.0316) * 0.125\big) * 0.88) + ((0.106 * 25) + \big((1 - 0.106) * 0.625\big) * 0.12))$$

$$EM_A = 2326 g/day$$

In the asphalt used on these locations, 5% PMB is added and 5% of the PMB is SBS rubber.

The estimated SBS rubber at Bryn is therefore:

$$SBS = EM_A * 0.0025$$

$$SBS = 5.8\ g/day$$

The combined mass of SBR+BR+SBS for Bryn is then estimated at 195.9g/day, for the first level for road wear emissions. In percentage, SBS contributes 3% of the total rubber mass. All three levels of SBS is calculated for each location and used in the following equations 5 and 6 (Rødland et al., 2022).

Equation 5

$$M_T = \frac{M_S - (M_S * R_{SBS}) * Sc}{(S_{PV} * R_{PV}) + (S_{HV} * R_{HV})}$$

Equation 6

$$M_{PMB} = \frac{(M_S * R_{SBS})}{C_{PMB}}$$

where

M_T is the mass of tire in a sample (mg);

M_{PMB} is the mass of PMB in a sample (µg);

M_S is the mass of SBR+BR+SBS in a sample (µg);

R_{SBS} is the estimated ratio of SBS from the total SBR+BR+SBS concentration for each location;

Sc is the conversion factor for styrene content in standards vs tires;

S_{PV} is the mass of SBR+BR in personal vehicle tires (µg/mg);

R_{PV} is the ratio of personal vehicles at the sampling location;

$S_{HV}$is the mass of SBR+BR in heavy vehicle tires (µg/mg);

R_{HV} is the ratio of heavy vehicles at the sampling location;

C_{PMB} is the conversion factor for SBS to PMB, based on the percentage SBS in PMB (0.05).

Example from Bryn 0m. The measured concentration of SBR+BR+SBS was 107333.5 µg/L. The input variables for each site is found in Tables SI-X.

Equation 5

$$M_T = \frac{M_S - (M_S * R_{SBS}) * Sc}{(S_{PV} * R_{PV}) + (S_{HV} * R_{HV})}$$

$$M_T = \frac{107333.5 - (107333.5 * 0.047) * 1}{(278.6 * 0.88) + (318.0 * 0.12)}$$

$$M_T = 360.9\ mg/L$$

The M_T concentration is calculated using Crystal Ball Monte Carlo simulation, where RSBS has a triangular distribution pattern with 4.7% as the mean value, SPV has a logistic distribution with a mean of 278.6 µg/mg rubber in winter tires and SHV has a beta distribution with 318.0 µg/mg rubber in winter tires. The

model runs for 100 000 predictions and the summary statistics used from this is the predicted mean value, standard deviation, median, 10th, 25th, 75th and 90th percentiles. These are given in Table SX.

Equation 6

$$M_{PMB} = \frac{(M_S * R_{SBS})}{C_{PMB}}$$

$$M_{PMB} = \frac{(107.3 * 0.047)}{0.05}$$

$$M_{PMB} = 101.7\ mg/L$$

The M_{PMB} concentration is calculated using the Crystal Ball Monte Carlo simulation, where RSBS has a triangular distribution pattern with 4.7% as the mean value.

SI-6 Results summarized from using Equation 5

Table S6. The table summarizes the results from using Equation 5, where the input variables RSBS, SPV and SHV (in yellow) have a distribution assumption fitted to the values and the variables M_S, S_C, R_{PV} and RT (in white) are constant. The output value M_T (in blue) is then predicted with 100 000 Monte Carlo simulations, which gives an average M_T and the standard deviation for each sample. The average M_T and standard deviation for all samples is calculated based on the predicted average M_T.

	Output values	Input variables							Predicted values						
Sample	M_T (mg/mL)	M_S (µg/mL)	R_{SBS}	S_C	S_{PV} (µg/mg)	S_{HV} (µg/mg)	R_{PV}	R_{HV}	Average M_T (mg/mL)	Standard deviation (mg/mL)	Median (mg/mL)	10th (mg/mL)	25th (mg/mL)	75th (mg/mL)	90th (mg/mL)
Bryn 0 m	360.9	107333.5	0.047	1.00	278.6	318.0	0.88	0.12	383	360	351	282	316	417	493
Bryn 1 m	673.3	200277.4	0.047	1.00	278.6	318.0	0.88	0.12	714	672	654	527	590	779	920
Bryn 3 m	2632.49	782996.0	0.036	1.00	278.6	318.0	0.88	0.12	2790	2630	2560	2060	2310	3050	3600
Carl Berner 0 m	1893.6	557960.2	0.036	1.00	278.6	318.0	0.86	0.14	2120	1890	37000	1480	1660	2200	2590
Carl Berner 1 m	560.9	165283.4	0.036	1.00	278.6	318.0	0.86	0.14	628	560	11000	439	491	649	765
Carl Berner 3 m	214.6	63229.9	0.036	1.00	278.6	318.0	0.86	0.14	240	214	4200	168	188	248	293
Frogner 0 m	108.6	31709.2	0.036	1.00	278.6	318.0	0.93	0.07	117	108	254	84.7	95.0	126	149
Frogner 3 m	133.6	38992.5	0.036	1.00	278.6	318.0	0.93	0.07	143	133	312	104	117	155	184
Holstad 0 m	398.3	118590.6	0.046	1.00	278.6	318.0	0.86	0.14	446	398	7730	312	349	461	543
Holstad 3 m	233.7	69594.9	0.046	1.00	278.6	318.0	0.86	0.14	262	233	4540	183	205	270	319
Ila 0 m	698.4	204956.0	0.037	1.00	278.6	318.0	0.90	0.10	753	697	9130	546	612	808	957
Ila 1 m	376.1	110357.0	0.037	1.00	278.6	318.0	0.90	0.10	405	375	4920	294	329	435	515
Ila 3 m	96.8	28406.2	0.037	1.00	278.6	318.0	0.90	0.10	104	96.6	1270	75.7	84.8	112	133
Lysaker 0 m	14058.0	4438411.9	0.108	1.00	278.6	318.0	0.92	0.08	14500	13900	135000	10900	12200	16200	19200
Lysaker 1 m	3741.6	1181295.4	0.108	1.00	278.6	318.0	0.92	0.08	3860	3710	35900	2900	3260	4310	5120
Lysaker 3 m	491.7	155246.6	0.108	1.00	278.6	318.0	0.92	0.08	507	488	4710	382	428	566	672
Skullerud 0 m	2092.4	622340.5	0.047	1.00	278.6	318.0	0.88	0.12	2220	2090	2030	1640	1830	2420	2860
Skullerud 1 m	1648.4	490296.6	0.047	1.00	278.6	318.0	0.88	0.12	1750	1640	1600	1290	1440	1910	22540

Skullerud 3 m	100.8	29980.9	0.047	1.00	278.6	318.0	0.88	0.12	107	101	97.8	78.9	88.3	117	138
Storo 0 m	12792.3	3747325.4	0.037	1.00	278.6	318.0	0.91	0.09	13700	12800	31500	1000	11200	14800	17500
Storo 1 m	8438.7	2471993.6	0.037	1.00	278.6	318.0	0.91	0.09	9010	8420	20800	6590	7390	9760	11600
Tøyen 0 m	143.4	41780.0	0.036	1.00	278.6	318.0	0.94	0.06	153	143	430	112	125	166	198
Tøyen 1 m	71.1	20729.5	0.036	1.00	278.6	318.0	0.94	0.06	76.0	70.9	214	55.4	62.2	82.4	98.1
Tøyen 3 m	329.5	95997.3	0.036	1.00	278.6	318.0	0.94	0.06	352	328	989	257	288	381	454
Ullevål 0 m	1670.3	489291.0	0.037	1.00	278.6	318.0	0.91	0.09	1780	1670	4160	1310	1460	1930	2290
Ullevål 1 m	1280.4	375079.3	0.037	1.00	278.6	318.0	0.91	0.09	1370	1280	3190	1000	1120	1480	1760
Ullevål 3 m	793.8	232537.5	0.037	1.00	278.6	318.0	0.91	0.09	848	792	1980	620	695	918	1090
Vinterbro 0 m	1240.6	362923.8	0.046	1.00	278.6	318.0	0.92	0.08	1290	1240	12000	969	1090	1440	1700
Vinterbro 1 m	1566.9	458363.5	0.046	1.00	278.6	318.0	0.92	0.08	1620	1560	15100	1220	1370	1810	2150
Vinterbro 3 m	391.2	115515.0	0.046	1.00	278.6	318.0	0.92	0.08	405	390	3750	305	342	452	537

Table S7. The table summarizes the PMB results from using Equation 6, where the input variables RSBS (in yellow) have a distribution assumption fitted to the values and the variables M_S and C_{PMB} (in white) are constant. The output value M_{PMB} (in blue) is then predicted with 100 000 Monte Carlo simulations, which gives an average M_{PMB} and the standard deviation for each sample. The average M_{PMB} and standard deviation for all samples are calculated based on the predicted average M_{PMB}.

	Output values	Input variables							Predicted values						
Sample	M_{PMB} (mg/mL)	M_S (mg/mL)	R_{SBS}	S_C	S_{PV} (µg/mg)	S_{HV} (µg/mg)	R_{PV}	R_{HV}	Average M_{PMB} (mg/mL)	Standard deviation (mg/mL)	Median (mg/mL)	10th (mg/mL)	25th (mg/mL)	75th (mg/mL)	90th (mg/mL)
Bryn 0 m	101.7	107.3	0.047	1.00	278.6	318.0	0.88	0.12	102	104	104	17.0	81.5	91.8	116
Bryn 1 m	189.7	200.3	0.047	1.00	278.6	318.0	0.88	0.12	190	194	193	31.7	152	171	217
Bryn 3 m	741.8	783.0	0.036	1.00	278.6	318.0	0.88	0.12	742	760	755	124	595	670	848
Carl Berner 0 m	398.2	558.0	0.036	1.00	278.6	318.0	0.86	0.14	398	414	411	75.9	314	359	468
Carl Berner 1 m	118.0	165.3	0.036	1.00	278.6	318.0	0.86	0.14	118	123	122	22.5	93.0	106	139
Carl Berner 3 m	45.1	63.2	0.036	1.00	278.6	318.0	0.86	0.14	45.1	46.9	46.5	8.60	35.6	40.7	53.0
Frogner 0 m	22.9	31.7	0.036	1.00	278.6	318.0	0.93	0.07	22.9	23.7	23.5	4.23	18.1	20.6	26.7
Frogner 3 m	28.1	39.0	0.036	1.00	278.6	318.0	0.93	0.07	28.1	29.1	28.9	5.21	22.3	25.4	32.8
Holstad 0 m	108.6	118.6	0.046	1.00	278.6	318.0	0.86	0.14	109	112	111	19.5	86.4	98.1	126
Holstad 3 m	63.7	69.6	0.046	1.00	278.6	318.0	0.86	0.14	63.7	65.8	65.3	11.4	50.7	57.6	74.0
Ila 0 m	152.1	205.0	0.037	1.00	278.6	318.0	0.90	0.10	152	156	155	26.6	121	137	175
Ila 1 m	81.9	110.4	0.037	1.00	278.6	318.0	0.90	0.10	81.9	84.2	83.7	14.3	65.2	73.9	94.4
Ila 3 m	21.1	28.4	0.037	1.00	278.6	318.0	0.90	0.10	21.1	21.7	21.5	3.68	16.8	19.0	24.3
Lysaker 0 m	9546.0	4438.4	0.108	1.00	278.6	318.0	0.92	0.08	9546	10000	9930	1330	8310	9050	11000
Lysaker 1 m	2540.7	1181.3	0.108	1.00	278.6	318.0	0.92	0.08	2541	2670	2640	354	2210	2410	2920
Lysaker 3 m	333.9	155.2	0.108	1.00	278.6	318.0	0.92	0.08	334	351	347	46.5	291	317	384
Skullerud 0 m	589.6	622.3	0.047	1.00	278.6	318.0	0.88	0.12	590	603	600	98.8	472	532	674

Skullerud 1 m	464.5	490.3	0.047	1.00	278.6	318.0	0.88	0.12	464	475	473	77.8	372	419	531
Skullerud 3 m	28.4	30.0	0.047	1.00	278.6	318.0	0.88	0.12	28.4	29.1	28.9	4.76	22.7	25.6	32.5
Storo 0 m	2756.1	3747.3	0.037	1.00	278.6	318.0	0.91	0.09	2756	2840	2820	490	2190	2480	3190
Storo 1 m	1818.1	2472.0	0.047	1.00	278.6	318.0	0.91	0.09	1818	1870	1860	324	1450	1640	2110
Tøyen 0 m	29.8	41.8	0.047	1.00	278.6	318.0	0.94	0.06	29.8	31.0	30.7	5.66	23.5	26.9	35.0
Tøyen 1 m	14.8	20.7	0.036	1.00	278.6	318.0	0.94	0.06	14.8	15.4	15.3	2.81	11.7	13.3	17.4
Tøyen 3 m	68.5	96.0	0.036	1.00	278.6	318.0	0.94	0.06	68.5	71.2	70.6	13.0	54.1	61.8	80.4
Ullevål 0 m	359.9	489.3	0.036	1.00	278.6	318.0	0.91	0.09	360	371	369	63.8	287	325	416
Ullevål 1 m	275.9	375.1	0.036	1.00	278.6	318.0	0.91	0.09	276	284	283	48.9	220	249	319
Ullevål 3 m	171.0	232.5	0.036	1.00	278.6	318.0	0.91	0.09	171	176	175	30.3	136	154	198
Vinterbro 0 m	332.2	362.9	0.036	1.00	278.6	318.0	0.92	0.08	332	343	341	59.8	264	300	386
Vinterbro 1 m	419.6	458.4	0.046	1.00	278.6	318.0	0.92	0.08	420	433	430	75.5	334	378	487
Vinterbro 3 m	105.7	115.5	0.046	1.00	278.6	318.0	0.92	0.08	106	109	108	19.0	84.1	95.4	123

SI-7 All concentration data summarized

Table S8. The table summarizes all concentration data in the study. The SBR+BR+SBS concentration (mg/L, mg/m²) and TSS (mg/L, mg/m²) are the measured values. The meltwater concentrations (mg(L) of tire and PMB are calculated using Crystal ball Monte Carlo simulation and includes the predicted mean value and the predicted standard deviation value. The meltwater concentrations of tire and PMB are used to calculate the mass load concentrations (mg/m²) of tire and PMB.

Road type	Site	Code	Distance	SBR+BR+SBS		TSS		Tire		Tire		PMB		PMB	
Unit				Mean. mg/L	Mean. mg/m²	Mean. mg/L	Mean, mg/ m2	Mean, mg/L	s.d., mg/L	Mean, mg/m²	s.d., mg/m²	Mean, mg/L	s.d., mg/L	Mean, mg/ m²	s.d., mg/m²
Inter-city Highway	Holstad	IC-1	0	119	179	65600	99300	446	398	672	599	109	112	164	169
			3	69.6	109	7660	11900	262	233	408	364	63.7	65.8	99.4	103
	Skullerud	IC-2	0	622	3460	54500	302000	2220	2090	12300	11600	590	603	3270	3350
			1	490	1890	37400	144000	1750	1640	6750	6330	465	475	1790	1830
			3	30	86.4	4210	12100	107	101	308	290	28.4	29.1	81.8	83.7
	Vinterbro	IC-3	0	363	932	26000	66700	1290	1240	3310	3180	332	343	853	881
			1	458	1360	46400	137000	1620	1560	4790	4610	420	433	1240	1281
			3	116	1370	14600	173000	405	390	4820	4630	106	109	1260	1300
	All sites		All	283	1170	32100	118000	1012	804	4170	4070	264	214	1100	1080
			0	368	1520	48800	156000	1319	887	5440	6110	343	241	1430	1630
			1	474	1620	41900	141000	1685	92	5770	1390	442	31.7	1520	390
			3	71.7	522	8810	65700	258	149	1840	2570	66.0	38.7	479	673
City Highway	Bryn	CH-1	0	107	636	29900	177000	383	360	2270	2130	102	104	603	617
			1	200	1180	27300	160000	714	672	4200	3950	190	194	1110	1140
			3	783	5840	72100	538000	2790	2630	20800	19600	742	760	5540	5670
	Lysaker	CHC-	0	4440	13400	208000	629000	14500	13900	43800	42000	9550	10000	28800	30200

		2													
			1	1180	2860	67500	163000	3860	3710	9330	8970	2540	2670	6140	6450
			3	155	359	15700	36300	507	488	1170	1130	334	351	772	811
	Storo	CH-3	0	3750	29700	355000	2810000	13700	12800	109000	101000	2760	2840	21800	22500
			1	2470	9170	219000	814000	9010	8420	33400	31200	1820	1870	6750	6940
	Ullevål	CH-4	0	489	2960	48100	291000	1780	1670	10779	10100	360	371	2180	2250
			1	375	1390	30400	112000	1370	1280	5060	4730	276	284	1020	1050
			3	233	975	22700	95200	848	792	3550	3320	171	176	717	739
	All sites		All	1290	6230	99600	530000	4500	5350	22100	31900	1710	2780	6860	9550
			0	8790	46700	153000	1240000	7590	7550	48200	48200	3190	4400	14100	14100
			1	4230	14600	86100	312000	3740	3770	13000	13800	1210	1160	3760	3120
			3	1170	7170	36800	223000	1380	1490	8520	11700	416	372	2340	3000
City Urban	Carl Berner	CU-1	0	558	2750	56900	281000	2120	1890	10500	9320	398	414	1960	2040
			1	165	712	20900	90000	628	560	2710	2410	118	123	508	528
			3	63.2	272	4610	19800	240	214	1030	920	45.1	46.9	194	201
	Frogner	CU-2	0	31.7	119	3030	11300	117	108	436	405	22.9	23.7	85.5	88.6
			3	39	187	6090	29200	143	133	687	638	28.1	29.1	135	140
	Ila	CU-3	0	205	930	18000	81800	753	697	3410	3160	152	156	690	709
			1	110	612	9910	54900	405	375	2250	2079	81.9	84.2	454	467
			3	28.4	61	3780	8050	104	97	222	206	21.1	21.7	45.0	46.2
	Tøyen	CU-4	0	41.8	168	5090	20500	153	143	616	574	29.8	31.0	120	125
			1	20.7	72.5	1810	6340	76	71	266	248	14.8	15.4	51.7	53.8
			3	96	432	8160	36800	352	328	1590	1480	68.5	71.2	309	321
	All sites		All	124	574	12600	58100	463	593	2150	2950	89.1	112	414	556
			0	209	992	20800	98600	786	908	3730	4550	151	170	715	853
			1	98.8	465	10900	50400	370	278	1740	1300	71.5	52.4	338	249
			3	56.7	238	5660	23400	210	111	882	575	40.7	21.1	171	111
	All samples		Mean	594	2810	49700	247000	2090	3700	10000	21100	731	1810	2960	6410

All samples	Min	20.7	60.5	1810	6340	76.0	222	14.8	50.0
All samples	Max	4440	29700	355000	2810000	14500	109000	9550	28800

SI-8 Regression analysis of TSS versus SBR+BR+SBS

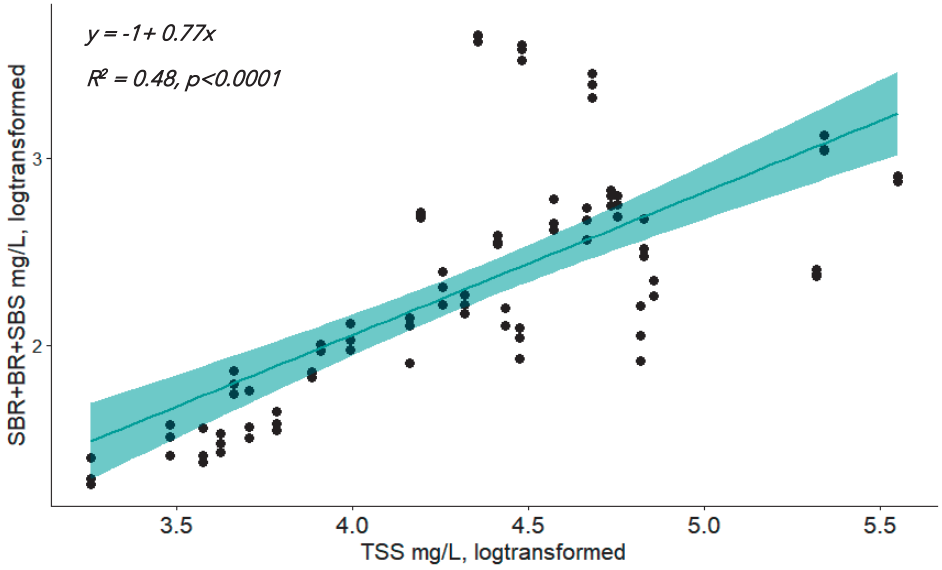

Figure S2. Linear regression of TSS (mg/L, log transformed) and rubber (SBR+BR+SBS, mg/m2, log transformed), showing a R^2 = 0.48 ($p<0.0001$)) and y= -1 + 0.77x. Residuals of regression model are normally distributed (Anderson Darling, p = 0.33)

SI-9 Results from RDA analysis on mass load dataset

*Table S8. Results from RDA analysis on the mass load concentrations of SBR+BR+SBS rubber. The variation in the dataset was explored using two sets of variables. The first analysis was performed using all variables (road group, speed limit, AADT, AADT*speed limit, distance, STOP-GO, %personal vehicles (%PV), % heavy vehicles (%HV), % studded tires (%STD). Only the variables with significant results (p<0.05) is reported in the table. The second analysis was performed without the road group variable. Only the variables with significant results (p<0.05) is reported in the table.*

MELTWATER mg/L All variables	Explains %	pseudo-F	P-value
Simple Effects RDA			
Group-City-Highway	34.4	46.1	0.0001
Group-City-Urban	29.6	37.0	0.0001
Speed limit	22.31	25.3	0.0001
Distance	14.68	15.1	0.0006
*AADT*speed limit*	11.58	11.5	0.0019
AADT	11.53	11.5	0.0008
Conditional Effects RDA			
Group-City-Highway	34.4	46.1	0.0001
Distance	11.7	18.9	0.0002
Speed limit	8.8	16.8	0.0004
Group-City-Urban	3.0	6.0	0.0161
%HV	3.0	6.9	0.0096
%STD	2.8	6.0	0.0176
AADT	2.6	6.3	0.0132
MASS LOAD mg/m²	Explains %	pseudo-F	P-value
All variables			
Simple Effects RDA			
Group-City-Highway	33.8	45.0	0.0001
Group-City-Urban	22.7	25.8	0.0001
Speed limit	15.5	16.1	0.0005
AADT	14.4	14.8	0.0008
*AADT*Speed limit*	13.5	13.7	0.0006
Distance	13.1	13.3	0.001
Conditional Effects RDA			
Group-City-Highway	33.82	45.0	0.0001
Distance	10.35	16.1	0.0003
Speed limit	4.62	7.8	0.0062
Group-City-Urban	2.94	5.2	0.0244

SI-10 Snow core sample data

Table S9. Summary table of all sample data for the collected snow cores and calculation of SWE.

Sample name	Snow core height (cm)	Snow core diameter cm	Total weight of sample g	Total amount of sample mL	Snow volume cm3	Snow density g/cm3	SWE cm
Holstad 0m	7.62						
Holstad 0m	6.35						
Holstad 0m	6.35						
Holstad 0m	5.08						
Holstad 0m	10.16						
Total	35.56	4.2	208.78	64	492.66	0.42	15.07
Holstad 1m	8.89						
Holstad 1m	6.35						
Holstad 1m	7.62						
Holstad 1m	10.16						
Holstad 1m	8.89						
Total	41.91	4.2	194.6	64	580.64	0.34	14.05
Holstad 3m	11.43						
Holstad 3m	10.16						
Holstad 3m	10.16						
Holstad 3m	7.62						
Holstad 3m	10.16						
Total	49.53	4.2	216.18	64	686.21	0.32	15.60
Vinterbro 0m	13.208						
Vinterbro 0m	15.24						
Vinterbro 0m	8.89						
Vinterbro 0m	10.16						
Vinterbro 0m	11.43						
Total	58.928	4.2	355.72	64	816.41	0.44	25.68

Vinterbro 1m	13.97						
Vinterbro 1m	17.78						
Vinterbro 1m	13.97						
Vinterbro 1m	15.748						
Vinterbro 1m	7.62						
Total	69.088	4.2	409.62	264	957.17	0.43	29.57
Vinterbro 3m	48.26						
Vinterbro 3m	49.53						
Vinterbro 3m	45.72						
Vinterbro 3m	33.02						
Vinterbro 3m	40.64						
Total	217.17	4.2	1646.12	2064	3008.77	0.55	118.82
Skullerud 0m	19.05						
Skullerud 0m	17.78						
Skullerud 0m	24.13						
Skullerud 0m	21.59						
Skullerud 0m	16.51						
Total	99.06	4.2	769.48	1264	1372.42	0.56	55.54
Skullerud 1m	16.51						
Skullerud 1m	13.97						
Skullerud 1m	21.59						
Skullerud 1m	19.05						
Skullerud 1m	8.89						
Total	80.01	4.2	534.34	664	1108.49	0.48	38.57
Skullerud 3m	13.97						
Skullerud 3m	12.7						
Skullerud 3m	11.43						
Skullerud 3m	16.51						
Skullerud 3m	15.24						

Total	69.85	4.2	399.01	714	967.73	0.41	28.80
Bryn 0 m	13.97						
Bryn 0 m	22.86						
Bryn 0 m	20.32						
Bryn 0 m	22.86						
Bryn 0 m	24.13						
Total	104.14	4.2	821.06	240	1442.80	0.57	59.26
Bryn 1 m	22.86						
Bryn 1 m	31.5						
Bryn 1 m	22						
Bryn 1 m	25.5						
Bryn 1 m	25.5						
Total	127.36	4.2	813.72	992	1764.50	0.46	58.73
Bryn 3 m	32.5						
Bryn 3 m	24						
Bryn 3 m	21						
Bryn 3 m	17.5						
Bryn 3 m	17.5						
Total	112.5	4.2	1033.95	240	1558.62	0.66	74.63
Storo 0 m	22						
Storo 0 m	24.5						
Storo 0 m	18.5						
Storo 0 m	30						
Storo 0 m	23						
Total	118	4.2	1097.52	1564	1634.82	0.67	79.22
Storo 1 m	11						
Storo 1 m	11.5						
Storo 1 m	7.5						
Storo 1 m	17.5						

Storo 1 m	13						
Total	60.5	4.2	514.16	564	838.19	0.61	37.11
Lysaker 0 m	14						
Lysaker 0 m	6						
Lysaker 0 m	9						
Lysaker 0 m	12.5						
Lysaker 0 m	8						
Total	49.5	4.2	418.62	160	685.79	0.61	30.22
Lysaker 1 m	10						
Lysaker 1 m	8						
Lysaker 1 m	9						
Lysaker 1 m	9						
Lysaker 1 m	7.5						
Total	33.5	4.2	334.88	144	464.12	0.72	24.17
Lysaker 3 m	4.5						
Lysaker 3 m	4						
Lysaker 3 m	3.5						
Lysaker 3 m	3						
Lysaker 3 m	3						
Lysaker 3 m	7.5						
Lysaker 3 m	2						
Lysaker 3 m	6						
Lysaker 3 m	6.5						
Lysaker 3 m	8						
Total	48	4.2	320.35	208	665.01	0.48	23.12
Ullevål st. 0 m	17						
Ullevål st. 0 m	22						
Ullevål st. 0 m	24.5						
Ullevål st. 0 m	19.5						

Ullevål st. 0 m	25						
Total	108	4.2	839	1064	1496.28	0.56	60.56
Ullevål st. 1 m	19						
Ullevål st. 1 m	14						
Ullevål st. 1 m	6.5						
Ullevål st. 1 m	15						
Ullevål st. 1 m	21						
Total	75.5	4.2	511.48	732	1046.01	0.49	36.92
Ullevål st. 3 m	8						
Ullevål st. 3 m	10.5						
Ullevål st. 3 m	9.5						
Ullevål st. 3 m	10.5						
Ullevål st. 3 m	6						
Ullevål st. 3 m	8						
Ullevål st. 3 m	7						
Ullevål st. 3 m	10						
Ullevål st. 3 m	9						
Ullevål st. 3 m	6						
Total	84.5	4.2	580.68	714	1170.70	0.50	41.91
Frogner 0 m	7						
Frogner 0 m	7.5						
Frogner 0 m	7.5						
Frogner 0 m	7						
Frogner 0 m	4						
Frogner 0 m	2						
Frogner 0 m	3						
Frogner 0 m	10						
Frogner 0 m	15						
Frogner 0 m	15						

Total	78	4.2	517.95	814	1080.65	0.48	37.39
Frogner 3 m	7						
Frogner 3 m	7						
Frogner 3 m	10						
Frogner 3 m	9						
Frogner 3 m	16						
Frogner 3 m	10						
Frogner 3 m	14						
Frogner 3 m	18						
Frogner 3 m	11.5						
Frogner 3 m	13.5						
Total	116	4.2	663.97	864	1607.11	0.41	47.92
Ila 0 m	22						
Ila 0 m	18						
Ila 0 m	17						
Ila 0 m	12						
Ila 0 m	8						
Total	77	4.2	628.35	732	1066.79	0.59	45.35
Ila 1 m	22						
Ila 1 m	19.5						
Ila 1 m	26.5						
Ila 1 m	22						
Ila 1 m	20						
Total	110	4.2	767.79	882	1523.99	0.50	55.42
Ila 3 m	7						
Ila 3 m	9.5						
Ila 3 m	8						
Ila 3 m	8						
Ila 3 m	8						

Total	40.5	4.2	295.47	164	561.10	0.53	21.33
Tøyen 0 m	11						
Tøyen 0 m	16						
Tøyen 0 m	20						
Tøyen 0 m	14						
Tøyen 0 m	10						
Total	71	4.2	557.08	1064	983.66	0.57	40.21
Tøyen 1 m	15						
Tøyen 1 m	12						
Tøyen 1 m	17						
Tøyen 1 m	15						
Tøyen 1 m	14						
Total	73	4.2	484.39	664	1011.37	0.48	34.96
Tøyen 3 m	15						
Tøyen 3 m	16						
Tøyen 3 m	18						
Tøyen 3 m	21						
Tøyen 3 m	19.5						
Total	89.5	4.2	623.99	864	1239.97	0.50	45.04
Carl Berner 0m	11.5						
Carl Berner 0m	15						
Carl Berner 0m	21						
Carl Berner 0m	19						
Carl Berner 0m	22						
Total	88.5	4.2	683.33	632	1226.12	0.56	49.32
Carl Berner	12						

1m							
Carl Berner 1m	17.5						
Carl Berner 1m	16						
Carl Berner 1m	24						
Carl Berner 1m	14						
Total	83.5	4.2	596.89	1132	1156.84	0.52	43.08
Carl Berner 3m	21						
Carl Berner 3m	4						
Carl Berner 3m	25						
Carl Berner 3m	22.5						
Carl Berner 3m	17						
Total	89.5	4.2	594.96	1064	1239.97	0.48	42.94
Referanse	18						
Referanse	15						
Referanse	12.5						
Referanse	15						
Referanse	18						
Total	78.5	4.2	417.6	814	1087.57	0.38	30.14

References

Bakløkk L, Horvli I, Myran T. Piggdekkslitasje og støvutvikling. Status-Litteraturstudie. SINTEF Bygg og miljøteknikk, Avdeling Vegteknikk, 1997.

Horvli I. Generelt. Dekketyper, egenskaper og bruksområder, EVU-kurs Asfaltdekker 2003. Notat 949, March 1996. Institutt for bygg, anlegg og transport, NTNU, 1996.

Klein J., Molnár-in 't Veld H., Geilenkirchen G., Hulskotte J., Ligterink N., Dellaert S., et al. Methods for calculating transport emissions in the Netherlands. Force on Transportation of the Dutch Pollutant Release and Transfer Register. PBL Netherlands Environmental Assessment Agency. , 2017, pp. 75.

Moghadas S, Paus KH, Muthanna TM, Herrmann I, Marsalek J, Viklander M. Accumulation of Traffic-Related Trace Metals in Urban Winter-Long Roadside Snowbanks. . Water, Air & Soil Pollution 2015; 226: 404.

Rødland ES, Samanipour S, Rauert C, Okoffo ED, Reid MJ, Heier LS, et al. A novel method for the quantification of tire and polymer-modified bitumen particles in environmental samples by pyrolysis gas chromatography mass spectroscopy. Journal of Hazardous Materials 2022; 423: 127092.

Snilsberg B. Pavement wear and airborne dust pollution in Norway-Characterization of the physical and chemical properties of dust particles. . PhD. NTNU, 2008.

Snilsberg B, Saba RG, Uthus N. Asphalt pavement wear by studded tires – Effects of aggregate grading and amount of coarse aggregate. 6th Euroasphalt & Eurobitume Congress, Prague Czech Republic, 2016.

Paper IV

Characterization of Tire and Road Wear Microplastic Particle contamination in a Road Tunnel: from surface to release

Elisabeth S. Rødland[1,2], Ole Christian Lind[2], Malcolm Reid[1], Lene S. Heier[3], Emelie Skogsberg[1,2], Brynhild Snilsberg[3], Dagfin Gryteselv[3], Sondre Meland[1,2]

[1]Norwegian Institute for Water Research, Økernveien 94, NO-0579 Oslo, Norway
[2]Norwegian University of Life Sciences, Center of Excellence in Environmental Radioactivity (CERAD), Faculty of Environmental Sciences and Natural Resource Management, P.O. Box 5003, 1433 Ås, Norway
[3]Norwegian Public Roads Administration, N-2605 Lillehammer, Norway

TOC

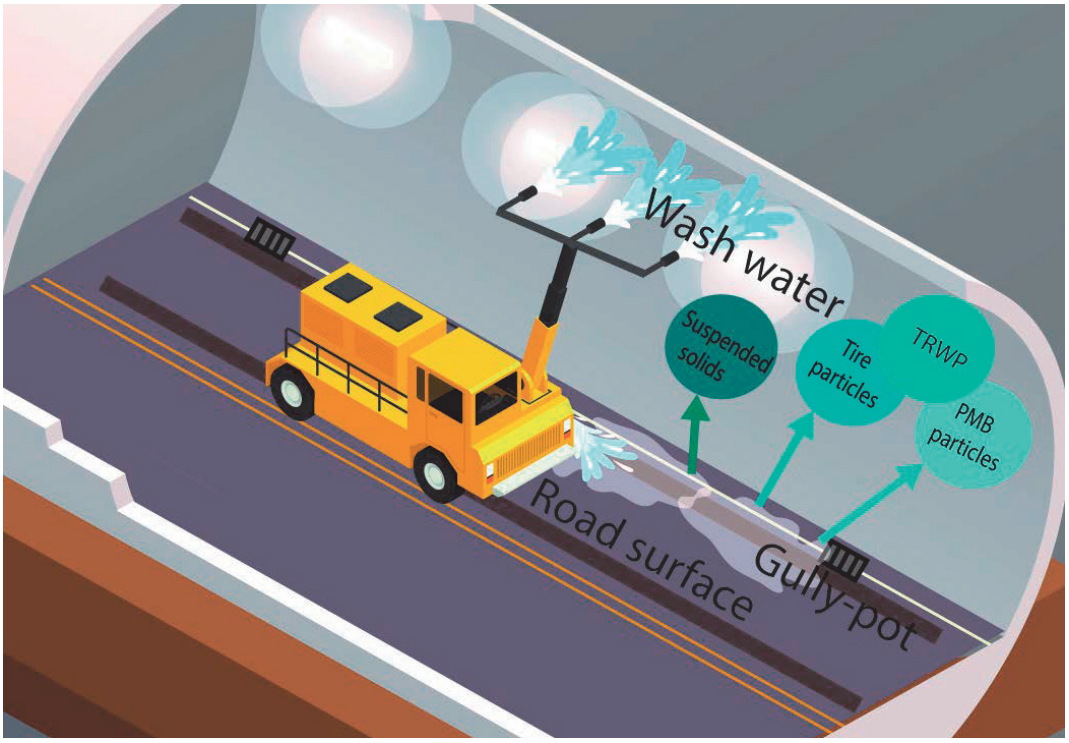

Abstract

Road pollution is one of the major sources of microplastic particles to the environment. The distribution of tire, polymer-modified bitumen (PMB) and tire and road wear particles (TRWP) in different tunnel compartments were explored: road surface, gully-pots and tunnel wash water. A new method for calculating TRWP using Monte Carlo simulation is presented. The highest concentrations on the surface were in the side bank (tire:13.4±5.67;PMB:9.39±3.96; TRWP:22.9±8.19 mg/m^2), comparable to previous studies, and at the tunnel outlet (tire:7.72±11.2; PMB:5.40±7.84; TRWP:11.2±16.2 mg/m^2). The concentrations in gully-pots were highest at the inlet (tire:24.7±26.9; PMB:17.3±48.8; TRWP:35.8±38.9 mg/g) and comparable to values previously reported for sedimentation basins. Untreated wash water was comparable to road runoff (tire:38.3±10.5; PMB:26.8±7.33; TRWP:55.3±15.2 mg/L). Sedimentation treatment retained 63% of tire and road wear particles, indicating a need to increase the removal efficiency to prevent these from entering the environment. A strong linear relationship (R2-adj=0.88, $p<0.0001$) between total suspended solids (TSS) and tire and road wear rubber were established, suggesting a potential for using TSS as a proxy for estimating rubber loads for monitoring purposes. Future research should focus on a common approach to analysis and calculation of tire, PMB and TRWP and address the uncertainties related to these calculations.

1 Introduction

Road tunnels are considered pollution "hot spots", accumulating pollutants from both vehicles and the road surface over time. Several studies have therefore characterized and assessed the levels of traffic-associated pollutants in tunnel wash water, with examples of pollutants such as zinc (Zn), lead (Pb), copper (Cu), polycyclic aromatic hydrocarbons (PAH), and abrasion particles from brakes, tires, and the road surface (Allan et al., 2016; Hallberg et al., 2014; Meland et al., 2010a). Recently, attention has been given to microplastic particles associated with roads and traffic, as tire wear particles and road wear particles contain synthetic rubbers, and contribute a substantial amount of rubbers to the overall microplastic particle release into the environment (Boucher et al., 2020; Knight et al., 2020; Sundt et al., 2021). Previous studies have defined particles released from tire wear and subsequently mixed with road wear mineral particles as the hetero-aggregated tire and road wear particle (TRWP) (Kreider et al., 2010). These are estimated to contain 50% tire tread and 50% road wear (Kreider et al., 2010), in which the rubber concentration (SBR+BR) in the tire is estimated at 50% (Unice et al., 2012; Unice et al., 2013). However, the assumption of road wear content in TRWP is based on a small number of studies and the use of a fixed percentage estimation of 50% road wear in TRWP has been questioned by a recent study (Klöckner et al., 2021). Also, the assumption that all tires contain 50% synthetic rubber have recently been discussed, as new research show a large variation in Styrene Butadiene rubber (SBR) and Butadiene rubber (BR) between different tires (Rauert et al., 2021; Rødland et al., 2022b). It has also been reported that polymer-modified bitumen (PMB) typically added to the road asphalt where traffic density is high, also contain a synthetic rubber similar to the rubber used in tires (Rødland et al., 2022b). However, PMB concentrations have so far only been reported for road-side snow (Rødland et al., 2022a).

The present study aimed to provide a characterization of total suspended solids (TSS) and road-associated microplastic particles, including tire particles, PMB particles and TRWP, through a road tunnel system, from the road surface of various parts of the tunnel to the release of tunnel wash water, with an assessment of levels

retained in gully-pots and sedimentation treatment. Previous studies of tunnels have reported that most of the road dust accumulates in the side bank area close to the tunnel walls and between wheel tracks and low particle concentrations are found in the wheel tracks, as well as reporting higher concentrations in the tunnel inlets compared to the outlets (NPRA, 2017; NPRA, 2021b).Most tunnels have drainage systems that convey the tunnel wash water out of the tunnel. Gully-pots are an important part of the drainage system and are used to trap sediment, debris, and larger particles to avoid clogging of the pipes. Previous literature has however suggested that these gully-pots have a limited effect in removing TRWP from tunnel wash water due to the density of TRWP and the design of most gully-pots (Andersson et al., 2018; Vogelsang et al., 2018). In some tunnels, treatment facilities have been built, to remove pollutants before the water is released into the environment. The correlation between pollutants and TSS makes sedimentation an efficient treatment of tunnel wash water (Allan et al., 2016; Hallberg et al., 2014; Paruch and Roseth, 2008; Roseth and Amundsen, 2003; Roseth and Meland, 2006). Based on these previous studies, it has been assumed that sedimentation treatment potentially also retains a substantial portion of tire and road wear particles. The most common treatment methods for tunnel wash water are sedimentation ponds and basins (Meland et al., 2010a) , as 40-90% of pollutants are bound to particles (Meland et al., 2010b; Roseth and Amundsen, 2003). TSS removal of >80% is demanded of a sedimentation treatment built for road and tunnel runoff in Norway (NPRA, 2021a), which has been confirmed possible with laboratory tests (TSS removal of 74 – 87%); (Garshol et al., 2015; Nyström et al., 2019)).

There is a need to generate concentration data of tire particles, PMB particles and TRWP for road runoff and tunnel wash water, especially for untreated tunnel wash water that is released directly into the environment. Currently there are no published studies on the tire, PMB and TRWP mass concentrations in tunnel wash water. One recent study, using Zn as a marker for tire wear, reports mass concentrations of TRWP between 110 and 120 mg/g (dry weight; dw) in tunnel road dust (Klöckner et al., 2021). This is approximately ten times higher mass

concentration of TRWP than previously reported for road dust outside of tunnels using Zn (Klöckner et al. (2020); 76.7-9.4 mg/g). This suggests that TRWP do accumulate in tunnels and that tunnel wash water potentially contains high mass concentrations of TRWP compared to the levels currently reported for road runoff (3 – 180 mg/L) (Baumann and Ismeier, 1998; Kumata et al., 2000; Kumata et al., 1997; Kumata et al., 2002; Parker-Jurd et al., 2021; Reddy and Quinn, 1997; Wik and Dave, 2009).

The main hypotheses of this study were:

I. Concentrations of tire and road wear particles on the road surface accumulates in the bank area close to the tunnel walls and in the outlet of the tunnel
II. Tire and road wear particles are not retained in gully-pots in tunnels
III. Untreated tunnel wash water contains higher concentrations of tire and road wear particles compared to road runoff
IV. Treatment of tunnel wash water by sedimentation is efficient in removal of tire and road wear particles (<80%)

2 Experimental

2.1 Sample collection and preparation

All samples were collected in the Smestad tunnel (westbound tube), which is 495 m long and consists of two tubes with two driving lanes in each direction (Oslo, Norway, 22 000 vehicles per day per tube (Annual Average Daily Traffic, AADT), 70 km/h speed limit, 59°56'10.4"N 10°40'47.7"E). Three different types of samples were collected: road surface particles suspended in water, gully-pot sediment, and tunnel wash water (Figure 1).

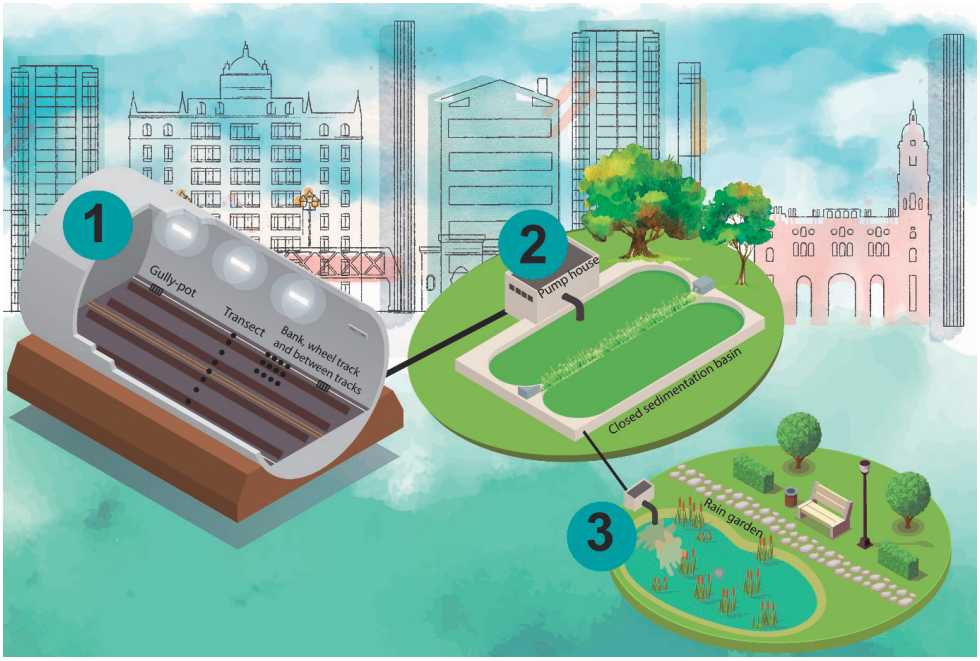

Figure 1.Conceptual drawing of sampling locations: 1) Inside the Smestad tunnel (Road surface: transect of driving lane, road-side bank, in wheel tracks and between wheel tracks, and gully-pots), 2) the pump house (untreated tunnel wash water) and 3) outlet to the raingarden (treated tunnel wash water). Treatment was performed in the closed sedimentation basin before release to the rain garden.

2.1.1 Sampling from the road surface

The road surface samples were collected before a tunnel wash on November 6th, 2019. The road surface was collected with a Wet Dust Sampler (WDS II) (Gustafsson et al., 2019; Lundberg et al., 2019). Sampling was focused on the right driving lane as it is used for normal traffic, while the left lane is for passing traffic. In the inlet and outlet of the tunnel (100m in), samples were collected in the right lane at the roadside bank (B), in the right wheel track (IW) and between wheel tracks (BW) (Figure 2). In the middle of the tunnel, samples were taken across the right and left lane, from B, right IW, BW, left IW, middle between the lanes (M), right IW, BW, left IW and B (Figure 2). The WDS II collects particles (<5mm) in a small area (0.0028m^2) of the surface by applying 330mL high pressurized water in one "shot". Each area was collected by three "shots" and the sample from two areas along the road surface were pooled together (a+b, c+d). All WDS samples were collected in

2L plastic bottles (HDPE plastic bottles, VWR Avantor) and stored at room temperature until analysis.

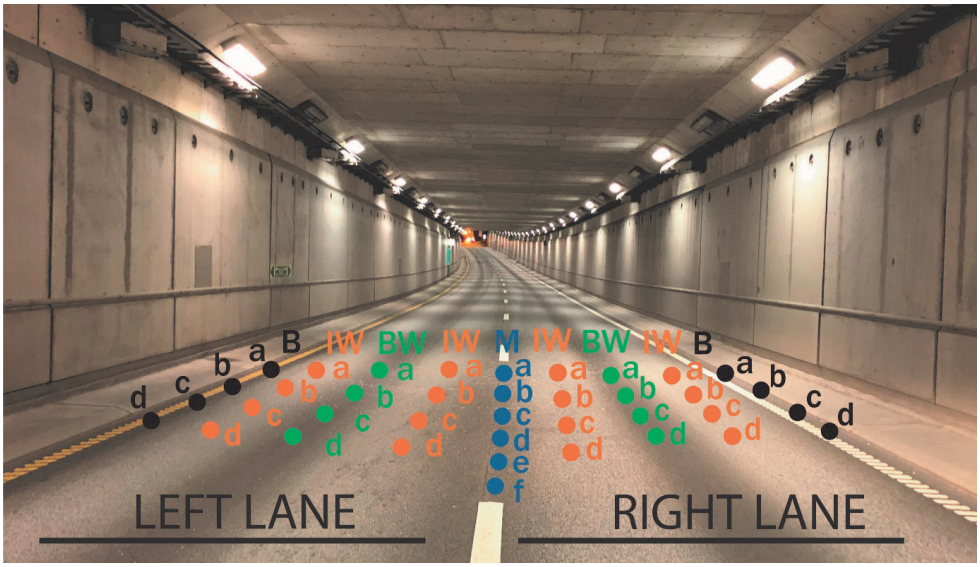

Figure 2. Illustration of sampling with the Wet Dust Samples (WDS II) in Smestad tunnel. The circles indicate the "shot" where pressurized water has been applied to collect particles from the road surface. At the inlet, outlet and middle of the tunnel, samples are collected in the right lane in the bank (B), between wheel tracks (BW) and in right wheel tracks (IW). In the middle of the tunnel, samples were collected in B, BW, left and right IW for both left and right lane and in the middle between the two lanes (M). Photo: Kjersti W. Kronvall, NPRA

2.1.2 Sampling from gully-pots

Sediments from gully-pots were sampled at 100m (GP-1), 250m (GP-2) and 400 m (GP-3) from the tunnel entrance before the tunnel wash on the November 6th, 2019. The sediment was sampled using a small van Veen grab sampler. The gully-pots in this tunnel had not been emptied since February 2019. Multiple grab samples were collected in pre-cleaned (rinsed with RO-water) aluminium foil trays. Triplicate samples from each gully pots were pooled into glass jars (pre-treated in muffle furnace at 480°C, Nabertherm, Germany).

2.1.3 Sampling of tunnel wash water

Untreated tunnel wash water was collected in a pre-basin in the pump house during the tunnel wash on April 21st, 2020, using a small drain pump (Brand Biltema) submerged in the water column. Samples were collected every third minute from the start to the end of the washing event, 14 samples in total. From the pump house, the tunnel wash water was pumped into sedimentation basins, one for each tunnel tube, where the water is let to settle for 21 days. After the 21day sedimentation period, the water is released back into the pre-basin and then pumped into a rain garden. As the water is released into the rain garden, water samples were collected in a time series of 5x5min, 6x10mins and 3x15mins (May 12th, 2020). All wash water samples were collected in 1L plastic bottles (high density polyethylene (HDPE) plastic bottles, VWR Avantor) and stored cool (4°C) until analysis.

2.2 Sample treatment

WDS and tunnel wash water samples were shaken to ensure representative subsampling. For samples with high particle content (by visual inspection), 30 mL water was first transferred to 50 mL Falcon tubes and centrifuged (Thermo Scientific Multifuge 3S/S-R Heraeus, 3000rpm/min), in order to make the filtration step more efficient. Separation of the particles from the water by centrifugation will help to get a larger column of water through the filters, before adding the particle fraction. The supernatant was filtered (13mm glass fibre filter, GF/A, Whatman, pore size 1.6 µm pre-treated in muffle furnace at 480°C) using glass filtration equipment under vacuum. The particle fall-out as resuspended with a small volume (2mL) of filtered RO-water and filtered onto the same filter and dried. Filters were weighed before and after filtration to obtain the mass of total suspended solids (TSS, >1.6 µm) in mg/L filtered water. The TSS measurements for tunnel wash water were performed on 1L replicate samples using 47mm RTU filters (1.5 µm) (analysed by Eurofins Norway). The whole 13 mm filter was folded up and put directly into pyrolysis cups before analysis.

For size distribution in tunnel wash water, the distribution (0.4-2000µm) was measured by laser diffraction (Beckman Coulter LS 13 320; Pye & Blott, 2004). Samples were prepared by mixing the samples (250 mL) with a dispersant (~15 % 0.05 M tetrasodium pyrophosphate) and ultrasonicating for 5 minutes. All samples were analysed for 60 seconds four times and reported as an average of the four. The obscuration limit was set between 8 and 12%. Fraunhofer's optical model was applied for the analysis (refraction index 1.333 and absorbation index 0.1). The size distribution was calculated on a volume percentage, and classification was based on a previous size distribution of TRWP (Kreider et al., 2010).

For the sediment samples from the gully-pots, the glass jars were frozen (-20C, >24H) and freeze dried (3-4 days, Leybold Heraeus Lyovac GT2). Next, the sediment samples were dry sieved (1 mm sieve, VWR) and weighed directly into pyrolysis cups (3.4-13.3 mg/cup) before analysis.

2.3 Pyrolysis GC-MS

Samples were analysed with a Multi-Shot Pyrolyzer (EGA/PY-3030D) equipped with an Auto-Shot Sampler (AS-1020E) (Frontier lab Ltd., Fukushima, Japan) coupled to gas chromatography mass spectrometer (GC/MS) (5977B MSD with 8860 GC, Agilent Technologies Inc., CA, USA), following the method of Rødland et al. (2022b). Samples were pyrolyzed in single-shot mode at 700 °C for 0.2 min (12 s). Injections were made using a 50:1 split and with a pyrolyzer interface temperature at 300 °C. The selected markers for Styrene Butadiene rubber (SBR), Butadiene Rubber (BR) and Styrene Butadiene Styrene (SBS) consisted of m/z 78 Da for benzene, m/z 118 Da for α-methylstyrene, m/z 117 Da for ethylstyrene and m/z 91 Da for butadiene trimer, and the method uses the combined peak heights of the four markers normalized against an internal standard (deuterated Polybutadiene, d6- PB). To demonstrate the presence of the four markers, the total ion chromatograms (TIC, pyrogram) of one tunnel wash water sample (TW-1-1) and one 30 µg SBR (quality control) sample are presented in the SI (SI-6). The calibration curve was created with three different ratios of SBR and SBS (20:80, 40:60 and 80:20). A total mass of SBR +

SBS of 1 µg, 5 µg, 25 µg, 50µg and 100 µg was inserted into pyrolysis cups (n = 3 for each ratio of SBR:SBS) and spiked with 25 µg d6-PB as internal standard. The normalized sum peak of all marker compounds is plotted against the mass of SBR + SBS at each calibration level to form the calibration curve (R = 0.99) (Figure SI-1).The signal to noise ratio (S/N) is determined by the Agilent Masshunter software for each of the selected markers. The limit of detection (LOD) is calculated as 3 x S/N and the limit of quantification (LOQ) is calculate as 10 x S/N. The lowest limit for any marker compound (if they are different) will determine the LOD and LOQ for the analysis.

2.4 Concentration calculations

2.4.1 Tire and PMB concentrations

Tire and PMB concentrations are calculated based on the SBR+BR+SBS concentrations following the method described in detail in Rødland et al. (2022a). A detailed calculation example is given in SI-4 and SI-5. The value for SBR+BR+SBS for each sample is reported in the Supplementary for each tunnel compartment (SI-2 and SI-3).

2.4.2 TRWP calculations

TRWP are defined as the hetero-aggregates of tire and road wear particles, where the tire tread is mixed with mineral particles from the road surface when abraded. According to previous morphology studies, the mineral encrustment of tire particles collected from road surfaces ranges from 6% to 53% (Kreider et al., 2010; Sommer et al., 2018). The encrustment level was found to be highest where the speed limit is lower and with higher frequency of "stop and go" driving, as more road wear particles are left on the road surface and available for mixing with the tire wear particles (Sommer et al., 2018). Based on density analysis, a recent study of tunnel road dust reported a 25% mineral content of TRWP (Klöckner et al., 2021). To calculate the TRWP concentrations, a Monte Carlo simulation (Crystal Ball) was performed with the predicted mean concentration of tire particles and the expected

level of encrustment based on previous studies. A triangular distribution was chosen to incorporate the minimum (6%), mean (30%) and maximum (53%) encrustment levels.

$$M_{TRWP} = \frac{M_T}{1 - R_{ENCR}} * 1$$

where

M_{TRWP} is the mass of tire particles with road wear encrustment in a sample (mg);

M_T is the mass of tire in a sample (mg);

R_{ENCR} is the ratio of encrustment covering the tire particle

2.5 Statistical analysis

The tire and PMB concentrations were calculated and predicted by Monte Carlo Simulation (Crystal Ball Add-In, Microsoft Excel), as described in Rødland et al.(2022b). Normal distribution was applied for both datasets of personal vehicle (PV) and heavy vehicle (HV) tires and triangular distribution for the SBS dataset. The TRWP concentration was predicted by Monte Carlo Simulation with a triangular distribution for the mineral content data for TRWP. For all three models, 100,000 simulations were applied, and the prediction statistics obtained for tire, PMB and TRWP were mean, median, standard deviation, minimum, maximum, and the 10th, 25th, 75th and 90th percentiles for each sample.

The statistical analysis of the data was conducted in RStudio 1.3.109 (Team, 2020), R version 4.0.4 (2021-02-15), using the ggplot2-package (Lai et al., 2016) (gplot2_3.3.3), the car-package (Fox J and Weisberg S . A, 2019) and the dplyr-package (Wickham et al., 2018) for creating boxplot graphs, linear regression and for performing Analysis of Variance (ANOVA).

All ANOVAs for WDS were performed on log-transformed data and all ANOVA for GP and TWW were performed on original data. The assumption of

normal distribution of residuals was tested using an Andersen-Darling normality test. The assumption of equal variance was tested using Levene's Test of Homogeneity of Variance. Whenever this assumption was not met, Welch's one-way ANOVA was used. The statistically significant level was set to p=0.05.

Linear regression was used to assess the relationship between TSS and total concentration of SBR+BR+SBS in tunnel wash water. The residuals of the regression model were checked for normality using an Andersen Darling Normality test.

The variation in size distribution of tunnel wash water was tested using Aitchison-weighted-logratio-PCA/Aitchison-weighted-logratio-RDA for compositional data (Canoco 5.12,Braak and S̃milauer (2018)).

3 Results

3.1 Limit of detection and limit of quantification

Different types of blank samples were analysed. For the sampling with WDS, 6 field blank samples and 3 lab blank samples were analysed. No SBR+BR+SBS were detected in these. For the tunnel wash water, 6 lab blanks were analysed. No SBR+BR+SBS were detected in these. During the pyrolysis runs, three blanks were analysed per 48 samples (autosampler), 12 blanks in total. These were blanks run without pyrolysis cups, to evaluate carry-over between samples. No SBR+BR+SBS were detected in these. Blank samples of the solvent used for the calibration samples and internal standard (Chloroform) were also analysed (n=2). No SBR+BR+SBS were detected in these. The limit of detection (LOD, 3xS/N) for the four pyrolysis markers was <1 µg of SBR+SBS. The limit of quantification (LOQ, 10xS/N) was <1 µg.

Table 1. Summary of the Limit of detection (LOD) and the Limit of quantification (LOQ) based on the average signal to noise (S/N) of 1µg of Styrene Butadiene rubber (SBR) and Styrene Butadiene Styrene (SBS) analysed in ratios of 20:80, 60:40 and 80:20.

1 µg SBR+SBS	Average S/N	LOD (3 x S/N)	LOQ (10 x S/N)	Concentration of SBR+SBS
m/z 78	58.5	175.4	584.8	<1
m/z 117	7.3	21.9	73.1	<1
m/z 118	0.3	0.9	2.9	<1
m/z 91	0.5	1.6	5.4	<1

3.2 Road surface

The total concentration of particles (TSS) collected per square meter road surface (m^2) varied greatly between the sample locations within each area (bank, in wheel track and between wheel tracks) and between inlet, middle and outlet of the tunnel (Figure 3, SI Table SI-10). The average TSS concentration across all locations was 47.8 g/m^2, with a large standard deviation of 56.9 g/m^2 (n=27). Comparing the inlet, mid area and outlet of the tunnel, the highest concentrations of TSS were found in the inlet (103 ± 74.7 g/m^2), the second highest in the mid area (34.0 ± 45.1 g/m^2 and the lowest in outlet (23.9 ± 10.9 g/m^2). The concentration of tire particles, PMB and TRWP were highest in the bank area of the outlet and lowest in the wheel track of the middle area right lane (Figure 3, Table SI-10, Table SI-11). Tire particles were reported in the range of 25.3-4820 mg/m^2 (893 ± 1210 mg/m^2), the PMB in the range of 20.2-3840 mg/m^2 (712± 960 mg/m^2) and the TRWP in the range of 36.6-6970 mg/m^2 (1290 ± 1740 mg/m^2). The difference between inlet, middle and outlet, as well as between the right and left lane in the middle, was not statistically significant (ANOVA, $p>0.05$). The difference between the sampling locations (B, IW, BW, M) was statistically significant (ANOVA, $p<0.0001$). The percentage of tire, PMB and TRWP were highest in the outlet (tire: 6.4%, PMB: 5.1%, TRWP: 9.2%), compared to the middle (tire: 2.1%, PMB: 1.7%, TRWP: 3.1%)

and the inlet (tire: 0.94%, PMB: 0.75%, TRWP: 1.4%). The relative standard deviation of the predicted mean tire concentrations using Monte Carlo simulation was 9.4% (Table SI-1). The relative standard deviation of the predicted mean PMB concentration was 11% (Table SI-2). Overall, the relative standard deviation of the predicted mean values of TRWP using Monte Carlo simulation was 14.2% across all samples (Table SI-3). For comparison with previous literature on tunnel and road dust, the concentration of TRWP on the road surface is also reported in mg/g, where the concentrations ranged between 0.835 and 373 mg/g (57.2 ± 99.1mg/g).

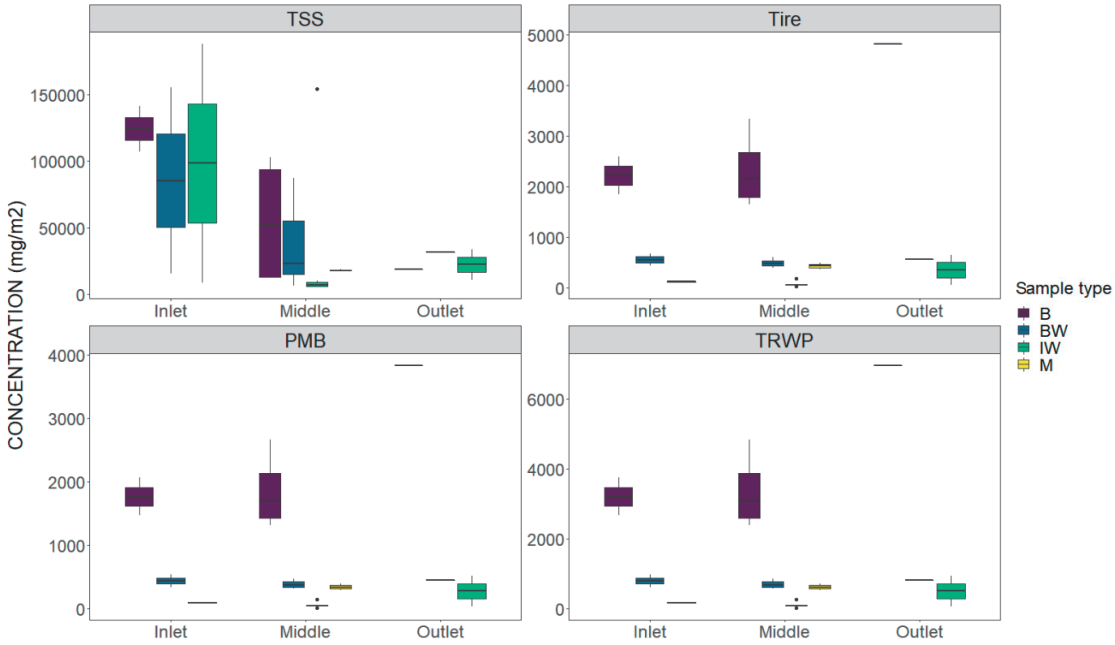

Figure 3. Concentration of TSS, tire PMB and TRWP through the tunnel from inlet, middle and outlet of the tunnel, as well as across the driving lane from the bank area (B), between wheel tracks (BW) in the wheel tracks (IW) and in the middle between lanes (M).

3.3 Gully-pots

The tire and PMB concentrations found at the inlet (GP-1: tire: 53.1 ± 1.33 mg/g; PMB: 42.3 ± 1.06 mg/g) were an order of magnitude higher compared to the middle of the tunnel (GP-2: tire: 4.75 ± 1.53; PMB: 3.78 ± 1.22 mg/g) and the outlet (GP-3: tire: 7.32 ± 2.86; PMB: 5.83 ± 2.28 mg/g) (Figure 4, SI Table SI-12). The difference between the three gully-pots was statistically significant (ANOVA, $p<0.0001$; Tukey post hoc, $p<0.0001$). By visual inspection, the sediments at the middle and outlet of the tunnel were significantly drier compared to the inlet sediment. The predicted standard deviation of the tire and PMB concentrations in the gully-pot samples was 9.4% and 11%, respectively (Table SI-4 and SI-5). The results for TRWP in the gully pots varied between 4.37 and 78.4 mg/g (31.4 ± 34.2 mg/g), with the highest concentrations found for the inlet. The predicted % standard deviation of the TRWP values were 14.1% (Table SI-6).

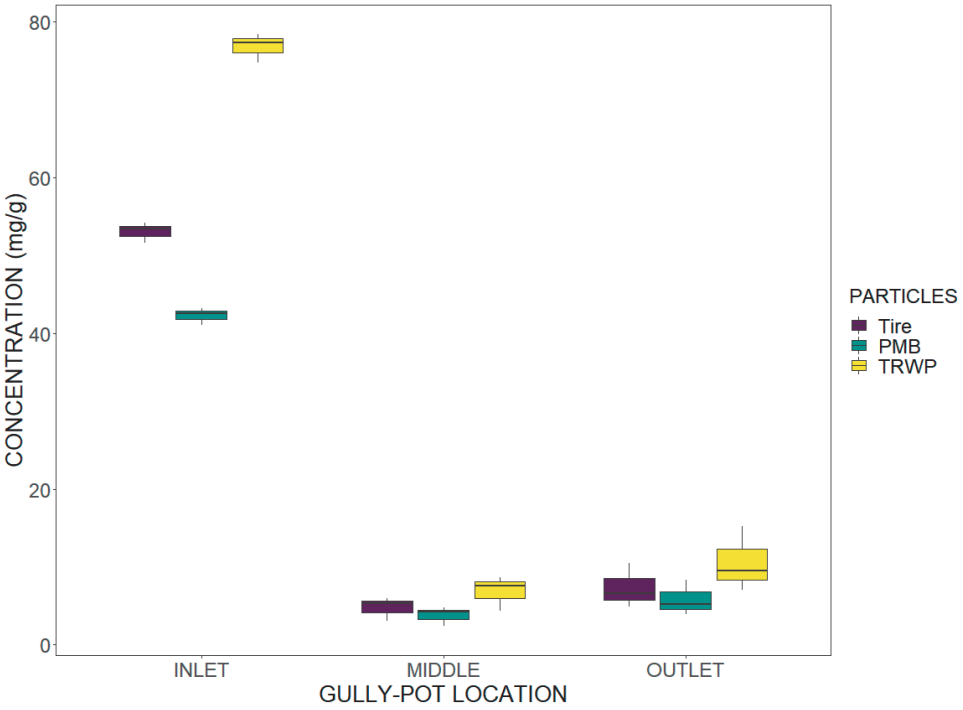

Figure 4. Concentration of tire, PMB and TRWP particles in gully-pots from the inlet, middle and outlet of the tunnel

3.4 Tunnel wash water

The average total suspended solids (TSS) concentration for tunnel wash water before treatment ranged from 930-3500 mg/L (1620 ± 930 mg/L; Figure 5, Table SI-13, Table SI-14). The predicted concentration of tire particles before treatment ranged between 14.5 and 47.8 mg/L (33.6 ± 9.20) and had standard deviation in the Monte Carlo simulation of 9.4% for all samples (Table SI-7). For the PMB, the concentration ranged from 11.5-38.1 mg/L (26.8 ± 7.33 mg/L) and the predicted standard deviation was 11% for all samples (Table SI-8). The percentage of tire, PMB and TRWP compared to TSS increased slightly between the untreated samples (tire: 2.2%, PMB: 1.8%, TRWP: 3.2%) and the treated samples (tire: 3.1%, PMB: 2.5%, TRWP: 4.5%), due to sample TWW-15, which had 5 times higher percentage of tire, PMB and TRWP compared to the average across all samples. The predicted concentration of TRWP before treatment ranged from 20.9 to 69.2 mg/L before treatment (48.6 ± 13.3 mg/L), with a predicted standard deviation of 14.2% (Figure 5, Table SI-7, Table SI-13, Table SI-14).

After treatment, the average concentration of TSS was reduced by 69% (average 500 ± 300 mg/L), with a range of 82-1,300 mg/L. The predicted concentration of tire ranged from 6.78-29.4 mg/L (12.5 ± 6.00 mg/L) and the standard deviation of the prediction was 9.4% for all samples. The predicted PMB concentration ranged from 5.40-23.4 mg/L (10.0 ± 4.78 mg/L), with a 11% standard deviation of the Monte Carlo prediction. The concentrations of TRWP varied between 9.81 and 42.5 mg/L after treatment (18.1 ± 8.68 mg/L) with an 11.2% standard deviation from the Monte Carlo simulation (Figure 5, Table SI-7, Table SI-13, Table SI-14).

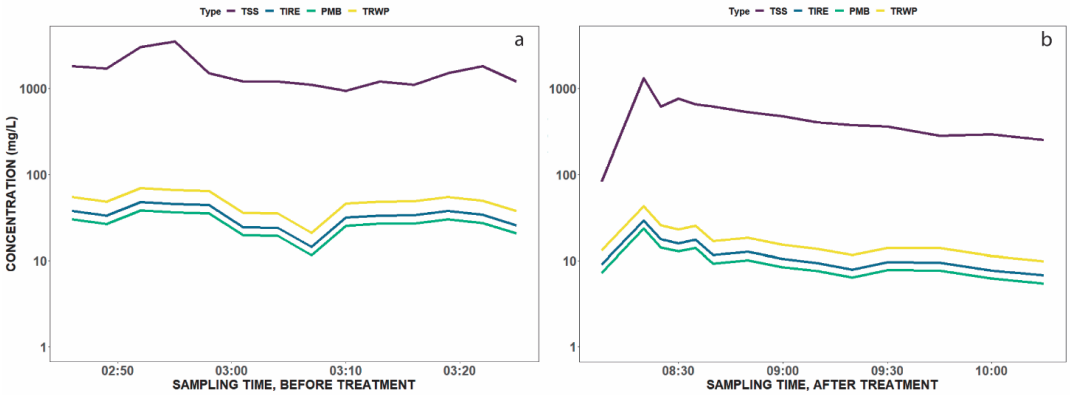

Figure 5. Concentrations of total suspended solids (TSS), tire particles, PMB particles and tire and road wear particles (TRWP) in the tunnel wash water before (a) and after (b) treatment. The samples are displayed as a time-series for the sampling, from 02:46 to 03:25 (April 21st, 2020) before treatment and from 08:08 to 10:15 (May 12th, 2020).

The first sample collected after treatment (TWW-15), had low TSS (82 mg/L) compared to the average of 500 mg/L as well as a high percentage of tire and PMB (12%) compared to the overall percentage excluding TWW-15 (2.57%). For the relationship between TSS and tire, PMB and TRWP, the linear regression was performed on the SBR+BR+SBS rubber values and not the predicted values, to reduce the uncertainty related to the prediction of these values. A strong relationship between TSS and SBR+BR+SBS was confirmed (adjusted R^2= 0.88, Figure 6). This relationship indicates that TSS is a possible proxy for SBR+BR+SBS rubber and subsequently tire and road wear particles in tunnel wash water.

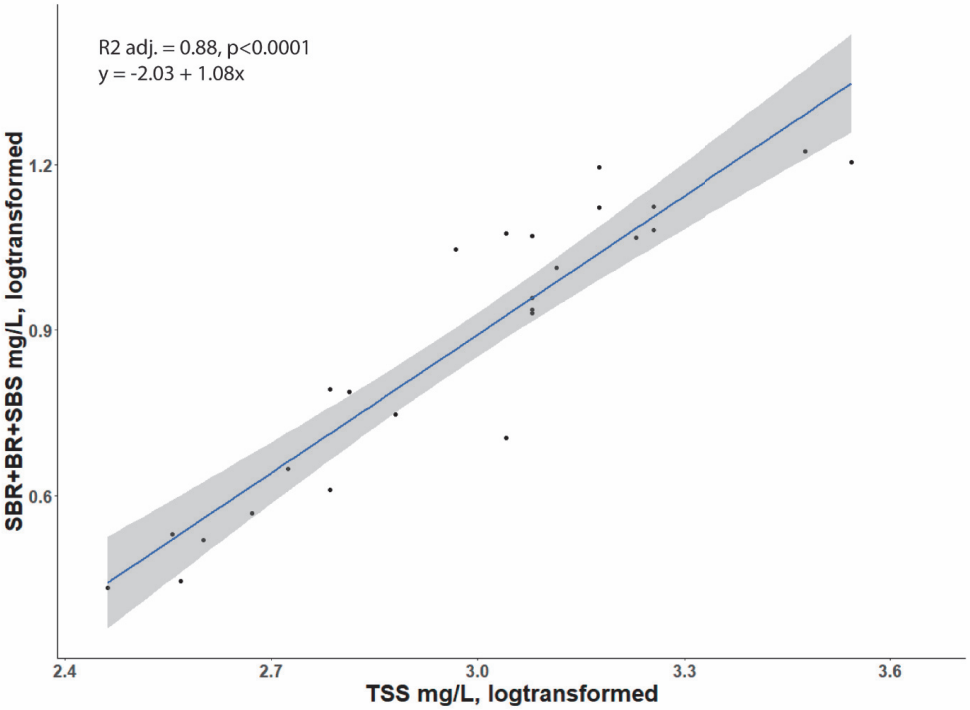

Figure 6: Linear regression between TSS (log transformed) and SBR+BR+SBS (log transformed) for all samples before and after treatment, except TWW-15 (low TSS)

The difference in size distribution of particles in the tunnel wash water before and after treatment was small, but significant (RDA, p=0.008, Figure 7, Table SI-15) when sample TW-15 is excluded as an outlier. The most visible difference between the before and after samples was the presence of particles >350µm after treatment (TWW-16, TWW-17and TWW-18), which were not present in the samples before treatment. The largest mass of particles was found in the 10-30µm size class, with an average contribution of 42% in the untreated samples and 47% in the treated samples. In fact, over 83% of the particles in both untreated and treated samples were <30µm in size. The untreated samples had a higher percentage of the smallest particles (>2.5µm and 2.5-10µm) For the fraction 50-350 µm, where the main mass of tire particles is expected (Kreider et al., 2010), the mass of particles was 6.4% before treatment and reduced to 5.3% after treatment. The difference in

concentration of tire and PMB before and after treatment was statistically significant (ANOVA, p <0.0001).

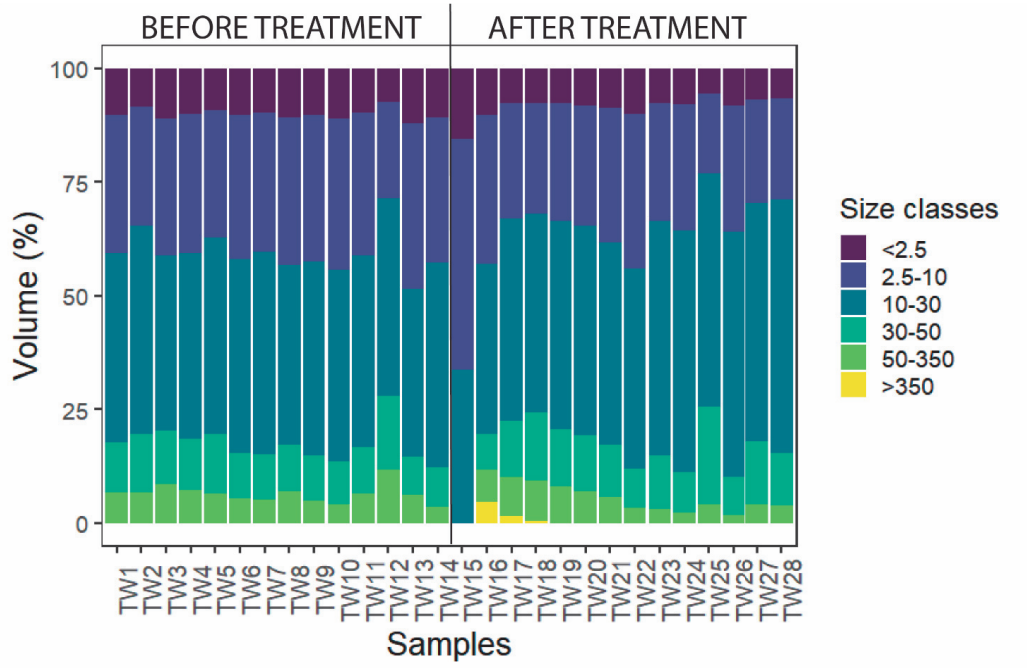

Figure 7. Size distribution of particles (total suspended solids <2000µm) in tunnel wash water before and after treatment. Sample TW15 is the first sample released of the treated tunnel water and differs significantly from the others (outlier). The difference between samples before and after treatment was significant (RDA, p=0.008)

4 Discussion

4.1 Road surface

The concentrations of tire, PMB and TRWP were highest in the outlet and bank area, which supports hypothesis I. For TSS, the high accumulation in the bank area agrees with previous studies of tunnel road dust using WDS (NPRA, 2017; NPRA, 2021b), however, in these studies the concentrations were higher in the inlet compared to the outlet and the overall concentrations reported in the present study were significantly lower compared to previous studies using WDS (200-400 g/m^2 (Gustafsson et al., 2019; NPRA, 2021b)).

Previous studies have reported up to 10% organic components in tunnel road dust (NPRA, 2017), which agrees with the percentage of tire, PMB and TRWP found at the tunnel outlet in the present study. However, the percentage of tire, PMB and TRWP was significantly lower in the inlet and in the middle of the tunnel. The reason for this difference could be that the inlet area is the highest point of the tunnel and receives a lot of runoff from outside of the tunnel. This could potentially include a higher concentration of other particles, which therefore dilutes the concentration of tire and PMB particles in this area. Another reason might be that tire and PMB particles are transported through the tunnel by the suspension made by traffic and wind (piston effect; Moreno et al. (2014)), as well as runoff when it precipitates, and accumulating in the lower areas of the tunnel. Another possibility is that a larger portion of the tire and PMB particles in the inlet area ends up in the gully-pots of that area.

The macrostructure of the pavement can have a substantial impact when comparing the particle load retained in the road surface (Lundberg et al., 2017). In the Smestad tunnel, the road surface is asphalt concrete (maximum aggregate size of 11 mm), which has a lower texture and less area for particles to be retained (especially in the wheel tracks), compared to coarser stone mastic asphalts with maximum aggregate size of 16 mm (Gustafsson et al., 2019; NPRA, 2017). The number of comparable studies for the mass of tire and road-wear rubber, tire particles, PMB and TRWP is limited. However, one study of street runoff from

Germany (Eisentraut et al., 2018) used a mass-based analysis (Thermal Desorption GC/MS) and found SBR concentrations between 3.9 and 8.9 mg/g in the street runoff, which is over 40 times lower than the highest values of rubber reported for tunnel road surface in this present study, although the rubber concentration in the present study also includes SBS rubber from the PMB surface. One likely reason for this major difference may be the sampling procedure. A previous study using a Wet Dust Sampler has demonstrated that 90% of particles (<180µm) are collected using three shots of each area (NPRA, 2021b), whereas only 60% of particles 180-5000µm were collected by three shots. Compared to a previous study of tunnel road dust (Klöckner et al., 2021), where the middle bank area (110 mg/g) and the outlet bank area (120 mg/g) were analysed, the TRWP concentration in Smestad reported in the present study is more than three times higher for both areas. Another study analysed road dust mixtures collected by road sweeper trucks (Klöckner et al., 2020) and the concentrations were more than four times lower (8.1-14 mg/g) than the average concentrations in road dust in the present study. Different sampling procedures, such as using multiple sample shots with a WDS compared to applying a commercial vacuum cleaner, might be the main reasons for these differences. Other explanations might be local, such as the different length, slope and AADT for the different roads analysed.

4.2 Gully-pots

The results for the gully-pots confirmed that tire, PMB and TRWP can be retained in high concentrations and thus supported a rejection of hypothesis II. Previous studies where the possibility of retention in gully-pots are discussed, have suggested low treatment efficiency for tire and road wear particles gully-pots (Blecken, 2016; Vogelsang et al., 2018) due the density and size of the particles. Studies that have tested the efficiency of gully-pots have found that the efficiency depends on the particle size, the particle geometry and the flow within the gully-pot, where the efficiency decreases as the sediment builds up in the gully pot (Rietveld et al., 2020). The concentration of TRWP at the tunnel inlet in the present study was comparable to the concentrations found in gully-pots from municipality roads (0.8-150mg/g; (Mengistu et al., 2021) and sediment from a road runoff treatment (130 ± 15 mg/g; Klöckner et al. (2019)), while it should be kept in mind that these studies were based on different analytical approaches. The major difference between the inlet gully-pot and the outlet in the current study is the opposite of the results for the road surface, where the concentration in the outlet was significantly higher compared to the other areas. One possible reason for the differences between inlet and outlet, as was also observed for the road surface, is that the inlet area is the highest point of the tunnel and receives a lot more runoff from outside of the tunnel. This runoff is likely to flow into the gully-pots, causing a higher percentage of tire and PMB particles to accumulate in the gully-pot sediment, as well as bringing in a higher percentage of other particles from outside of the tunnel to the inlet area. The particle concentration in mid area and the outlet of the tunnel are affected by the traffic inside the tunnel with little water flowing through during normal conditions. This is also supported by the observation of drier sediment present in the middle and outlet gully-pots.

4.3 Tunnel wash water

Compared to previous studies, the concentrations of TRWP in untreated tunnel wash water agrees with values reported for road runoff (3-180 mg/L: (Baumann and Ismeier, 1998; Kumata et al., 2000; Kumata et al., 1997; Kumata et al., 2002); Parker-Jurd et al. (2021; (Reddy and Quinn, 1997; Wik and Dave, 2009)). It should be noted that these studies all represent different analytical methods and calculations, so comparisons should be made with caution. A recent study has also reported TRWP in the range of 6.4 - 18 mg/L in an Australian urban creek receiving stormwater runoff (Rauert et al., 2022), although these values represent the diluted runoff mixed with the river water. The hypothesis that untreated tunnel wash would far exceed the road runoff concentrations due to the accumulation in tunnels was not supported based on these comparisons. On the contrary, the concentrations of tire and PMB particles found in the untreated tunnel wash water were significantly lower compared to a recent study of tire and PMB particles in road-side snow in Oslo, Norway (Rødland et al., 2022a). One explanation might be that the tire, PMB and TRWP particles in the tunnel system are divided between different tunnel compartments, such as the road surface and the gully-pots, whereas the road-side snow traps more of the total tire, PMB and TRWP production and therefore features higher concentrations. Different types of road surfaces could be one contributing factor, as discussed in the study of road-side snow that the sites with concrete asphalt had a higher concentration of TSS and a higher calculated contribution of SBS based on road abrasion factors for concrete asphalt (Rødland et al., 2022a). As the road surface in the Smestad tunnel is also made of concrete asphalt, the observed high TSS compared to tire, PMB and TRWP might indicate that there is a higher road wear contribution here compared to sites with stone mastic asphalt.

The strong correlations found between TSS and SBR+BR+SBS rubber could potentially provide a valuable tool for environmental monitoring of tunnel wash water. Applying online sensors in tunnels, the TSS and turbidity data could then be collected in real-time for a large number of tunnels, and TSS and turbidity could be used as proxy tire, PMB and TRWP concentrations. More data is needed to establish the basis for such a tool, however, the impact on environmental

monitoring could be high, as monitoring with sensors would potentially reduce the costs for sampling and analysis.

The retention efficiency reported in this study (63%) is lower than expected according to the previous assumption of >80% retention in sedimentation treatment. This supports the rejection of hypothesis IV, stating that the current treatment of tunnel wash water in Smestad is efficient in retaining tire, PMB and TRWP. The possible issues with the sedimentation treatment in Smestad are also highlighted by sample TW-15. This is the first treated sample released into the rain garden, and it was characterized by low TSS (5 times lower than the average) and a high percentage of tire and PMB compared to the average and particle sizes >30µm. This indicates that the first samples may represent the water that has been treated inside the pump house basin and not the treated water from the sedimentation basin. The following samples may have higher TSS and particle size distribution due to the turbulence and resuspension of particles upon the release. This is also supported by the size distribution analysis, where the difference in size distribution before and after treatment was low. A small decrease in the volume of particles >50 µm was observed for the after-treatment samples compared to before treatment, however, three of the after-treatment samples also contained particles >350 µm, which had not been observed in the previous samples. This further indicates that turbulence and resuspension of particles occurs when the treated water is released into the rain garden and may be the reason why the retention efficiency for TSS, tire and PMB was lower than expected for this tunnel.

The size distribution data may provide us with more understanding of the treatment process. Although the total particle retention (TSS) had a 69% retention in the treatment basin, this did not have a significant impact on the size distribution. Only a small decrease was observed in the second largest size class (50-350 µm), where the main mass of tire particles is expected to be found (Kreider et al., 2010). The Swedish road authorities have reported that treatment by sedimentation is not suitable for particle sizes <10µm, where infiltration treatment is needed (Anderson et al., 2018). As 41% of the particles before treatment and 37% after treatment were <10um, this indicates that the sedimentation basin is less efficient in the removal of

particle-bound pollutants. Although low efficiency was found for this tunnel, different tunnels do have different types of treatment, and these should be investigated to evaluate to overall efficiency of wash water treatment for tire, PMB and TRWP.

Other factors that could impact the treatment efficiency is the use of soap. As previously mentioned, soap is applied in the Smestad tunnel, and the percentage of soap used in this specific tunnel is approximately 0.2% (NPRA, 2022). However, the use of soap has been demonstrated to lower the treatment efficiency for several metals (Aasum, 2014): the use of 0.3% soap in the wash water reduced the retention of Zn from 98% (no soap) to only 33%, and for Cu, the use of 3 % soap reduced the retention from 99% without soap to as low as 25% retention. The treated tunnel wash water in Smestad still had soap in it when released into the rain garden, indicating that the soap could be a crucial factor in the low treatment efficiency. Furthermore, temperature could impact the treatment of tunnel wash water, where lower temperatures (4°C) cause slower sedimentation compared to higher temperatures (20°C) (Garshol et al., 2015). The average outdoor temperature for the treatment period was 8.4°C (Yr, 2020), which could have an impact on the treatment efficiency.

4.4 Uncertainty evaluation

For studies applying mass-based methods such as pyrolysis GC/MS, the use of reliable pyrolysis markers with low variability is crucial. This has been discussed as a major issue when it comes to analysing tire particles, as different pyrolysis products have displayed large variations in different reference tires tested (Rauert et al., 2021; Rødland et al., 2022b). The major impacting factor causing variability is the different microstructures in the composition of SBR and BR rubber, which can cause variability in the pyrolysis products (Choi, 2001; Choi and Kwon, 2020; Miller et al., 2021). The use of different types of SBR in tires, such as emulsion-SBR and solution-SBR has also been brought to attention in previous literature (Miller et al., 2021; Rødland et al., 2022b). Another important aspect, which has also been

brought to attention by Wagner et al. (2022), is the need to address how aging of tire particles in the environment impacts the SBR+BR content and the pyrolysis products used as marker compounds. Aging is also important for the SBS rubber content in PMB. The presence of SBS rubber in samples has so far only been addressed by one environmental study from Norway (Rødland et al., 2022b), however, several countries such as Australia, United Kingdom, Russia, Denmark and Sweden apply PMB asphalt on roads with high traffic volume (EAPA, 2018). As various polymers and rubbers, not just SBS, can be applied, it is important to investigate the presence of SBS in the road surface before analysing samples for SBR+BR. SBR and SBS have identical pyrolysis products, as well as BR sharing overlapping products with SBS, so without separation between SBR+BR and SBS, TRWP concentrations will be overestimated in a sample that contains both. To reduce the uncertainty caused by variations in the pyrolysis products, the present study applies a method where the combination of four different pyrolysis products (*benzene, α-methylstyrene, ethylstyrene and butadiene trimer*) are used for quantification. This method has displayed lower variability (40% S.D) in reference tires compared to the single markers previously proposed by other studies (62-85% S.D.) (Rødland et al., 2022b), suggesting that the method reduces the uncertainty related to variation in single markers compared to previous methods. A second challenge in analysing tire particles concerns the variable rubber content in different commercial tires. Previous studies have reported a rubber content of 50% in personal vehicle tires (44% SBR+BR) and 50% in truck tires (45% NR) (Unice et al., 2012), however, in our recent study we found large variations of SBR+BR content in commercial tires, not in line with the 50% assumption (PV: 19-47% SBR+BR, HV: 11-68% SBR+BR) (Rødland et al., 2022b). Variations in commercial tires have also been reported by other studies (Goßmann et al., 2021; Rauert et al., 2021). To reduce the uncertainty in calculations from rubber concentrations to tire concentrations, the SBR+BR concentrations in relevant seasonal tires are used in the present study, and the calculations are applied in Monte Carlo simulations to predict the tire concentrations present in a sample. The use of these simulations allows us to predict the possible mean concentrations of tire present in the sample, as well as a

variety of statistics such as predicted standard deviations, minimum and maximum values and percentiles. For the tire concentrations, % predicted standard deviation from the predicted mean was 9.4% (SI Table SI-1, SI-4 and SI-7), which demonstrates that there are some uncertainties related to the calculation of tire particles. This uncertainty is influenced by the large variation of SBR+BR content in the PV tires (96.8%, Crystal ball sensitivity analysis), which underlines the need for relevant and reliable reference tires. The estimated SBS rate contributes 2.4% to the variation, whereas the SBR+BR variation in HV tires only contributes 0.8% of the variation. For the PMB particles, the variation of SBS reported in PMB asphalt is low compared to the variation in tires because the input data has a lower variance and the model is only influenced by the SBS ratio for Smestad (100%, Crystal Ball sensitivity analysis), and therefore the % predicted standard deviation of PMB concentrations is lower (11%).

Uncertainty is also important to consider for the calculated TRWP concentrations. Previous literature has suggested that urban roads with lower speed limits and traffic density have a high percentage of encrusted particles (>73%, Klöckner et al. (2020)) compared to highways with higher speed limits and traffic density (<10%:Sommer et al. (2018); 25%: Klöckner et al. (2021)). Increased speed limit and traffic density increases the distance a tire wear particle is transported from the point of release (Gustafsson et al., 2009; Rødland et al., 2022a), thus, decreasing the potential mixing with mineral particles from the road surface. In tunnels, the semi-enclosure of the tunnel walls inhibits the transportation, however, as demonstrated by the present study and others (NPRA, 2017; NPRA, 2021b), a substantial proportion of tire and road wear particles accumulate in the side bank area, which is outside of the driving lane and not contributing to the increased mixing of tire and mineral particles on the surface. Thus, assuming a generalized 50% mineral encrustment (Kreider et al., 2010; Unice et al., 2013) may overestimate TRWP concentrations for highways, including in road tunnels, as well as underestimating the TRWP concentrations for urban roads. In the present study, Monte Carlo simulation was applied to calculate the predicted TRWP concentrations based on tire concentrations and the reported distribution of

mineral encrustment. However, the available data on mineral encrustment on TRWP for different road types and sample matrices are currently limited to three studies (Klöckner et al., 2021; Kreider et al., 2010; Sommer et al., 2018), hence these calculations are associated with large uncertainties. Even so, the use of Monte Carlo simulations for predicting the expected TRWP concentrations in the sample is promising and the method can be improved by increasing the data available for mineral encrustment of TRWP. Future studies should investigate the impact on mineral content by different variables such as driving conditions (highway, urban, rural), traffic speed, the use of studded tires and different types of road surfaces. As the input variable in the TRWP model is the predicted tire values, the TRWP model is also subject to the variations in tire reference data. Hence, improving both the data available for mineral encrustment and SBR+BR content in relevant reference tires will improve the prediction of TRWP. Another aspect not mentioned in any previous literature is how road wear particles with polymer-modified bitumen interacts with and impacts the TRWP. In this study, tire and PMB particles are reported and discussed as separate particles. This is mainly because there is not enough research available on how these particles interact with each other in the environment. To fully understand the transport mechanisms and the possibilities with mass-based analysis, more research is needed on the impact of PMB particles on TRWP.

The demonstrated use of multiple pyrolysis products as markers as well as Monte Carlo simulations for tire, PMB and TRWP calculations demonstrates the possibility of applying local conditions relevant for each sample (reference tires, asphalt abrasion, mineral encrustment) to improve the results and reduce the uncertainties.

5 Conclusions

The lowest concentrations of tire and PMB particles were found on the road surface of the tunnel, with the second highest concentration in the gully pots and the highest concentration in the tunnel wash water. For the road surface, the concentrations were high compared to previous studies, and validated the first part of hypothesis I, that most of these particles accumulate in the side bank area. However, in contrary to previous studies, the highest concentrations were found in the outlet of the tunnel and not in the inlet, rejecting the second part of hypothesis I. Our findings confirm that it is important to clean the surface both before the tunnel wash and after the wash. This will reduce the particle load in the tunnel wash water, which will decrease the release of pollutants from tunnels without water treatment. Removing particles in the smaller size range (<50 µm), which had the highest number of particles, from the road surface may also increase the retention efficiency of sedimentation treatment. Cleaning the road surface again after the tunnel wash helps to remove particles from the surface before it settles in the road surface macrostructure. High concentration of tire, PMB and TRWP were also reported in the inlet gully-pot, with concentrations comparable to sediment in road treatment basins. This was in contrast to previous studies, thus rejecting hypothesis II. The concentration was lower in the middle and outlet gully-pots, also displaying a different pattern compared to the accumulation of tire, PMB and TRWP on the road surface.

For the tunnel wash water, the concentration of tire, PMB and TRWP in untreated water was comparable to previous studies of road runoff, however, significantly lower compared to meltwater from road-side snow, thus rejecting hypothesis III. The retention of tire, PMB and TRWP (63%) and TSS (69%) were also lower than expected (>80%) based on previous literature for tunnel wash water, rejecting hypothesis IV. Factors such as soap and temperature could be influencing the treatment, as well as the large fraction of small sized particles that potentially hampers removal by sedimentation alone. The second treatment step at Smestad (rain garden) could not be analysed and assessed in this study, and future research on this tunnel should aim to include this second treatment step for comparison. The concentrations of tire,

PMB and TRWP in the untreated tunnel wash water are relevant for the high number of tunnels in Norway that release untreated tunnel wash water into freshwater and marine recipients.

There are still issues related to using different analytical approaches in different studies, making comparisons between different matrices such as road runoff, road-side snow or road dust difficult. Large uncertainties are also related to the analysis of tire and road wear rubber with Pyrolysis GC/MS, as well as the calculations of tire, PMB and TRWP based on the rubber concentrations. Future research should focus on finding a common approach to both analysis and calculation of tire, PMB and TRWP, as well as addressing the uncertainties related to these calculations. The impact of aging on the pyrolysis markers applied should be addressed, and an increase of available data for SBR+BR content in tires, road abrasion including PMB and mineral content of TRWP is needed.

6 Acknowledgements

The analysis of particle size distribution was performed by Christian Solheim at Norwegian University of Life Sciences. We thank Kjersti W. Kronvall (NPRA) for contributing the photo for Figure 2 and we thank Rachel Hurley for commenting on the final draft paper.

7 Funding sources

This work was funded in collaboration between the Norwegian Institute for Water Research (NIVA) (funded by the Research Council of Norway, grant number 160016) and the NordFoU-project REHIRUP (grant number 604133), consisting of the Norwegian Public Roads Administration, the Swedish Transport Administration, and the Danish Road Directorate. Part of the work is also supported by the Norwegian University of Life Sciences (NMBU) and the Centre for Environmental Radioactivity (CERAD) (funded by the Research Council of Norway through its Centers of Excellence funding scheme, project number 223268/F50)

8 Author Contributions

The manuscript was written through contributions of all authors. All authors have given approval to the final version of the manuscript.

9 Supplementary information

Supplementary information to this article is provided.

References

Allan IJ, O'Connell SG, Meland S, Bæk K, Grung M, Anderson KA, et al. PAH Accessibility in Particulate Matter from Road-Impacted Environments. Environmental Science & Technology 2016; 50: 7964-7972.

Andersson J, Mácsik J, van der Nat D, Norström A, Albinsson M, Åkerman S, et al. Reducing Highway Runoff Pollution (REHIRUP). Sustainable design and maintenance of stormwater treatment facilities. 2018:155, 2018.

Baumann W, Ismeier M. Emissionen beim bestimmungsgemässen Gebrauch von Reifen. Kautschuk und Gummi, Kunststoffe 1998; 51: 182-186.

Blecken GW. Kunskapssammanställning – Dagvattenrening. In: Vatten S, Utveckling., editors, 2016.

Boucher J, Billard G, Simeone E, Sousa JT. The marine plastic footprint. 2831720281. IUCN, Gland, Switzerland, 2020.

Braak CJFt, S̃milauer P. Canoco reference manual and user's guide : software for ordination (version 5.10). Biometris, Wageningen University & Research, Wageningen, 2018.

Choi S-S. Characteristics of pyrolysis patterns of polybutadienes with different microstructures. Journal of Analytical and Applied Pyrolysis 2001; 57: 249-259.

Choi S-S, Kwon H-M. Considering factors on determination of microstructures of SBR vulcanizates using pyrolytic analysis. Polymer Testing 2020; 89: 106572.

EAPA. HEAVY DUTY SURFACES THE ARGUMENTS FOR SMA. Technical review. In: Association EAP, editor, Brussels, Belgium, 2018.

Eisentraut P, Dümichen E, Ruhl AS, Jekel M, Albrecht M, Gehde M, et al. Two Birds with One Stone—Fast and Simultaneous Analysis of Microplastics: Microparticles Derived from Thermoplastics and Tire Wear. Environmental Science & Technology Letters 2018; 5: 608-613.

Fox J, Weisberg S . A. n R Companion to Applied Regression. Thousand Oaks CA.: Sage, 2019.

Garshol FK, Estevez MM, Eftekhar Dadkhah M, Stang P, Rathnaweera SS, Sahu A, et al. Laboratorietester – rensing av vaskevann fra Nordbytunnelen. Inklusive datarapport og resultater med vann hentet 31.08. 2014 og 18.03.2015. In: NORWAT, editor. Report No. 521, Norway, 2015, pp. 131.

Goßmann I, Halbach M, Scholz-Böttcher BM. Car and truck tire wear particles in complex environmental samples – A quantitative comparison with "traditional" microplastic polymer mass loads. Science of The Total Environment 2021; 773: 145667.

Gustafsson M, Blomqvist G, Gudmundsson A, Dahl A, Jonsson P, Swietlicki E. Factors influencing PM10 emissions from road pavement wear. Atmospheric Environment 2009; 43: 4699-4702.

Gustafsson M, Blomqvist G, Järlskog I, Lundberg J, Janhäll S, Elmgren M, et al. Road dust load dynamics and influencing factors for six winter seasons in Stockholm, Sweden. Atmospheric Environment: X 2019; 2: 100014.

Hallberg M, Renman G, Byman L, Svenstam G, Norling M. Treatment of tunnel wash water and implications for its disposal. Water Science and Technology 2014; 69: 2029-2035.
Klöckner P, Reemtsma T, Eisentraut P, Braun U, Ruhl AS, Wagner S. Tire and road wear particles in road environment – Quantification and assessment of particle dynamics by Zn determination after density separation. Chemosphere 2019; 222: 714-721.
Klöckner P, Seiwert B, Eisentraut P, Braun U, Reemtsma T, Wagner S. Characterization of tire and road wear particles from road runoff indicates highly dynamic particle properties. Water Research 2020; 185: 116262.
Klöckner P, Seiwert B, Weyrauch S, Escher BI, Reemtsma T, Wagner S. Comprehensive characterization of tire and road wear particles in highway tunnel road dust by use of size and density fractionation. Chemosphere 2021; 279: 130530.
Knight LJ, Parker-Jurd FNF, Al-Sid-Cheikh M, Thompson RC. Tyre wear particles: an abundant yet widely unreported microplastic? Environ Sci Pollut Res Int 2020; 27: 18345-18354.
Kreider ML, Panko JM, McAtee BL, Sweet LI, Finley BL. Physical and chemical characterization of tire-related particles: Comparison of particles generated using different methodologies. Science of the Total Environment 2010; 408: 652-659.
Kumata H, Sanada Y, Takada H, Ueno T. Historical Trends of N-Cyclohexyl-2-benzothiazolamine, 2-(4-Morpholinyl)benzothiazole, and Other Anthropogenic Contaminants in the Urban Reservoir Sediment Core. Environmental Science & Technology 2000; 34: 246-253.
Kumata H, Takada H, Ogura N. 2-(4-Morpholinyl)benzothiazole as an Indicator of Tire-Wear Particles and Road Dust in the Urban Environment. Molecular Markers in Environmental Geochemistry. 671. American Chemical Society, 1997, pp. 291-305.
Kumata H, Yamada J, Masuda K, Takada H, Sato Y, Sakurai T, et al. Benzothiazolamines as Tire-Derived Molecular Markers: Sorptive Behavior in Street Runoff and Application to Source Apportioning. Environmental Science & Technology 2002; 36: 702-708.
Lai FY, O'Brien J, Bruno R, Hall W, Prichard J, Kirkbride P, et al. Spatial variations in the consumption of illicit stimulant drugs across Australia: A nationwide application of wastewater-based epidemiology. Science of The Total Environment 2016; 568: 810-818.
Lundberg J, Blomqvist G, Gustafsson M, Janhäll S. Texture influence on road dust load. In: Pollution T-TaA, editor. Proceedings of the 22nd International Transportation and Air Pollution Conference, 2017.
Lundberg J, Blomqvist G, Gustafsson M, Janhäll S, Järlskog I. Wet Dust Sampler—a Sampling Method for Road Dust Quantification and Analyses. Water, Air, & Soil Pollution 2019; 230: 180.
Meland S, Borgstrøm R, Heier LS, Rosseland BO, Lindholm O, Salbu B. Chemical and ecological effects of contaminated tunnel wash water runoff to a small Norwegian stream. Science of The Total Environment 2010a; 408: 4107-4117.

Meland S, Heier LS, Salbu B, Tollefsen KE, Farmen E, Rosseland BO. Exposure of brown trout (Salmo trutta L.) to tunnel wash water runoff – Chemical characterisation and biological impact. Science of The Total Environment 2010b; 408: 2646-2656.
Mengistu D, Heistad A, Coutris C. Tire wear particles concentrations in gully pot sediments. Science of The Total Environment 2021; 769: 144785.
Miller JV, Maskrey JR, Chan K, Unice KM. Pyrolysis-Gas Chromatography-Mass Spectrometry (Py-GC-MS) Quantification of Tire and Road Wear Particles (TRWP) in Environmental Matrices: Assessing the Importance of Microstructure in Instrument Calibration Protocols. Analytical Letters 2021: 1-13.
Moreno T, Pérez N, Reche C, Martins V, de Miguel E, Capdevila M, et al. Subway platform air quality: Assessing the influences of tunnel ventilation, train piston effect and station design. Atmospheric Environment 2014; 92: 461-468.
NPRA. Road cleaning in tunnel and street, 2016. Strindheim tunnel and Haakon VII street in Trondheim, Stordal tunnel in Møre and Romsdal. In: Snilsberg B, Gryteselv D, editors. Norwegian Public Roads Administration, Trondheim, 2017.
NPRA. Håndbok N200 Vegbygging Norwegian Public Roads Administration

2021a.
NPRA. Tunnel cleaning experiment 2019-2020. Reduced washing frequency in the Strindheim tunnel. In: Snilsberg B, Gryteselv D, Veivåg ILS, Peckolt Fordal K, Indo K, Monsen E, editors. Norwegian Public Roads Administration, Trondheim, 2021b.
NPRA. Use of soap in the Smestad tunnel. In: Rødland E, editor, 2022.
Nyström F, Nordqvist K, Herrmann I, Hedström A, Viklander M. Treatment of road runoff by coagulation/flocculation and sedimentation. Water Science and Technology 2019; 79: 518-525.
Parker-Jurd FNF, Napper IE, Abbott GD, Hann S, Thompson RC. Quantifying the release of tyre wear particles to the marine environment via multiple pathways. Marine Pollution Bulletin 2021; 172: 112897.
Paruch AM, Roseth R. Treatment of tunnel wash waters – experiments with organic sorbent materials. Part II: Removal of toxic metals. Journal of Environmental Sciences 2008; 20: 1042-1045.
Rauert C, Charlton N, Okoffo ED, Stanton RS, Agua AR, Pirrung MC, et al. Concentrations of Tire Additive Chemicals and Tire Road Wear Particles in an Australian Urban Tributary. Environmental Science & Technology 2022.
Rauert C, Rødland ES, Okoffo ED, Reid MJ, Meland S, Thomas KV. Challenges with Quantifying Tire Road Wear Particles: Recognizing the Need for Further Refinement of the ISO Technical Specification. Environmental Science & Technology Letters 2021; 8: 231-236.
Reddy CM, Quinn JG. Environmental Chemistry of Benzothiazoles Derived from Rubber. Environmental Science & Technology 1997; 31: 2847-2853.
Rietveld M, Clemens F, Langeveld J. Solids dynamics in gully pots. Urban Water Journal 2020; 17: 669-680.

Roseth R, Amundsen CE. Vaskevann fra vegtunneler - forurensningsstoffer og behandling. Kommunalteknikk. 5, 2003, pp. 16-19.
Roseth R, Meland S. Forurensning fra sterkt trafikkerte vegtunneler. Norwegian Public Roads Administration and Jordforsk, 2006.
Rødland ES, Lind OC, Reid MJ, Heier LS, Okoffo ED, Rauert C, et al. Occurrence of tire and road wear particles in urban and peri-urban snowbanks, and their potential environmental implications. Science of The Total Environment 2022a; 824: 153785.
Rødland ES, Samanipour S, Rauert C, Okoffo ED, Reid MJ, Heier LS, et al. A novel method for the quantification of tire and polymer-modified bitumen particles in environmental samples by pyrolysis gas chromatography mass spectroscopy. Journal of Hazardous Materials 2022b; 423: 127092.
Sommer F, Dietze V, Baum A, Sauer J, Gilge S, Maschowski C, et al. Tire Abrasion as a Major Source of Microplastics in the Environment. Aerosol and Air Quality Research 2018; 18: 2014-2028.
Sundt P, S. R, Haugedal TR, Schulze P-E. Norske landbaserte kilder til mikroplast (Norwegian land-based sources to microplastics). MEPEX, Oslo, 2021, pp. 88.
Team R. RStudio: Integrated Development for R. RStudio, PBC, Boston, MA, 2020.
Unice KM, Kreider ML, Panko JM. Use of a Deuterated Internal Standard with Pyrolysis-GC/MS Dimeric Marker Analysis to Quantify Tire Tread Particles in the Environment. International Journal of Environmental Research and Public Health 2012; 9.
Unice KM, Kreider ML, Panko JM. Comparison of Tire and Road Wear Particle Concentrations in Sediment for Watersheds in France, Japan, and the United States by Quantitative Pyrolysis GC/MS Analysis. Environmental Science & Technology 2013; 47: 8138-8147.
Vogelsang C, Lusher AL, Dadkhah ME, Sundvor I, Umar M, Ranneklev SB, et al. Microplastics in road dust – characteristics, pathways and measures, 2018.
Wagner S, Klöckner P, Reemtsma T. Aging of tire and road wear particles in terrestrial and freshwater environments – A review on processes, testing, analysis and impact. Chemosphere 2022; 288: 132467.
Wickham H, François R, Henry L, Müller K. R package version 0.7.6. dplyr: A Grammar of Data Manipulation., 2018.
Wik A, Dave G. Occurrence and effects of tire wear particles in the environment - A critical review and an initial risk assessment. Environmental Pollution 2009; 157: 1-11.
Yr. Historical weather data for Oslo (Blindern station). In: Corporation NMIatNB, editor, 2020.
Aasum JH. Effekter av vaskemiddel (TK601) på mobilitet av metaller ved sedimentering av tunnelvaskevann fra Nordbytunnelen (E6), Ås kommune, Akershus : et laboratorieforsøk. Master of Science. Norwegian University of Life Sciences, Ås, Norway, 2014.

SUPPLEMENTARY INFORMATION

Characterization of Tire and Road Wear Microplastic Particle contamination in a Road Tunnel: from surface to release

Elisabeth S. Rødland[1,2], Ole Christian Lind[2], Malcolm Reid[1], Lene S. Heier[3], Emelie Skogsberg[1,2], Brynhild Snilsberg[3], Dagfin Gryteselv[3], Sondre Meland[1,2]

[1]Norwegian Institute for Water Research, Økernveien 94, NO-0579 Oslo, Norway
[2]Norwegian University of Life Sciences, Center of Excellence in Environmental Radioactivity (CERAD), Faculty of Environmental Sciences and Natural Resource Management, P.O. Box 5003, 1433 Ås, Norway
[3]Norwegian Public Roads Administration, N-2605 Lillehammer, Norway

SI-1 Calibration curve

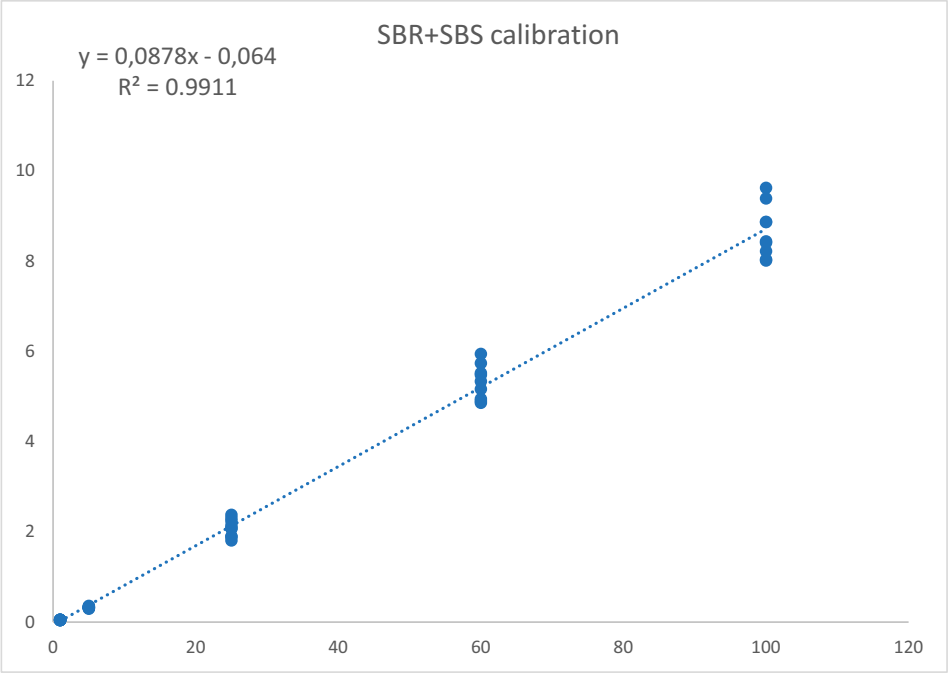

Figure S1. Calibration curve for mixture calibration of SBR and SBS. Calibration points 1 µg, 2µg, 25 µg, 60µg and 100 µg. Three ratios of SBR:SBS (20:80, 40:60, 80:20) and three replicates for each ratio at all calibration points.

SI-2 Tire, PMB and TRWP Monte Carlo simulation results

ROAD SURFACE

Table SI-1 *Results for tire prediction for road surface samples. Sample codes: B = Bank. IW = In the Wheeltrack. BW = Between the Wheeltrack. BL = Between the Lanes. RL = Right Lane (for middle area transect), LL = Left Lane (for middle area transect). AB and BC = Two and two areas are collected and pooled together in one sample.*

	Output values	**Input variables**							**Predicted values**									
Sample	*MT*	*MS*	*RSBS*	*SC*	*SPV*	*SHV*	*RPV*	*RT*	Average MT	S.D.	*Min*	*Max*	*Median*	*10th*	*25th*	*75th*	*90th*	*S.D.*
	mg/L	*µg/L*							mg/L	mg/L	mg/L	mg/L	mg/L	mg/L	mg/L	mg/L	mg/L	%
INLET-B-AB	5.26	1850	0.110	0.9	279	318	0.920	0.080	5.28	5.24	0.50	3.81	8.51	4.68	4.93	5.58	5.93	9.4
INLET-B-CD	7.39	2597	0.110	0.9	279	318	0.920	0.080	7.41	7.35	0.70	5.35	11.94	6.57	6.92	7.83	8.33	9.4
INLET-IW-AB	0.39	138	0.110	0.9	279	318	0.920	0.080	0.39	0.39	0.04	0.28	0.63	0.35	0.37	0.42	0.44	9.4
INLET-IW-CD	0.31	109	0.110	0.9	279	318	0.920	0.080	0.31	0.31	0.03	0.22	0.50	0.27	0.29	0.33	0.35	9.4
INLET-BW-AB	1.23	433	0.110	0.9	279	318	0.920	0.080	1.23	1.22	0.12	0.89	1.99	1.09	1.15	1.30	1.39	9.4
INLET-BW-CD	1.92	676	0.110	0.9	279	318	0.920	0.080	1.93	1.91	0.18	1.39	3.11	1.71	1.80	2.04	2.17	9.4
MID-B-RL-AB	9.51	3345	0.110	0.9	279	318	0.920	0.080	9.55	9.47	0.90	6.88	15.38	8.47	8.91	10.09	10.73	9.4
MID-B-RL-CD	4.71	1656	0.110	0.9	279	318	0.920	0.080	4.73	4.69	0.45	3.41	7.62	4.19	4.41	5.00	5.31	9.4
MID-IW-RL-RIGHT-AB	0.52	184	0.110	0.9	279	318	0.920	0.080	0.53	0.52	0.05	0.38	0.85	0.47	0.49	0.56	0.59	9.4
MID-IW-RL-RIGHT-CD	0.07	25.3	0.110	0.9	279	318	0.920	0.080	0.07	0.07	0.01	0.05	0.12	0.06	0.07	0.08	0.08	9.4
MID-BW-RL-AB	1.12	394	0.110	0.9	279	318	0.920	0.080	1.13	1.12	0.11	0.81	1.81	1.00	1.05	1.19	1.26	9.4
MID-BW-RL-CD	1.72	604	0.110	0.9	279	318	0.920	0.080	1.72	1.71	0.16	1.24	2.78	1.53	1.61	1.82	1.94	9.4
MID-IW-RL-RIGHT-AB	5.24	1843	0.110	0.9	279	318	0.920	0.080	5.26	5.22	0.50	3.79	8.47	4.66	4.91	5.56	5.91	9.4
MID-IW-RL-RIGHT-CD	7.00	2462	0.110	0.9	279	318	0.920	0.080	7.03	6.97	0.66	5.07	11.32	6.23	6.56	7.43	7.89	9.4
MID-IW-LL-RIGHT-AB	0.17	61.3	0.110	0.9	279	318	0.920	0.080	0.18	0.17	0.02	0.13	0.28	0.16	0.16	0.19	0.20	9.4
MID-IW-LL-RIGHT-CD	0.19	67.3	0.110	0.9	279	318	0.920	0.080	0.19	0.19	0.02	0.14	0.31	0.17	0.18	0.20	0.22	9.4
MID-IW-LL-LEFT-AB	0.19	67.4	0.110	0.9	279	318	0.920	0.080	0.19	0.19	0.02	0.14	0.31	0.17	0.18	0.20	0.22	9.4
MID-IW-LL-LEFT-CD	0.17	58.2	0.110	0.9	279	318	0.920	0.080	0.17	0.16	0.02	0.12	0.27	0.15	0.16	0.18	0.19	9.4

MID-IW-RL-LEFT-AB	0.22	78.4	0.110	0.9	279	318	0.920	0.080	0.22	0.22	0.02	0.16	0.36	0.20	0.21	0.24	0.25	9.4
MID-IW-RL-LEFT-CD	0.16	56.5	0.110	0.9	279	318	0.920	0.080	0.16	0.16	0.02	0.12	0.26	0.14	0.15	0.17	0.18	9.4
MID-BW-LL-AB	1.36	477	0.110	0.9	279	318	0.920	0.080	1.36	1.35	0.13	0.98	2.19	1.21	1.27	1.44	1.53	9.4
MID-BL-AB	1.42	499	0.110	0.9	279	318	0.920	0.080	1.43	1.41	0.13	1.03	2.30	1.26	1.33	1.51	1.60	9.4
MID-BL-AB	1.05	368	0.110	0.9	279	318	0.920	0.080	1.05	1.04	0.10	0.76	1.69	0.93	0.98	1.11	1.18	9.4
OUTLET-B-AB	13.72	4824	0.110	0.9	279	318	0.920	0.080	13.8	13.7	1.30	9.93	22.2	12.2	12.9	14.6	15.5	9.4
OUTLET-IW-AB	1.87	656	0.110	0.9	279	318	0.920	0.080	1.87	1.86	0.18	1.35	3.02	1.66	1.75	1.98	2.10	9.4
OUTLET-IW-CD	0.16	55.0	0.110	0.9	279	318	0.920	0.080	0.16	0.16	0.01	0.11	0.25	0.14	0.15	0.17	0.18	9.4
OUTLET-BW-CD	1.61	566	0.110	0.9	279	318	0.920	0.080	1.62	1.60	0.15	1.17	2.60	1.43	1.51	1.71	1.82	9.4

Table SI-2. Results for PMB prediction for road surface samples. Sample codes: B = Bank. IW = In the Wheeltrack. BW = Between the Wheeltrack. BL = Between the Lanes. RL = Right Lane (for middle area transect), LL = Left Lane (for middle area transect). AB and BC = Two and two areas are collected and pooled together in one sample.

	Output values	**Input variables**		**Predicted values**									
Sample	*MPMB*	*MS*	*RSBS*	Average MPMB	S.D.	*Min*	*Max*	*Median*	*10th*	*25th*	*75th*	*90th*	*S.D.*
	mg/L	*µg/L*		mg/L	mg/L	mg/L	mg/L	mg/L	mg/L	mg/L	mg/L	mg/L	%
INLET-B-AB	4058	1850	0.110	4207	4173	470	3142	5426	3597	3865	4539	4868	11.2
INLET-B-CD	5697	2597	0.110	5905	5859	660	4411	7618	5050	5426	6372	6833	11.2
INLET-IW-AB	302	138	0.110	313	311	35.0	234	404	268	288	338	363	11.2
INLET-IW-CD	238	109	0.110	247	245	27.6	184	319	211	227	267	286	11.2
INLET-BW-AB	949	433	0.110	983	976	110	735	1269	841	904	1061	1138	11.2
INLET-BW-CD	1484	676	0.110	1538	1526	172	1149	1984	1315	1413	1660	1780	11.2
MID-B-RL-AB	7337	3345	0.110	7605	7545	849	5680	9811	6503	6989	8207	8800	11.2
MID-B-RL-CD	3633	1656	0.110	3766	3736	421	2813	4858	3221	3461	4064	4358	11.2
MID-IW-RL-RIGHT-AB	405	184	0.110	419	416	46.8	313	541	359	385	453	485	11.2
MID-IW-RL-RIGHT-CD	55.6	25.3	0.110	57.6	57.1	6.4	43.0	74.3	49.2	52.9	62.1	66.6	11.2
MID-BW-RL-AB	865	394	0.110	897	890	100	670	1157	767	824	967	1037	11.2
MID-BW-RL-CD	1325	604	0.110	1374	1363	153	1026	1772	1175	1262	1482	1590	11.2
MID-IW-RL-RIGHT-AB	4042	1843	0.110	4190	4157	468	3129	5405	3583	3850	4521	4848	11.2
MID-IW-RL-RIGHT-CD	5401	2462	0.110	5598	5554	625	4181	7221	4787	5144	6041	6477	11.2
MID-IW-LL-RIGHT-AB	135	61.3	0.110	139	138	15.6	104	180	119	128	151	161	11.2
MID-IW-LL-RIGHT-CD	148	67.3	0.110	153	152	17.1	114	197	131	141	165	177	11.2
MID-IW-LL-LEFT-AB	148	67.4	0.110	153	152	17.1	114	198	131	141	165	177	11.2
MID-IW-LL-LEFT-CD	128	58.2	0.110	132	131	14.8	98.9	171	113	122	143	153	11.2
MID-IW-RL-LEFT-AB	172	78.4	0.110	178	177	19.9	133	230	152	164	192	206	11.2
MID-IW-RL-LEFT-CD	124	56.5	0.110	128	127	14.3	95.9	166	110	118	139	149	11.2
MID-BW-LL-AB	1047	477	0.110	1085	1077	121	811	1400	928	997	1171	1256	11.2
MID-BL-AB	1095	499	0.110	1136	1127	127	848	1465	971	1043	1225	1314	11.2

MID-BL-AB	808	368	0.110	838	831	93.5	626	1080	716	770	904	969	11.2
OUTLET-B-AB	10582	4824	0.110	10969	10882	1225	8192	14149	9379	10079	11836	12692	11.2
OUTLET-IW-AB	1439	656	0.110	1492	1480	167	1114	1924	1276	1371	1610	1726	11.2
OUTLET-IW-CD	121	55.0	0.110	125	124	14.0	93.4	161	107	115	135	145	11.2
OUTLET-BW-CD	1242	566	0.110	1288	1277	144	962	1661	1101	1183	1389	1490	11.2

Table SI-3. *Results for tire and road wear particle (TRWP) prediction for road surface samples. Sample codes: B = Bank. IW = In the Wheeltrack. BW = Between the Wheeltrack. BL = Between the Lanes. RL = Right Lane (for middle area transect), LL = Left Lane (for middle area transect). AB and BC = Two and two areas are collected and pooled together in one sample.*

	Output values	**Input variables**		**Predicted values**									
Sample	*MTRWP*	*MT*	*RENCR*	Average MTRWP	S.D.	*Min*	*Max*	*Median*	*10th*	*25th*	*75th*	*90th*	*% S.D.*
INLET-B-AB	4058	5.28	0.295	7.64	7.49	1.08	5.62	11.2	6.32	6.82	8.29	9.20	14.2
INLET-B-CD	5697	7.41	0.295	10.7	10.5	1.52	7.90	15.7	8.87	9.58	11.6	12.9	14.2
INLET-IW-AB	302	0.393	0.295	0.569	0.558	0.0808	0.419	0.834	0.471	0.508	0.618	0.685	14.2
INLET-IW-CD	238	0.310	0.295	0.448	0.440	0.0637	0.330	0.657	0.371	0.401	0.487	0.540	14.2
INLET-BW-AB	949	1.23	0.295	1.79	1.75	0.253	1.31	2.62	1.48	1.59	1.94	2.15	14.2
INLET-BW-CD	1484	1.93	0.295	2.79	2.74	0.396	2.06	4.09	2.31	2.49	3.03	3.36	14.2
MID-B-RL-AB	7337	9.55	0.295	13.8	13.5	1.96	10.2	20.2	11.4	12.3	15.0	16.6	14.2
MID-B-RL-CD	3633	4.73	0.295	6.84	6.71	0.971	5.04	10.0	5.66	6.11	7.43	8.24	14.2
MID-IW-RL-RIGHT-AB	405	0.526	0.295	0.761	0.747	0.108	0.561	1.12	0.630	0.680	0.827	0.917	14.2
MID-IW-RL-RIGHT-CD	55.6	0.072	0.295	0.105	0.103	0.0148	0.0770	0.153	0.0865	0.0934	0.114	0.126	14.2
MID-BW-RL-AB	865	1.13	0.295	1.627	1.60	0.231	1.20	2.39	1.35	1.45	1.77	1.96	14.2
MID-BW-RL-CD	1325	1.72	0.295	2.493	2.45	0.354	1.84	3.66	2.06	2.23	2.71	3.00	14.2
MID-IW-RL-RIGHT-AB	4042	5.26	0.295	7.61	7.46	1.08	5.60	11.2	6.30	6.79	8.26	9.16	14.2
MID-IW-RL-RIGHT-CD	5401	7.03	0.295	10.2	9.97	1.44	7.48	14.9	8.41	9.08	11.0	12.2	14.2
MID-IW-LL-RIGHT-AB	135	0.175	0.295	0.253	0.248	0.0360	0.186	0.371	0.210	0.226	0.275	0.305	14.2
MID-IW-LL-RIGHT-CD	148	0.192	0.295	0.278	0.273	0.0394	0.205	0.407	0.230	0.248	0.302	0.335	14.2
MID-IW-LL-LEFT-AB	148	0.192	0.295	0.278	0.273	0.0395	0.205	0.408	0.230	0.249	0.302	0.335	14.2
MID-IW-LL-LEFT-CD	128	0.166	0.295	0.240	0.236	0.0341	0.177	0.352	0.199	0.215	0.261	0.289	14.2
MID-IW-RL-LEFT-AB	172	0.224	0.295	0.323	0.317	0.0459	0.238	0.474	0.268	0.289	0.351	0.390	14.2
MID-IW-RL-LEFT-CD	124	0.161	0.295	0.233	0.229	0.0331	0.172	0.342	0.193	0.208	0.253	0.281	14.2
MID-BW-LL-AB	1047	1.36	0.295	1.97	1.93	0.280	1.45	2.89	1.63	1.76	2.14	2.37	14.2
MID-BL-AB	1095	1.43	0.295	2.06	2.02	0.293	1.52	3.02	1.71	1.84	2.24	2.48	14.2
MID-BL-AB	808	1.05	0.295	1.52	1.49	0.216	1.12	2.23	1.26	1.36	1.65	1.83	14.2

OUTLET-B-AB	10582	13.8	0.295	19.9	19.5	2.83	14.7	29.2	16.5	17.8	21.6	24.0	14.2
OUTLET-IW-AB	1439	1.87	0.295	2.71	2.66	0.385	1.99	3.97	2.24	2.42	2.94	3.26	14.2
OUTLET-IW-CD	121	0.157	0.295	0.227	0.223	0.0322	0.167	0.333	0.188	0.203	0.247	0.274	14.2
OUTLET-BW-CD	1242	1.62	0.295	2.34	2.29	0.3319	1.72	3.43	1.93	2.09	2.54	2.82	14.2

GULLY-POT

Table SI-4. Results for tire prediction for gully-pot samples. GP1 (inlet), GP2 (middle) and GP-3 (outlet) are analyzed in triplicates. The % s.d. is 9.4% for all. MS unit µg/mg. MT unit mg/mg

	Output values	**Input variables**							**Predicted values**								
Sample	*MT*	*MS*	*RSBS*	*SC*	*SPV*	*SHV*	*RPV*	*RT*	Average MT	S.D.	*Min*	*Max*	*Median*	*10th*	*25th*	*75th*	*90th*
GP-1-1	0.0540	13301	0.110	0.9	279	318	0.92	0.08	0.0542	0.0538	0.00512	0.0391	0.0874	0.0481	0.0506	0.0573	0.0609
GP-1-2	0.0532	11687	0.110	0.9	279	318	0.92	0.08	0.0534	0.0530	0.00505	0.0385	0.0861	0.0474	0.0499	0.0565	0.0600
GP-1-3	0.0514	16767	0.110	0.9	279	318	0.92	0.08	0.0516	0.0512	0.00488	0.0372	0.0832	0.0458	0.0482	0.0546	0.0580
GP-2-1	0.00594	15986	0.110	0.9	279	318	0.92	0.08	0.00596	0.00591	0.000563	0.00430	0.00960	0.00528	0.00556	0.00630	0.00670
GP-2-2	0.00301	15644	0.110	0.9	279	318	0.92	0.08	0.00302	0.00300	0.000286	0.00218	0.00487	0.00268	0.00282	0.00320	0.00340
GP-2-3	0.00525	8657	0.110	0.9	279	318	0.92	0.08	0.00527	0.00522	0.000498	0.00380	0.00849	0.00467	0.00492	0.00557	0.00592
GP-3-1	0.0104	8531	0.110	0.9	279	318	0.92	0.08	0.0105	0.0104	0.000990	0.00756	0.0169	0.00929	0.00978	0.0111	0.0118
GP-3-2	0.00488	5070	0.110	0.9	279	318	0.92	0.08	0.00490	0.00486	0.000463	0.00354	0.00790	0.00435	0.00458	0.00518	0.00551
GP-3-3	0.00656	11110	0.110	0.9	279	318	0.92	0.08	0.00658	0.00652	0.000621	0.00474	0.0106	0.00583	0.00614	0.00695	0.00739

Table SI-5. Results for PMB prediction for gully-pot samples. GP1 (inlet), GP2 (middle) and GP-3 (outlet) are analyzed in triplicates. MS unit μg/mg. MPMB unit mg/mg. % s.d. for all samples were 11.2%

	Output values	**Input variables**		**Predicted values**								
Sample	*MPMB*	*MS*	*RSBS*	Average MPMB	S.D.	*Min*	*Max*	*Median*	*10th*	*25th*	*75th*	*90th*
GP-1-1	41.7	13301	0.110	43.2	42.9	4.83	32.3	55.7	36.9	39.7	46.6	50.0
GP-1-2	41.1	11687	0.110	42.6	42.2	4.75	31.8	54.9	36.4	39.1	45.9	49.3
GP-1-3	39.7	16767	0.110	41.1	40.8	4.59	30.7	53.1	35.2	37.8	44.4	47.6
GP-2-1	4.58	15986	0.110	4.75	4.71	0.53	3.55	6.12	4.06	4.36	5.12	5.49
GP-2-2	2.33	15644	0.110	2.41	2.39	0.27	1.80	3.11	2.06	2.21	2.60	2.79
GP-2-3	4.05	8657	0.110	4.20	4.16	0.47	3.13	5.41	3.59	3.86	4.53	4.86
GP-3-1	8.05	8531	0.110	8.35	8.28	0.93	6.23	10.8	7.14	7.67	9.01	9.66
GP-3-2	3.77	5070	0.110	3.91	3.87	0.44	2.92	5.04	3.34	3.59	4.21	4.52
GP-3-3	5.06	11110	0.110	5.24	5.20	0.59	3.92	6.76	4.48	4.82	5.66	6.07

Table SI-6. Results for TRWP prediction for gully-pot samples. GP1 (inlet), GP2 (middle) and GP-3 (outlet) are analyzed in triplicates. MS unit mg/mg. MTRWP unit mg/mg. % s.d. for all samples were 14.2%

	Output values	**Input variables**		**Predicted values**								
Sample	*MTRWP*	*MT*	*RENCR*	Average MTRWP	S.D.	*Min*	*Max*	*Median*	*10th*	*25th*	*75th*	*90th*
GP-1-1	0.0769	0.0542	0.295	0.0784	0.0770	0.0111	0.0578	0.1150	0.0649	0.0701	0.0852	0.0945
GP-1-2	0.0758	0.0534	0.295	0.0773	0.0758	0.0110	0.0569	0.1133	0.0640	0.0690	0.0839	0.0931
GP-1-3	0.0732	0.0516	0.295	0.0747	0.0733	0.0106	0.0550	0.1095	0.0618	0.0667	0.0811	0.0900
GP-2-1	0.00845	0.00596	0.295	0.00862	0.00846	0.0012	0.00635	0.0126	0.00713	0.00770	0.00936	0.0104
GP-2-2	0.00429	0.00302	0.295	0.00437	0.00429	0.0006	0.00322	0.00641	0.00362	0.00391	0.00475	0.00527
GP-2-3	0.00747	0.00527	0.295	0.00762	0.00748	0.00108	0.00561	0.0112	0.00631	0.00680	0.00827	0.00918
GP-3-1	0.0149	0.0105	0.295	0.0152	0.0149	0.00215	0.0112	0.0222	0.0125	0.0135	0.0165	0.0183
GP-3-2	0.00695	0.00490	0.295	0.00709	0.00696	0.00101	0.00522	0.0104	0.00587	0.00633	0.00770	0.00854
GP-3-3	0.00933	0.00658	0.295	0.00951	0.00934	0.00135	0.00701	0.0140	0.00788	0.00850	0.0103	0.0115

TUNNEL WASH WATER

Table SI-7. Results for tire prediction for tunnel wash water. Samples TWW-1 to TWW-14 are untreated tunnel wash water collected in the pump house during the wash. Samples TWW-14 to TWW-28 are treated tunnel wash samples collected from the outlet to the raingarden after sedimentation treatment. MS unit is µg/L MT unit is mg/L. % s.d. for all samples is 9.4%.

	Output values	Input variables							Predicted values								
Sample	*MT*	*MS*	*RSBS*	*SC*	*SPV*	*SHV*	*RPV*	*RT*	Average MT	S.D.	*Min*	*Max*	*Median*	*10th*	*25th*	*75th*	*90th*
TWW-1	37.83	13301	0.110	0.9	279	318	0.920	0.080	38.0	37.6	3.59	27.4	61.2	33.7	35.4	40.1	42.7
TWW-2	33.24	11687	0.110	0.9	279	318	0.920	0.080	33.4	33.1	3.15	24.1	53.7	29.6	31.1	35.3	37.5
TWW-3	47.68	16767	0.110	0.9	279	318	0.920	0.080	47.8	47.5	4.52	34.5	77.1	42.4	44.7	50.6	53.8
TWW-4	45.46	15986	0.110	0.9	279	318	0.920	0.080	45.6	45.2	4.31	32.9	73.5	40.5	42.6	48.2	51.3
TWW-5	44.49	15644	0.110	0.9	279	318	0.920	0.080	44.6	44.3	4.22	32.2	71.9	39.6	41.7	47.2	50.2
TWW-6	24.62	8657	0.110	0.9	279	318	0.920	0.080	24.7	24.5	2.33	17.8	39.8	21.9	23.1	26.1	27.8
TWW-7	24.26	8531	0.110	0.9	279	318	0.920	0.080	24.3	24.1	2.30	17.6	39.2	21.6	22.7	25.7	27.4
TWW-8	14.42	5070	0.110	0.9	279	318	0.920	0.080	14.5	14.3	1.37	10.4	23.3	12.8	13.5	15.3	16.3
TWW-9	31.60	11110	0.110	0.9	279	318	0.920	0.080	31.7	31.4	3.00	22.9	51.1	28.1	29.6	33.5	35.6
TWW-10	33.45	11763	0.110	0.9	279	318	0.920	0.080	33.6	33.3	3.17	24.2	54.1	29.8	31.3	35.5	37.7
TWW-11	33.81	11891	0.110	0.9	279	318	0.920	0.080	33.9	33.7	3.21	24.5	54.7	30.1	31.7	35.9	38.1
TWW-12	37.69	13253	0.110	0.9	279	318	0.920	0.080	37.8	37.5	3.57	27.3	60.9	33.5	35.3	40.0	42.5
TWW-13	34.26	12047	0.110	0.9	279	318	0.920	0.080	34.4	34.1	3.25	24.8	55.4	30.5	32.1	36.3	38.6
TWW-14	25.85	9091	0.110	0.9	279	318	0.920	0.080	25.9	25.7	2.45	18.7	41.8	23.0	24.2	27.4	29.2
TWW-15	9.02	3172	0.110	0.9	279	318	0.920	0.080	9.05	8.98	0.86	6.53	14.6	8.03	8.45	9.57	10.17
TWW-16	29.30	10304	0.110	0.9	279	318	0.920	0.080	29.4	29.2	2.78	21.2	47.4	26.1	27.5	31.1	33.0

TWW-17	17.61	6192	0.110	0.9	279	318	0.920	0.080	17.7	17.5	1.67	12.7	28.5	15.7	16.5	18.7	19.9
TWW-18	15.85	5575	0.110	0.9	279	318	0.920	0.080	15.9	15.8	1.50	11.5	25.6	14.1	14.9	16.8	17.9
TWW-19	17.45	6135	0.110	0.9	279	318	0.920	0.080	17.5	17.4	1.65	12.6	28.2	15.5	16.3	18.5	19.7
TWW-20	11.59	4075	0.110	0.9	279	318	0.920	0.080	11.6	11.5	1.10	8.4	18.7	10.3	10.9	12.3	13.1
TWW-21	12.63	4442	0.110	0.9	279	318	0.920	0.080	12.7	12.6	1.20	9.1	20.4	11.2	11.8	13.4	14.2
TWW-22	10.50	3691	0.110	0.9	279	318	0.920	0.080	10.5	10.4	1.00	7.6	17.0	9.3	9.8	11.1	11.8
TWW-23	9.40	3307	0.110	0.9	279	318	0.920	0.080	9.44	9.36	0.89	6.81	15.2	8.37	8.81	9.97	10.6
TWW-24	7.91	2781	0.110	0.9	279	318	0.920	0.080	7.94	7.87	0.75	5.72	12.8	7.04	7.41	8.39	8.92
TWW-25	9.64	3389	0.110	0.9	279	318	0.920	0.080	9.67	9.59	0.91	6.97	15.6	8.58	9.03	10.2	10.9
TWW-26	9.53	3350	0.110	0.9	279	318	0.920	0.080	9.56	9.48	0.90	6.90	15.4	8.48	8.92	10.1	10.7
TWW-27	7.71	2711	0.110	0.9	279	318	0.920	0.080	7.74	7.67	0.73	5.58	12.5	6.86	7.22	8.18	8.69
TWW-28	6.76	2377	0.110	0.9	279	318	0.920	0.080	6.78	6.73	0.64	4.89	10.9	6.02	6.33	7.17	7.62

Table SI-8. Results for PMB prediction for tunnel wash water. Samples TWW-1 to TWW-14 are untreated tunnel wash water collected in the pump house during the wash. Samples TWW-14 to TWW-28 are treated tunnel wash samples collected from the outlet to the raingarden after sedimentation treatment. MS unit is mg/L MPMB unit is mg/L. % s.d. for all samples is 11.2%.

	Output values	**Input variables**		**Predicted values**								
Sample	*MPMB*	*MS*	*RSBS*	Average MPMB	S.D.	*Min*	*Max*	*Median*	*10th*	*25th*	*75th*	*90th*
TWW-1	29178	13301	0.110	30245	30006	3378	22589	39014	25862	27791	32635	34996
TWW-2	25637	11687	0.110	26575	26364	2968	19848	34280	22724	24419	28675	30749
TWW-3	36780	16767	0.110	38125	37824	4258	28475	49180	32601	35033	41139	44115
TWW-4	35068	15986	0.110	36351	36063	4060	27150	46890	31083	33402	39224	42061
TWW-5	34317	15644	0.110	35572	35291	3973	26568	45886	30418	32687	38384	41160
TWW-6	18989	8657	0.110	19684	19528	2198	14702	25391	16832	18087	21240	22776
TWW-7	18714	8531	0.110	19399	19245	2167	14489	25023	16588	17825	20932	22446
TWW-8	11121	5070	0.110	11528	11437	1287	8610	14870	9857	10593	12439	13339
TWW-9	24372	11110	0.110	25263	25063	2821	18869	32588	21602	23214	27260	29232
TWW-10	25804	11763	0.110	26748	26537	2987	19978	34504	22872	24578	28862	30950
TWW-11	26083	11891	0.110	27037	26824	3020	20194	34877	23119	24844	29174	31284
TWW-12	29072	13253	0.110	30135	29897	3366	22507	38872	25768	27691	32517	34869
TWW-13	26426	12047	0.110	27392	27176	3059	20459	35334	23423	25170	29557	31695
TWW-14	19942	9091	0.110	20671	20508	2309	15439	26665	17676	18995	22305	23919
TWW-15	6959	3172	0.110	7213	7156	806	5387	9305	6168	6628	7783	8346
TWW-16	22602	10304	0.110	23429	23244	2617	17499	30222	20034	21528	25281	27109
TWW-17	13582	6192	0.110	14079	13967	1572	10515	18161	12039	12937	15191	16290
TWW-18	12229	5575	0.110	12677	12576	1416	9468	16352	10840	11648	13679	14668
TWW-19	13457	6135	0.110	13950	13839	1558	10419	17994	11928	12818	15052	16141
TWW-20	8940	4075	0.110	9267	9194	1035	6921	11954	7924	8515	9999	10723
TWW-21	9743	4442	0.110	10100	10020	1128	7543	13028	8636	9280	10898	11686
TWW-22	8097	3691	0.110	8394	8327	937	6269	10827	7177	7713	9057	9712

TWW-23	7254	3307	0.110	7519	7460	840	5616	9699	6430	6909	8114	8700
TWW-24	6100	2781	0.110	6323	6273	706	4722	8156	5406	5810	6822	7316
TWW-25	7433	3389	0.110	7705	7644	861	5755	9939	6589	7080	8314	8916
TWW-26	7348	3350	0.110	7617	7557	851	5689	9826	6513	6999	8219	8814
TWW-27	5946	2711	0.110	6164	6115	688	4604	7951	5271	5664	6651	7132
TWW-28	5214	2377	0.110	5405	5362	604	4037	6972	4622	4966	5832	6254

Table SI-9. Results for tire and road wear (TRWP) prediction for tunnel wash water. Samples TWW-1 to TWW-14 are untreated tunnel wash water collected in the pump house during the wash. Samples TWW-14 to TWW-28 are treated tunnel wash samples collected from the outlet to the raingarden after sedimentation treatment. MT unit is mg/L MTRWP unit is mg/L. % s.d. for all samples is 14.2%.

	Output values	**Input variables**		**Predicted values**								
Sample	*MTRWP*	*MT*	*RENCR*	Average MTRWP	S.D.	*Min*	*Max*	*Median*	*10th*	*25th*	*75th*	*90th*
TWW-1	53.8	38.0	0.295	54.9	53.9	7.8	40.4	80.5	45.5	49.0	59.6	66.1
TWW-2	47.3	33.4	0.295	48.2	47.3	6.8	35.5	70.7	39.9	43.1	52.4	58.1
TWW-3	67.9	47.8	0.295	69.2	67.9	9.8	51.0	101.5	57.3	61.8	75.2	83.4
TWW-4	64.7	45.6	0.295	66.0	64.8	9.4	48.6	96.7	54.6	58.9	71.7	79.5
TWW-5	63.3	44.6	0.295	64.6	63.4	9.2	47.6	94.7	53.5	57.7	70.1	77.8
TWW-6	35.0	24.7	0.295	35.7	35.1	5.1	26.3	52.4	29.6	31.9	38.8	43.0
TWW-7	34.5	24.3	0.295	35.2	34.6	5.0	25.9	51.6	29.2	31.5	38.2	42.4
TWW-8	20.5	14.5	0.295	20.9	20.5	3.0	15.4	30.7	17.3	18.7	22.7	25.2
TWW-9	45.0	31.7	0.295	45.9	45.0	6.5	33.8	67.2	38.0	41.0	49.8	55.2
TWW-10	47.6	33.6	0.295	48.6	47.6	6.9	35.8	71.2	40.2	43.4	52.7	58.5
TWW-11	48.1	33.9	0.295	49.1	48.2	7.0	36.1	72.0	40.6	43.8	53.3	59.1
TWW-12	53.6	37.8	0.295	54.7	53.7	7.8	40.3	80.2	45.3	48.9	59.4	65.9
TWW-13	48.8	34.4	0.295	49.7	48.8	7.1	36.6	72.9	41.2	44.4	54.0	59.9
TWW-14	36.8	25.9	0.295	37.5	36.8	5.3	27.6	55.0	31.1	33.5	40.8	45.2
TWW-15	12.8	9.05	0.295	13.1	12.8	1.9	9.6	19.2	10.8	11.7	14.2	15.8
TWW-16	41.7	29.4	0.295	42.5	41.7	6.0	31.3	62.4	35.2	38.0	46.2	51.2
TWW-17	25.1	17.7	0.295	25.6	25.1	3.6	18.8	37.5	21.2	22.8	27.8	30.8
TWW-18	22.6	15.9	0.295	23.0	22.6	3.3	16.9	33.7	19.1	20.6	25.0	27.7
TWW-19	24.8	17.5	0.295	25.3	24.8	3.6	18.7	37.1	21.0	22.6	27.5	30.5
TWW-20	16.5	11.6	0.295	16.8	16.5	2.4	12.4	24.7	13.9	15.0	18.3	20.3
TWW-21	18.0	12.7	0.295	18.3	18.0	2.6	13.5	26.9	15.2	16.4	19.9	22.1
TWW-22	14.9	10.5	0.295	15.2	15.0	2.2	11.2	22.3	12.6	13.6	16.5	18.4
TWW-23	13.4	9.44	0.295	13.6	13.4	1.9	10.1	20.0	11.3	12.2	14.8	16.4

TWW-24	11.3	7.94	0.295	11.5	11.3	1.6	8.5	16.8	9.5	10.3	12.5	13.8
TWW-25	13.7	9.67	0.295	14.0	13.7	2.0	10.3	20.5	11.6	12.5	15.2	16.9
TWW-26	13.6	9.56	0.295	13.8	13.6	2.0	10.2	20.3	11.4	12.4	15.0	16.7
TWW-27	11.0	7.74	0.295	11.2	11.0	1.59	8.24	16.4	9.26	10.0	12.2	13.5
TWW-28	9.62	6.78	0.295	9.81	9.63	1.39	7.23	14.4	8.12	8.76	10.7	11.8

SI-3 Combined results for TSS, SBR+BR+SBS, Tire, PMB and TRWP

Road surface

Table S-10. Summary of the results for road surface: total suspended solids (TSS) in mg/L and mg/m², styrene butadiene styrene + butadiene rubber + styrene butadiene styrene (SBR+BR+SBS) in mg/L, mg/m² and mg/g, predicted mean tire in mg/L, mg/m2 and mg/g, predicted polymer-modified bitumen (PMB) in mg/L, mg/m² and mg/g, and predicted tire and road wear particles (TRWP) in mg/L, mg/m² and mg/g.

Sample	Volume	TSS	TSS	SBR+BR+SBS	SBR+BR+SBS	SBR+BR+SBS	Tire	Tire	Tire	PMB	PMB	PMB	TRWP	TRWP	TRWP
	L	*mg/L*	*mg/m2*	*mg/L*	*mg/m²*	*mg/g*	*mg/L*	*mg/m²*	*mg/g*	*mg/L*	*mg/m²*	*mg/g*	*mg/L*	*mg/m²*	*mg/g*
INLET-B-AB	1.98	306	106988	1.85	6.05	648	5.28	1849	17.3	4.21	1473	13.8	7.64	2674	25.0
INLET-B-CD	1.98	403	141224	2.60	6.44	909	7.41	2595	18.4	5.91	2068	14.6	10.7	3753	26.6
INLET-BW-AB	1.98	45.0	15756	0.433	9.61	151	1.23	432	27.4	0.983	344	21.9	1.79	625	39.7
INLET-BW-CD	1.98	443	155229	0.676	1.53	237	1.93	676	4.4	1.54	539	3.47	2.79	978	6.30
INLET-IW-AB	1.98	25.3	8870	0.138	5.44	48.2	0.393	138	15.5	0.313	110	12.4	0.57	199	22.5
INLET-IW-CD	1.98	537	187909	0.109	0.202	38.0	0.310	109	0.6	0.247	86.5	0.460	0.45	157	0.8
MID-B-RL-AB	1.98	37.3	13072	3.34	89.6	1171	9.55	3342	256	7.61	2663	203.7	13.8	4834	370
MID-B-RL-CD	1.98	37.7	13189	1.66	44.0	580	4.73	1655	125	3.77	1319	100.0	6.84	2394	181
MID-B-LL-AB	1.98	260	91037	1.84	7.09	645	5.26	1841	20.2	4.19	1467	16.1	7.61	2663	29.3
MID-B-LL-CD	1.98	293	102708	2.46	8.39	862	7.03	2460	24.0	5.60	1960	19.1	10.2	3558	34.6
MID-BW-RL-AB	1.98	250	87535	0.394	1.58	138	1.13	394	4.5	0.897	314	3.59	1.63	570	6.5
MID-BW-RL-CD	1.98	19.3	6769	0.604	31.2	212	1.72	604	89.2	1.37	481	71.1	2.49	873	129
MID-BW-LL-AB	1.98	66.7	23343	0.477	7.16	167	1.36	477	20.4	1.09	380	16.3	1.97	690	29.6
MID-IW-RL-RIGHT-AB	1.98	440	154062	0.1845	0.419	64.6	0.526	184	1.2	0.419	147	0.95	0.76	267	1.73
MID-IW-RL-RIGHT-CD	1.98	21.7	7586	0.0253	1.17	8.87	0.0723	25	3.3	0.0576	20.2	2.66	0.10	36.6	4.82

MID-IW-LL-RIGHT-AB	1.98	17.7	6186	0.0613	3.47	21.5	0.175	61	9.9	0.139	48.8	7.90	0.25	88.6	14.3
MID-IW-LL-RIGHT-CD	1.98	17.0	5952	0.0673	3.96	23.6	0.192	67	11.3	0.153	53.6	9.00	0.28	97.3	16.3
MID-IW-LL-LEFT-AB	1.98	25.0	8754	0.0674	2.70	23.6	0.192	67	7.7	0.153	53.7	6.13	0.28	97.4	11.1
MID-IW-LL-LEFT-CD	1.98	18.3	6419	0.0582	3.18	20.4	0.166	58	9.1	0.132	46.3	7.22	0.24	84.1	13.1
MID-IW-RL-LEFT-AB	1.98	17.3	6069	0.0784	4.52	27.4	0.224	78	12.9	0.178	62.4	10.3	0.32	113	18.7
MID-IW-RL-LEFT-CD	1.98	29.0	10154	0.0565	1.95	19.8	0.161	56	5.6	0.128	44.9	4.43	0.23	81.6	8.03
MID-BL-AB	1.98	53.3	18674	0.499	9.36	175	1.43	499	26.7	1.14	398	21.3	2.06	722	38.6
MID-BL-AB	1.98	50.0	17507	0.368	7.37	129	1.05	368	21.0	0.838	293	16.8	1.52	532	30.4
OUTLET-B-AB	1.98	53.3	18674	4.82	90.4	1689	13.8	4820	258	10.97	3841	205.7	19.9	6971	373
OUTLET-BW-CD	1.98	91.1	31902	0.566	6.2147	198	1.62	566	17.7	1.29	451	14.1	2.34	818	25.7
OUTLET-IW-AB	1.98	31.7	11088	0.656	20.7	230	1.87	656	59.1	1.49	522	47.1	2.71	948	85.5
OUTLET-IW-CD	1.98	96.7	33847	0.0550	0.569	19.3	0.157	55	1.62	0.125	43.8	1.29	0.23	79.5	2.35

Table S-11. Average total suspended solids (TSS), styrene butadiene styrene + butadiene rubber + styrene butadiene styrene (SBR+BR+SBS), tire, polymer-modified bitumen (PMB) and tire and road wear particles (TRWP) on the tunnel road surface. Concentrations are summarized for all samples within the inlet, mid and outlet area of the tunnel, and by bank area (B), in the wheel tracks (IW), between the wheel tracks (BW) and middle between lanes (BL) for inlet, mid and outlet pooled. The average for tire, PMB and TRWP are predicted mean from 100,000 Monte Carlo simulations.

BANK (B)	TSS	SBR+BR+SBS	Tire	PMB	TRWP	TRWP
	mg/m²	mg/m²	mg/m²	mg/m²	mg/m²	mg/g
AVERAGE	69600	929	2650	2110	3840	149
SD	53300	392	1120	892	1620	162
MIN	13100	580	1660	1320	2390	25.0
MAX	141000	1690	4820	3840	6970	373
BETWEEN WHEELTRACKS (BW)						
AVERAGE	53400	184	525	418	759	39.4
SD	57400	38	108	86.3	157	45.8
MIN	6770	138	394	314	570	1.63
MAX	155000	237	676	539	978	129
IN WHEELTRACKS (IW)						
AVERAGE	37200	45.4	130	103	187	16.6
SD	63300	60.0	171	136	247	22.8
MIN	5950	8.87	25.3	20.2	36.6	0.835
MAX	188000	230	656	522	948	85.5
BETWEEN LANES (BL)						
AVERAGE	18100	152	434	345	627	34.5
SD	825	32.4	92.6	73.8	134	5.83
MIN	17500	129	368	293	532	30.4
MAX	18700	175	499	398	722	38.6
INLET AREA						
AVERAGE	103000	339	966	770	1398	20.1
SD	74700	358	1022	814	1478	14.3
MIN	8870	38.0	109	86.5	157	0.835
MAX	188000	909	2595	2070	3753	39.7
MIDDLE AREA						
AVERAGE	34000	252	720	574	1040	55.1
SD	45100	347	992	790	1430	93.9
MIN	5950	8.9	25.3	20.2	36.6	1.73
MAX	154000	1170	3340	2660	4830	370
OUTLET AREA						
AVERAGE	23900	534	1524	1210	2200	122
SD	10900	776	2213	1760	3200	171
MIN	11100	19.3	55.0	43.8	79.5	2.35
MAX	33800	1690	4820	3840	6970	373
ALL SAMPLES						

AVERAGE	47800	313	894	712	1290	57.2
SD	56900	422	1200	961	1744	99.1
MIN	5950	8.87	25.3	20.2	36.6	0.835
MAX	188000	1690	4820	3840	6970	373

Gully-pot

SI-12. Summary of all results for gully-pots: GP-1 is located in the inlet of the tunnel, GP-2 in the middle and GP-3 in the outlet. Total suspended solids (TSS), styrene butadiene styrene + butadiene rubber + styrene butadiene styrene (SBR+BR+SBS) predicted mean tire, predicted polymer-modified bitumen (PMB), and predicted tire and road wear particles (TRWP). All presented in mg/g dry weight sediment.

Sample	SBR+BR+SBS (µg/mg)	Tire (mg/g)	PMB (mg/g)	TRWP mg/g
GP-1-1	19.0	54.2	43.2	78.4
GP-1-2	18.7	53.4	42.6	77.3
GP-1-3	18.1	51.6	41.1	74.7
Average	18.6	53.1	42.3	76.8
Standard deviation	0.467	1.33	1.06	1.93
GP-2-1	2.09	5.96	4.75	8.62
GP-2-2	1.06	3.02	2.41	4.37
GP-2-3	1.85	5.27	4.20	7.62
Average	1.66	4.75	3.78	6.87
Standard deviation	0.537	1.53	1.22	2.22
GP-3-1	3.67	10.5	8.35	15.2
GP-3-2	1.72	4.90	3.91	7.09
GP-3-3	2.31	6.58	5.24	9.51
Average	2.56	7.32	5.83	10.6
Standard deviation	1.00	2.86	2.28	4.14
All				
Average	7.61	21.7	17.3	31.4
Standard deviation	8.28	23.6	18.8	34.2
Median	2.31	6.58	5.24	9.51
Max	19.0	54.2	43.2	78.4
Min	1.06	3.02	2.41	4.37

Tunnel wash water

Table SI-13. Summary of all results for tunnel wash water (TWW): Total suspended solids (TSS), styrene butadiene styrene + butadiene rubber + styrene butadiene styrene (SBR+BR+SBS) predicted mean tire, predicted polymer-modified bitumen (PMB), and predicted tire and road wear particles (TRWP). All presented in mg/L.

Sample	Treatment	TSS	SBR+BR+SBS	Tire	PMB	TRWP	Tire + PMB
		mg/L	*mg/L*	*mg/L*	*mg/L*	*mg/L*	*%*
TWW-1	Before	1800	13.3	37.6	30.2	54.9	3.77
TWW-2	Before	1700	11.7	33.1	26.6	48.2	3.51
TWW-3	Before	3000	16.8	47.5	38.1	69.2	2.85
TWW-4	Before	3500	16.0	45.2	36.4	66.0	2.33
TWW-5	Before	1500	15.6	44.3	35.6	64.6	5.32
TWW-6	Before	1200	8.7	24.5	19.7	35.7	3.68
TWW-7	Before	1200	8.5	24.1	19.4	35.2	3.63
TWW-8	Before	1100	5.1	14.3	11.5	20.9	2.35
TWW-9	Before	930	11.1	31.4	25.3	45.9	6.10
TWW-10	Before	1200	11.8	33.3	26.7	48.6	5.00
TWW-11	Before	1100	11.9	33.7	27.0	49.1	5.52
TWW-12	Before	1500	13.3	37.5	30.1	54.7	4.51
TWW-13	Before	1800	12.0	34.1	27.4	49.7	3.42
TWW-14	After	1200	9.1	25.7	20.7	37.5	3.87
TWW-15	After	82	3.17	8.98	7.21	13.1	19.7
TWW-16	After	1300	10.3	29.2	23.4	42.5	4.05
TWW-17	After	610	6.19	17.5	14.1	25.6	5.18
TWW-18	After	760	5.57	15.8	12.7	23.0	3.74
TWW-19	After	650	6.13	17.4	13.9	25.3	4.82
TWW-20	After	610	4.08	11.5	9.27	16.8	3.41
TWW-21	After	530	4.4	12.6	10.1	18.3	4.28
TWW-22	After	470	3.69	10.4	8.39	15.2	4.01
TWW-23	After	400	3.31	9.36	7.52	13.6	4.22
TWW-24	After	370	2.78	7.87	6.32	11.5	3.84
TWW-25	After	360	3.39	9.59	7.71	14.0	4.80
TWW-26	After	280	3.35	9.48	7.62	13.8	6.11
TWW-27	After	290	2.71	7.67	6.16	11.2	4.77
TWW-28	After	250	2.38	6.73	5.40	9.81	4.85

Table S-14. Summary statistics of total suspended solids (TSS), styrene butadiene styrene + butadiene rubber + styrene butadiene styrene (SBR+BR+SBS), tire, polymer modified bitumen (PMB) and tire and road wear particles (TRWP) in tunnel wash water for all samples, samples before treatment and samples after treatment.

Tunnel wash water	Unit mg/L	Mean (n=28)	STD (n=28)	MIN (n=28)	MAX (n=28)	Treatment efficiency
TSS	ALL	1060	800	82	3500	
	Before treatment	1620	747	930	3500	
	After treatment	497	295	82	1300	69%
SBR+BR+SBS	ALL	8.08	4.61	2.38	16.8	
	Before treatment	11.8	3.22	5.07	16.8	
	After treatment	4.39	2.10	2.38	10.4	63%
Tire predicted	ALL	23.1	13.2	6.78	47.8	
	Before treatment	33.6	9.20	14.5	47.8	
	After treatment	12.5	6.00	6.78	29.4	63%
PMB predicted	ALL	18.4	10.5	5.40	38.1	
	Before treatment	26.8	7.33	11.5	38.1	
	After treatment	10.0	4.78	5.40	23.4	63%
TRWP predicted	ALL	33.4	19.0	9.81	69.2	
	Before treatment	48.6	13.3	20.9	69.2	
	After treatment	18.1	8.68	9.81	42.5	63%

Table SI-15. Summary of the size distribution of particles in tunnel wash water (TWW). TWW-1 to TWW-14 are untreated samples and TWW-15 to TWW-28 are treated samples. Values are presented as a %volume of the total number of particles.

Sample	<2.5 μm	2.5-10 μm	10-30 μm	30-50 μm	50-350 μm	>350 μm
TWW-1	10.2	30.4	41.7	10.9	6.83	0.00
TWW-2	8.48	26.1	45.8	12.9	6.60	0.00
TWW-3	11.0	30.2	38.6	11.7	8.53	0.00
TWW-4	10.0	30.6	40.8	11.5	7.13	0.00
TWW-5	9.20	28.2	43.1	13.0	6.59	0.00
TWW-6	10.3	31.6	42.6	10.1	5.31	0.00
TWW-7	9.90	30.6	44.4	10.0	5.15	0.00
TWW-8	10.8	32.5	39.5	10.2	6.95	0.00
TWW-9	10.3	32.3	42.5	9.94	4.94	0.00
TWW-10	11.0	33.5	42.1	9.36	4.13	0.00
TWW-11	9.82	31.4	42.2	10.2	6.36	0.00
TWW-12	7.44	21.2	43.5	16.3	11.7	0.00
TWW-13	12.0	36.5	37.0	8.22	6.29	0.02
TWW-14	10.8	32.1	44.9	8.56	3.67	0.00
TWW-15	15.6	50.8	33.6	0.00	0.00	0.00
TWW-16	10.3	32.8	37.4	7.84	7.10	4.51
TWW-17	7.74	25.3	44.7	12.2	8.51	1.57
TWW-18	7.65	24.3	43.6	15.1	8.97	0.32
TWW-19	7.65	25.9	45.8	12.7	7.90	0.00
TWW-20	8.14	26.6	46.1	12.1	7.10	0.00
TWW-21	8.70	29.5	44.6	11.5	5.70	0.00
TWW-22	10.2	33.8	44.1	8.66	3.26	0.00
TWW-23	7.62	26.1	51.5	11.9	2.96	0.00
TWW-24	7.98	27.8	53.1	8.97	2.17	0.00
TWW-25	5.68	17.4	51.5	21.3	4.15	0.00
TWW-26	8.17	27.8	53.9	8.41	1.74	0.00
TWW-27	7.05	22.6	52.4	13.8	4.09	0.00
TWW-28	6.78	22.1	55.8	11.6	3.75	0.00

SI-4 Calculation example for tire and road abrasion

Emission factors for road and tire abrasion

Table SI16: Road abrasion values for different road surfaces (EFA) for studded personal vehicles (PV-st) and non-studded PV (PVnst), studded heavy vehicles (HV-st) and non-studded HV (HV-nst). Values are modified after reported values for studded PV tires, with reported 5 times higher emission for all HV tires and a 40 times lower emission from non-studded tires (Bakløkk et al., 1997; Horvli, 1996; Snilsberg, 2008; Snilsberg et al., 2016)

Road surface	$EFA_{PV\text{-}st}$ (g/vkm)	$EFA_{HV\text{-}st}$ (g/vkm)	$EFA_{PV\text{-}nst}$ (g/vkm)	$EFA_{HV\text{-}nst}$ (g/vkm)
Stone mastic asphalt (SMA)	5-10	25-50	0.125-0.25	0.625-1.25
Asphalt concrete (AC)	15-20	75-100	0.375-0.5	1.875-2.5
Topeca	<15	<75	<0.375	<1.875
Porpus asphalt	18-25	90-125	0.45-0.625	2.25-3.125
Asphalt concrete with more gravel	15-30	75-150	0.375-0.75	1.875-3.75

Table SI17: Emission factors for tires for highway (EFT_H) and urban driving (EFT_U) for personal vehicles (PV) and heavy vehicles (HV), reported by (Klein J. et al., 2017)l

Tire	PV	HV
EFT_H	0.104	0.668
EFT_U	0.132	0.850

Table SI18: Calculating the ratio of SBR+BR to SBS using emission factors reported in tables S3 and S4, and traffic values for each location.

Site	Smestad
Type of road	CA
AÅDT (v/day)	44060
PV (ratio)	0.92
HV (ratio)	0.08
Ratio of studded tires HV	0.106
Ratio of studded tires PV	0.0316
Driving mode	Urban
EF_PV_tire (g/vkm)	0.132
EF_HV_tire (g/vkm)	0.85
EF_PV_road (g/vkm) ST	15-20
EF_HV_road	75-100
EF_PV_road (g/vkm) NST	0.375-0.500
EF_HV_road (g/vkm) NST	1.875-2.50
SBS (g/day)	23.2-43.1
Ratio of SBR, winter tires	0.3
Mass_SBR (g/day)	250.4
% of SBS	8.5-14.7
Mean % of SBS at location	11

SI-5 Calculation example from SBR+BR+SBS to tire and PMB concentrations

1) Calculate the ratio of SBR+BR vs SBS rubber in the sample

The calculations are described in detail in Rødland et al. (2022). Here we use the emission factors available to calculate the expected SBR+BR and SBS values for the specific site based on AADT, percentage of personal (PV) and heavy vehicles (HV), percentage of studded tires. A road length is needed for the emission calculations and this is set to 0.1km for all sites.

Equation 2

$$EM_T = (L_r * N_{v,r,t} * ((R_{PV} * EFT_{PV}) + (R_{HV} * EFT_{HV}))$$

Equation 3

$$EM_A = L_r * N_{v,r,t} * (((R_{PV-st} * EFA_{PV-st}) + (R_{PV-nst} * EFA_{PV-nst}) * R_{PV}) + ((R_{HV-st} * EFA_{HV-st}) + (R_{HV-nst} * EFA_{PV-nst}) * R_{HV}))$$

Where:

EM_T is estimated mass of tire in a sample (mg);

EM_A is the estimated mass of asphalt in a sample (mg);

L_r is the length of the particular road stretch *r* (km);

$N_{v,r,t}$ is the number of vehicles that have travelled the particular road stretch *r* during the given time period *t*;

EFT_{PV} is the emission factor for personal vehicle tires (mg/vkm);

EFT_{HV} is the emission factor for heavy vehicle tires (mg/vkm);

R_{PV} is the ratio of personal vehicles at the sampling location;

R_{HV} is the ratio of heavy vehicles at the sampling location;

EFA_{PV-st} is the emission factor for asphalt based on studded personal vehicle tires (mg/vkm);

EFA_{PV-nst} is the emission factor for asphalt based on non-studded personal vehicle tires (mg/vkm);

EFA_{HV-st} is the emission factor for asphalt based on studded heavy vehicle tires (mg/vkm);

EFA_{PV-nst} is the emission factor for asphalt based on non-studded heavy vehicle tires (mg/vkm);

R_{PV-st} is the ratio of personal vehicles (PV) with studded tires at the sampling location, compared to all PV vehicles;

R_{PV} is the ratio of personal vehicles (PV) at the sampling location compared to all vehicles;

R_{HV-st} is the ratio of heavy vehicles (HV) with studded tires at the sampling location, compared to all HV vehicles;

R_{HV} is the ratio of heavy vehicles (HV) at the sampling location, compared to all vehicles.

Example Smestad (values from Table SI-18)

Equation 3:

$$EM_T = (L_r * N_{v,r,t} * ((R_{PV} * EFT_{PV}) + (R_{HV} * EFT_{HV}))$$

$$EM_T = 0.1 * 44060 * ((0.92 * 0.132) + (0.08 * 0.85))$$

$$EM_T = 834.67 g/day$$

SBR+BR in Norwegian winter tires (mean value for PV and HV) = 30%

$$SBR+BR = EM_T * 0.3$$

$$SBR+BR = 834.67 * 0.3$$

$$SBR+BR = 250.4 g/day$$

Equation 3

The road wear emission factors are based on the estimated release of 15-20g/vkm for studded PV. As this is a range, we calculate the road wear for three levels: 15, 17.5 and 20g/vkm and then find the average for each site. For HV the release is estimated at 5 x the PV emissions (75g/vkm). For non-studded vehicles, the release for both PV (0.375g/vkm) and HV (1.875g/vkm) are estimated to be 40 times lower than for studded tires.

The calculation below is for the first level, 15g/vkm.

$$EM_A = L_r * N_{v,r,t} * (((R_{PV-st} * EFA_{PV-st}) + (EFA_{PV-nst} * (R_{PV-nst} * EFA_{PV-nst}) * R_{PV}) + ((R_{HV-st} * EFA_{HV-st}) + (EFA_{HV-st} * (R_{HV-nst} * EFA_{PV-nst}) * R_{HV}))$$

$$EM_A = 0.1 * 44060 * ((((0.0316 * 15) + (0.375 * (1 - 0.0316)) * 0.92)) + (((0.106 * 75) + (1.875 * (1 - 0.106)) * 0.08)))$$

$$EM_A = 6786 g/day$$

In the asphalt used on these locations, 5% PMB is added and 5% of the PMB is SBS rubber.

The estimated SBS rubber at Bryn is therefore:

$$SBS = EM_A * 0.0025$$

$$SBS = 16.9\ g/day$$

The combined mass of SBR+BR+SBS for Smestad is then estimated at 267.3g/day, for the first level for road wear emissions. In percentage, SBS contributes 6.3% of the total rubber mass. All three levels of SBS is calculated for each location and used in the following equations 5 and 6 (Rødland et al., 2022).

Equation 5

Equation 6

$$M_T = \frac{M_S - (M_S * R_{SBS}) * Sc}{(S_{PV} * R_{PV}) + (S_{HV} * R_{HV})}$$

$$M_{PMB} = \frac{(M_S * R_{SBS})}{C_{PMB}}$$

where

M_T is the mass of tire in a sample (mg);

M_{PMB} is the mass of PMB in a sample (µg);

M_S is the mass of SBR+BR+SBS in a sample (µg);

R_{SBS} is the estimated ratio of SBS from the total SBR+BR+SBS concentration for each location;

Sc is the conversion factor for styrene content in standards vs tires;

S_{PV} is the mass of SBR+BR in personal vehicle tires (µg/mg);

R_{PV} is the ratio of personal vehicles at the sampling location;

S_{HV} is the mass of SBR+BR in heavy vehicle tires (µg/mg);

R_{HV} is the ratio of heavy vehicles at the sampling location;

C_{PMB} is the conversion factor for SBS to PMB, based on the percentage SBS in PMB (0.05).

Example from Smestad tunnel, Tunnel wash water sample 1(TWW-1). The measured concentration of SBR+BR+SBS was 13301 µg/L. The input variables for each site is found in Tables SI-7.

Equation 5

$$M_T = \frac{M_S - (M_S * R_{SBS}) * Sc}{(S_{PV} * R_{PV}) + (S_{HV} * R_{HV})}$$

$$M_T = \frac{13301 - (13301 * 0.110) * 0.9}{(279 * 0.92) + (318 * 0.08)}$$

$$M_T = 37.8\, mg/L$$

The M_T concentration is calculated using Crystal Ball Monte Carlo simulation, where RSBS has a triangular distribution pattern with 11% as the mean value, SPV has a normal distribution with a mean of 278.6 µg/mg rubber in winter tires and SHV has a normal distribution with 318.0 µg/mg rubber in winter tires. The model runs for 100 000 predictions and the summary statistics used from this is the predicted mean value, standard deviation, median, 10th, 25th, 75th and 90th percentiles. These are given in Table S7.

Equation 6

$$M_{PMB} = \frac{(M_S * R_{SBS})}{C_{PMB}}$$

$$M_{PMB} = \frac{(13301 * 0.11)}{0.05}$$

$$M_{PMB} = 29178\, mg/L$$

The M_{PMB} concentration is calculated using the Crystal Ball Monte Carlo simulation (100 000 simulations), where RSBS has a triangular distribution pattern with 11% as the mean value.

SI-6 Example of Total Ion Chromatogram

1) Styrene Butadiene rubber (SBR) 30µg used for quality control in between sample runs

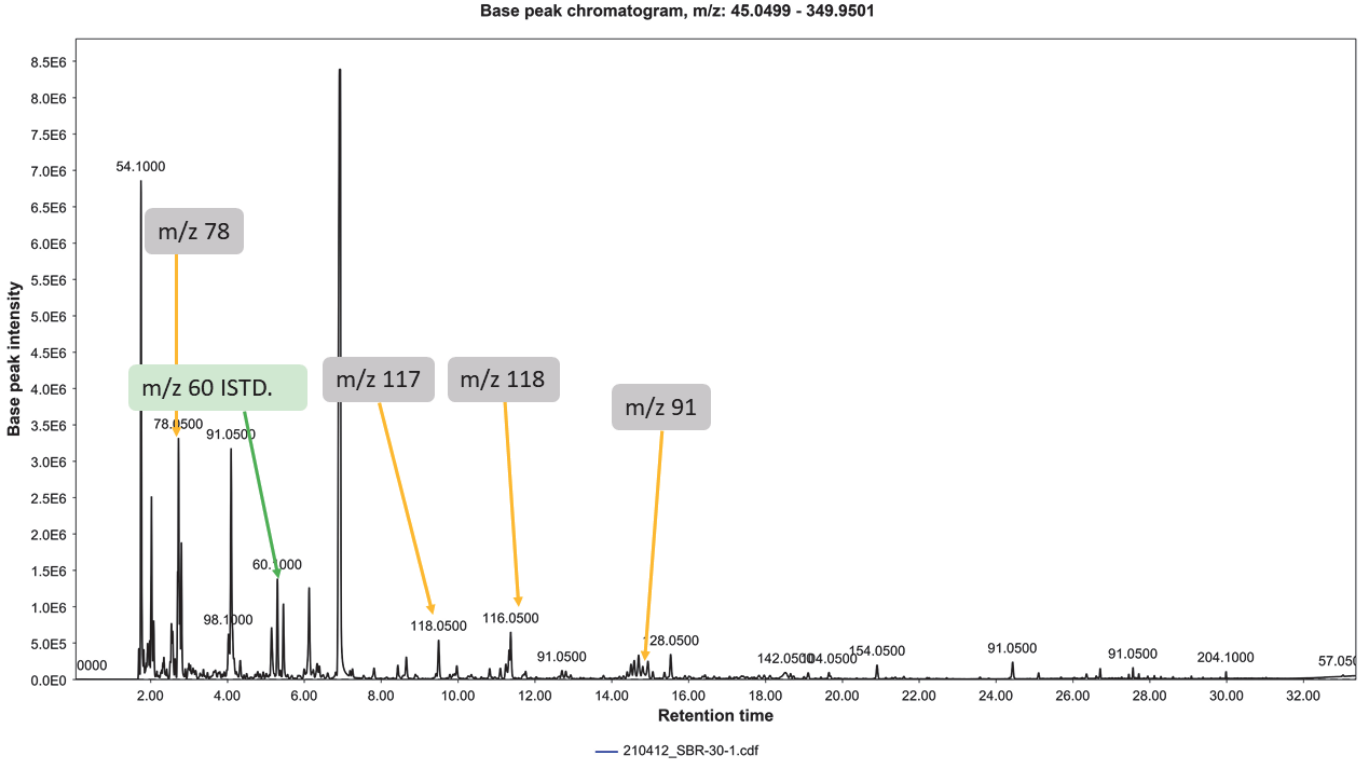

2) Tunnel wash water sample (untreated) TW-1-1

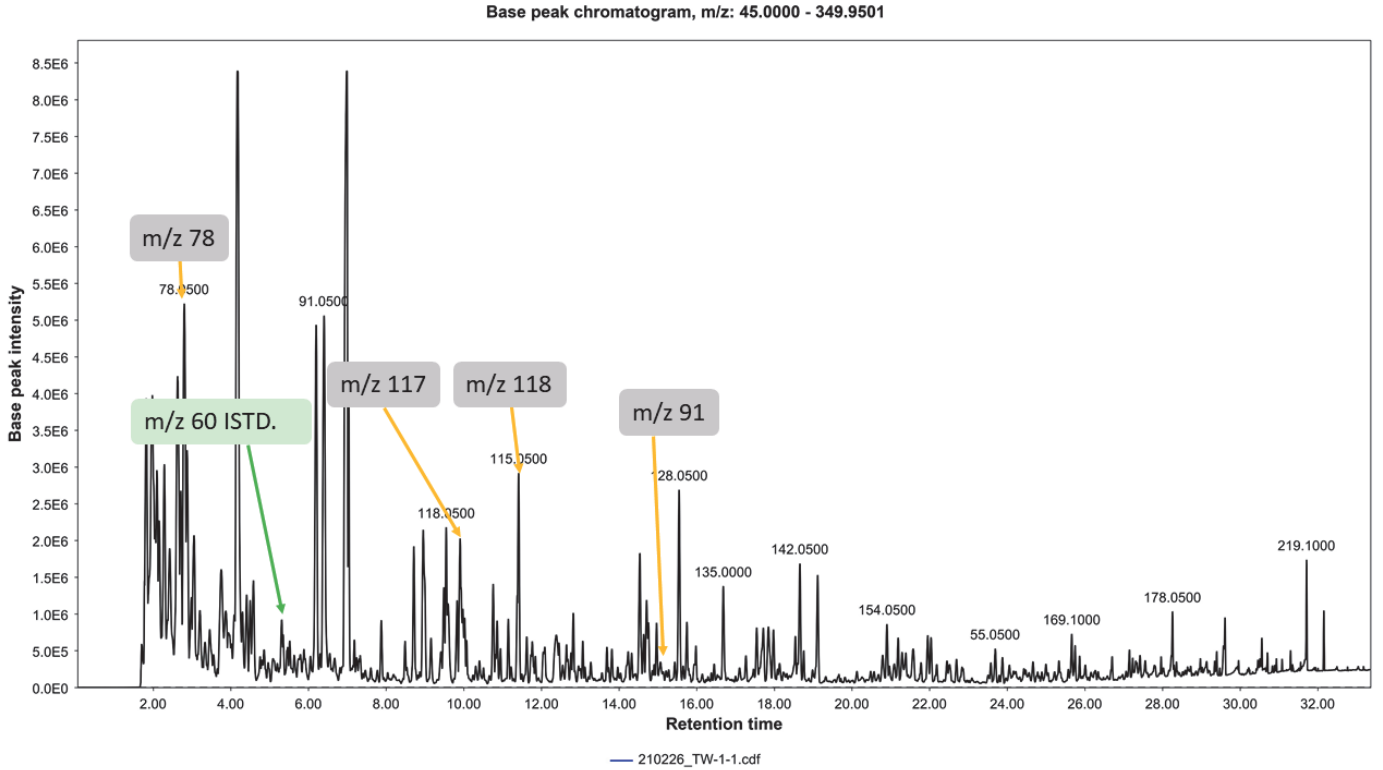
Base peak chromatogram, m/z: 45.0000 - 349.9501
Base peak intensity
8.5E6
8.0E6
7.5E6
7.0E6
6.5E6
6.0E6
5.5E6
5.0E6
4.5E6
4.0E6
3.5E6
3.0E6
2.5E6
2.0E6
1.5E6
1.0E6
5.0E5
0.0E0
m/z 78
78.0500
91.0500
m/z 117
m/z 118
m/z 91
m/z 60 ISTD.
115.0500
128.0500
118.0500
142.0500
135.0000
154.0500
55.0500
169.1000
178.0500
219.1000
2.00
4.00
6.00
8.00
10.00
12.00
14.00
16.00
18.00
20.00
22.00
24.00
26.00
28.00
30.00
32.00
Retention time
210226_TW-1-1.cdf

ISBN: 978-82-575-1906-3
ISSN: 1894-6402

Norwegian University
of Life Sciences

Postboks 5003
NO-1432 Ås, Norway
+47 67 23 00 00
www.nmbu.no